Acta Universitatis Szegediensis

Visit us at
www2.sci.u-szeged.hu/ABS

Acta Biologica Szegediensis

Volume 58, Number 2, 2014

University of Szeged, Szeged, Hungary

Acta Biologica Szegediensis

Acta Biologica Szegediensis (ISSN 1588-385X print form; ISSN 1588-4082 online form) is an international peer-reviewed, open access journal published by the University of Szeged yearly, in two issues per volume.

Acta Biologica Szegediensis publishes novel findings in various fields of biology with special focus on innovative research in modern experimental life sciences. The journal publishes experimental and theoretical papers, reviews, short communications, and descriptions of new methods. Letters to the editor and conference proceedings may also be published, subject to the approval of the Editor-in-Chief.

Acta Biologica Szegediensis provides peer review by expert researchers, fast publication times, no page charge and free online accessibility. Table of contents and all issues of the journal are available at http://www2.sci.u-szeged.hu/ABS.

Acta Biologica Szegediensis is indexed in BIOSIS Database, EMBASE, Excerpta Medica, Elsevier BIOBASE (Current Awareness in Biological Sciences), Scopus, SCImago and Zoological Record.

Editor-in-Chief: Csaba Vágvölgyi

Senior Editors: László Erdei and Károly Gulya

Editorial Board:

Imre Boros *(Biochemistry, Molecular Biology)*
Mihály Boros *(Experimental Surgery)*
Milan Certik *(Biotechnology)*
Gyula Farkas *(Anthropology)*
László Gallé *(Ecology)*
Zoltán Janka *(Psychiatry)*
Kornél Kovács *(Biotechnology)*
János Lonovics *(Internal Medicine)*
Péter Maróti *(Biophysics)*
Péter Maróy *(Genetics)*
Erzsébet Mihalik *(Botany)*
András Mihály *(Anatomy, Embryology, Histology)*
Manikandan Palanisamy *(Medical Mycology)*
Attila Pál *(Obstetrics and Gynecology)*
Aurél J. Simonka *(Traumatology, Surgery)*
Mária Szűcs *(Biochemistry, Pharmacology)*
József Toldi *(Comparative Physiology)*
László Vécsei *(Neurology)*
László Vígh *(Biochemistry)*
Kerstin Voigt *(Microbiology)*

Technical Editor: Tamás Mikola
Manuscript Editor and Editorial Assistant: Tamás Papp

Subscriptions

All subscriptions relate to the calendar year and must be pre-paid. The annual subscription rate is currently 100 USD and includes air mail delivery and handling.

Editor-in-Chief: Csaba Vágvölgyi
Department of Microbiology, Faculty of Science and Informatics
University of Szeged, Közép fasor 52., H-6726 Szeged, Hungary
Phone: 36 (62) 544-822, fax: 36 (62) 544-823
E-mail: csaba@bio.u-szeged.hu

Technical Editor: Tamás Mikola
Acta Biologica Szegediensis, Editorial Office
Közép fasor 52., H-6726 Szeged, Hungary
Phone: 36 (62) 544-822, fax: 36 (62) 544-823
E-mail: abs@bio.u-szeged.hu

ACTA BIOLOGICA SZEGEDIENSIS VOLUME 58(2), 2014

Table of Contents

Articles

On the cover: picture of *Spirodela polyrhiza* (L.) Schleiden (giant duckweed) (see Oláh et. al. in this issue).

Volume 58(2):95-101, 2014
Acta Biologica Szegediensis
http://www2.sci.u-szeged.hu/ABS

ARTICLE

Antioxidant enzyme changes in response to osmotic stress in wheat (*Triticum aestivum* L.) seedling

Rana Naderi[1]*, Mostafa Valizadeh[1], Mahmoud Toorchi[1], Mohammad Reza Shakiba[2]

[1]Department of Plant Breeding and Biotechnology, Faculty of Agriculture, University of Tabriz, Tabriz, Iran, [2]Department of Plant Eco-Physiology, Faculty of Agriculture, University of Tabriz, Tabriz, Iran

ABSTRACT In order to evaluate the effects of osmotic stress on behavioral responses of antioxidant enzymes including superoxide dismutase (SOD), peroxidase (POX), catalase (CAT), glutathione reductase (GR) and ascorbate peroxidase (APX), a factorial experiment was carried out under laboratory conditions with three groups of wheat genotypes (tolerant, intermediate and susceptible) and three osmotic stress levels induced by PEG (control, mild and severe). Electrophoretic analyses were performed for three antioxidant enzymes SOD, POX and CAT in shoots of wheat seedlings using 7.5% slab polyacrylamide gels. The activities of GR and APX were determined spectrophotometrically. For SOD, POX and CAT, two, seven and one isozymes were observed, respectively. Statistical analysis showed that osmotic stress has a significant effect on enzymatic activities in wheat seedlings. POX, CAT, GR and APX activities were increased significantly in the severe stress compared with control condition about 31, 61, 129 and 149 percent, respectively. Whereas, SOD activity increased significantly by 41% in the mild stress compared with control treatment. The highest enzymatic activity was belonged to tolerant group under severe stress conditions for almost all of isozymes and enzymes. Among the antioxidant enzymes, APX activity was increased most drastically in severe stress condition. The extent of damage to the wheat seedlings seems to depend on genotype and severity of osmotic stress.
Acta Biol Szeged 58(2):95-101 (2014)

KEY WORDS

antioxidant enzyme
osmotic stress
seedling
wheat

The stress factors especially drought, negatively affect plant growth and development and causes a sharp decrease of plants productivity. The limitation in the availability of water induces osmotic stress (Molinari et al. 2007). In certain tolerant crop plants morphological and metabolic changes occur in response to osmotic stress, which contribute towards adaptation to such unavoidable environmental constraints (Sinha et al. 1986). Among crop plants, wheat (*Triticum aestivum* L.), is an attractive study system because of the natural genetic variation in traits related to water deficit tolerance (Loggini et al. 1999). Water deficit stress induces oxidative reactions by producing reactive oxygen species (ROS), which attack the most sensitive biological macromolecules and membranes to impair their function (Foyer et al. 1994; Noctor and Foyer 1998; Mitller 2002). Strategies to minimize oxidative damage are a universal feature of plant defense responses. The plant response to water deficit stress would depend on the species inherent "strategy" as well as on the duration and severity of the stress period.

Mechanisms of ROS detoxification in several plants by enzymatic and non-enzymatic antioxidants are well documented (Dhindsa et al. 1981; Asada and Takahashi 1987; Foyer and Noctor 2000). The measure of specific antioxidant enzyme activities and/or expression analysis during water deficit stress treatments has been generally accepted as an approach to assess the involvement of the scavenging system during water stress (Cruz de Carvalho 2008). However, contradictory results (increment, reduction or remaining unchanged) have been obtained through the much more analysis of plants antioxidant in different conditions. In sunflower seedlings and in grass plants (*Aegilops squarrosa*) a decrease in SOD activity was detected under water deficit stress (Badiani et al. 1990). The reverse was those also found in wheat (Badiani et al. 1990) and rice (Sharma and Dubey 2005) where water stress increased SOD activity. Simova-Stoilova et al. (2010) reported increased CAT activity in wheat under drought stress being higher especially in sensitive varieties. In another study, Sharma and Dubey (2005) reported a decrease in CAT activity in rice seedlings following drought stress. It was shown that APX and/or GR activities were enhanced during water stress in wheat seedlings (Keles and Oncel 2002) and alfalfa (Rubio et al. 2002). A time course measure of APX and GR activities under a mild water stress imposed by a PEG treatment (-0.7 MPa) on maize detached leaves also showed a significant increase in both above mentioned enzyme activities (Jiang and Zhang 2002). In a field study, it was observed that when plants subjected to mild drought stress in the seedling stage,

Accepted Sept 24, 2014
*Corresponding author. E-mail: Naderi.rana@gmail.com

Table 1. List and characteristics of studied wheat genotypes belonging to three groups.

No.	Families	Group	Reference
1	Unknown-1	Tolerant	Mohammadi et al. 2010
2	1-27-6149/Sabalan// 84.40023	Tolerant	Mohammadi et al. 2010
3	Ghafghaz//F9.10/Maya"s" IRW92-1-D-474-OMA-OMA-OMA-OMA-IMA-OMA	Tolerant	Mohammadi et al. 2010
4	DARIC95-010-OMA-OMA-OMA-OMA-6MA-OMA	Tolerant	Roostaei 2008; Valizadeh et al. 2012
5	Azarbaijan/Gobostan	Tolerant	Mollasadeghi et al. 2011
6	Azarbaijan/Roozi-84	Tolerant	Mollasadeghi et al. 2011
7	Tous	Tolerant	Mollasadeghi et al. 2011
8	Azar-2	Tolerant	Mohammadi et al. 2010
9	Sardari	Tolerant	Mohammadi et al. 2010
10	DARIC95-010-OMA-OMA-OMA-OMA-8MA-OMA	Intermediate	Roostaei 2008; Valizadeh et al. 2012
11	Manning/Sdv1//Dogu88	Intermediate	Mohammadi et al. 2010
12	RECITL/TIA.2//TRK13	Intermediate	Mohammadi et al. 2010
13	Vrz/3/Orf1.148/Td1/Blo/4/Sabalan	Intermediate	Roostaei 2008; Valizadeh et al. 2012
14	HK16/7/KVZ/T171/3/MAYA//BB/INIA/4/KAR/JCWH99034-0AP- OAP-OAp-OMAR-6MAR	Susceptible	Roostaei 2008; Valizadeh et al. 2012
15	FKG13/4/NWT/3/TAST/SPRW// TCI98-0139-OAP-OAP-OMAR-5MAR	Susceptible	Roostaei 2008; Valizadeh et al. 2012
16	JANZ QT3685-OAUS	Susceptible	Roostaei 2008; Valizadeh et al. 2012
17	RINA-11	Susceptible	Roostaei 2008; Valizadeh et al. 2012
18	Azarbaijan/Saratoveskaya-29	Susceptible	Mollasadeghi et al. 2011
19	Cimmyt/Saysonz	Susceptible	Mollasadeghi et al. 2011

the drought-tolerant wheat cultivar acclimatized better than the drought- susceptible cultivar by maintaining favorable water relations and lower membrane injury due to low H_2O_2 accumulation and antioxidant defense in the leaves under severe water-deficit conditions (Khanna-Chopra and Selote, 2007).

Polyethylene glycol (PEG) compounds have been used to simulate water stress effect in plants (Murillo-Amadaor et al. 2002). PEG of higher molecular weight is considered to cause blockage of the pathway of water movement, reducing water absorption and causing desiccation of the plant (Lawlor 1970). It is envisaged from the above findings that PEG solution can be frequently used in the laboratory for screening drought tolerant genotypes at early stage.

Therefore, the present study aimed to determine the effect of PEG-induced osmotic stress on enzymatic antioxidant systems in tolerant, intermediate and susceptible wheat genotype's seedlings and to evaluate the activity changes in antioxidant enzymes in the three groups of wheat genotypes.

Material and Methods

Plant material and experimental conditions

The experiment was conducted in factorial form, using a completely randomized design with three replications. Three groups of wheat genotypes (9 tolerant, 4 intermediate and 6 susceptible), (Roostaei 2008; Mohammadi et al. 2010; Mollasadeghi et al. 2011) (Table 1) were evaluated under laboratory conditions. Seeds of wheat genotypes were surface sterilized with 0.01% $HgCl_2$ solution for three minutes, followed by washing several times by distilled water. Ten seeds of each genotype then were placed on the moist Whatman germination papers in Petri dishes and were germinated using distilled water for 3 days under control conditions (light/dark regime of 16/8 h at 25/20 °C, relative humidity of 60-70%. Light intensity during the daytime was 350 µmol m^{-2} s^{-1}). After 3 days, osmotic stress was imposed by application of PEG-6000 (polyethylene glycol) for 5 days. Using the Michel-Kaufmann equation, 139 and 203 g of PEG-6000 was dissolved in 200 ml of distilled water and total volume was raised up to one liter to produce solutions of mild (–0.4MPa) and severe (–0.8MPa) osmotic potential, respectively (Michel and Kaufmann 1973). The activities of five antioxidant enzymes were evaluated on shoots of 8-day-old seedlings in Faculty of Agriculture, University of Tabriz during 2012.

Native polyacrylamide gel electrophoresis

The activities of SOD, POX and CAT were determined in native PAGE (Polyacrylamide gel electrophoresis). The crude extract of fresh and healthy shoots were prepared with separate mortars and pestles in a Tris-HCl extraction buffer pH 7.5 (Tris 50 mM, sucrose 5%, ascorbic acid 50 mM, sodium metabisulfite 20 mM, PEG 2% and 2-mercaptoethanol 0.1%) before use with a ratio of 0.1 gr μl^{-1} (W:V) and centrifuged (Model EBA 12R) at 4 °C and 10 000 rpm for 10 minutes (Valizadeh et al. 2011). Enzyme extracts were immediately absorbed onto 3×5 mm wicks cut from Whatman 3 mm filter paper and loaded onto 7.5% horizontal slab polyacrylamide gels (0.6×15×12 cm), prepared by Poulik buffer (Soltis and

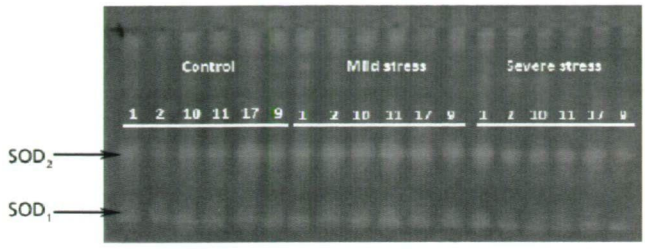

Figure 1. Example of isozyme pattern and relative activity of SOD in the shoots of wheat seedlings for three stress conditions (No.1, 2, 9: tolerant- 10, 11: intermediate and 17: susceptible genotypes).

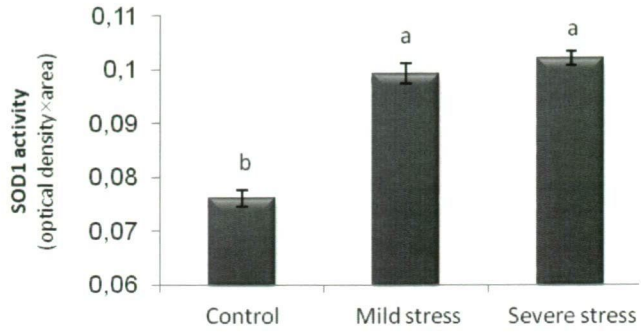

Figure 2. Mean comparison of SOD_1 in three stress conditions.

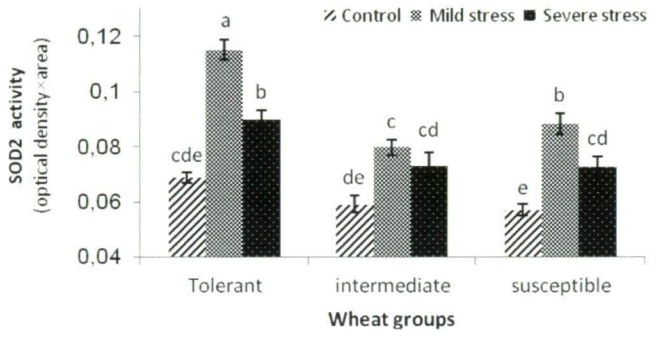

Figure 3. Treatment combination means of wheat groups and PEG-mediated osmotic stress for SOD_2.

Soltis 1990) using TBE (Tris-Borate-EDTA) electrode buffer (pH 8.8). Electrophoresis was carried out at 4 °C for 3 hours (constant current of 30 mA, and voltage of about 180 V). For each genotype, analysis was repeated three times, each time from bulked material of at least five seedlings. After electrophoresis, two slices of slab gel were prepared. The staining protocol for SOD and CAT was performed according to Soltis and Soltis (1990) and POX according to Olson and Varner (1993). The gels were fixed and scanned immediately after staining. An image analysis program (MCID Analysis Evaluation 0.7) was used to measure D×A (optical density × area) parameter for each isozyme band to evaluate the enzymatic activity.

Spectrophotometer analysis

The activities of GR and APX were determined spectrophotometrically (Model RAY LEIGH UV-2601). GR activity was determined by measuring the reduction kinetics of oxidized glutathione (O'Kane et al. 1996). APX activity was determined following the oxidation of ascorbate to dehydroascorbate, as described by Nakano and Asada (1981).

Protein determination

The protein contents of the enzyme extracts were determined by Bradford (1979) method using bovine serum albumin (BSA) as a standard.

Statistical analysis

Data were analyzed using the general linear model procedure in SAS program (SAS Institute, Cary, USA). The assumptions of variance analysis were tested by ensuring that the residuals were random and homogenous, with a normal distribution. Enzymatic activity means were compared by LSD and SNK using the SAS program.

Results and Discussion

Assessment of electropherograms for SOD, CAT and POX in 19 wheat genotypes displayed two, one and seven isozymes, respectively. Analysis of variances for 10 above mentioned isozymes activities and two antioxidant enzymes, including GR and APX, studied spectrophotometrically, showed that the osmotic stress has a significant effect on enzymatic activities in wheat seedlings. But, the differences between three groups of wheat (susceptible, tolerant and intermediate) were significant only for one SOD (SOD_2) and two POXs (POX_1 and POX_7). Stress × wheat groups interactions were significant for all enzymes except one SOD (SOD_2) and one POX (POX_2) isozymes (variance analysis not shown).

Superoxide dismutase

The specific SOD activity was increased in the shoots of wheat seedlings under stress conditions. Increase in enzyme activity coincided with a variable increment in the individual isoform expression. Two isozymes (SOD 1 and 2) were detected in the shoot with SOD_2 being the major one (Fig. 1). Mean comparison of SOD_1 in three levels of stress conditions is presented in Figure 2. SOD_1 activity was significantly increased in both mild and severe stress conditions, having non-significant stress wheat group interaction. The SOD_2 expression showed a concomitant increase with the total SOD activity. The stress × wheat group interaction was significant for SOD_2 (Fig. 3). A significant difference between severe and mild stress was observed in tolerant and susceptible groups

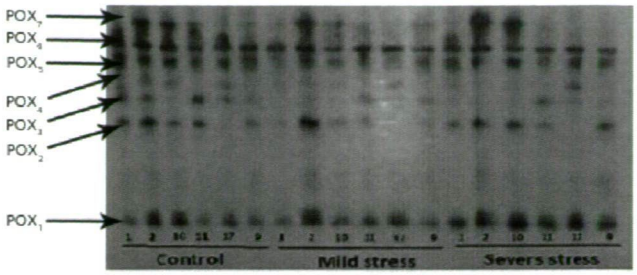

Figure 4. Example of isozyme pattern and relative activity of POX in the shoots of wheat seedlings for three stress conditions (No.1, 2, 9: tolerant- 10, 11: intermediate and 17: susceptible genotypes).

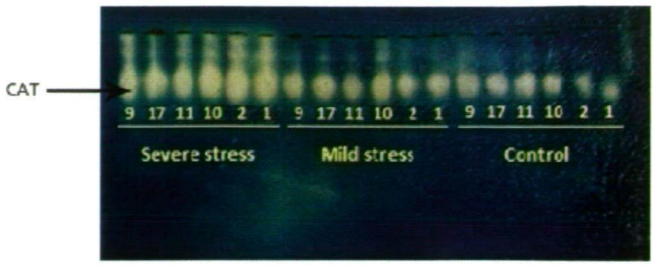

Figure 6. Example of enzyme pattern and relative activity of CAT in the shoots of wheat seedlings for three drought conditions (No.1, 2, 9: tolerant- 10, 11: intermediate and 17: susceptible genotypes).

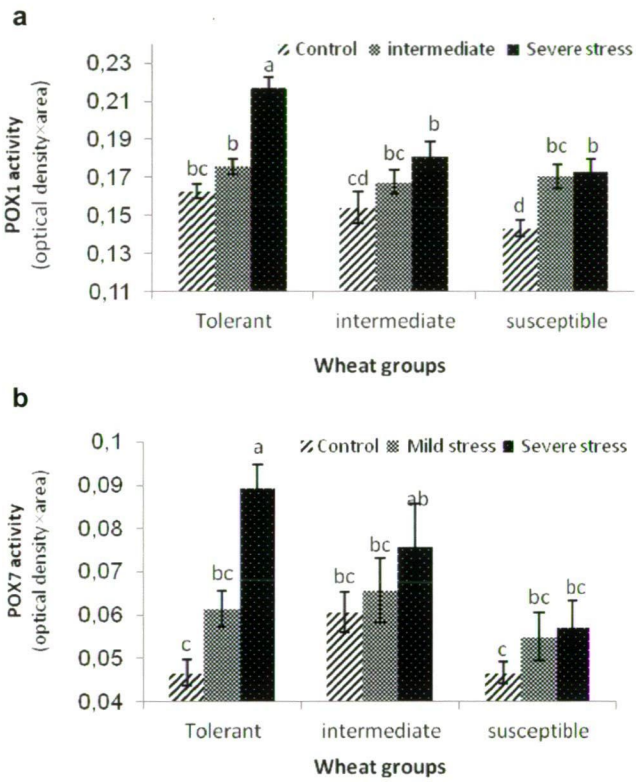

Figure 5. Treatment combination means of wheat groups and PEG-mediated osmotic stress for POX_1 (a) and POX_7 (b).

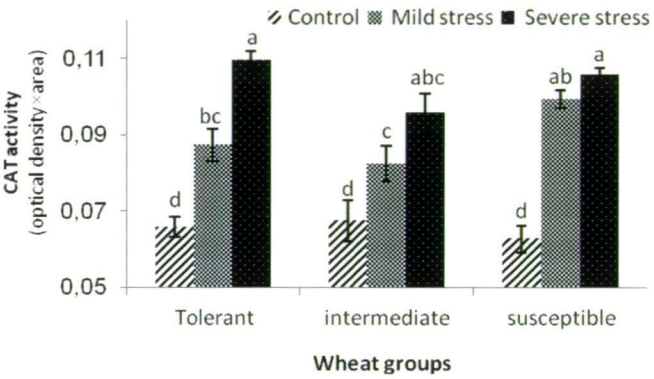

Figure 7. Treatment combination means of wheat groups and PEG-mediated osmotic stress for CAT activity.

for SOD_2, whereas in intermediate group there was no significant difference and the maximum activity was obtained in tolerant group at mild (-0.4 MPa) stress.

Interestingly, mild water stress resulted in a maximum and significant up-regulation of SOD_2 in both tolerant and susceptible groups compared with intermediate group (Fig. 1 and 3). The ability of plants to overcome oxidative stress partly relies on the induction of SOD activity and subsequently on the up-regulation of other downstream antioxidant enzymes (Alscher et al. 2002). According to this fact that SOD processing is known to be substrate inducible) Tsang et al. 1991), an increment in the SOD activity may be attributed to the increased production of the superoxide ($O_2^{\bullet-}$) as substrate that lead to induced expression of genes encoding SOD. In sunflower seedlings a decrease in SOD activity was detected under water stress (Badiani et al. 1990). The reverse was true in wheat (Badiani et al. 1990; Bakalova et al. 2004) and rice (Sharma and Dubey 2005) where water stress increased SOD activity. Our results are consistent with Badiani et al. (1990) and Bakalova et al. (2004). Higher SOD activity in tolerant group compared with susceptible and intermediate groups can also be explained by less efficiency susceptible group in scavenging of $O_2^{\bullet-}$ under severe stress conditions.

Peroxidase

Seven isozymes were detected (Fig. 4) in the shoots of wheat seedlings with POX_1 and POX_7 being the major ones, having significantly different activities between wheat groups. Differences of genotypes within group and stress × wheat group interaction were significant for all POX isozymes except for POX_2 (data not shown). The highest enzymatic activity increment was belonged to tolerant group of wheat under severe

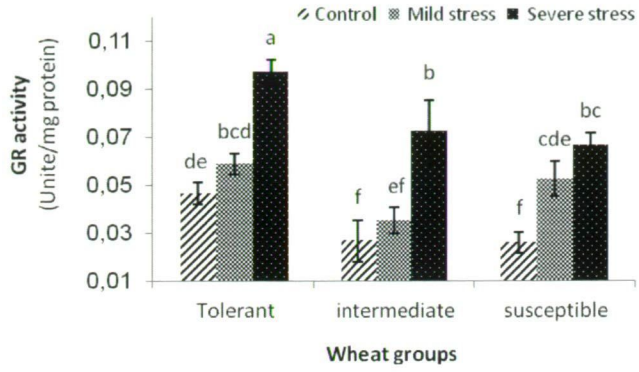

Figure 8. Treatment combination means of wheat groups and PEG-mediated osmotic stress for GR activity.

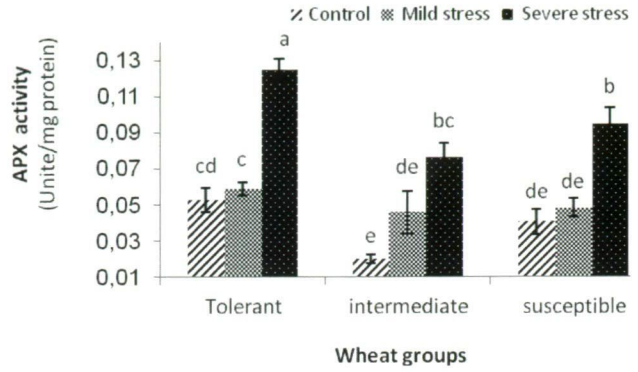

Figure 9. Treatment combination means of wheat groups and PEG-mediated osmotic stress for APX activity.

stress conditions (-0.8 MPa) for most of POX isozymes, especially for POX_1 and POX_7 (Fig. 5a, b).

POX, APX and CAT are three important H_2O_2 scavenging antioxidant enzymes functioning in different sub cellular compartments (Noctor and Foyer 1998). Increase in POX activity in leaves of drought tolerant and susceptible wheat cultivars has also been reported earlier under water deficit stress. Sairam and Saxena (2000) reported that tolerant genotypes, with highest peroxidase activity, had the lowest lipid peroxidation and highest membrane stability under water stress at different stages after anthesis, while the susceptible genotypes exhibited the lowest antioxidant enzyme activity, membrane stability and the highest lipid peroxidation.

Acar et al. (2001) reported an increase in POX activity in tolerant barely variety but non changed activity in susceptible one. Shao et al. (2005) observed variation in peroxidase activity in wheat genotypes under soil water deficits at maturation stage and suggested that water stress tolerance was closely associated with POX activities. An increase in POX activity in drought tolerant as well as susceptible maize genotypes at seedling stage under 72 h drought stress has been reported by Chugh et al. (2011). In a review applied at seedling stage of wheat cultivars, antioxidant enzymes activities were increased with the decrease of osmotic potential in both tolerant and sensitive cultivars. The tolerant cultivar exhibited a higher antioxidant activity compared to the sensitive one (Valifard et al. 2012), supporting our results in the present study.

Catalase

A single band of CAT was detected in the shoots of wheat seedlings upon native PAGE separation. In severe stress condition, CAT showed higher activity as compared with mild stress and control condition (Fig. 6). Stress × wheat group and stress × genotype within group interaction for CAT were also significant (data not shown). A significant difference was observed between severe and mild stress in tolerant wheat group alone (Fig. 7).

Reports on catalase activity under stress condition are heterogeneous. CAT activity has been shown to increase in maize (Kolarovic et al. 2009), wheat (Luna et al. 2004) and also to remain unchanged or even decrease under water stress in sunflower (Zhang and Kirkham 1992). Luna et al. (2004) reported leaf H_2O_2 content increased even though total CAT activity doubled in wheat seedling under severe stress conditions. Our results are consistent with works reporting the increased CAT activity in response to osmotic stress in wheat seedling.

Glutathione reductase

Effect of water deficit stress was significant on GR activity, measured spectrophotometrically. Stress × wheat group interactions and genotype within group were significant. Figure 8 indicates the mean GR activity values, for treatment combinations. The highest and significant GR activity was obtained for tolerant wheats in severe stress conditions.

Several authors have reported increased activity of GR in rice seedlings (Sharma and Dubey 2005) and alfalfa (Rubio et al. 2002) under environmental stresses. Lascano et al. (2001) reported an increase in glutathione reductase (GR) activities in the tolerant wheat cultivars and a higher decline in reduced glutathione (GSH), ascorbate content and less oxidative damage than in the susceptible cultivar.

Ascorbate peroxidase

APX activity showed significant difference for osmotic stress, genotype within group conditions, stress × wheat group and stress × genotype within group interactions. In spite of genotype differences within groups (data are not shown), the interaction effect between stress and groups of wheat

revealed that (Fig. 9), the tolerant group of wheats under severe stress displays a substantially increased activity for APX as for GR.

Khanna-Chopra and Selote (2007) reported that drought tolerant wheat cultivars had the highest APX activity during severe water deficit stress in post-anthesis period as our finding for wheat seedling. Al-Ghamdi (2009) reported that drought acclimated (by cessation of watering for 8 days) wheat seedling exhibited systematic increase in the activity of H_2O_2 scavenging enzymes, particularly APX and CAT and maintenance of ascorbate redox pool by efficient function of APX enzyme.

Acknowledgements

The present study was supported by the research grant offered to Prof. M. Valizadeh from the University of Tabriz. The authors wish to thank Dr. M. Roostaei (Dry Land Agricultural Research Institute, Maragheh, Iran) and Dr. R. Shahryari (Islamic Azad University, Ardabil, Iran) for providing some wheat genotypes.

References

Al-Ghamdi AA (2009) Evaluation of oxidative stress tolerance in two wheat (*Triticum aestivum* L.) cultivars in response to drought. Int J Agric Biol 11:7-12.

Acar O, Turkan I, Ozdamir F (2001) Superoxide dismutase and peroxidase activities in drought sensitive and resistant barley (*Hordeum vulgare* L.) varieties. Acta Physiol 23:351-356.

Alscher RG, Erturk N, Heath LS (2002) Role of superoxide dismutases (SODs) in controlling oxidative stress. J Exp Bot 53:1331-1341.

Asada K, Takahashi M (1987) Production and scavenging of active oxygens in chloroplasts. In: Kyle DJ, Osmond CB, Arntzen CJ, eds. Photoinhibition. Amsterdam: Elsevier 1987:227-287.

Badiani M, De Biasi MG, Cologna M, Artemi F (1990) Catalase, peroxidase and superoxide dismutase activities in seedlings submitted to increasing water deficit. Agrochim 34:90-102.

Bakalova S, Nikolova A, Wedera D (2004) Isoenzyme profiles of peroxidase catalase and superoxide dismutase as affected by dehydration stress and ABA during germination of wheat seeds. Plant Physiol 30:64-77.

Bradford M (1979) A rapid and sensitive method for the quantitation of microgram quantities of protein utilizing the principle of protein-dye binding. Anal Biochem 72:248-254.

Chugh V, Kaur N, Gupta AK (2011) Evaluation of oxidative stress tolerance in maize (*Zea mays* L.) seedlings in response to drought. Ind J Biochem Biophys 48:47-53.

Cruz de Carvalho MH (2008) Drought stress and reactive oxygen species. Plant Signal Behav 3:156-165.

Dhindsa RS, Plumb-Dhindsa P, Thorpe TA (1981) Leaf senescence: correlated with increased levels of membrane permeability and lipid peroxidation, and decreased levels of superoxide dismutase and catalase. J Exp Bot 32:93-101.

Foyer CH, Lelandais M, Kunert KJ (1994) Photo oxidative stress in plants. Plant Physiol 92:696-717.

Foyer CH, Noctor G (2000) Oxygen processing in photosynthesis: Regulation and signaling. New Phytol 146:359-388.

Jiang M, Zhang J (2002) Water stress-induced abscisic acid accumulation triggers the increased generation of reactive oxygen species and up-regulates the activities of antioxidant enzymes in maize leaves. J Exp Bot 53:2401-2410

Keles Y, Oncel I (2002) Response of the antioxidative defence system to temperature and water stress combinations in wheat seedlings. Plant Sci 163:783-90.

Khanna-Chopra R, Selote DS (2007) Acclimation to drought stress generates oxidative stress tolerance in drought-resistant than susceptible wheat cultivar under field conditions. Environ Exp Bot 60:276-283.

Kolarovic L, Valentovic P, Luxova M, Gasparıkova O (2009) Changes in antioxidants and cell damage in heterotrophic maize seedlings differing in drought sensitivity after exposure to short-term osmotic stress. Plant Growth Reg 59:21-26.

Lascano HR, Antonicelli GE, Luna CM, Melchiorre MN, Gomez LD, Racca RW, Trippi VS, Casano LM (2001) Antioxidant system response of different wheat cultivars under drought: Field and in vitro studies. Aust J Plant Physiol 28:1095-1102.

Lawlor DW (1970) Absorption of PEG by plants and their effects on plant growth. New Phytol 69:501-13.

Loggini B, Scartazza A, Brugnoli E, Navari-Izzo F (1999) Antioxidant defense system, pigment composition, and photosynthetic efficiency in two wheat cultivars subjected to drought. Plant Physiol 119:1091-1099.

Luna CM, Pastori GM, Driscoll S, Groten K, Bernard S, Foyer CH (2004) Drought controls on H_2O_2 accumulation, catalase (CAT) activity and CAT gene expression in wheat. J Exp Bot 56:417-23.

Michel BE, Kaufmann MR (1973) The osmotic potential of polyethylene glycol 6000. Plant Physiol 51:914-917.

Mittler R (2002) Oxidative stress, antioxidants and stress tolerance. Trends Plant Sci 7:405-410.

Mohammadi R, Roostaei M, Haghparast R, Roohi E, Kazemi S, Ahmadi MM, Abediasl G, Amri A (2010) Genotype × Environment interaction for grain yield in rainfed winter wheat Multi-Environmental trials in Iran. Agronomy J 102:1500-1510.

Molinari HBC, Marur CJ, Daros E, de Campos MKF, de Carvalho JFR, PFilho LFP, Pereira JCB, Vieira LGE (2007) Evaluation of the stress-inducible production of proline in transgenic sugarcane (*Saccharum* spp.): osmotic adjustment, chlorophyll fluorescence and oxidative stress. Physiol Plant 130:218-229.

Mollasadeghi V, Valizadeh M, Reza Shahryari R, Imani AA (2011) Evaluation of end drought tolerance of 12 wheat genotypes by stress indices. Middle-East J Sci Res 7(2):241-247.

Murillo-Amadaor B, Lopez-Aguilar R, Kaya C, Larrinaga-Mayoral J, Flores-Hernandez A (2002) Comparative effects of NaCl and polyethylene glycol on germination, emergence and seedling growth of cowpea. J Agron Crop Sci 188:235-247.

Nakano Y, Asada K (1981) Hydrogen peroxide is scavenged by ascorbate-specific peroxidase in spinach chloroplasts. Plant Cell Physiol 22:867-880.

Noctor G, Foyer CH (1998) Ascorbate and glutathione: keeping active oxygen under control. Ann Rev Plant Physiol Plant Mol Biol 49:249-279.

O'Kane D, Gill V, Boyd P, Burdon R (1996) Chilling, oxidative stress and antioxidant responses in *Arabidopsis thaliana* callus. Planta 198:371-377.

Olson PD, Varner JE (1993) Hydrogen peroxides and lignifications. Plant J 4:887-892.

Roostaei M (2008) Genetic analysis of drought tolerance in wheat by morpho- physiological traits and molecular analysis. PhD Thesis. Submitted: Plant Breeding. Science and Research Unit Tehran, Iran.

Rubio MC, González EM, Minchin FR, Webb KJ, Arrese-Igor C, Ramos J, Becana M (2002) Effects of water stress on antioxidant enzymes of leaves and nodules of transgenic alfalfa overexpressing superoxide dismutases. Physiol Planta 115:531-540.

Sairam RK, Saxena DC (2000) Oxidative stress and antioxidant in wheat genotypes: possible mechanism of water stress tolerance. J Agron Crop Sci 184:55-61.

Shao HB, Liang ZS, Shao MA (2005) Changes of some anti-oxidative enzymes under soil water deficits among 10 wheat genotypes at maturation stage. Colloids and Surfaces B: Biointerfaces 45:7-13.

Sharma P, Dubey RS (2005) Modulation of nitrate reductase activity in rice seedlings under aluminium toxicity and water stress: role of osmolytes as enzyme protectant. J Plant Physiol 162:854-864.

Simova-Stoilova L, Vaseva I, Grigorova B, Demirevska K, Feller U (2010) Proteolytic activity and cysteine protease expression in wheat leaves under severe soil drought and recovery. Plant Physiol Biochem 48:200-206.

Sinha SK, Aggarwal PK, Chaturvedi GS, Singh AK, Kailasnathan KK (1986) Performance of wheat and triticale cultivars in a variable soil–water environment. I Grain yield stability Field Crops Res 13:289-299.

Soltis DE, Soltis PS (1990) Isozymes in Plant Biology. Chapman and Hall London, pp. 259.

Tsang EWT, Bowler C, Herouart D, Van CW, Villarroel R, Genetello C, Van MM, Inze D (1991) Differential regulation of superoxide dismutase in plants exposed to environmental stress. Plant Cell 3:783-792.

Valifard M, Moradshahi A, Kholdebarin B (2012) Biochemical and physiological responses of two wheat (*Triticum aestivum* L.) cultivars to drought stress applied at seedling stage. J Agr Sci Tech 14:1567-1578.

Valizadeh M, Mohayeji M, Yasinzadeh N, Nasrullazadeh S, Moghaddam M (2011) Genetic diversity of synthetic alfalfa generations and cultivars using tetrasomic inherited allozyme markers. J Agr Sci Tech 13:425-430.

Valizadeh M, Mahmoodian Z, Jalaly HM, Ghafari A, Roostaei M (2012) Response of advanced winter wheat genotypes to drought stress using agronomic traits and protein patterns. Cer Res 1(1):1-24 [*in Persian*].

Zhang J, Kirkham MB (1992) Antioxidant responses to drought in sunflower and sorghum seedlings. New Phytol 132:361-73.

Volume 58(2):103-108, 2014
Acta Biologica Szegediensis
http://www2.sci.u-szeged.hu/ABS

ARTICLE

Cadmium-induced turion formation of *Spirodela polyrhiza* (L.) Schleiden

Viktor Oláh[1], Anna Hepp[1], Gyula Lakatos[2], Ilona Mészáros[1]*

[1]Department of Botany, Faculty of Science and Technology, University of Debrecen, Debrecen, Hungary, [2]Department of Ecology, Faculty of Science and Technology, University of Debrecen, Debrecen, Hungary

ABSTRACT *Spirodela polyrhiza* (L.) Schleiden (giant duckweed) is an extensively studied representative of duckweeds (Lemnoideae subfamily, Araceae). Despite its widespread application in numerous research areas and well-known capability for producing turions, the effects of various toxicants on turion production are sporadically discussed in the scientific literature. Our aim was to study the growth of *S. polyrhiza* under cadmium stress and to test its potential interference with turion production. Effects of cadmium were assessed in axenic cultures of a local *S. polyrhiza* clone in 7-days-long duckweed growth inhibition tests. Our results indicated that higher cadmium concentrations decreased the relative growth rates of cultures within 3 days and growth inhibition reached its maximum between the 3rd and 5th days with 0.080 mg l^{-1} IC_{50}. Parallel with slowed frond production - by mirror image pattern - induction of turion formation was observed. The first turions protruded by the 5th day of treatments in the 0.075-0.75 mg l^{-1} concentration range. Such rapid onset of turion formation is indicative of an almost immediate switch between normal and turion mode of meristem function upon cadmium stress. The consideration of this mechanism in practical applications of *S. polyrhiza* is recommended.
Acta Biol Szeged 58(2):103-108 (2014)

KEY WORDS

Spirodela polyrhiza
duckweed
cadmium
growth inhibition
turion
vegetative propagule

Spirodela polyrhiza (L.) Schleiden (giant duckweed) is a cosmopolite representative of the Lemnoideae subfamily (Araceae). Although *Lemna gibba* L. and *L. minor* L. are the commonly used species in standardized ecotoxicological test procedures (Environment Canada 2007) *S. polyrhiza* is also widely applied as a model organism in plant physiology, ecotoxiciology and bioremediation studies (Gaur et al. 1994; Oláh et al. 2008). This special attention could partly be attributed to its special way of propagation (Chaloupková and Smart 1994). Duckweeds usually produce descendants vegetatively by their meristematic 'pockets' at the proximal end of their fronds. A considerable portion of the subfamily (15 out of 37 species according to Appenroth 2002), however, can produce not only daughter fronds but turions or turion-like fronds as well, which serve as dormant buds for surviving unfavorable periods (Jacobs 1947). *S. polyrhiza* is the most extreme example of this strategy since in temperate regions its winter survival relies exclusively on its turions because normal fronds cannot tolerate low temperatures (Appenroth 2002). Turions are produced by the same meristematic regions as normal vegetative fronds. Jacobs (1947) observed that the growing primordium loses its ability to reversibly switch between normal and turion developmental paths when it reaches approximately 0.2 mm length. According to Smart and Trewavas (1983) the developing primordium crosses this limit when cell expansion tends to dominate over cell division and the developmental switch is regulated by the internal level of abscisic acid (ABA). The mesophyll of turions is less differentiated, contains high amounts of starch, and lacks aerenchyma, and, as a result, turions sink to the water bottom during unfavorable periods (Jacobs 1947). Structural simplicity and small size of fronds, rapid growth, and easy observation of turion formation qualify *S. polyrhiza* as an ideal model system for investigating regulation of morphogenesis and dormancy in plants (Chaloupková and Smart 1994). Besides their popularity in plant physiological and ecotoxicological research, common advantages of duckweed species make these plants suitable for various fields of practical applications (Wang et al. 2014). Recently duckweeds are considered as potential candidates for bioremediation, waste water treatment, and raw material (e.g. protein and starch) production (Cheng and Stomp 2009).

Despite its extensive application in ecotoxicology and phytoremediation research, the effects of heavy metals on turion formation of *S. polyrhiza* are sparingly discussed and the results are rather contradictory. Xyländer et al. (1993) found that the presence of either cadmium (Cd) or nickel in the nutrient medium inhibited formation of turions. Contrary to that, Srivastava and Jaiswal (1989) found Cd to induce turion formation. Susplugas et al. (2000) reported similar effect of hexavalent chromium. Since the induction or suppression

Accepted Dec 11, 2014
*Corresponding author. E-mail: immeszaros@unideb.hu

Table 1. Relative growth rates (RGR, mean±SE, n=12) of control samples, lowest observed effect Cd-concentrations (LOEC), median growth inhibiting Cd-concentrations (IC_{50}, ±95% confidence intervals), mortality- ('Mortality') and turion formation-inducing concentrations ('Turion formation') of Cd as calculated for the periods between counting days 0th, 3rd, 5th and 7th, respectively. 'Mortality' and 'Turion formation' denote the Cd concentration ranges where negative mean RGRs or protruding turions, respectively, were observed.

	0th-3rd days	3rd-5th days	5th-7th days
$RGR_{control}$ (frond frond^{-1} day^{-1})	0.401 (±0.011)	0.398 (±0.013)	0.275 (±0.012)
LOEC (mg Cd l^{-1})	0.075	0.01	0.05
IC_{50} (mg Cd l^{-1})	0.297 (±0.088)	0.080 (±0.016)	0.100 (±0.030)
Mortality (mg Cd l^{-1})	-	-	0.5-1
Turion formation (mg Cd l^{-1})	-	0.075-0.75	0.075-0.75

of turion formation could affect both realized growth rates and quality of the produced biomass, the effects of various chemicals on turion formation are important factors considering the practical applicability of duckweeds. The aim of the present study was to assess the effects of Cd on growth of *S. polyrhiza* over a wide concentration range and to test its potential interference with turion production.

Materials and Methods

Test conditions

Effects of Cd were investigated in duckweed growth inhibition tests. Axenic stock culture of *Spirodela polyrhiza* (L.) Schleiden. was initiated from plants collected in 2004 at lake Kis-Balaton (W. Hungary). Stock cultures were maintained on Steinberg medium (pH 5.5±0.2, Environment Canada 2007) in tissue culturing room of Department of Botany, University of Debrecen (Hungary), under constant temperature (22±2 °C) and irradiation (warm white fluorescent lamps, PPFD: 60±10 µmol m^{-2} s^{-1}). 7-10 days prior to growth inhibition tests several plants were subcultured aseptically in 300 cm^3 Erlenmeyer's flasks containing 100 ml sterile Steinberg medium in order to maintain exponential growth of cultures. The applied conditions assured that no turion formation occurred during pre-culturing and tests in control cultures.

7-days-long, static growth inhibition tests were performed in 80 mm (diameter) crystallizing dishes containing 100-100 ml test solutions. Cd was applied in form of $3CdSO_4$ x $8H_2O$ salt (Reanal, Hungary) in final concentrations of 0, 0.0001, 0.0075, 0.01, 0.025, 0.05, 0.075, 0.1, 0.175, 0.25, 0.375, 0.5, 0.75 and 1 mg Cd l^{-1}, respectively. 2-3 colonies (10±2 fronds) per vessel were used as starting inoculum at the beginning of tests. Growth was characterized by the change in total frond number (FN) of cultures. Each culture was photographed digitally at 0th, 3rd, 5th, and 7th days of tests (Environment Canada 2007). Then digital images were used for counting FN by means of ImageJ (Abramoff et al. 2004). All living, distinguishable fronds were considered.

The same digital images were used for assessing turions produced during the tests. All distinguishable turion primordia were counted irrespective of their detachment from mother frond.

Data analysis

Relative growth rate (RGR) of cultures was calculated for periods between counting days according to the Environment Canada (2007) guidelines:

$$RGR\ (\text{frond frond}^{-1}\ \text{day}^{-1}) = (\ln(FN_j) - \ln(FN_i)) / t_j - t_i$$

where FN_i and FN_j are the observed frond numbers at days t_i and t_j

Based on newly formed turions and fronds the turion yield ratio (T%) of cultures that is production of turions in percentage of total new offshoots during a given period was calculated as follows:

T% = turions / (turions + new fronds)

Each applied Cd concentration was tested in 4 parallel cultures per test, and in 2 or 3 independent experiments. For assessing effects of Cd respective results of all parallel treatments were pooled (n = 8-12). Medians were compared by Kruskal-Wallis test and *post-hoc* Mann-Whitney pairwise comparisons using Past 3.01 (Hammer et al. 2001). Effects of different Cd concentrations were considered as significantly different at $p<0.05$ levels. The lowest observed effect concentration (LOEC) was considered as the lowest applied Cd concentration which resulted in significant ($p<0.05$) growth inhibition as compared to control. IC_{50} that is Cd concentration resulting in 50% growth inhibition for a given period of treatments was calculated performing non-linear regressions by means of Sigmaplot 10 (Systat Software). Four parameter logistic curves were fit to mean RGRs plotted as percentage of respective control means.

Results

Inhibiting effects of Cd on FN of *S. polyrhiza* cultures evolved very fast. By the 3rd day of treatments 0.075 mg l^{-1} and higher concentrations significantly ($p<0.05$) reduced RGR and 0.75 and 1 mg l^{-1} Cd almost completely stopped growth of cultures (Fig. 1, Table 1). Prolonged exposure to low Cd concentrations slowed the growth of plants as well. Growth of cultures

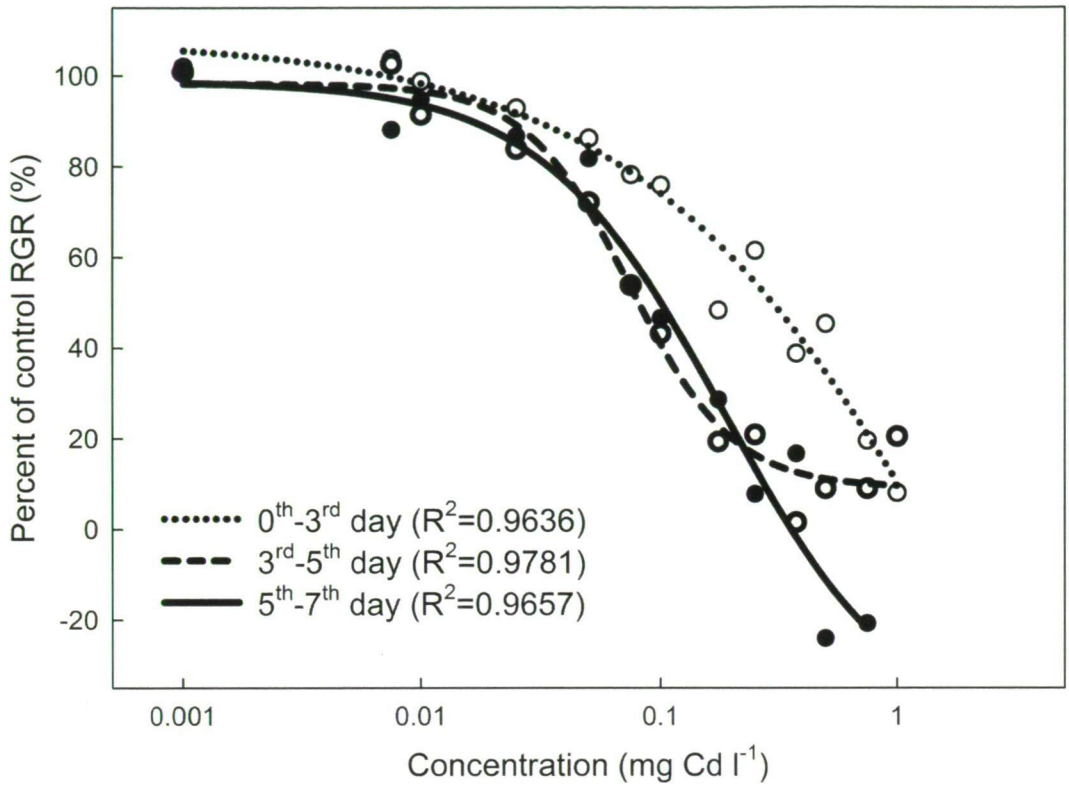

Figure 1. Relative growth rates (RGR) of *S. polyrhiza* cultures calculated on the basis of frond number changes between 0th-3rd, 3rd-5th and 5th-7th days of cadmium treatments, respectively. Regression lines are 4 parameter logistic curves with coefficients of determination in brackets. Symbols denote mean of 8-12 samples as percentiles of mean control RGR.

was significantly ($p<0.05$) inhibited between the 3rd and 5th days of treatments at 0.01 mg dm^{-3} and higher concentrations. In this period 0.175-1 mg l^{-1} and higher concentrations lowered growth rates of cultures below 0.1 frond $frond^{-1}$ day^{-1} that is increased the doubling times of fronds over 8 days. There was no considerable difference in pattern of growth inhibition over the applied Cd concentration range between periods of 3rd-5th days and 5th-7th days (Fig. 1). 0.25 mg l^{-1} and higher concentrations stopped entirely production of new fronds or even induced 'negative growth' that is resulted in mortality of existing fronds (Table 1). At 1 mg l^{-1} Cd proved to be lethal for test cultures within 7 days.

The LOEC and IC_{50} values showed strong decrease as comparing the periods of 0th-3rd and 3rd-5th days, respectively. However, later (5th-7th days) both LOEC and IC_{50} showed slight increase (Table 1).

Formation of turions was first observed at the 5th day of exposures. At this point, protruding turions were visible in the 0.075-0.75 mg l^{-1} concentration range (Table 1). Comparing the turion-inducing Cd concentrations, there was no difference at the 5th and 7th days of exposures, respectively (Table 1). Differentiation of primordia between the 3rd and 7th days of exposures was concentration-dependent and showed clearly mirror image pattern (Fig. 2). Increase in Cd concentration elevated T% suggesting that a growing proportion of newly formed offshoots became turion. Beyond 0.1 mg l^{-1} production rate of new fronds dropped strongly and in line with that T% exceeded 45% (Fig. 2). At 0.5 mg dm^{-3} Cd formation of turions became almost exclusive (85±8%) among offshoots in the test cultures. 0.75 mg l^{-1} Cd -the highest applied non-lethal concentration- accelerated the inhibition on the meristematic activity further and thus both formation of fronds and turions declined. This resulted in still high but somewhat lower T% (63±15%) than 0.5 mg l^{-1} Cd.

Discussion

Due to rapid doubling of duckweed cultures Cd-induced growth retention took place within a short time interval, even 3 days of exposure proved to be effective. The calculated IC_{50} values for the assessed three periods (0.297; 0.080 and 0.100 mg l^{-1} for 0th-3rd, 3rd-5th, and 5th-7th days, respectively) indicate that growth inhibition reached its maximum by the 5th day of exposure stopping completely the production of new fronds at higher concentrations after which the mortality of fronds took place resulting in negative growth rates of cultures. The observed effective concentrations were in the similar range as

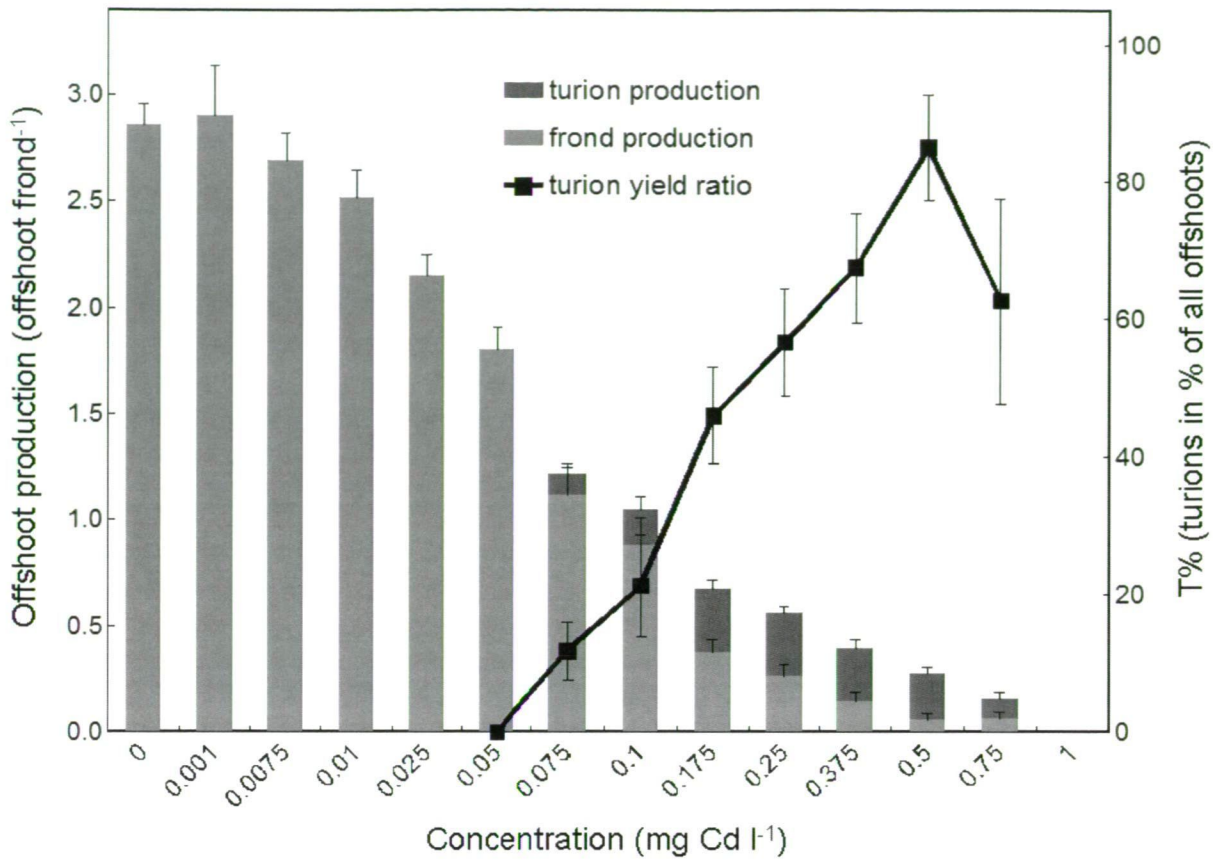

Figure 2. Average number of fronds and turions produced by one mother frond between the 3rd and 7th days of cadmium treatments (offshoot production) and relative proportion of turions in total offshoot production (T%), respectively. Error bars denote standard errors of means (n=8-12).

the literature data. On the basis of fresh weight change Gaur et al. (1994) calculated 0.09 mg l^{-1} IC_{50} for *S. polyrhiza* after 4 days of Cd treatments. In 7 days long growth inhibition tests with similar test conditions to ours Naumann et al. (2007) reported 0.323 mg l^{-1} IC_{50} based on FN of *L. minor* cultures.

Although *S. polyrhiza* is widely studied in ecotoxicology and bioremediation research effects of heavy metals on its turion formation are scarcely mentioned. The only available report on turion-inducing effect of Cd was provided by Srivastava and Jaiswal (1989). In their paper growth and turion formation of duckweed cultures was monitored at 10th, 20th and 30th days of treatments. Turion formation was first observed after 10 days due to 10 mg l^{-1} Cd. Although this concentration is one order of magnitude higher than the lethal concentration in our experiments, it induced similar extent of inhibition in growth rate (35%) also leading to turion production. Since they applied similar light and temperature conditions to those in our experiments we assume that the different growth media might be the potential reason for the higher inhibiting dose of Cd. Srivastava and Jaiswal (1989) used different concentrations of major nutrients and also applied 1% sucrose in the growth medium which might improve the tolerance of plants to Cd.

Rapid onset of turion production in our study suggests that switch of mother frond meristems from normal mode to turion formation takes place almost immediately after exposure to Cd. Since developmental path of offshoot primordium is irreversibly determined after a distinct period of morphogenesis (Jacobs 1947; Smart and Trewavas 1983) production of normal fronds continued during the first few days irrespective of Cd treatments. After protrusion of those fronds, the next generation of offshoots clearly reflected turion-inducing effects of Cd. The observed lag in turion formation fits the time range reported for plants under phosphate deficiency (3 days, Appenroth 2002) and ABA treatments (within 4 days, Smart et al. 1995).

Appenroth (2002) grouped turion inducing factors into 2 classes: those in the first one influence turion yield by total productivity of the system (e.g. via conditions of carbon assimilation), while those in the second one are signals for switching between normal and turion mode of meristematic pockets. Rapid appearance of turions in our experiments

suggests that Cd stress serves as a factor for triggering turion mode similarly to the latter group of factors.

Differentiation of primordia into normal fronds versus turions between the 3rd and 7th days of exposures showed distinct bell-shaped response of T% as a function of the applied Cd concentration (Fig. 2). This pattern is very similar to that reported by Smart and Trewavas (1983): they found that turion formation induced by ABA treatments was always accompanied by decreasing rate of frond production and after reaching maximum T% it decreased in parallel with the declining meristematic activity. Srivastava and Jaiswal (1989) and Susplugas et al. (2000) also observed a decrease in vegetative growth when turion formation had started as a result of Cd and chromate stress, respectively.

Although the regulating factors of Cd-induced turion formation were not assessed directly in our study we suggest at least two mechanisms for explanation for formation of turions under Cd stress as based on former reports:

i) Induction of turion formation by Cd might be attributed to its interference with mineral nutrition especially to imbalanced uptake of phosphate (Srivastava and Jaiswal 1989), a well described factor triggering turion formation (Appenroth 2002). Cd is known to inhibit phosphate nutrition of plants (Das et al. 1997) and in the rapidly growing duckweed plants P-deficiency might develop within short time. Appenroth (2002) observed rapid onset of turion formation (3 days) as a result of phosphate limitation which supports the former assumption.

ii) Similarly to other abiotic stress factors heavy metals influence the hormonal regulation of plants (Manara 2012). Enhanced synthesis of stress-related hormones such as ABA, ethylene and salicylic acid and decreased concentration of cytokinins might promote senescence of plants. Internal level of ABA and its relative concentration to cytokinins were proved to be directly linked to turion formation of *S. polyrhiza* by e.g. Smart and Trewavas (1983), Chaolupková and Smart (1994) and Smart et al. (1995).

Further efforts are needed to reveal which of the above mechanisms or perhaps a third one is responsible for alteration of primordium developmental pathway in response to Cd stress. Latest transcriptome analyses on both active *S. polyrhiza* fronds and turions published by Wang et al. (2014) revealed that ABA-responsive element binding factors, ethylene-responsive element binding factors, heat-shock transcription factors, and WRKY transcription factors –which also regulate plants' stress defense – play role in switch from normal to turion mode of meristems.

Based on our results it could be concluded that turion formation of *S. polyrhiza* should have been taken into consideration when this species is used in basic and applied research. Despite the widespread application of giant duckweed in ecotoxicology and plant physiology, turion formation as a response to various toxicants is reported scarcely. Our results indicate that the switch to turion mode of meristems can occur within the time period of frequently applied growth inhibition tests. Thus, the onset of turion formation may provide important additional information on special physiological effects of a given toxicant.

Another interesting aspect of turion formation might emerge when potential use of duckweeds is discussed as tools for phytoremediation. Such techniques apply plants rapidly increasing their biomass and exhibiting a relatively high affinity to absorb toxicants. As some of these toxicants seem to induce or at least enhance turion production, this mechanism might significantly reduce the expected growth rates of the applied species.

Acknowledgements

This work was supported by TÁMOP-4.2.2.B-10/1 and TÁMOP-4.2.3-12/1/KONV-2012-0048 projects. Anna Hepp is grateful for scholarship supported by the European Union and the State of Hungary, co-financed by the European Social Fund in the framework of TÁMOP 4.2.4. A/2-11-1-2012-0001 'National Excellence Program'.

References

Abràmoff MD, Magalhães PJ, Ram SJ (2004) Image processing with ImageJ. Biophotonics Int 11:36-42.

Appenroth K-J (2002) Co-action of temperature and phosphate in inducing turion formation in *Spirodela polyrhiza* (Great duckweed). Plant Cell Environ 25:1079-1085.

Chaloupková K, Smart CC (1994) The abscisic acid induction of a novel peroxidase is antagonized by cytokinin in *Spirodela polyrrhiza* L. Plant Physiol 105:497-507.

Cheng JJ, Stomp AM (2009) Growing duckweed to recover nutrients from wastewaters and for production of fuel ethanol and animal feed. Clean: Soil, Air, Water 37:17-26.

Das P, Samantaray S, Rout GR (1997) Studies on cadmium toxicity in plants: a review. Environ Pollut 98:29-36.

Environment Canada (2007) Biological Test Method - Test for measuring the inhibition of growth using the freshwater macrophyte Lemna minor. Environmental Protection Service, Report EPS 1/RM/37, 2nd ed. Method Development and Applications Section, Environmental Technology Centre, Environment Canada, Ottawa. 112 p.

Gaur JP, Noraho N, Chauhan YS (1994) Relationship between heavy metal accumulation and toxicity in *Spirodela polyrhiza* (L.) Schleid. and *Azolla pinnata* R. Br. Aquat Bot 183-192.

Hammer Ø, Harper DAT, Ryan PD (2001) PAST: Paleontological Statistics Software Package for Education and Data Analysis. Palaeontologia Electronica 4:9. URL: http://palaeo-electronica.org/2001_1/past/issue1_01.htm.

Jacobs DL (1947) An ecological life-history of *Spirodela polyrhiza* (greater duckweed) with emphasis on the turion phase. Ecol Monogr 17:437-469.

Manara A (2012) Plant responses to heavy metal toxicity. In Furini A, ed., Plants and Heavy Metals. Springer Briefs in Biometals. Springer, New York, 27-53.

Naumann B, Eberius M, Appenroth K-J (2007) Growth rate based dose-response relationships and EC-values of ten heavy metals using the duckweed growth inhibition test (ISO 20079) with *Lemna minor* L. clone St. J Plant Physiol 164:1656-1664.

Oláh V, Tóth GD, Szöll si E, Kiss T (2008) Comparative study on sensitivity

of different physiological properties of *Spirodela polyrrhiza* (L.) Schleiden to Cr (VI) treatments. Acta Biol Szeged 52:181-182.

Smart CC, Fleming AJ, Chaloupková K, Hanke DE (1995) The physiological role of abscisic acid in eliciting turion morphogenesis. Plant Physiol 108:623-632.

Smart CC, Trewavas AJ (1983) Abscisic-acid-induced turion formation in *Spirodela polyrrhiza* L. I. Production and development of the turion. Plant Cell Environ 6:507-514.

Srivastava A, Jaiswal VS (1989) Effect of cadmium on turion formation and germination of *Spirodela polyrrhiza* L. J Plant Physiol 134:385-387.

Susplugas S, Srivastava A, Strasser RJ (2000) Changes in the photosynthetic activities during several stages of vegetative growth of *Spirodela polyrhiza*: Effect of chromate. J Plant Physiol 157:503-512.

Xyländer M, Augsten H, Appenroth K-J (1993) Influence of nickel on the life cycle of the duckweed *Spirodela polyrhiza* (L.) Schleiden. J Plant Physiol 142:208-213.

Wang W, Wu Y, Messing J (2014) RNA-Seq transcriptome analysis of *Spirodela* dormancy without reproduction. BMC Genomics 15:60.

Volume 58(2):109-113, 2014
Acta Biologica Szegediensis
http://www2.sci.u-szeged.hu/ABS

ARTICLE

Morphological and physiological behavior in soybean (*Glycine max*) genotypes to drought stress implemented at pre- and post-anthesis stages

Nesa Sepanlo, Reza Talebi*, Asad Rokhzadi, Hayedeh Mohammadi

Department of Agronomy and Plant Breeding, College of Agriculture, Sanandaj Branch, Islamic Azad University, Sanandaj, Iran

ABSTRACT In order to evaluate the morphological and physiological responses of soybean genotypes to water deficit, a field experiment with 3 different soybean genotypes at three different irrigation regimes was carried out. Plants were grown either under optimum condition (irrigated), drought stress implemented before the flowering (pre-anthesis) and pod-filling stage (post-anthesis). Seed yield and measured morphological characters, except for number of seeds per plant and seed protein content, decreased from normal irrigation regime to water deficit stress in both flowering and pod filling growing stages. Leaf relative water content (RWC) was significantly decreased in all genotypes by water deficit at both growing stages, as well as both stressed environments had progressive fall in chemical osmolytes and chlorophyll content. With the present results, it can be concluded that drought stress retards the growth and metabolic activity of soybean genotypes. These parameters showed considerable variability under drought stress at different growth stages in soybean. **Acta Biol Szeged 58(2):109-113 (2014)**

KEY WORDS

Soybean
drought stress
morphology
chlorophyll
soluble sugar

Plants are subjected to several harsh environmental stresses that adversely affect their growth, metabolism, and yield. Drought is a meteorological term and defined as a period without sufficient rainfall for crop growth and productivity. This limitation for water supply in agriculture is likely to increase in the future due to growth of population and economical sectors other than agriculture (Araus 2004). Soybean is considered a species sensitive to several abiotic stresses (Van Heerden and Krüger 2000), when compared with other tropical legumes, such as *Vigna unguiculata* and *Phaseolus vulgaris* (Roy-Macauley et al. 1992; Silveira et al. 2003), as well as others species as *Gossypium hirsutum*, *Sorghum bicolor* (Younis et al. 2000) and chickpea (Talebi et al. 2013). Drought stress is the most important limiting factor at the initial phase of plant growth and establishment (Jaleel et al. 2009). Soybean is particularly sensitive to the lack of moisture during the blooming process (growth stages R1 and R2) and during the legume and seed growing processes (growth stages R3 – R6) (Doss et al. 1974; Sionit et al. 1987). Mederski et al. (1973) claim that water stress during the blooming process (growth stages R1 and R2) and legume growing process (growth stages R3 and R4) was noticed as a factor responsible for a flower and legume abortion, however, the seed size was reduced by the stress during the seed growing process (growth stages R5 and R6) (Krivosudská and Filová 2013). The responses of different crops to the decrease of water potential caused by drought may vary considerably among species (Save et al. 1995). In most of the crops, yield losses might be the result of decreasing in water supply during the vegetative phase, due to drought during reproductive development or due to terminal drought at the end of the crop cycle (Serraj et al. 2004). In term of morphological responses to drought stress, the remarkable reduction in growth, dry mater and harvestable yield in a number of plant species were recorded, but the tolerance of species to this menace varies remarkably (Serraj et al. 2004; Talebi et al. 2013). Various physiological responses of plants to drought with their tolerance mechanisms were reported in different crops (Dhanda et al. 2004; Serraj et al. 2004; Benjamin and Nielsen 2006; Kalefetoğlu and Ekmekci 2009; Praba et al. 2009; Talebi et al. 2013). Soybean is planted over a wide range of conditions, but information related to morphological and physiological changes in the plant organs under drought stress is lacking. The aim of the present work was to examine the effects of drought on several morphological and physiological parameters of soybean under different water regimes.

Materials and Methods

Three soybean (*Glycine max* cv. Sambaiba) accessions (Habit, L17 and M7) were chosen for the study based on their reputed differences in growth habit and yield performance. Experiments were conducted at the experimental field of Islamic

Accepted Nov 5, 2014
*Corresponding author. E-mail: srtalebi@yahoo.com

Azad University of Sanandaj (35°10'N, 46°59E; 1393 m above sea level), in Kurdistan province (northwest of Iran) in 2012. Some of the soil physicochemical characteristics were: sand 25.4%, silt 32.6%, clay 42%, pH 7.6, organic carbon 0.62%, electrical conductivity 0.50 dS m–1, and available P and K 9.3 and 340 mg L^{-1}, respectively. The experiment was laid out in a split-plot arrangement with randomized complete block design and three replications. Three different irrigation regimes including irrigation every 4th day (a1), irrigation every 4th day with withholding irrigation at flowering stage for 15 days (a2) and irrigation every 4th day with withholding irrigation at pod filling stage for 15 days (a3) were compared in main plots. In well-watered control experiment, water level at field capacity (between 80 to 90%) was maintained throughout the experiment. For drought treatments, water was withheld for 15 days until the water level at field capacity decreased to 50%. Three different soybean genotypes were assigned in sub-plots. Each sub-plot contained three sowing rows 3 m in length. Inter- and intra-row spacing was 50 and 15 cm, respectively.

Six plants were randomly chosen from each plot to measure the number of seeds per plant, number of seeds per pod, plant height, 100-seeds weight, biological yield and grain yield (g m^{-2}) was measured by harvesting each plot at crop maturity. Leaf relative water content (RWC) was determined according to Turner (1981), based on the following equation:

$$RWC = (FM - DM) / (SM - DM) \times 100$$

where FM is leaf fresh mass, DM is dry mass of leaves after drying at 85 °C for 3 days, and SM is the turgid mass of leaves after soaking in water for 4 h at room temperature (approximately 20 °C). Half of the third (from the top) fully expanded leaf was used. Samples for chlorophyll and carotenoid determination were taken from soybean leaves using a 0.8 cm diameter cork borer, weighted quickly in pre-weighted clean glass vials and 5 ml of 80% acetone was added to these samples. The leaf material was bleached and decanted off. The optical density was read at $\lambda = 663$, 646 and 470 nm using 80% acetone as a blank by a spectrophotometer (Spectronic Genesys-5, Milton Roy). Content of chlorophyll a, chlorophyll b and carotenoids (μg g^{-1}) was calculated according to Lichtenthaler and Wellburn (1983) using the following formulae:

$$\text{Chlorophyll } a = 12.21\ OD_{663} - 2.81\ OD_{646};$$

$$\text{Chlorophyll } b = 20.13\ OD_{646} - 5.03\ OD_{663};$$

$$\text{Carotenoids} = (1000\ OD_{470} - 3.27\ \text{Chlorophyll } a - 104\ \text{Chlorophyll } b) / 229$$

Soluble sugars were determined based on the method of phenol-sulfuric acid (Dubois et al. 1956). 0.5 g fresh weight of soybean leaves was homogenized with deionized water, extract was filtered and treated with 5% phenol and 98% sulfuric acid, mixture remained for 1 h and then absorbance at 485 nm was determined by spectrophotometer. Contents of soluble sugar were expressed as mg g^{-1} FW.

Leaf soluble proteins were extracted from 2 g leaf dry weight of each sample into 5 ml Tris-HCl buffer (pH=8.0) containing 26.8 ml 0.2N HCl, 17.2% sucrose, 1% ascorbic acid and was then centrifuged. 1 ml of reagent D was added into 0.05 ml of the resulting solution and kept at room temperature. Then, 3 ml of reagent E was added and the sample was kept in Bain-marie at 50 °C. The absorbance was measured spectrophotometrically at 625 nm. Protein was calculated based on μM g^{-1} FW. For seed oil content, crude oils were extracted with n-hexane in a Soxhiet apparatus for 12 hs. After drying the solution with anhydrous sodium sulphate, solvent was removed by vacuum distillation at 30 °C. Oil percentages were determined by weight difference. Seed protein content was determined by the Kjeldahl method and it was converted to protein content by using the conversion factor 6.25 (AOAC 1980).

All collected data were subjected to analysis of variance operations and means of treatments were compared with the least significant difference (LSD) test at $P \leq 0.05$. The statistical calculations were performed with MSTAT-C software version 2.10.

Results

Seed yield and yield components

Drought stress had significant effects on seed yield and morphological traits. Seed yield and measured morphological characters, except for number of seeds per plant and seed protein content, decreased from normal irrigation regime to water deficit stress in both flowering and pod filling growing stages (Table 1). Interestingly, seed oil content increased significantly by water deficit stress. Between the genotypes, Habit showed higher seed yield and oil content (Table 1). The interactive effects of irrigation regimes and genotypes for seed yield and morphological characters are presented in Table 2. Seed yield and most of the measured traits were significantly decreased in stress treatments compared to normal irrigation environment (Table 2). Habit showed higher seed yield and 100-seed weight in stressed environments compared to other genotypes, while seed oil content in L17 and M7 was dramatically higher than in Habit (Table 2).

RWC and leaf biochemical characters

Leaf relative water content (RWC) was significantly decreased in all genotypes by water deficit at both growing stages as well as both stressed environments (a1 and a2) had progressive fall in chemical osmolytes and chlorophyll content (Table 3). Interactive effects of genotypes and irrigation regimes for RWC and leaf biochemical attributes showed less decrease in early flowering stress (a2), while when plants subjected to water stress at pod filling stage (a3) these characters significantly decreased and genotypes differed in response

Table 1. Main effects of irrigation regimes and genotypes on seed yield and yield components traits. Data are means from three replications. Means followed by same letters in a group of a column are not significantly different at $P \leq 0.05$ according to LSD test.

Treatment	NPP	NSP	TSW	Y (t/ha)	BY (t/ha)	PH	Seed oil (%)	Seed protein (%)
Normal irrigation (a1)	127.7±11.22 a	2.4±0.41 a	13.1±1.12 a	6.23±2.14 a	15.05±3.78 a	90.2±7.49 a	15.9±0.49 b	34.2±0.77 a
Water stress at flowering (a2)	73.3±8.63 b	2.1±0.28 a	11.7±0.58 b	2.26±0.98 b	6.42±2.18 b	63.5±7.91 b	16.8±0.78 b	34.2±0.33 a
Water stress at pod filling (a3)	80.9±9.11 b	2.5±0.29 a	11.3±0.47 b	2.67±1.08 b	7.46±2.58 b	91.7±8.17 a	19.04±1.14 a	28.9±0.79 a
Habit	110.9±9.01 a	2.2±0.11 a	13.4±0.98 a	5.38±0.34 a	11.43±1.07 a	60.6±4.78 b	15.7±0.30 b	33.03±0.77 a
L17	87.2±7.14 b	2.3±0.09 a	10.3±0.68 b	2.93±0.45 b	8.73±0.91 b	94.7±7.11 a	17.4±0.24 a	31.70±0.46 a
M7	83.8±6.89 b	2.4±0.07 a	12.5±0.49 a	2.86±0.51 b	8.81±1.08 b	90.1±8.79 a	18.7±0.41a	32.80±0.24 a

NPP=Number of pods/plant; NSP=Number of seeds/plant; TSW=100-seed weight; Y=seed yield (t/ha); BY=Biological yield (t/ha); PH=Plant height (cm)

Table 2. Interaction effect of irrigation regimes × genotype on seed yield and morphological characteristics. Data are means from three replications. Means in each column followed by same letters are not significantly different at $P \leq 0.05$ according to LSD test.

Treatment	Genotype	NPP	NSP	TSW	Y
	Habit	129.5±10.11 a	2.35±0.19 a	13.96±0.97 a	10330±478.9 a
Normal irrigation (a1)	L17	149.6±9.77 a	2.47±0.17 a	11.27±1.08 ab	5036.6±325.8 b
	M7	103.7±11.07 ab	2.44±0.10 a	14.01±1.45 a	3340±279.58 c
	Habit	94.5±9.14 b	2.06±0.08 a	13.62±1.11 a	2793.4±215.21 c
Water stress at flowering (a2)	L17	51.4±8.11 c	2.02±0.09 a	9.74±0.54 b	1346.7±425.14 c
	M7	74.2±7.19 c	2.19±0.11 a	11.77±1.57 a	2636.6±478.14 c
	Habit	108.56±10.11 ab	2.29±0.12 a	12.54±1.14 a	3010±521.14 c
Water stress at pod filling (a3)	L17	60.56±4.01 c	2.53±0.19 a	9.75±0.78 b	2400±615.25 c
	M7	73.5±5.14 c	2.55±0.21 a	11.6±1.86 ab	2603±397.78 c

Treatment	Genotype	BY	PH	Seed oil (%)	Seed protein (%)
	Habit	19330±2478.15 a	46.5±28.37 d	13.86±2.47 b	36±1.28 a
Normal irrigation (a1)	L17	13476.6±1987.45 b	115.66±29.14 a	16.43±0.98 ab	34.24±2.12 a
	M7	12363.3±2135.17 b	108.99±17.15 a	17.56±1.65 a	32.35±1.48 a
	Habit	7000±2745.25 c	56.44±8.14 cd	16.10±1.73 ab	33.87±1.38 a
Water stress at flowering (a2)	L17	5316.6±1798.54 c	69.88±5.18 c	15.90±1.98 ab	33.24±1.47 a
	M7	6953.3±1796.35 c	64.22±6.16 c	18.50±1.11 a	35.52±1.65 a
	Habit	7880±2014.34 c	79.44±8.19 bc	17.21±1.36 a	25.24±1.29 b
Water stress at pod filling (a3)	L17	7400±1978.24 c	98.66 ±10.14ab	20±0.98 a	26.36±1.37 b
	M7	7101.3±2078.39 c	97±14.77 ab	19.91±0.79 a	30.38±2.79 ab

NPP=Number of pods/plant; NSP=Number of seeds/plant; TSW=100-seed weight; Y=seed yield (t/ha); BY=Biological yield (t/ha); PH=Plant height (cm)

to drought stress (Table 4). It seems that, M7 is able to keep or accumulate more RWC and other biochemical osmolytes when compared to Habit and L17, while Habit showed higher seed yield and other yield components than the other two genotypes. The yield reductions in M7 and L17 under water deficit stress are less than that in Habit. The role of RWC and osmolytes accumulation in tolerance to water deficit in L17 and M7 is noticeable.

Discussion

Irrigation regimes and genotypes both differed significantly for all morphological characters, except for number of seeds per plant and seed protein content, that can be considered useful for screening soybean germplasm under water stress. Compared with control conditions (a1), progressive water stress decreased number of pods per plant, seed yield, biological yield and plant height. The reduction in the number of pods and seed size in the stress treatments appears through the reduction of dry matter production (Oya et al. 2004). The reduction in relative water content (RWC) in both stress environments (a1 and a2) was provoked by the water losses in soil, because during the photosynthesis water loss occurs through the stomatal mechanism and the water assimilation rate is negatively affected during drought stress (Verslues et al. 2006; Lobato et al. 2008). The reduction in the total soluble proteins detected in the plants under water stress is

Table 3. Main effects of irrigation regimes and genotypes on relative water content (RWC) and some leaf biochemical characteristics. Data are means from three replications. Means followed by same letters in a group of a column are not significantly different at $P \leq 0.05$ according to LSD test.

Treatment	RWC	Soluble sugar	Soluble protein	*Chl a*	*Chl b*	Carotenoid
Normal irrigation (a1)	0.68±0.6 a	0.072±0.07 ab	0.061±0.04 a	13.2±1.12 a	16±1.37 a	1.6±0.14 a
Water stress at flowering (a2)	0.64±0.5 a	0.080±0.06 a	0.053±0.02 b	9.47±0.79 b	7.31±2.79 b	1.6±0.27 a
Water stress at pod filling (a3)	0.55±0.3 b	0.062±0.05 b	0.041±0.04 c	7.81±1.09 b	16.81±3.97 a	0.6±0.71 b
Habit	0.64±0.7 a	0.061±0.05 b	0.059±0.07 a	9.3±0.63 a	12.3± 0.77 b	1.2±0.01 a
L17	0.62±0.7 a	0.072±0.04 a	0.062±0.08 a	10.8±0.99 a	12.6 ±0.71 b	1.2±0.01 a
M7	0.62±0.6 a	0.063±0.04 a	0.042±0.09 b	10.3±0.83 a	15.2±1.01 a	1.3 ±0.01a

RWC=Relative water content; *Chla*=Chlorophyll a; *Chlb*=Chlorophyll b

Table 4. Interaction effect of irrigation regimes × genotype on physiological parameters. Data are means from three replications. Means in each column followed by same letters are not significantly different at $P \leq 0.05$ according to LSD test.

Treatment	Genotype	RWC (%)	Soluble sugar	Soluble protein	*Chl a*	*Chl b*	*Carotenoid*
	Habit	0.63±0.11 a	0.07±0.01 a	0.063±0.009 a	10.71±1.13 b	13.65±0.54 b	1.47±0.39 bc
Normal irrigation (a1)	L17	0.43±0.08 b	0.07±0.02 a	0.063±0.007 a	13.35±0.45 a	15.24±1.21 a	1.38±0.27 bc
	M7	0.51±0.05 a	0.06±0.02 a	0.057±0.005 a	15.50±1.88a	19.35±2.89 a	1.57±0.49 bc
	Habit	0.50±0.03 a	0.07±0.01 a	0.047 ±0.006ab	10.66 ±1.15b	7.62±1.28 c	0.73±0.47 c
Water stress at flowering (a2)	L17	0.43±0.04 b	0.08±0.03 a	0.053±0.005 a	9.77±1.34 b	7.80±1.24 c	0.65±0.42 c
	M7	0.41±0.04 b	0.08±0.02 a	0.060 a	7.77±1.01 b	6.48±2.64 c	0.77±0.38 c
	Habit	0.47±0.04 ab	0.06±0.02 a	0.040±0.003 b	6.51±1.12 c	16.04 ±1.25a	2.24±0.66 b
Water stress at pod filling (a3)	L17	0.47±0.03 ab	0.06 ±0.01a	0.037±0.006 b	9.28±0.77 b	14.69±0.57 a	3.78±0.59 a
	M7	0.51±0.01 a	0.07±0.01 a	0.047±0.005ab	7.56±0.88 bc	19.72±3.24a	1.39±0.77 bc

RWC=Relative water content; *Chla*=Chlorophyll a; *Chlb*=Chlorophyll b

due to probable increase of the protease enzyme activities, in which these protease enzymes promote the breakdown of the proteins and consequently decrease the protein amount present in the plant under abiotic stress conditions (Debouba et al. 2006; Lobato et al. 2008; Jaleel et al. 2009). In inadequate conditions to the plant the pathway of protein breakdown is active, because the plant uses the proteins for the synthesis of nitrogen compounds as amino acids that might be auxiliary for the plant osmotic adjustment (Sankar et al. 2007). In conclusion, alternative and significant variation was found for morphological and physiological characteristics in tested soybeans under water deficit environments, which underlines the susceptibility of this crop to drought stress. Based on the present results it can be concluded that drought stress retards the growth and metabolic activity of soybean genotypes. These parameters showed considerable variability under drought stress at different growth stages in soybean. This study may help to understand some adaptive mechanisms developed by soybean genotypes and contribute to identify useful traits for soybean breeding programmes.

References

AOAC (Association of Official Analytical Chemists) (1980) Official Methods of Analysis of the Association of Official Analytical Chemists. Horwitz, W. (Ed.). 13th Ed. Washington D.C. USA.

Araus JL (2004) The problem of sustainable water use in the Mediterranean and research requirements for agriculture. Annal Appl Biol 144:259-272.

Benjamin JG, Nielsen DC (2006) Water deficit effects on root distribution of soybean, field pea and chickpea. Field Crop Res 97:248-253.

Debouba M, Gouia H, Suzuki A, Ghorbel MH (2006) NaCl stress effects on enzymes involved in nitrogen assimilation pathway in tomato "*Lycopersicon esculentum*" seedlings. J Plant Physiol 163:1247-1258.

Dhanda SS, Sethi GS, Behl RK (2004) Indices of drought tolerance in wheat genotypes at early stages of plant growth. J Agric Crop Sci 190:6-12.

Doss BD, Pearson RW, Rogers HT (1974) Effect of soil water stress at various growth stages on soybean yield. Agron J 66:297-299.

Dubois M, Gilles KA, Hamilton JK, Rebers PA, Smith F (1956) Colorimetric method for determination of sugars and related substances. Anal Chem 28:350-356.

Jaleel CA, Manivannan P, Wahid A, Farooq M, Somasundaram R, Panneerselvam R (2009) Drought stress in plants: a review on morphological characteristics and pigments composition. Int J Agric Biol 11:100-105.

Kalefetoğlu MT, Ekmekci Y (2009) Alterations in photochemical and physiological activities of chickpea (*Cicer arietinum* L.) cultivars under drought stress. J Agron Crop Sci 195:335-346.

Krivosudská E, Filová A (2013) Evaluation of selected soybean genotypes (*Glycine max* L.) by physiological responses during water deficit. J Cent Eur Agric 14:691-706.

Lichtenthaler HK, Wellburn AR (1983) Determinations of total carotenoids and chlorophylls a and b of leaf extracts in different solvents. Biochem Soc Trans 11:591-592.

Lobato AKS, Costa RCL, Oliveira Neto CF, Santos Filho BG, Cruz FJR, Freitas JMN, Cordeiro FC (2008) Morphological changes in soybean

under progressive water stress. Int J Bot 4:231-235.

Mederski HJ, Jeffers DL, Peters DB (1973) Water and water relations. In: Caldwell BE, ed. Soybeans: Improvement, production, and uses. American Society of Agronomy, Madison, WI, pp. 239-266.

Oya T, Nepomuceno AL, Neumaier N, Farias JRB, Tobita S, Ito O (2004) Drought tolerance characteristics of Brazilian soybean cultivars – evaluation and characterization of drought tolerance of various Brazilian soybean cultivars in the field. Plant Prod Sci 7:129-137.

Praba ML, Cairns JE, Babu RC, Lafitte HR (2009) Identification of physiological traits underlying cultivar differences in drought tolerance in rice and wheat. J Agron Crop Sci 195:30-46.

Roy-Macauley H, Zuily-Fodil Y, Kidric M, Pham Thi AT, Silva JV (1992) Effects of drought stress on proteolytic activities in *Phaseolus* and *Vigna* leaves from sensitive and resistant plants. Physiol Plant 85:90-96.

Sankar B, Jaleel CA, Manivannan P, Kishorekumar A, Somasundaram R, Panneerselvam R (2007) Drought-induced biochemical modifications and proline metabolism in *Abelmoschus esculentus* (L.) Moench. Acta Bot Croat 66:43-56.

Save R, Biel C, Domingo R, Ruiz-Sanchez MC, Torrecillas A (1995) Some physiological and morphological characteristics of citrus plants for drought resistance. Plant Sci 110:167-172.

Serraj R, Krishnamurthy L, Kashiwagi J , Kumar J, Chandra S, Crouch JH (2004) Variation in root traits of chickpea (*Cicer arietinum* L.) grown under terminal drought. Field Crop Res 88:115-127.

Silveira JAG, Costa RCL, Viegas RA, Oliveira JTA, Figueiredo MVB (2003) N-Compound accumulation and carbohydrate shortage on N_2 fixation in drought-stressed and rewatered cowpea plants. Span J Agric Res 1:65-75.

Sionit N, Strain BR, Flint EP (1987) Interaction of temperature and CO_2 enrichment on soybean: Photosynthesis and seed yield. Can J Plant Sci 67:629-636.

Talebi R, Ensafi MH, Baghebani N, Karami E, Mohammadi KH (2013) Physiological responses of chickpea (*Cicer arietinum*) genotypes to drought stress. Environ Exp Biol 11:9-15.

Turner NC (1981) Techniques and experimental approaches for the measurement of plant water status. Plant Soil 58:339-366.

Van Heerden PDR, Krüger GHJ (2000) Photosynthetic limitation in soybean during cold stress. South Afr J Sci 96:201-206.

Verslues PE, Agarwal M, Katiyar-Agarwal S, Zhu J, Zhu JK (2006) Methods and concepts in quantifying resistance to drought, salt and freezing, abiotic stresses that affect plant water status. Plant J 45:523-539.

Younis ME, El-Shahaby OA, Abo-Hamed SA, Ibrahim AH (2000) Effects of water stress on growth, pigments and $^{14}CO_2$ assimilation in three sorghum cultivars. J Agron Crop Sci 185:73-82.

Volume 58(2):115-122, 2014
Acta Biologica Szegediensis
http://www2.sci.u-szeged.hu/ABS

ARTICLE

Accumulation of water stress-responsive class-III type of boiling stable peroxidases (BsPOD) in different cultivars of wheat (*Triticum aestivum*)

Arun Dev Sharma*, Nadia Dhuria, Gurmeen Rakhra, Shubhneet Mamik

PG Department of Biotechnology, Lyallpur Khalsa College, Jallandhar-144001, Punjab, India

ABSTRACT Drought is one of the most important abiotic stress that affects plant growth and productivity. Class-III Peroxidases (PODs) are known to maintain oxidative stress induced-ROS at sub-lethal levels in plants under abiotic stress conditions, but, studies documenting how drought regulates boiling stable class-III PODs are still a matter of conjecture. In this study, changes in total protein content (TPC), water content (WC), H_2O_2, malondialdehyde (MDA) and ROS scavenging class-III boiling stable POD were studied in the shoots of seven cultivars of wheat at different stages of drought treatment (3 days: D3, 5 days: D5 and 7 days: D7) followed by recovery from stress (post stress: PS). Simultaneous analysis of H_2O_2, MDA contents and activities of ROS-scavenging class-III boiling stable POD (BsPOD) enzymes gave an integrative view of physiological state and detoxifying potential under conditions of sensitivity and tolerance. Drought stress increased TPC and decreased WC in all the cultivars of wheat. H_2O_2 content decreased considerably under various stage of drought stress in a genotype dependent manner. As a result, amount of MDA, a product of lipid peroxidation, was also less in all the cultivars at all stress durations. During initial stress conditions (D3), a marked increase in BsPOD activity was observed in cultivars PBW343, PBW550, PBW175, DBW17 and HD2967. An especially high increase (55-fold) was noticed in PBW175 accompanied by enhanced expression of boiling stable POD isoenzyme(s) suggesting that this cultivar has more efficient mechanisms to scavenge ROS species. In addition, this cultivar has also maintained higher BsPOD activity when the stress duration increased from D3 to D7. The other cultivars having lowest enzyme activities are mentioned as cultivars sensitive to drought stress. Compared to stress, significantly higher soluble protein content accompanied by BsPOD activity was observed after the exposure to recovery conditions in the majority of cultivars. Based on these results, the possible role of BsPOD activity and isoenzyme(s) to perform biological antioxidative reactions to combat drought-induced oxidative stress was discussed.
Acta Biol Szeged 58(2):115-122 (2014)

KEY WORDS

Boiling stable proteins
Class-III Peroxidase
isoenzymes
wheat

In nature, plants frequently encounter environmental conditions that may include stresses such as biotic and abiotic conditions, which drastically affects crop both in terms of quality and quantity (Chaves and Oliveira 2004; Kotak et al. 2007). Drought is one of the environmental stresses, which is the most significant factor restricting plant growth and crop productivity in the majority of agricultural fields of the world (Tas and Tas 2007). Compelling evidences have indicated that drought is associated with oxidative stress in plant cells and can cause the generation of reactive oxygen species (ROS) such as H_2O_2 (hydrogen peroxide), $O_2^{\cdot-}$ (superoxide) and OH (hydroxyl) radicals in a tissue dependent manner (Gao et al. 2008). Among them, H_2O_2 seems best suited to play the role of a signaling molecule due to its higher stability and longer half-life (Hung et al. 2005). If H_2O_2 serves as a stress signal, the fluctuation of the H_2O_2 level in plants should spatially and temporally reflect changes in the environment. Under normal conditions, ROS are inevitable generating from the essential aerobic metabolism including chloroplastic and mitochondrial processes, per-oxidation of membrane lipids and plasma membrane linked electron transport systems (Bi et al. 2009). Besides dangerous cytotoxic molecules, ROS have been shown to act as second messengers involved in the various stress signal transduction pathways, which control and regulate such biological processes as programmed cell death and hormone signaling (Graper and Dolan 2006). However, excessive ROS synthesis can cause an extensive peroxidation and de-esterification of membrane lipids as well as damages plants by oxidizing photosynthetic pigments, membrane lipids, proteins and nucleic acids, if the plant is not efficient in scavenging these molecules (Mittler 2002; Baruah et al. 2009). Besides this, increase and accumulation of ROS could cause lipid peroxidation leading to cell death. Malondialdehyde (MDA), which is the most abundant aldehydic lipid breakdown product, is considered as a suitable

Accepted Oct 29, 2014
*Corresponding author. E-mail: arundevsharma47@gmail.com

marker for membrane lipid peroxidation (Goel and Sheoran 2003). A decrease in membrane stability reflects the extent of lipid peroxidation caused by ROS. Oxidative stress arises due to an imbalance between generation and elimination of ROS, which can lead to changes in membrane permeability and membrane leakage. All these observations suggest the dual role of ROS in plant biology as dangerous molecules and key regulators of growth and defence pathways. Plants have ability to sense ROS and re-programme their gene expression in response to changing conditions of their environment. Microarray studies involving mutants and antisense lines that lack ROS-scavenging enzymes revealed that ROS act as signaling molecules involved in the expression of a large number of genes and biological processes (Miller et al. 2008). In order to combat ROS, plants have the detoxification mechanism that includes both enzymatic and non-enzymatic antioxidant components (Scandalios 2005). Enzymatic antioxidants systems involve the activity of superoxide dismutase (SOD), peroxidase (POD), catalase (CAT), ascorbate peroxidase (APX), glutathione reductase (GR) and dehydroascorbate reductase (DHAR) (Gill and Tuteja 2010). Non-enzymatic components includes ascorbate (AsA), glutathione (GSH), flavonoids, phenolic compounds, alkaloids, tocopherol and carotenoids, which act as antioxidant buffers (Mittler 2002; Foyer and Noctor 2005; Gratao et al. 2005). Out of the antioxidative enzymes involved in mitigating the effect of oxidative stress, class-III peroxidases (PODs) are the major antioxidative enzymes grouped in a super-family utilizing guaiacol as electron donor. They are located in the cytosol, cell wall and involved in the decomposition of H_2O_2 through the oxidation of phenolic compounds. Generally, peroxidases (PODs/PRXs) are divided in three different classes. Class-I mainly includes ascorbate peroxidases and cytochrome C peroxidases (CcPs); class-II contains fungal manganese and lignin peroxidases, while class-III involves all the secretary plant peroxidases (PODs) (for review, see Cosio and Dunand 2009). Several key roles have been attributed to plant class-III PODs in response to biotic and abiotic stresses, such as the modification of cell wall via suberin polymerization, cross-linking of structural non-enzymatic proteins, and cleaving cell wall polysaccharides; they may affect leaf expansion, fruit growth, germination and nodulation (Cosio and Dunand 2009). They may have diverse roles possibly due to the large number of their isoforms (isoenzymes). The quantitative and qualitative changes in the expression of antioxidant enzymes are often related to the levels of resistance to water stress. Some studies indicated that activities of antioxidant enzymes are correlated with plant tolerance to abiotic stress (Ozkur et al. 2009; Wang et al. 2009).

Many water-stress inducible proteins (e.g. HSPs and LEAs) are highly hydrophilic and remain soluble even after boiling. Thereafter, they have been termed as "boiling soluble proteins" (BSPs) (Jacobsen and Shaw1989). Many proteins, which were detected in total protein extracts, are lost after boiling the extracts (Pelah et al.1995). Earlier research also indicated that hydrophilins represent less than 0.2% of the total protein of a given genome, however, it represents the most significant part of the proteome in regulating tolerance to abiotic stresses in plants (for review, see Battaglia et al. 2008). Hence, to better elucidate the role of these boiling soluble proteins (BSPs), it is a prerequisite to examine their expression not only under water stress, but also after boiling of extracts. Moreover, the role of class-III type boiling stable peroxidases (BsPODs) under drought treatment is not well documented. Therefore, in the present study, we have analyzed the effect of drought on the biochemical activity and isoenzyme expression profile of BsPODs along with H_2O_2 and MDA contents in the shoots of different wheat cultivars. Analysis of isoforms of BsPOD coupled with biochemical analysis will provide new insights into drought-induced oxidative stress. Wheat is one of the most important crops in arid and semi arid areas worldwide and it is sensitive to drought and temperature stress. In order to facilitate the detection of BSPs, heat stable (HS) fractions that resist coagulation upon heating at 100 °C were focused.

Material and Methods

Seed germination and growth conditions

Seeds of commercially relevant lines of seven wheat (*Triticum aestivum* L.) cultivars (PBW343, PBW621, PBW527, PBW550, PBW175, DBW17 and HD2967) (Table 1) were selected for experimental purposes. All the cultivars were obtained from PAU Ludhiana, Punjab, India. They were selected as all are locally grown and a comparison of their responses could give a better understanding of the susceptibility/tolerance to the different varieties to drought. Seeds were surface sterilized with 1% (w/v) mercuric chloride followed by 70% (v/v) ethanol (Sharma et al. 2006). Seeds were thoroughly rinsed with deionized water and imbibed for 6 h. After imbibitions, seeds were placed in petri plates containing sterile filter sheets, moistened with water. Then, the seeds were incubated at 25±1 °C in a seed germinator in darkness and allowed to grow for 6 days. To impart water stress, watering of plants was completely withheld for the test period when plants were 6 days old. Sampling was done on the 3rd (D3), 5th (D5) and 7th (D7) day to study response of plants to the length of drought. In all experiments, samplings were also done at zero day of drought, which was designated as control. To study the post-stress (PS) effect, after the 7th day of drought stress, plants were re-watered. Water content (WC) was measured after imposing stress treatments. Fresh weights (FW) were determined within 2 h after collection. Dry weights (DW) were obtained after oven drying the samples for 72 h at 70 °C. WC was calculated from the following equation:

WC = FW-DW/FW.

Extraction of Boiling Stable Proteins

Boiling stable proteins were extracted as described previously (Sharma et al. 2006; Sharma et al. 2012). Briefly, tissues were homogenized with chilled mortar and pestle in extraction buffer (50 mM Tris buffer, pH 7.0). Crude extracts were centrifuged at 10 000 g for 10 min. The total extract was boiled for 15 min in order to get boiling stable protein fractions. The total soluble protein content in the supernatant was determined according to Lowry et al. (1951) using BSA as a standard.

BsPOD activity analysis

The BsPOD activity was measured according to the method described in Sharma et al. (2013). The mixture contained 50 mM TRIS (pH 7.0), 10 mM guaiacol and 5 mM H_2O_2. To this mixture An aliquot of 120 µg of protein was added to this mixture adjusting the total volume to 1 ml. The increase in absorbance was measured at 470 nm at intervals of 30 s. The activity was calculated as per min per milligram of tetraguaiacol production by using the extinction coefficient for tetraguaiacol of 26/mM/cm.

Isoenzyme analysis of BsPODs

Boling stable proteins were extracted as described above. For in-gel activity analysis, the proteins (240 µg) were separated by a non-denaturing 12% polyacrylamide gel electrophoresis as described by Sambrook et al. (1989). When electrophoresis was complete, the gel was washed three times in 50 mM sodium acetate buffer (pH 5.0). Peroxidase activity was visualized by incubating the gel in 50 ml of a solution containing 50 mM sodium acetate buffer (pH 5.0), 330 µl of guaiacol (9 M) and 1.5 ml of 6.6% H_2O_2. The gel was incubated at room temperature in dark until reddish-brown bands appeared. The gel was washed in distilled water and used for further analysis. Relative abundance of isoenzymes was quantified by Ultraquant software 13.3.26 of gel documentation system (Omega Lum USA)

Estimation of hydrogen peroxide content

The H_2O_2 content was measured by the method described by Mamik and Sharma (2014). The reaction mixture contained 0.5 ml of Tris-HCl buffer pH 7.0, 0.5 ml of 0.1% trichloroacetic acid (TCA), 120 µg of protein, 2 ml of 1 M KI. After 1 h of reaction in dark, the absorbance was measured at 390 nm. The amount of hydrogen peroxide (µM/gFW) was calculated using a standard curve prepared with known concentrations of H_2O_2.

Statistical analysis

The plants were distributed over a completely randomized design, with 175 treatment combinations, forming a 7×5×5 factorial (7 genotypes, 5 watering regimes and 5 samplings) at vegetative and reproductive phases. Statview ANOVA program was used for statistical analysis of the data. Values were compared using one-way analysis of variance and student's *t*-test for differences between pairs of data if the ANOVA ($LSD_{0.05}$) revealed significance. Means were tested by LSD at P 0.05 level ($LSD_{0.05}$).

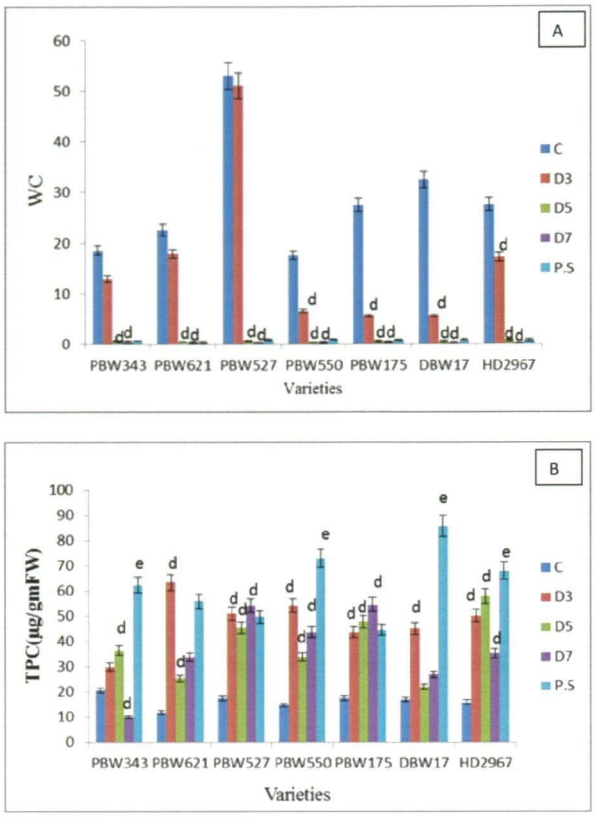

Figure 1. Effect of drought stress and recovery on WC (A), and TPC (B) in the shoots of different cultivars of *Triticum aestivum*. Data shown are averages ± SD (n=3). [d] represents significant difference with respect to control p≤0.5. [e] represents significant difference of PS relative to D7 p≤0.5.

Results and Discussion

Drought stress triggers the change of a wide variety of responses ranging from physiological to metabolic processes in plants. In the present study, effect of drought stress on BsPOD enzymes and other parameters were studied in seven different cultivars of wheat by imposing drought stress for 3 days (D3), 5 days (D5) and 7 days (D7) and followed by recovery from drought stress (PS).

Changes in the physiological parameters

As shown in Figure 1A, compared to the control (zero day), water content (WC) in all wheat cultivars showed a progres-

sive decrease as the intensity of stress increased from D3 to D7. However, only in PBW527, no substantial change in WC at D3 was observed. Most research has shown decreased WC in response to drought stress (Chakraborty and Pradhan 2012; Sanchez-Blanco et al. 2002; Chakraborty et al. 2002). Moreover, compared to D7, a notable increase (about 2- to 7-folds) in WC was observed following post stress recovery period (PS) in all cultivars, except PBW343 and PBW621.

The changes of total protein content (TPC) in the leaves of wheat cultivars treated with drought stress are shown in Figure 1B. Significantly increased TPCs were detected during the drought stress. Relative to the control, TPC increased significantly at all stages of drought in PBW621, PBW527, PBW550, PBW175 and HD2967. At the same time, in PBW343, a substantial decrease in TPC was observed at D7. Earlier studies reported that drought stress affects gene expression and protein synthesis (Lobato et al. 2008). Lee and Lee (2000) described elevated soluble protein content following water stress. As indicated by earlier studies, protein degradation under drought stress might be due to increased activity of proteases and catabolic enzymes or to fragmentation of proteins because of the toxic effects of ROS. These processes may result in reduced protein contents. Compared to D7, TPC increased considerably in cvs PBW343, PBW621, PBW550, DBW17 and HD2967 during the PS period.

Changes in MDA content

The drought-induced changes were further examined by measuring the accumulation of thiobarbituric acid (TBA)-reactive compounds, such as malondialdehyde (MDA). These compounds are by products of lipid peroxidation, a process resulting in the generation of ROS (Dhindsa et al. 1981). Lipid peroxidation in the cell membranes is said to be one of the most challenging and detrimental effect of water stress in the membranes of all cells exposed to various degree of stress (Thankamani et al. 2003). The degree of lipid peroxidation was measured in terms of MDA content which is one of the determinants indicating the severity of stress experienced by any plant. Compared to the control, significantly higher concentrations of TBA-reactive compounds were observed in drought stressed leaves of HD2967 and DBW17 at all stages (D3, D5, D7) of drought (Fig. 2A). In PBW621 and PBW527, the maximum MDA level was observed at D7. In PBW343, a linear increase of the MDA values were observed as stress duration raised from D3 to D5. Jiang and Huang (2001) reported increased MDA accumulation and reduced WC and photosynthetic pigment content under prolonged drought. Terzi and Kadioglu (2006) reported similar transient changes in MDA contents under drought stress. Earlier, Tatar and Gevrek (2008) also reported that MDA content increases in wheat with the increasing degree of stress. Tian et al (2012) also reported increased MDA content in the leaves and petals of Marigold plant in response to drought stress. Notably, in

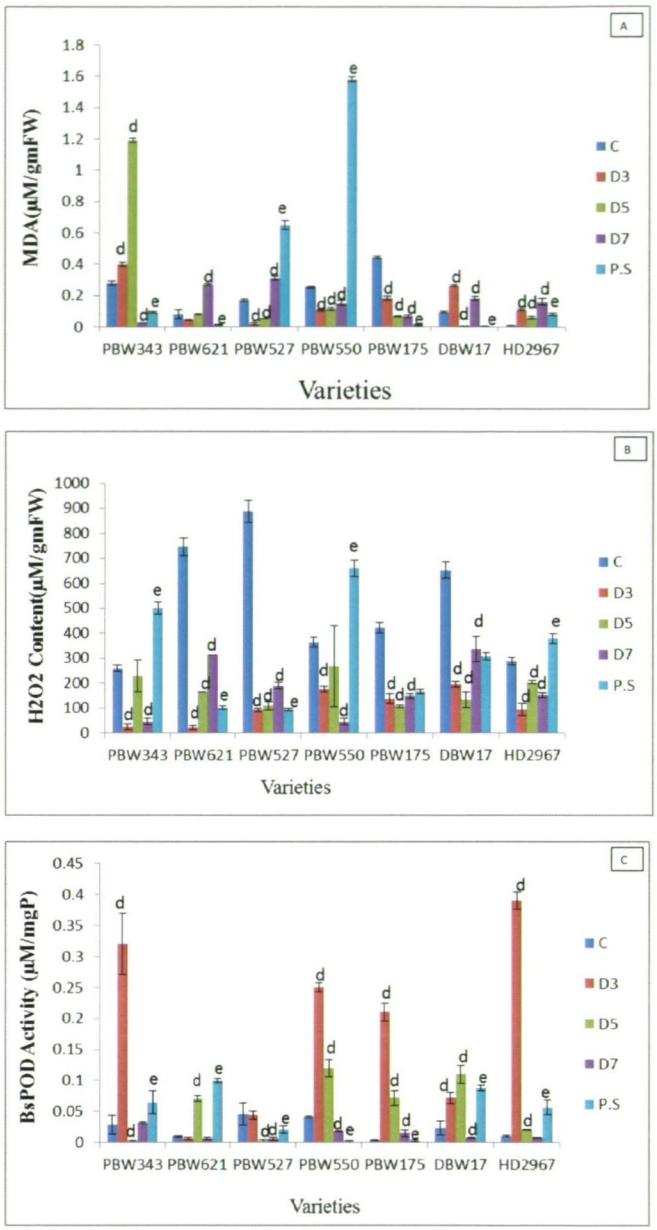

Figure 2. Effect of drought on MDA (A), and H_2O_2 (B) content and specific activity of BsPOD (C) in the shoots of different cultivars of *Triticum aestivum*. Data shown are averages ± SD (n=3). ^{d} represents significant difference relative to the control $p \leq 0.5$. ^{e} represents significant difference of PS relative to D7 $p \leq 0.5$.

PBW550 and PBW175, a substantial decrease in MDA levels were observed at D3, D5 or D7, suggesting that drought-induced BsPODs provided sufficient protection as seen in Figure 3A. The lower values of MDA in PBW175 and PBW550 may indicate that these cvs may have an efficient free radical quenching system, which can maintain higher membrane stability and lower peroxidation under drought treatment. These speculations are in agreement with previous studies

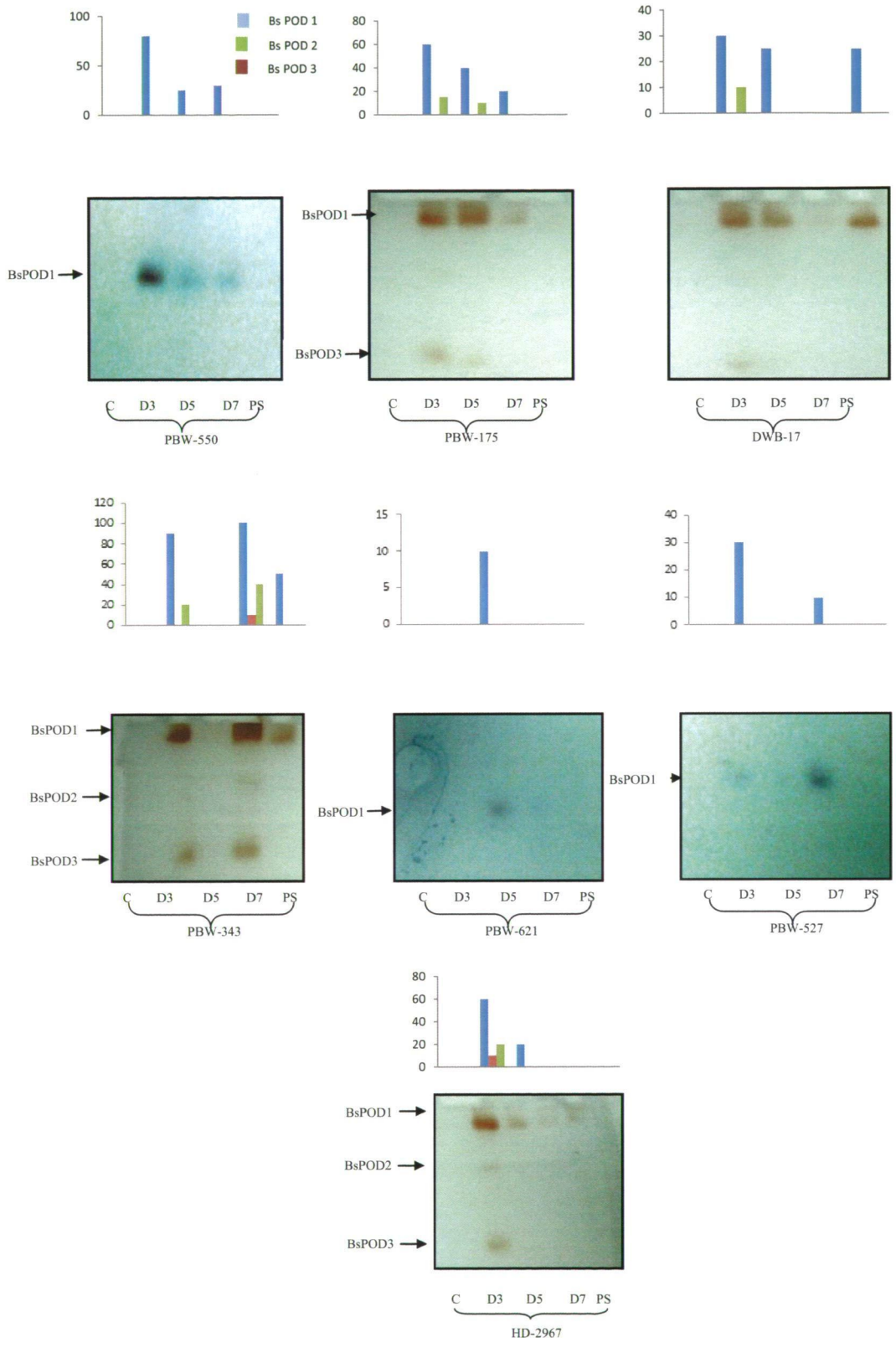

Figure 3. Drought-induced changes in BsPOD isoenzymes in shoots of different cultivars of *Triticum aestivum*. Bar graphs as shown in the top of panels indicate relative band intensities, which were determined using Ultraquant software of Gel Visualization, Documentation and Analysis system (Omega-Lum, USA).

of Sairam et al. (2000), Terzi et al. (2010) and Zhang et al. (2011) who found that low MDA levels were associated with drought stress tolerance in artichoke plans, common beans, and wheat, respectively. In PBW343, DBW17 and HD2967, MDA content increased in the early period of drought but it decreased during the further periods. During PS, MDA content was observed to be decreased in PBW621, PBW175, DBW17 and HD2967 while it increased substantially in PBW343 and PBW550. Earlier Simova-Stoilova et al. (2008) reported similar results in wheat varieties, which showed an increased MDA content on release of water stress.

Changes in H_2O_2

While ROS have the potential to cause oxidative damage to cells during environmental stresses, recent studies have shown that ROS play a key role in plants as signal transduction molecules involved in the mediation of responses to pathogen infection, environmental stresses, programmed cell death and different developmental stimuli (Mittler 2002). Among ROS, H_2O_2 seems best suited to play the role of signaling molecule due to its higher stability and longer half-life (Hung et al. 2005). If H_2O_2 serves as a stress signal, the fluctuation of H_2O_2 level in plants should spatially and temporally reflect changes in the environment. H_2O_2 content significantly decreased at D3 in PBW343, PBW550, PBW175, DBW17 and HD2967 (Fig. 2B) which might be a consequence of the increased BsPOD activities in these cultivars indicating that BsPOD activity have been involved in the detoxification of H_2O_2. Earlier Simova-Stoilova et al. (2008) reported similar results in four wheat varieties, which when subjected to drought stress showed a progressive decrease in H_2O_2 content due to the increased POD activities. Lee and Lee (2000) also documented similar findings upon cold stress in cucumber. In the present study, lower level of H_2O_2 coupled with lower values of MDA in these cvs indicate that these cultivars have an efficient free radical quenching system that offers protection against oxidative stress. Although H_2O_2 content decreased significantly at D3 day in PBW621 and PBW527, BsPOD activity also decreased, which might indicate that other antioxidant enzymes (such as APX, GR or CAT) might be involved in the detoxification of H_2O_2 in these cultivars. Earlier studies also documented that, besides antioxidant enzymes, non-enzymatic metabolites such as ascorbate and glutathione are involved in ROS scavenging. Furthermore, they, together with alpha-tocopherol, have been reported as to be involved in suppression of peroxidation of membrane lipids by reducing the MDA content and thus protecting the integrity of the bio-membranes (Gill and Tuteja 2010).Our results were in agreement with the studies of Bandurska et al. (1997), in which roots of two barley genotypes subjected to drought stress showed significantly decreased H_2O_2 content without increased peroxidase activity indicating that other mechanisms may also be involved in the detoxification of H_2O_2. During the post stress period, however, H_2O_2 levels increased significantly in PBW343 and PBW550 compared to those at drought stress. In PBW621 and PBW527, H_2O_2 content decreased considerably relative to that at D7.

Changes in BsPOD activity

The metabolism of ROS, such as that of H_2O_2, depends on various functionally interrelated antioxidant enzymes, such as PODs. Although abiotic stresses have been shown to induce one or more antioxidant enzymes, there has been little information on the role of POD at boiling level under various drought stress stages and recovery. To control the steady-state ROS levels, PODs are important enzymes of the antioxidant system converting H_2O_2 to water (Cosio and Dunand 2009; Miller et al. 2008).The changes in BsPOD activities in shoots of different wheat cultivars are shown in Fig. 2C. Our results showed that the seven cultivars responded to drought stress differently in terms of activities of antioxidant enzyme. Compared to the control, imposition of drought stress treatment significantly induced the BsPOD activity at D3 in PBW343 (11-fold), PBW550 (6-fold), PBW175 (52-fold), DBW17 (3-fold) and HD2967 (35-fold). The increased antioxidant enzyme activity correlated with decreased H_2O_2 content in drought stressed shoots. On the other hand, PBW621 showed a sharp decline in BsPOD activity after drought treatment and no change was observed in PBW527 at D3 stage, indicating a genotype specific regulation of BsPODs. As the duration of drought stress increased to severe stress (at D5), the BsPOD activity increased considerably in PBW621 and DBW17. In PBW343, PBW527 and HD2967, a significant decrease in the BsPOD activity was observed at D5. It should be emphasis that, as the duration of stress further increased to D7, only PBW175 maintained higher BsPOD activity (3.7-fold) compared to the control. This indicates that BsPOD activity is involved in maintaining the level of ROS and the stability of bio-membranes by controlling lipid peroxidation. As adaptive enzymes of the antioxidant system, PODs are known to play an important role in protecting membrane lipids from peroxidation and reducing cell damage being caused by oxidative stress in plants (Abedi and Pakniyat 2010; Lee and Lee 2000). All other cultivars showed a substantial decrease in BsPOD activity, which may reflect the low ROS scavenging capacity and increased damage in these cultivars. Tian et al (2012) also reported that POD activity declined significantly with increasing drought stress. Therefore, from the above described observation, it can be postulated that, out of the 7 varieties, antioxidant mechanisms in terms of BsPOD activity is enhanced in PBW175, which can be considered potentially tolerant and designated as best variety. Higher POD activity has been correlated with the relative drought tolerance of crop plants (Abedi and Pakniyat 2010; Mafakheri et al. 2011; Chakraborty and Pradhan 2012)

On the removal of stress after D7, a notable increase in Bs-

POD activity was observed in PBW343, PBW621, PBW527, DBW17 and HD2967 emphasizing the importance of cellular mechanisms that protect protein integrity and enable damage repair upon stress relief. Earlier studies on oxidative stress have also shown that the level of some antioxidants in relation with GR and APX may be higher during the recovery period than during water stress, as observed for example in cotton (Ratnayaka et al. 2003) or in pea (Mittler and Zilinskas 1994). This might indicate that either stress had induced an antioxidant response that 'hardens' the plants for future stressful conditions or/and that antioxidant protection in pivotal under recovery period. On the other hand, in PBW175 and PBW550, the BsPOD activity decreased significantly. The oxidative damage to cellular components is limited under normal conditions due to the efficient control of ROS through well coordinated and rapidly responsive antioxidant system consisting of several enzymes. Earlier, Mafakheri et al. (2011) also reported decreased activity of peroxidase during recovery in chickpea after drought stress conditions.

Changes in BsPOD isoenzyme

Patterns of BsPOD isoenzymes are shown is Fig. 3. After native-PAGE analysis, three BsPOD isoenzymes were detected in a genotype dependent manner. Earlier, Abedi and Pakniyat (2010) and Gratao et al. (2005) reported that number of isoenzymes of POD varies from plant to plant. Utilization of multiple isoforms of antioxidant enzymes is one of the major control mechanisms of cellular ROS detoxification. Imposition of drought treatment drastically provoked the expression of BsPOD1 isoenzyme at D3 in almost all cultivars except in PBW621. At D5, BsPOD1 isoenzyme was also induced in PBW621, PBW550, PBW175 and DBW17. Accumulation of BsPOD1 decreased in PBW343 and PBW527, which may be related to the low ROS scavenging capacity of these cultivars to remove ROS under drought treatment. Upon removal of water stress (PS), the BsPOD1 isoform was induced in DBW17, suggesting that the BsPOD1 isoform have participated in the repair of the cellular damage. Moreover, induction of new isoform(s) was also observed in the drought stressed shoots. Two minor differential boiling stable POD isoforms (designated as BsPOD2 and BsPOD3) were observed in shoots under drought treatment in PBW343, HD2967 and PBW175. Utilization of multiple isoforms in shoots may be one of the primary control mechanisms in plants to detoxify ROS. BsPOD2 isoform was induced in PBW343 at D3 and in HD2967 at D7. BsPOD3 was accumulated in PBW343, PBW175 and HD2967 at D3. During post stress period, differential BsPOD2 and BsPOD3 isoforms were not detected. In the different cultivars, along with various stages of drought stress, expression profile of isoenzymes well correlated with the changes observed in the biochemical activity. In PBW550, PBW175 and DBW17 a good correlation was observed between BsPOD1 and BsPOD activity at all the stages of drought stress. Increased band intensity and appearance of new isoenzyme bands may be an indication of an increase in the BsPOD activity under drought stress. Terzi and Kadioglu (2006) and Abedi and Pakniyat (2010) have also suggested that increased POD activity under stress conditions appears to be due to changes in the isoforms populations. Temporal and spatial drastic changes in expression of antioxidant isoforms have been reported previously (Baek et al. 2000; Kim et al. 2005).

To conclude, our results suggest that increased BsPOD activities due to temporal regulation or induction of new isoforms during the stress regimes were thereby dependent on plant genotype. Different wheat cultivars responded differently in response to different stages of drought stress. These results can be used as markers while breeding crops for drought stress tolerance in arid regions. In addition, PBW175 with high BsPOD activities, which may represent a higher capacity to protect against drought-induced oxidative damage, could be introduced to farmers as drought tolerant cultivar for arid and semi-arid environments. Out of the seven tested varieties, PBW175 showed much more pronounced antioxidant mechanisms and hence seemed to be protected from the negative effects of water stress even at the longer duration and increased severity.

Acknowledgements

AD Sharma would like to thank UGC, Government of India for providing financial assistance for the present study.

References

Abedi T, Pakniyat H (2010) Antioxidant enzyme changes in response to drought stress in ten cultivars of oilseed rape (*Brassica napus* L.). Czech J Genet Plant Breed 46:27-34.

Baek SH, Kwon IS, Park TI, Yun SJ, KimJK, Choi KG (2000) Activities and isozyme profiles of antioxidant enzymes in intercellular compartment of overwintering barley leaves. J Biochem Mol Biol 33:385-390.

Bandurska H, Stroinski A, Zielezinska M (1997) Effect of water deficit stress on membrane properties, lipid peroxidation and hydrogen peroxide metabolism in the leaves of barley genotypes. Acta Soc Bot Pol 66:177-183.

Baruah A, Simkova K, Apel K, Laloi C (2009) *Arabidopsis* mutants reveal multiple singlet oxygen signaling pathways involved in stress response and development. Plant Mol Biol 70:547-563.

Battaglia M, Olvera-Carrillo Y, Garciarrubio A, Campos F, Covarrubias A (2008) The enigmatic LEA proteins and other hydrophilins. Plant Physiol 148:6-24.

Bi YH, Chen WL, Zhang WN, Zhou Q, Yun LJ, Xing D (2009) Production of reactive oxygen species, impairment of photosynthetic function and dynamic changes in mitochondria are early events in cadmium induced cell death in *Arabidopsis thaliana*. Biol Cell 101:629-643.

Chakraborty U, Pradhan B (2012) Oxidative stress in five wheat varieties (*Triticum aestivum* L.) exposed to water stress and study of their antioxidant enzyme defense system, water stress responsive metabolites and H2O2 accumulation. Braz J Plant Physiol 24:17-130.

Chakraborty U, Dutta S, Chakraborty BN (2002) Response of tea plants to water stress. Biol Plant 45:557-562.

Chaves M, Oliveira M (2004) Mechanisms underlying plant resilience

to water deficits: prospects for water-saving agriculture. J Expt Bot 55:2365-2384.

Cosio C, Dunand C (2009) Specific functions of individual class III peroxidase genes. J Expt Bot 60:391-408.

Dhindsa RH, Plumb-Dhindsa R, Thorpe TA (1981) Leaf senescence correlated with increased level of membrane permeability, lipid peroxidation and decreased level of SOD and CAT. J Expt Bot 32:93-101.

Foyer CH, Noctor G (2005) Redox homeostasis and antioxidant signalling: A metabolic interface between stress perception and physiological responses. Plant Cell 17:1866-1875.

Gao CJ, Xing D, Li L, Zhang LR (2008) Implication of reactive oxygen species and mitochondrial dysfunction in the early stages of plant programmed cell death induced by ultraviolet-C overexposure. Planta 227:755-767.

Gill SS, Tuteja N (2010) Reactive oxygen species and antioxidant machinery in abiotic stress tolerance in crop plants. Plant Physiol Biochem 48:909-930.

Goel A, Sheoran IS (2003) Lipid peroxidation and peroxide scavenging enzymes in cotton seeds under natural ageing. Biol Plant 46:429-434.

Graper C, Dolan L (2006) Control of plant development by reactive oxygen species. Plant Physiol 141:341-345.

Gratao PL, Polle A, Lea PJ, Azevedo RA (2005) Making the life of heavy metal-stressed plants a little easier. Funct Plant Biol 32:481-494.

Hung SH, Yu CW, Lin CH (2005) Hydrogen peroxide functions as a stress signal in plants. Bot Bull Acad Sinica 46:1-10.

Jacobsen JV, Shaw DC (1989) Heat-stable proteins and abscisic acid action in barley aleurone cells. Plant Physiol 91:1520-1526.

Jiang Y, Huang B (2001) Drought and heat injury to two cool seasons turf grasses in relation to antioxidant metabolism and lipid peroxidation. Crop Sci 41:436-442.

Kim SY, Lim JH, Park MR, Kim YK, Park TI, Seo YW, Choi KG, Yun SJ (2005) Enhanced antioxidant enzymes are associated with reduced hydrogen peroxide in barley roots under saline stress. J Biochem Mol Biol 38:218-224.

Kotak S, Larkindale J, Lee U, Koskull-Döring PV, Vierling E, Scharf KD (2007) Complexity of the heat stress response in plants. Curr Opin Plant Biol 10:310-316.

Lee DH, Lee CB (2000) Chilling stress-induced changes of antioxidant enzymes in the leaves of cucumber: in gel enzyme activity assays. Plant Sci 159:75-85.

Lobato AKS, Santos BG, Costa RCL, Oliveira CF, Meirelles ACS, Cruz FJR, Alves GAR, Neves HKB, Pita JD, Lopes MJS, Freitas JMN, Monteiro BS, Ferreira RR (2008) Physiological and biochemical changes in soybean (*Glycine max*) plants under progressive water deficit during the vegetative phase. J Agric 3:327-333.

Lowry OH, Rosebrough NJ, Farr AL, Randall RJ (1951) Protein measurement with the Folin phenol reagent. J Biol Chem 193:265-75.

Mafakheri A, Siosemardeh A, Bahramnejad B, Struik PC, Sohrabi Y (2011) Effect of drought stress and subsequent recovery on protein, carbohydrate contents, catalase and peroxidase activities in three chickpea (*Cicer arietinum*) cultivars. Aust J Crop Sci 5:1255-1260.

Mamik S, Sharma AD (2014) Analysis of boiling stable antioxidant enzymes in invasive alien species of *Lantana* under abiotic stress-like conditions. Braz J Bot 37:129-141.

Miller G, Shulaev V, Mittler R (2008) Reactive oxygen signalling and abiotic stress. Plant Physiol 133:481-489.

Mittler R (2002) Oxidative stress, antioxidants and stress tolerance. Trends Plant Sci 7:405-410.

Mittler R, Zilinskas BA (1994) Regulation of pea cytosolic ascorbate peroxidase and other antioxidant enzymes during the progression of drought stress and following recovery from drought. Plant J 5:397-405

Ozkur O, Ozdemir F, Bor M, Turkan I (2009) Physiochemical and antioxidant responses of the perennial xerophyte *Capparisovata* desf. to drought. Environ Expt Bot 66:487-492.

Pelah D, Shoseyov O, Altman A (1995) Characterization of BspA, a major boiling stable water stress responsive protein in Aspen (*Populus tremula*). Tree Physiol 15:673-678.

Ratnayaka HH, Molin WT, Sterling TM (2003) Physiological and antioxidant responses of cotton and spurred anoda under interference and mild drought. J Expt Bot 54:2293-2305.

Sairam RK, Saxena DC (2000) Oxidative stress and antioxidants in wheat genotypes: possible mechanism of water stress tolerance. J Agro Crop Sci 184:55-61.

Sambrook J, Fritsch EF, Maniatis T (1989) Molecular cloning: a laboratory manual, Cold Spring Harbour Laboratory Press, New York, 18.64-18.75.

Sanchez-Blanco MJ, Rodrgiuez P, Morales MA, Ortuo MF, Torrecillas A (2002) Comparative growth and water relations of *Citrus albidus* and *Citrus monspeliensis* plants during water deficit conditions and recovery. Plant Sci 162:107-113.

Scandalios JG (1993) Oxygen stress and superoxide dismutase. Plant Physiol 101:7-12.

Sharma AD, Rakhra G, Kaur S, Kaur H (2013) Expression of Boiling stable Peroxidase (PRX) isoenzymes under combined effect of drought and heat in different tissues of *Triticum aestivum*. J AgricTechnol 9:901-913.

Sharma AD, Rakhra G, Singh J (2012) Expression analysis of BsAPase14 acid phosphatase, a stress responsive boiling-stable protein from *Triticum aestivum*. J Crop Sci Biotechnol 15:41-45.

Sharma AD,Vasudeva R, Kaur R (2006) Expression of a boiling-stable protein (BsCyp) in response to heat shock, drought and ABA treatments in *Sorghum bicolor*. Plant Growth Regul 50:249-254.

Simova-Stoilova L, Demirevska K, Petrova T, Tsenov N, Feller U (2008) Antioxidative protection in wheat varieties under severe recoverable drought at seedling stage. Plant Soil Environ 54:529-536.

Tas S, Tas B (2007) Some physiological responses of drought stress in wheat genotypes with different ploidity in Turkiye. World J Agric Sci 3:178-183.

Tatar O, Gevrek MN (2008) Influence of water stress on proline accumulation, lipid peroxidation and water content of wheat. Asian J Plant Sci 7:409-412.

Terzi R, Saglam A, Kutlu N, Nar H, Kadioglu A (2010) Impact of soil drought stress on photochemical efficiency of photosystem 2 and antioxidant enzyme activity of *Phaseolus vulgaris* cultivar. Turk J Bot 34:1-10.

Terzi R, Kadioglu A (2006) Drought stress tolerance and the antioxidant enzyme system in *Ctenanthe setosa*. Acta Biol Cracov Botan 48:89-96.

Thankamani CK, Chempakam B, Ashokan PK (2003) Water stress induced changes in enzymatic activities and lipid peroxidation in black pepper (*Piper nigrum*). J Med Aro Plant Sci 25:646.

Tian Z, Wang F, ZhangW, Liu C, Zhao X (2012) Antioxidant mechanism and lipid peroxidation patterns in leaves and petals of marigold in response to drought stress. Hortic Environ Biotechnol 53:183-192.

Volume 58(2):123-126, 2014
Acta Biologica Szegediensis
http://www2.sci.u-szeged.hu/ABS

ARTICLE

Study of seed protein electrophoretic profiles in some *Erodium* (Geraniaceae) species native to Iran

Maryam Keshavarzi*, Elham Taghipour, Parinaz Ghadam and Zahra Nazem Bokaee

Faculty of Science, Biology Department, Alzahra University, Vanak, Tehran, Iran

ABSTRACT *Erodium* (L.) L'Hér. with 75 species is the third largest genus in Geraniaceae. *Erodium* is distributed in all continents but it shows a great diversity in the Mediterranean region. In Flora Iranica , Schonbeck-Temesy (1970), 15 species, four subsections and three subspecies have been mentioned for *Erodium* in Iran. Electrophoretic patterns of seed storage proteins in the genus *Erodium* has not been studied extensively. In this study for the first time seed protein electrophoretic patterns of seven *Erodium* species from different regions of Iran have been investigated. Protein extracts of seeds were obtained and protein concentration was determined by the Bradford method and analyzed with SDS-polyacrylamide gel electrophoresis (SDS-PAGE). Results were evaluated by multivariate analysis methods including cluster analysis and factor analysis. In the electrophoretic pattern of seed storage proteins, generally, 48 specific bands with molecular weight between 13-102 kDa were detected. Electrophoretic data confirmed sub-generic classification of *Erodium* (to *Plumosa* and *Erodium* sections). Species relationships are discussed.

Acta Biol Szeged 58(2):123-126 (2014)

KEY WORDS

Erodium
Geraniaceae
SDS-polyacrylamide gel electrophoresis
Iran

Erodium is the third largest genus of Geraniaceae with 75 species of annual or biennial herbaceous rosette form (Fiz et al. 2008). These taxa are distributed in all continents except Antarctica, but most of them are found in temperate and tropical regions of the world with a great diversification in Mediterranean region (Fiz et al. 2008; Takhtajan 2009). *Erodium* species are common weeds, but are used in traditional medicine because of its astringent properties (Gohar et al. 2003). L'Heritier (1789) was the first who used *Erodium* for this genus. Boissier (1867) divided *Erodium* into two sections: *Barbata* Boiss and *Plumosa* Boiss. Knuth (1912) in his study divided *Erodium* into two sections as *Plumosa* with five species and *Barbata* with the remaining species. Schonbeck-Temesy in Flora Iranica (1970) followed Boissier system, but used *Erodium* instead of *Barbata* for section name. However in 1972, Guittonneau considered these two parts as two subgenera *Plumosa* and *Barbata* (El Hadidi et al. 1984; El Naggar 1991). All mentioned classifications were based on different mericarp characters as beak and bristles condition. In *Plumosa* section, species have deciduous beak and hairy bristle, but in *Barbata* beak is persistent and there is no feather like bristles. Janighorban (2005) pointed to 15 species without any sectional classification for this genus in Iran.

In the present study the Schonbeck-Temesy (1970) classification has been used which defined two sections in *Erodium* as section *Plumosa* Boiss and section *Erodium* (*Barbata* Boiss) with *E. oxyrrhynchum* M. Bieb. is the only species of first section present in Iran. At the same time, *Erodium* section is composed of 5 subsections as *Gruina* Willk. et Lange. including *E. gruinum* (L.) L Hér. and *E. hoefftianum* C.A. Mey., subsection *Absinthioidea* (Brumh.) Guitt. including *E. ciconium* (L.) L Hér., *E. stephanianum* Willd., and *E. dimorphom* Wendelbo, subsection *Malacoidea* Brumh. with *E. malacoides* (L.) Willd., *E. neuradifollium* Del. Ex Godr. and *E. pulverulentum* (Cav.) Willd., subsection *Bovei* (Delile) Schonbeck-Temesy including *E. laciniatum* (Cav.) Willd. and finally subsection *Cicutaria* Willk. et Lange. including *E. cicutarium* L Hér., *E. moschatum* (L.) L Hér and *E. deserti* Eig.

Over the last decades, investigation of protein electrophoretic patterns was frequently used in plant taxonomic studies. In most cases, the seed was used as protein source, because it displays a certain stage of the plant life and is less affected by environmental stress than the leaves (Crawford 1990). Concerning *Erodium* species, the only study on seed protein electrophoretic patterns of the genus was conducted by Sharawy and Badr (2008) on 12 *Erodium* species of Egypt. In our present study, the electrophoretic protein profiles of seven *Erodium* species native to Iran are investigated.

Materials and Methods

Plant material

Sampling was carried out from distribution range of the seven studied *Erodium* species in 2012 and 2013 growth period. Accession details for studied species are displayed in Table 1.

Accepted Aug 10, 2014
*Corresponding author. E-mail: Keshavarzm@alzahra.ac.ir

Table 1. Voucher details of the investigated *Erodium* species.

Taxa	Locality	Herbarium number
E. cicutarium	Tehran, Vanak, Najafian & Taghipour. 1439 m. Tehran, Peykanshahr, Botanical Garden of Iran, Taghipour. 1270 m	911 918
E. ciconium	Tehran, Peykanshahr, Botanical Garden of Iran, Taghipour. 1261 m	913
E. oxyrrhynchum	Tehran, Peykanshahr, Botanical Garden of Iran, Taghipour. 1261 m	912
E. malacoides	Gilanegharb, Vizhnan, Najafian. 920 m	927
E. moschatum	Gilanegharb, Vizhnan, Najafian. 920 m	929
E. gruinum	Gilanegharb, Vizhnan, Najafian. 915 m	926
E. hoefftianum	Karaj, Kondor, Taghipour. 1897 m	9215

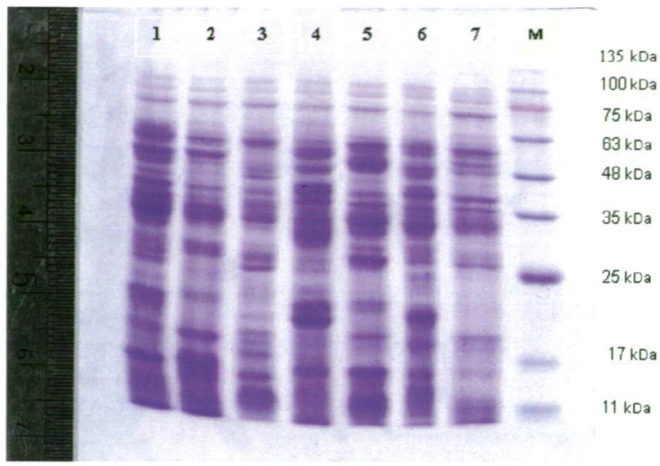

Figure 1. SDS-PAGE pattern of the examined isolates of Iranian *Erodium*. M: pre-stained protein ladder (10-170 kDa). Lane 1-7: *E. cicutrium, E. ciconium, E. oxyrrhynchum, E. moschatum, E. hoefftianum, E. malacoides*, and *E. gruinum*, respectively.

Extraction of Seed Proteins

In order to extract seed storage proteins, seeds pods were removed and 0.1 g of each seed sample was powdered and homogenized with 1 ml extraction buffer (0.2 M Tris-HCl, pH 8) in mortar in ice bath for 1 hour. Extractions were centrifuged in a cold room with 13400 rpm for 30 min. Supernatant was transferred to a clean tube and used immediately for electrophoresis (Laemmli 1970; Sharawy and Badr 2008).

Bradford method

The protein concentration was measured by Bradford (1976) method. To produce 100 ml of 0.01% Coomassie Brilliant Blue G250 solution, 10 mg of Coomassie Brilliant Blue G-250 was dissolved in 5 ml of 95% ethanol, then 10 ml 85% phosphoric acid was added and when the dye has completely dissolved, it diluted to 100 ml with distilled water, and filtered through Whatman #1 paper just before use. In this method, Bovine Serum Albumin (BSA) solution (1 g/l) in Tris-HCl buffer was prepared and used as standard protein solution. The different concentrations of BSA from 0 to 0.6 mg/ml were prepared using extraction buffer, then 5 ml of Coomassie Brilliant Blue G250 solution was added and their absorbances were read in 595 nm (Bradford 1976). A standard curve of absorbance versus mg/ml protein was prepared and the concentration of samples was determined from the curve.

SDS-polyacrylamide gel electrophoresis

Gel electrophoresis was performed with Tris-glycine running buffer (pH 8.3) at room temperature. SDS-PAGE was consisting of 4% stacking gel (pH 6.8) and 15% separating gel (pH 8.8). Electrophoresis was done in constant voltage (120 V) for 2 hours. The gel was stained with Coomassie Brilliant Blue R-250 in 50% methanol and 3.5% acetic acid for about 30 min, followed by destaining in 10% methanol and 10% acetic acid overnight or until the gel background was cleared (Laemmli 1970).

Proteins molecular weight measurement

For the preparation of a protein molecular weight standard curve a 10-170 kDa protein ladder was used. After electrophoresis of the sample protein solutions their relative mobility values (R_f) were calculated. The logarithm of the molecular weights of protein ladder against their R_fs were plotted. The molecular weights of the samples were calculated by comparison of their R_fs with the standard curve. Multivariate statistical analysis of data was performed using SPSS Software (version 18; SPSS, Chicago, IL, USA). Cluster analysis by WARD method (minimum variance) was used to illustrate branching patterns as an appropriate method for quantitative variables.

Results

For the first time, seed storage protein electrophoretic profile of *E. hoefftianum* is recorded. About 48 specific bands were observed and their molecular weights (13-102 kDa) were calculated (Fig. 1). Presence and absence of bands were considered as qualitative binary or multistate features in multivariate statistical analysis. Some bands were exclusively observed in certain species, for example six bands were only observed in *E. oxyrrhynchum,* four in *E. cicutarium* and other four bands only in *E. moschatum.* There was also one band in common in *E. moschatum, E. cicutarium* and also three bands in common in *E. malacoides* and *E. hoefftianum* species pairs.

Cluster analysis by WARD method (Fig. 2) showed that there are two main clusters in distance level 25. The first

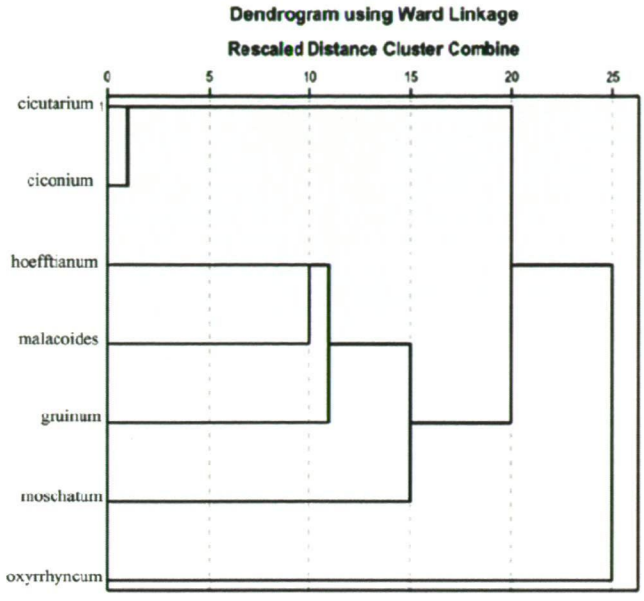

Figure 2. WARD dendrogram based on the electrophoretic data of *Erodium* seed proteins.

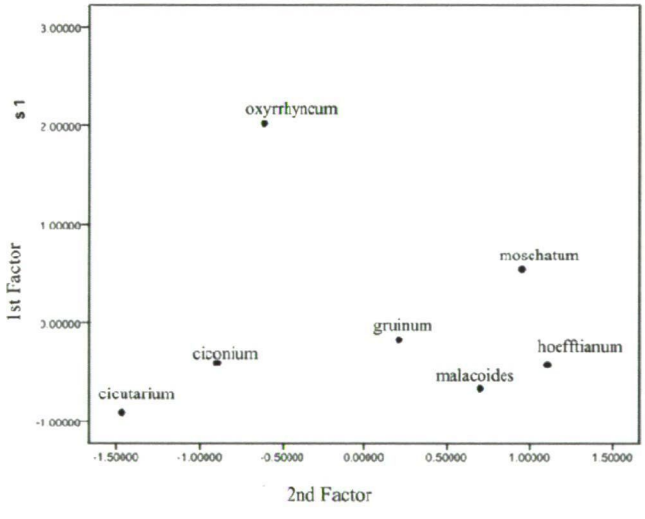

Figure 3. PCA scatter diagram based on the electrophoretic data for studied *Erodium* species. (Axis values are based on Principal Component Analysis).

cluster contains *Erodium* species of section *Erodium*. This is divided into two sub-clusters, which contain two closely related species as *E. ciconium* and *E. cicutarium*. The other sub-cluster comprises two species: *E. hoefftianum* and *E. malacoides* at a distance of about 10. The second main cluster contains *E. oxyrrhynchum* that belongs to *Plumosa* section.

In scatter diagram of Principal Component Analysis based on the first and second factors of electrophoretic data (Fig. 3), it is evident that *E. oxyrrhynchum* as the only species of *Plumosa* section, has been separated from other species (belonging to *Erodium* section).

Discussion

Comparison of the electrophoretic profiles revealed that the most common bands are observed between *E. cicutarium* and *E. ciconium* (possessed in common five bands) and also between *E. malacoides* and *E. hoefftianum* (possessed in common five bands). *E. cicutarium* and *E. ciconium,* and also *E. malacoides* and *E. hoefftianum* species pairs showed the highest similarities. According to WARD clustering pattern (Fig. 2), the two main clusters are in accordance with the Schonbeck-Temesy (1970) sectional classification (*Erodium* and *Plumosa*). In main cluster of *Erodium* section, *E. gruinum* and *E. hoefftianum* species of *Gruina* subsection, there were two near sub-clusters, which are in accordance with the Schonbeck-Temesy (1970) sub-sectional classification. The second major cluster contained *E. oxyrrhynchum* of *Plumosa* section. This is clearly separated from *Erodium* section. Cluster analysis by WARD method for *Erodium* species is somehow in accordance with Sharawy and Badr studies (2008) on Egyptian *Erodium*, especially in sectional separation, but there are some differences in species separation pattern, for example *E. cicutarium* from *Cicutaria* subsection and *E. ciconium* from *Absinthioidea* subsection are grouped in the same cluster in the present study. *E. malacoides* from *Malacoidea* subsection and *E. hoefftianum* from *Gruina* subsection are also grouped as closely related species in the same sub-cluster. *E. gruinum* and *E. hoefftianum* are elements of the same subsection, but are grouped in different sets. According to PCA graph based on electrophoretic data (Fig. 3), results clearly confirmed sub-sectional classification of *Erodium* presented by Schonbeck-Temesy (1970).

The results of seed storage protein electrophoresis for seven studied *Erodium* species of Iran showed that species separation at sectional level is in accordance with previous studies in Egypt (Sharawy and Badr 2008) and also confirmed the Schonbeck-Temesy opinion about sectional classification. The present study reinforced that electrophoretic profiles of seed storage proteins have taxonomic value in species delimitation in the genus *Erodium*.

References

Boissier A (1867) Flora Orientalis sive enumeratio plantarum in Oriente a Graecia et Aegypto ad Indiae fines hucusque observatarum. I: Geraniaceae. Genevae et Basileae.

Bradford MM (1976) A rapid and sensitive method for the quantitation of microgram quantitatives of protein dye binding. Anal Biochem 72:248-254.

Crawford DJ (1990) Plant Molecular Systematics: Macromolecular Approaches. Wiley InterScience Publ, New York.

El Hadidi MN, Fayed AA, El Naggar SM (1984) Systematic revision of *Erodium* (Geraniaceae) in Egypt. Plant Syst Evol 144:307-314.

El Naggar SM (1991) Numerical taxonomy of the genus *Erodium* L'Herit. (Geraniaceae) in Egypt. Feddes Repert 102(7-8):535-540.

Fiz O, Vargas P, Alarcón M, Aedo C, García JL, Aldasoro JJ (2008) Phylogeny and historical biogeography of Geraniaceae in relation to climate changes and pollination ecology. Syst Bot 33:326-342.

Gohar A, Lahloub M, Niwa M (2003) Antibacterial polyphenol from *Erodium glaucophyllum*. Z Naturforsch C 58:670-674.

Guittonneau G-G (1972) Contribution à l étude biosystématique du genre *Erodium* L Hér. dans le bassin méditérranéen occidental. Boissiera 20:1-154.

Janighorban M (2005) Geraniaceae, Flora of Iran Vol 62. 1st ed. Research Institute of Forest and Rangelands Publication, Tehran [Persian].

Knuth R (1912) Geraniaceae. In Engler A, ed., Das Pflanzenreich IV. 129 (Heft 53), Leizpig, Verlag.

L'Heritier CL (1789) *Erodium*. In Aiton W, ed., Hortus Kewensis, 2:414-416. Nicol, London.

Laemmli UK (1970) Cleavage of structural proteins during the assembly of the head bacteriophage T4. Nature 227:680-685.

Schonbeck-Temesy E (1970) Geraniaceae. 1-67. In Flora Iranica Vol 69, Rechinger KH (Ed). Graz Akademische Druck.

Sharawy SM, Badr A (2008) Systematic revision of *Erodium* species in Egypt as reflected by variation in morphological characters and seed protein electrophoretic profiles. Int J Bot 4(2):225-230.

Takhtajan A (2009) Diversity and classification of flowering plants. Columbia University Press, New York. p. 643.

Volume 58(2):127-132, 2014
Acta Biologica Szegediensis
http://www2.sci.u-szeged.hu/ABS

ARTICLE

Novel features of the rat model of inflammatory bowel disease based on 2,4,6-trinitrobenzenesulfonic acid-induced acute colitis

Zita Szalai[1], Krisztina Kupai[1], Médea Veszelka[1], Anikó Pósa[1], Szilvia Török[1], Anikó Magyariné Berkó[1], Zoltán Baráth[2], Ferenc A. László[1], Csaba Varga[1]*

[1]Department of Physiology, Anatomy and Neuroscience, Faculty of Science and Informatics, University of Szeged, Szeged, Hungary, [2]Department of Orthodontics and Paediatric Dentistry, Faculty of Dentistry, University of Szeged, Szeged, Hungary

ABSTRACT The 2,4,6-trinitrobenzenesulfonic acid (TNBS)-induced acute inflammatory bowel disease (IBD) model in the rat is discussed, focusing on the details of the TNBS instillation and highlighting the advantages and limitations of this model. For determination of the time-dependent action of 50% ethanol and different doses of TNBS, male Wistar rats were treated with 50% ethanol or 10 mg or 30 mg of TNBS dissolved in 50% ethanol. The TNBS-induced inflammation peaked 48-72 h after installation and the colitis caused by 30 mg of TNBS was more severe than that caused by 10 mg of TNBS. To test the effectiveness of sulfasalazine (SASP), male rats were treated with 10 mg of TNBS or with 10 mg of TNBS and SASP, and 72 h later the extent of mucosal damage was determined. Orally administered 50 mg/kg/day SASP proved to reduce the TNBS-induced colonic inflammation in rats significantly. The TNBS-induced colitis model facilitates a better understanding of the immunopathological mechanisms of IBD. Optimization of the dose of TNBS and oral SASP as positive control in TNBS-induced colitis in rats furnishes an appropriate test system for new anti-IBD drugs.
Acta Biol Szeged 58(2):127-132 (2014)

KEY WORDS

colitis
rat IBD model
TNBS

Inflammatory bowel disease (IBD) is a chronic disease of the gastrointestinal tract, primarily manifested as Crohn's disease (CD) and ulcerative colitis (UC). Environmental, genetic and immunological factors all contribute significantly to the pathophysiology of IBD, but the precise mechanisms remain unclear (Kaser et al. 2010). Epidemiological studies have revealed an increasing incidence of IBD in northwestern Europe, the USA and eastern Canada, suggesting that environmental and lifestyle factors play a major role in the development and progression of this disease (Vatn 2008; Kappelman et al. 2013; Ng et al. 2013).

Several animal models have been developed in attempts to understand the pathogenesis of IBD and to test pharmacological molecules and therapeutic targets. However, CD and UC are chronic diseases, while animal models are necessarily primarily acute, in order to limit the discomfort and the pain caused to the animals and to reduce the costs associated with the use of reagents and supplies. Invertebrate models of IBD, involving *Caenorhabditis elegans* (Chinnadurai et al. 2008; Kang et al. 2010) and *Drosophila melanogaster* (Liu et al. 2010; Apidianakis et al. 2011), have been used to investigate the genetic factors and signalling pathways involved in the pathogenesis of these diseases and to identify novel therapeutic agents (Lin et al. 2011). However, the various vertebrate models (most commonly mice and rats) more closely resemble the complexity of the human physiology than those with invertebrate animals, and may reflect the different subtypes of patients with IBD, and they are important in preclinical studies (Jurjus et al. 2004).

Rodent models of chemically induced IBD are widely used because of their simplicity and the possibility of the control of the degree of inflammation (Table 1). However, the differences in protocols lead to difficulties in reproducing reported experiments and in comparing measured parameters between studies. The inconsistent variables generally include the rodent strains used, the amounts and concentrations of chemical agents and the time of sacrifice in relation to the treatment.

The 2,4,6-trinitrobenzenesulfonic acid (TNBS) model was originally described by Morris et al. (Morris et al. 1989). TNBS (0.5 to 4.0 mg for mice and 10 to 30 mg for rats) is dissolved in 45% or 50% ethanol, which can lead to the destruction of the mucosal barrier. As a hapten, TNBS can bind to the endogenous proteins, giving rise to hapten-protein formation, which induces the interleukin-12 (IL-12) and T helper 1-mediated local immunological response. The activated macrophages produce inflammatory mediators,

Accepted Dec 2, 2014
*Corresponding author. E-mail: vacs@bio.u-szeged.hu

Table 1. Advantages and disadvantages of the most common chemically-induced animal models of IBD.

Models	Advantages	Disadvantages	References
TNBS	Widely applicable to vertebrate animals (rats, mice, guinea pigs, rabbits), in which the pathology closely resembles the human pathology. Can induce acute or chronic transmural inflammation.	Cannot mimic the relapsing phase of Crohn's disease.	Scheiffele et al. 2002 te Velde et al. 2006 Motavallian-Naeini et al. 2012 Alex et al. 2009
DSS	Can induce inflammation in acute, chronic or relapsing form.	Longer duration of experiment.	Rose et al. 2012 Chen et al. 2007 Perse et al. 2012
Acetic acid	The general health of the animals is similar to that of the controls.	The treatment is more complex.	Yamada et al. 1992 Fabia et al. 1992
Indomethacin	Induces inflammation not in the colon, but in the ileum and jejunum. Simple administration (subcutaneous) without anaesthesia.	The inflammation is not localized in the colon.	Yamada et al. 1993 Piepoli et al. 2005

TNBS = 2,4,6-trinitrobenzenesulfonic acid, DSS = dextran sulfate sodium

such as tumor necrosis factor- , IL-6 and IL-1 (Ishiguro et al. 2010; Strober et al. 1998), which in turn result in transmural inflammation with weight loss and diarrhoea. The TNBS model has many advantages, such as the simple process and the short duration of the experiment. Moreover, it is widely applicable to vertebrates, including mice (it is important to note, however, that the susceptibility to TNBS-induced colitis varies between different mouse strains: SJL and BALB/c mice are susceptible), rats, guinea pigs and rabbits, and can be used either acutely with a single TNBS treatment or chronically with the repeated administration of TNBS (Terai et al. 2014). On the other hand, this model has the major limitation that it cannot mimic the relapsing phase of CD (Table 1).

Among the reference drugs with anti-IBD effects, hydrocortisone acetate (20 mg/kg, i.p.), Asacol (100 mg/kg, p.o.) (Motavallian-Naeini et al. 2012), 5-aminosalicylic acid (5-ASA; 8, 25 or 75 mg/kg, intracolonal) (Horvath et al. 2008) and the 5-ASA-releasing sulfasalazine (SASP; 360 mg/kg, p.o.) (Byrav et al. 2013) have been found effective in ameliorating inflammation.

The primary aim of the present study was to investigate a TNBS-induced acute IBD model in the rat, focusing on the details of the TNBS instillation and highlighting the advantages and limitations of this model, in which anti-colitis drugs can be tested. A further aim was to describe a newly developed method for treatment with SASP as a positive control in a TNBS-induced acute colitis model.

Materials and Methods

Animals

Male Wistar rats (200-250 g, Toxi-Coop Zrt., Hungary) were housed in groups (4 or 5 rats in each cage). Food was withdrawn overnight before the induction of colitis; otherwise, the animals had access to food and drinking water *ad libitum* throughout the experiments. The animal care and research protocols were in full accordance with the guidelines of the University of Szeged.

Experimental design for determination of the time-dependent action of 50% ethanol or TNBS (10 or 30 mg) dissolved in 50% ethanol

The animals were randomly divided into three groups, to which 50% ethanol (n=36), 10 mg of TNBS (n=27) or 30 mg of TNBS (n=90) was administered. 12 h before the induction of colitis, the rats were fasted.

TNBS (also called picrylsulfonic acid, from Sigma-Aldrich) as received from the manufacturer was aliquoted and stored at -20 °C in order to prevent its effectiveness. The TNBS solution for administration was prepared immediately before treatment: 10 mg or 30 mg of TNBS was dissolved in 50% ethanol for instillation in a final volume of 250 µl per rat. Following dissolution, the TNBS solutions were protected from light, because they are light-sensitive and unstable at room temperature.

The intracolonic administration of the ethanol or the TNBS (dissolved in ethanol) was performed under transient ether anaesthesia with the aid of an 8 cm long plastic catheter (800/100/260PO, ReplantMed) attached to a 1 ml syringe. After the instillation, the rats were kept on their back for about 30 s before being returned to their cages.

The body weight was measured immediately before and 24, 48 and 72 h after ethanol or TNBS treatment.

Both before and 24, 48 and 72 h after treatment with 10 mg of TNBS, and 1.5, 3, 6, 12, 24, 48 and 72 h and 6 and 10 days after treatment with 30 mg of TNBS and 6, 12, 24 and 48 h after treatment with ethanol, rats (n=9 at each timepoint) were sacrificed by cervical dislocation under ether anaesthesia, and the 8 cm portion of the colon distal from the rectum

Table 2. Treatment groups.

Group (n=9)	Treatment	Route options	Schedule
Absolute control	-	-	-
Vehicle control	EtOH	Intracolonic	Single dose of 250 µl of 50% EtOH
TNBS-treated	TNBS in 50% EtOH	Intracolonic	Single dose of 10 mg/250 µl of 50% EtOH
Positive control (anti-IBD drug)	TNBS in 50% EtOH	Intracolonic	Single dose of 10 mg/250 µl of 50% EtOH
	+ SASP in 1% CMC	Oral	Daily 2 x 25 mg/ 250 µl 1% CMC
Test item	TNBS in 50% EtOH	Intracolonic	Single dose of 10 mg/250 µl of 50% EtOH
	+ test item	Oral	Twice daily

EtOH = ethanol, TNBS = 2,4,6-trinitrobenzenesulfonic acid solution, SASP = sulfasalazine, CMC = carboxymethylcellulose

was dissected, longitudinally opened, gently rinsed with ice-cold physiological saline, and photographed (Panasonic Lumix DMC-TZ6 digital camera) for determination of the extent of macroscopic colonic inflammatory damage.

Experimental design for tests of the effectiveness of a SASP in the TNBS model (Table 2)

The animals were randomly divided into 2 groups, for the administration of 10 mg of TNBS (n=9) or 10 mg of TNBS + SASP 50 mg/kg/day (positive control group, n=9). For 12 h before the induction of colitis, all of the rats were fasted. The animals were treated with TNBS (10 mg dissolved in 50% ethanol for a final volume of 250 µl per rat). The detailed steps of the TNBS treatment were described above.

The animals in the positive control group were treated with TNBS and SASP as follows: 25 mg/kg SASP was dissolved in 1% carboxymethylcellulose (CMC) for a final volume of 250 µl per rat. The animals were treated orally with SASP solution twice a day for 3 days, the first treatment taking place 2 h before the instillation of TNBS.

72 h after the treatment with TNBS, the 8 cm distal segment of the colon was collected as described above.

Parameters utilized to analyse the severity of the induced inflammation

Body weight change: the weight of each animal was measured every day, starting on the day before TNBS treatment, and the change in weight was calculated as a percentage, the baseline (100%) being taken as the weight on the day of the TNBS challenge.

Percentage of damaged mucosa: the extent of macroscopically apparent inflammation, ulceration and tissue disruption was determined in a randomized manner from colour images via computerized planimetry (proprietary computerized planimetry software, developed in our laboratory was used: Stat_2_1_1). The surface area of macroscopically visible mucosal involvement was calculated and expressed as a percentage of the surface area of the total 8 cm colonic segment under study.

Statistical analysis

Results are shown as means ± S.E.M; statistical comparisons were performed with the two-tailed Student *t*-test.

Results

Time-dependent changes in colonic inflammation induced by 50% ethanol, or by 10 mg or 30 mg of TNBS

Our findings revealed the role and time-dependent effects of ethanol (the vehicle of TNBS) and the different doses of TNBS in the development of acute colonic inflammation. 50% ethanol give rise to damage to the mucosal barrier 6-12 h after treatment, and the macroscopic changes were reversed after 2 days. The TNBS-induced inflammation peaked 48-72 h after instillation, and this was followed by a slow recovery process. The maximum extent of the lesion caused by 30 mg of TNBS (62.8 ± 5.5% of the 8 cm segment of the colon) was slightly greater than that caused by 10 mg of TNBS (58.0 ± 3.0% of the 8 cm segment of the colon) (Fig. 1A). Moreover, in the 30 mg TNBS group 5 rats died during the study, whereas in the 10 mg TNBS group there were no deaths.

Changes in body weight induced by treatment with 10 mg or 30 mg of TNBS

The rats treated with 30 mg of TNBS exhibited a significantly greater weight loss as compared with the animals challenged with 10 mg of TNBS on the third day (Fig. 1B).

SASP, a positive control for the TNBS colitis model

SASP administered orally twice a day in a dose of 25 mg/kg/day in 1% CMC significantly reduced the colonic inflamma-

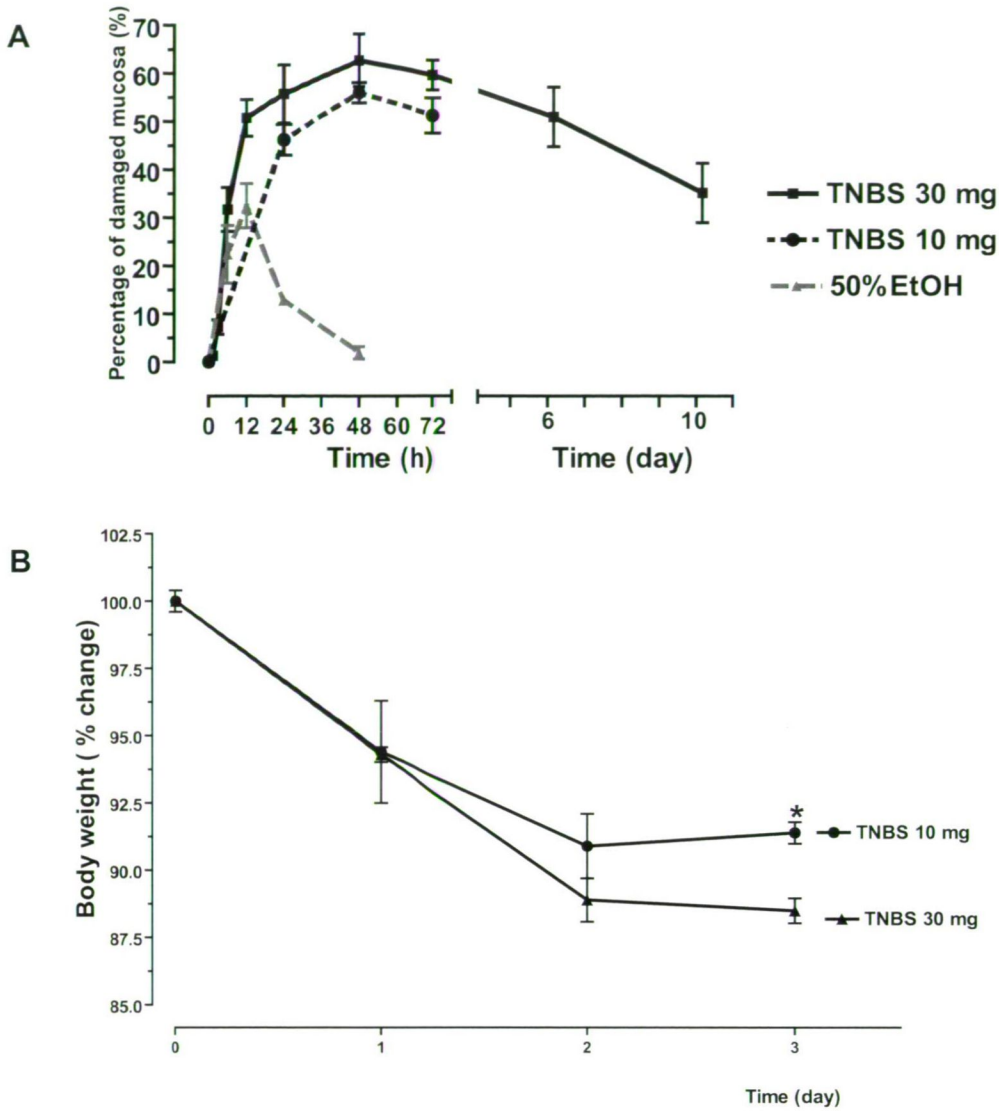

Figure 1. Time-dependent changes in the percentage of mucosal damage induced by 10 mg of TNBS, 30 mg of TNBS or 50% ethanol (A). (The intermittent x axis shows the time-scale: hours and days.) Results are given as means ± S.E.M., n=7-9. Time-dependent body weight changes caused by challenge with 10 mg or 30 mg of TNBS (B). Results are given as means ± S.E.M., *P<0.05 as compared with the 30 mg TNBS group on the 3rd day, n=7-9.

tion in the TNBS (10 mg)-treated rats, from 51.2 ± 3.7% to 28 ± 2.1% 72 h after the TNBS challenge (Fig. 2A).

The representative images demonstrate that the TNBS (10 mg) treatment caused macroscopic damage in the 8 cm segment of the colon, such as ulceration and wall thickening (Fig. 2B), while the SASP treatment exerted an anti-inflammatory effect on the TNBS (10 mg)-induced colitis (Fig. 2C).

Discussion

The use of animal models is important for the attainment of a better understanding of the pathological mechanisms involved in IBD, and such models can contribute to the development of new modes of treatments for humans. The present study related to a detailed protocol of TNBS treatment in the rat, with methods designed to monitor colonic inflammation, including the effects of different doses of TNBS, ethanol and SASP on the development of colonic inflammation.

TNBS-induced colitis can mimic many of the features of CD. The body weight loss is an indicator of the severity of the colitis, because TNBS/ethanol treatment causes diarrhoea, and the discomfort decreases the appetite (Ibrahim et al. 2011). In accordance with previous findings, we found that there was a greater decrease in body weight in the rats treated with 30 mg of TNBS at 72 h than in those treated with 10 mg

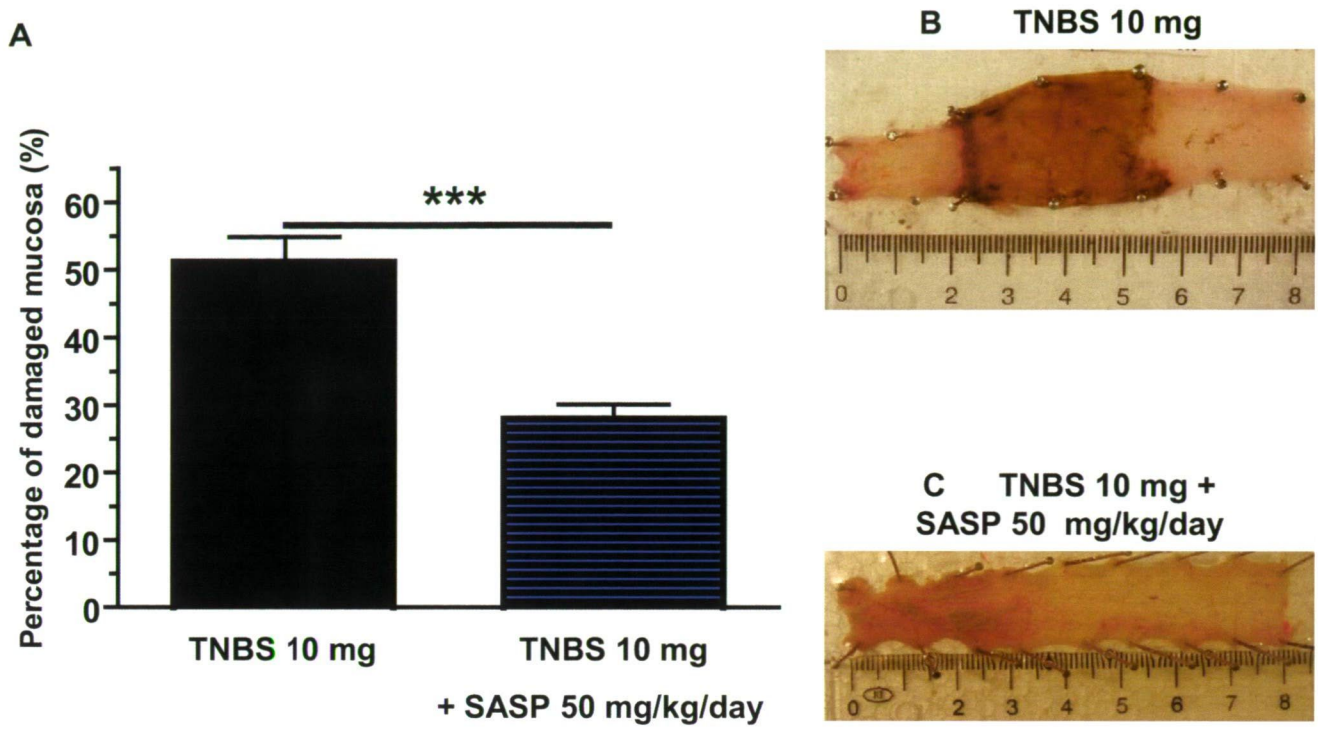

Figure 2. Effect of 50 mg/kg/day sulfasalazine (SASP) on the severity of colonic inflammation induced by 10 mg of TNBS (A). Results are given as means ± S.E.M., ***P<0.001 as compared with the TNBS group, n=9. Representative images of the 8 cm colonic segment from each group: TNBS 10 mg (B), TNBS 10 mg + SASP 50 mg/kg/day (C).

of TNBS. Moreover, in the 10 mg TBNS group, no rat died as a result of the TNBS treatment.

The dose of TNBS and the percentage of ethanol applied vary among the reported investigations. In agreement with previous studies, we found that the severity of TNBS-induced colonic inflammation is dose-dependent (Motavallian-Naeini et al. 2012, Brenna et al. 2013). Menozzi et al. observed that 30 mg of TNBS resulted in the need for a longer regeneration of the histological changes as compared with 10 mg of TNBS (Menozzi et al. 2006). The findings relating to the body weight changes, the mucosal damage and the survival rate following the treatments with the two different doses of TNBS suggest that 10 mg of TNBS is a more appropriate dose with which to induce colonic inflammation.

As the time-related changes in ethanol-induced mucosal damage indicated, ethanol plays an important role in the initial phase (12 h after treatment) of the development of inflammation. Hong-Yan Qin et al. demonstrated that the same dose of TNBS in different vehicle volumes caused different degrees of damage, TNBS in 25% ethanol gave rise to a lower pathological score and to a lower level of myeloperoxidase activity relative to those after TNBS in 50% ethanol (Qin et al. 2012).

We used SASP (brand names Azulfidine in the U.S., and Salazopyrin and Sulazine in Europe) as a positive control. SASP is a sulfa drug and a widely used anti-colitic agent in human IBD therapy. Earlier findings revealed that SASP and 5-ASA are poorly absorbed in the gut (Yen et al. 2012), while 5-ASA, the pharmacologically active metabolite of SASP, ingested directly into the colon is effective in decreasing colitis (Horvath et al. 2008). The oral administration of SASP is better than local ingestion of the drug into the inflamed colon, as there is then less risk of aggravation of the injury of the inflamed colon; moreover, the oral administration of SASP can serve as a positive control (Ghatule et al. 2014, Zhang et al. 2014). The present study has demonstrated that SASP given orally at a dose of 50 mg/kg/day twice a day resulted in an improvement in the colonic inflammation induced by 10 mg of TNBS.

In conclusion, this report has described a chemically-induced rodent model of intestinal inflammation focusing on TNBS-induced acute colitis in rats, a widely-used simple animal model characterized by transmural inflammation with weight loss. It emerged that 10 mg of TNBS is a more suitable dose than 30 mg of TNBS, and, as a reference drug, orally administered SASP is preferable to an enema (Horvath et al. 2008) for attenuation of acute TNBS inflammation in rats.

This model may promote a better understanding of the immunopathological mechanisms of IBD via the testing of new compounds in the preclinical phase. It is hoped that this

detailed description of the TNBS colitis protocol used in our laboratory will be helpful to other research teams.

Acknowledgements

This research was realized in the frames of TÁMOP 4.2.4. A/2-11-1-2012-0001 "National Excellence Program – Elaborating and operating an inland student and researcher personal support system". The project was subsidized by the European Union and co-financed by the European Social Fund.

References

Alex P, Zachos NC, Nguyen T, Gonzales L, Chen TE, Conklin LS, Centola M, Li X (2009) Distinct cytokine patterns identified from multiplex profiles of purine DSS and TNBS-induced colitis. Inflamm Bowel Dis 15:341-352.

Apidianakis Y, Rahme LG (2011) *Drosophila melanogaster* as a model for human intestinal infection and pathology. Dis Model Mech 4:21-30.

Brenna Ø, Furnes MW, Drozdov I, van Beelen Granlund A, Flatberg A, Sandvik AK, Zwiggelaar RT, Marvik R, Nordrum IS, Kidd M, Gustafsson BI (2013) Relevance of TNBS-colitis in rats: a methodological study with endoscopic, historical and transcripttomic characterization and correlation to IBD. PLoS One 8(1):e54543.

Byrav DSP, Medhi B, Prakash A, Chakrabarti A, Vaiphei K, Khanduja KL (2013) Comparative evaluation of different doses of PPAR- agonist alone and in combination with sulfasalazine in experimentally induced inflammatory bowel disease in rats. Pharmacol Rep 65:951-959.

Chen Y, Si JM, Liu WL, Cai JT, Du Q, Wang LJ, Gao M (2007) Induction of experimental acute ulcerative colitis in rats by administration of dextran sulfate sodium at low concentration followed by intracolonic administration of 30% ethanol. J Zhejiang Univ Sci B 8:632-637.

Chinnadurai G, Vijayalingam S, Gibson SB (2008) BNIP3 Subfamily BH3-only proteins: mitochondrial stress sensors in normal and pathological functions. Oncogene 27:S114-S127

Fabia R, Willen R, Ar'Rajab A, Andersson R, Ahren B, Bengmark S (1992) Acetic acid-induced colitis in the rat: a reproducible experimental model for acute ulcerative colitis. Eur Surg Res 24:211-225.

Ghatule RR, Gautam MK, Goel S, Singh A, Joshi VK, Goel RK (2014) Protective effects of *Aegle marmelos* fruit pulp on 2,4,6-trinitrobenzene sulfonic acid-induced experimental colitis. Pharmacogn Mag 10:S147-S152

Horvath K, Varga C, Berko A, Posa A, Laszlo F, Whittle BJ (2008) The involvement of heme oxygenase-1 activity in the therapeutic actions of 5-aminosalicylic acid in rat colitis. Eur J Pharmacol 581:315-323.

Ibrahim A, Mbodji K, Hassan A, Aziz M, Boukhettala N, Coeffier M, Savoye G, Dechelotte P, Marion-Letellier R (2011) Anti-inflammatory and anti-angiogenic effect of long chain n-3 polyunsaturated fatty acids in intestinal microvascular endothelium. Clin Nutr 30:678-687.

Ishiguro K, Ando T, Maeda O, Watanabe O, Goto H (2010) Novel mouse model of colitis characterized by hapten-protein visualization. Biotechniques 49:641-648.

Jurjus AR, Khoury NN, Reimund JM (2004) Animal models of inflammatory bowel disease. J Pharmacol Toxicol Methods 50:81-92.

Kang C, Avery L (2010) Death-associated protein kinase (DAPK) and signal transduction: fine-tuning of autophagy in *Caenorhabditis elegans* homeostasis. FEBS J 277:66-73.

Kappelman MD, Moore KR, Allen JK, Cook SF (2013) Recent trends in the prevalence of Crohn's disease and ulcerative colitis in a commercially insured US population. Dig Dis Sci 58:519-525.

Kaser A, Zeissig S, Blumberg RS (2010) Genes and environment: how will our concepts on the pathophysiology of IBD develop in the future? Dig Dis 28:395-405.

Lin J, Hackam DJ (2011) Worms, flies and four-legged friends: the applicability of biological models to the understanding of intestinal inflammatory diseases. Dis Model Mech 4:447-456.

Liu W, Singh SR, Hou SX (2010) JAK-STAT is restrained by Notch to control cell proliferation of the *Drosophila* intestinal stem cells. J Cell Biochem 109:992-999.

Menozzi A, Pozzoli C, Poli E, Lazzaretti M, Grandi D, Coruzzi G (2006) Long-term study of TNBS-induced colitis in rats: focus on mast cells. Inflamm Res 55:416-422.

Morris GP, Beck PL, Herridge MS, Depew WT, Szewczuk MR, Wallace JL (1989) Hapten-induced model of chronic inflammation and ulceration in the rat colon. Gastroenterology 96:795-803.

Motavallian-Naeini A, Andalib S, Rabbani M, Mahzouni P, Afsharipour M, Minaiyan M (2012) Validation and optimization of experimental colitis induction in rats using 2, 4, 6-trinitrobenzene sulfonic acid. Res Pharm Sci 7:159-169.

Ng SC, Bernstein CN, Vatn MH, Lakatos PL, Loftus EV, Jr., Tysk C, O'Morain C, Moum B, Colombel JF, Epidemiology and Natural History Task Force of the International Organization of Inflammatory Bowel Disease (IOIBD) (2013) Geographical variability and environmental risk factors in inflammatory bowel disease. Gut 62:630-649.

Perse M, Cerar A (2012) Dextran sodium sulphate colitis mouse model: traps and tricks. J Biomed Biotechnol 2012:718617.

Piepoli AL, De Salvatore G, De Salvia MA, Mitolo CI, Siro-Brigiani G, Marzullo A, Grattagliano I, Mitolo-Chieppa D, Palasciano G, Portincasa P (2005) Indomethacin-induced ileitis is associated with tensiometric, vascular and oxidative changes in the experimental rat model. Eur J Clin Invest 35:271-278.

Qin HY, Xiao HT, Wu JC, Berman BM, Sung JJ, Bian ZX (2012) Key factors in developing the trinitrobenzene sulfonic acid-induced post-inflammatory irritable bowel syndrome model in rats. World J Gastroenterol 18:2481-2492.

Rose WA, 2nd, Sakamoto K, Leifer CA (2012) Multifunctional role of dextran sulfate sodium for in vivo modeling of intestinal diseases. BMC Immunol 13:41.

Scheiffele F, Fuss IJ (2002) Induction of TNBS colitis in mice. Curr Protoc Immunol Chapter 15:Unit 15 19.

Strober W, Ludviksson BR, Fuss IJ (1998) The pathogenesis of mucosal inflammation in murine models of inflammatory bowel disease and Crohn disease. Ann Intern Med 128:848-856.

te Velde AA, Verstege MI, Hommes DW (2006) Critical appraisal of the current practice in murine TNBS-induced colitis. Inflamm Bowel Dis 12:995-999.

Terai T, Osawa S, Tani S, Oishi S, Arai Y, Yamada T, Sugimoto M, Furuta T, Kanaoka S, Miyajima H, Sugimoto K (2014) Induction of murine TNBS colitis is strictly controlled by a modified method using continuous inhalation anesthesia with sevoflurane. Dig Dis Sci 59:1415-1427.

Vatn MH (2008) Recent research in IBD epidemiology. Gastroenterol Hepatol (N Y) 4:413-415.

Yamada T, Deitch E, Specian RD, Perry MA, Sartor RB, Grisham MB (1993) Mechanisms of acute and chronic intestinal inflammation induced by indomethacin. Inflammation 17:641-662.

Yamada Y, Marshall S, Specian RD, Grisham MB (1992) A comparative analysis of two Models of colitis in rats. Gastroenterology 102:1524-1534.

Yen L, Wu J, Hodgkins PL, Cohen RD, Nichol MB (2012) Medication use patterns and predictors of nonpersistence and nonadherence with oral 5-aminosalicylic acid therapy in patients with ulcerative colitis. J Manag Care Pharm 18:701-712.

Zhang Y, Zhou R, Zhou F, Cheng H, Xia B (2014) Total glucosides of peony attenuates 2,4,6-trinitrobenzene sulfonic acid/ethanol-induced colitis in rats through adjustment of Th1/Th2 cytokines polarization. Cell Biochem Biophys 68:83-95.

Volume 58(2):133-137, 2014
Acta Biologica Szegediensis
http://www2.sci.u-szeged.hu/ABS

ARTICLE

Development and validation of an LC-MS/MS method for the analysis of L-DOPA in oat

Erika Varga, Mónika Varga*

Cereal Research Non-Profit Ltd. Co., Szeged, Hungary

ABSTRACT L-DOPA (L-3,4-dihydroxyphenylalanine), currently the most effective known therapeutic agent for the symptomatic relief of Parkinson's disease, is one of the highly active allelochemicals that inhibit the growth and development of certain plant species. A tropical legume, *Mucuna pruriens*, has been shown to contain from 2 to 7% L-DOPA. However, little is known about the L-DOPA contents of other plants. The aim of our work was to develop and validate a simple method for the LC-MS/MS determination of L-DOPA in different oat varieties. During the development of the method, various LC and MS parameters were optimized from the aspect of sensitivity. In the final method, the calibration curve was linear over the concentration range 10-10,000 pg/µl. L-DOPA could be detected at 18 µg/kg level through use of the $[(M+H)-NH_3]^+$ fragment of the $[M+H]^+$ molecular ion. The intraday precision and accuracy were all within acceptable ranges.

Acta Biol Szeged 58(2):133-137 (2014)

KEY WORDS

oat
L-DOPA
LC-MS/MS
validation

L-DOPA (L-3,4-dihydroxyphenylalanine) is currently widely accepted as the most effective therapeutic agent for the symptomatic relief of Parkinson's disease. This compound is produced by certain plants, and especially a tropical legume, *Mucuna pruriens* or velvet bean, which has been reported to contain up to 7% L-DOPA (Daxenbichler et al. 1971). *M. pruriens* is used in the traditional Indian therapeutics and a number of attempts have been made to utilize it as a modern medicine (Nagashayana et al. 2000). On the other hand, the legume demonstrates a significant allelopathic effect, which means that other plants can hardly live in its vicinity. This phenomenon has been ascribed to its high L-DOPA content (Nishihara et al. 2004). Allelopathic plants and allelochemicals are of considerable potential in agriculture as their application has the result that the amounts of artificial fertilizers can then be significantly decreased with them. If this is to be achieved, extended experiments are needed as regards the allelochemical contents of different plants. The aim of the present study was the determination of L-DOPA in oat, certain species of which exhibit notable allelopathy (Schumacher et al. 1983; Bertoldi et al. 2009)

Various methods are available for the quantitative analysis of L-DOPA. Modern capillary electrophoresis and high performance liquid chromatography (HPLC) methods are proper (Tsunoda 2006; Shalini et al. 2011), but the selectivity can be further increased by mass spectrometric (MS) detection, especially if the MS/MS mode is at hand (Manini et al. 2000; Bourcier et al. 2006).

Accepted Dec 2, 2014
*Corresponding author. E-mail: vargam@gabonakutato.hu

We therefore set out to develop and validate a simple method for the LC-MS/MS determination of L-DOPA in different oat varieties.

Materials and Methods

Materials

L-DOPA and L-tyrosine standards were purchased from SERVA (Hungary), while α-methyldopa, ascorbic acid standards and formic acid, acetic acid and ammonium acetate were from Sigma-Aldrich (Hungary). Membrane-filtered, deionized water for HPLC runs was produced with Millipore (Merck, Hungary) water purification equipment. HPLC-grade acetonitrile (ACN), methanol (MeOH) were purchased from Molar Chemicals (Hungary).

Stock solutions of L-DOPA, L-tyrosine and α-methyldopa were prepared by dissolution of the solid standards in an aqueous solution of 0.1% (v/v) formic acid and 0.1% (m/v) ascorbic acid to obtain a concentration of 1 mg/ml. Stock solutions were diluted to the necessary concentrations, typically to 10 ng/µl for parameter optimizations.

HPLC parameters

HPLC investigations were performed on an Agilent 1100 (Agilent, Palo Alto, USA) modular HPLC system, equipped with a degasser (G1379A), a binary pump (G1376A) and a micro-well plate autosampler (G1229A).

Separation was carried out on a Synergi Hydro-RP 250 x 2 mm, 4 µm analytical column (Gen-Lab, Hungary) in front of which a Hydro-RP 4 x 2.0 mm guard column (Gen-Lab,

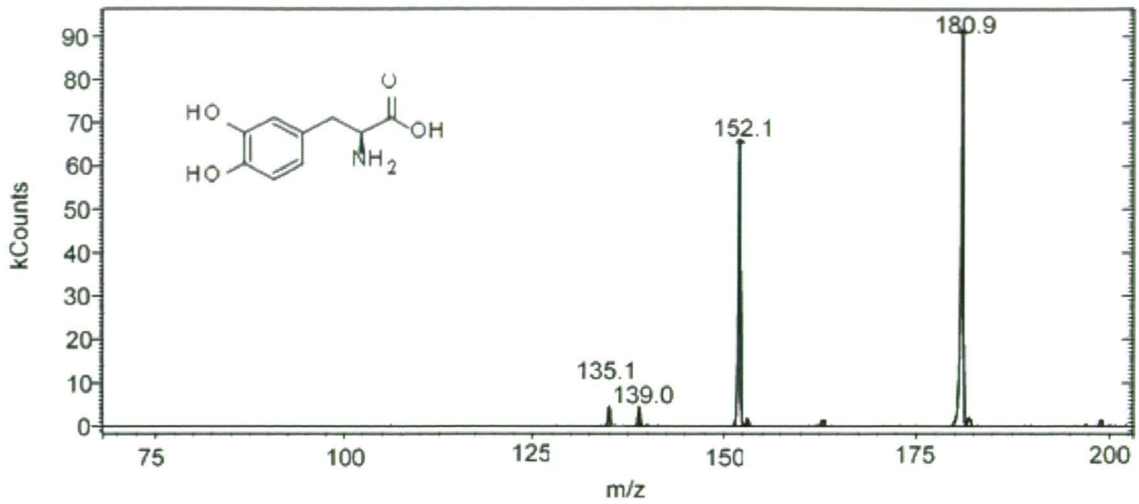

Figure 1. MS/MS spectrum of the L-DOPA after fragmentation of the molecular ion $[M+H]^+$ (*m/z* 198.2).

Hungary) was situated. The column temperature was maintained at 30 °C with a Jones Model 7990 Space column heater (Jones Chromatography, UK). Eluent A consisted of 0.1% (v/v) formic acid and 3% (v/v) eluent B. Eluent B contained ACN/MeOH at a volume ratio of 75/25 containing 0.1% (v/v) formic acid. The gradient elution started with 0% B, which was increased linearly to 100% B within 5 min, held there for 2 min, then decreased to 0% in 3 min, and kept there for 5 min. Before the next injection, a 5 min equilibration period was held. The flow rate was set to 200 µl/min. The injection volume was 5 µl. The retention times of L-DOPA, L-tyrosine and α-methyldopa were 5, 6.5 and 7.8 min, respectively.

The HPLC was controlled by Chemstation B.02.01 software.

Ion trap MS conditions

The MS measurements were performed with a Varian 500MS Ion Trap mass spectrometer equipped with an electrospray ionization (ESI) source. The ion trap parameters were tuned in positive ion mode by continuous infusion (5 µl/min) of the standard solutions (10 ng/µl) with the built-in syringe pump of the instrument. The parameters were set as follows: capillary voltage, 45V, RF loading, 67%; needle voltage, 4350 V; spray shield voltage, 600 V; fragmentation voltages, 0.5, 0.71 and 1.86 V for L-DOPA, L-tyrosine and α-methyldopa, respectively. The ion source parameters were optimized in flow injection analysis without a column. In the final experiments the ion source parameters were as follows: spray chamber temperature, 50 °C; drying gas (N_2) pressure and temperature, 25 psi and 350 °C, respectively; nebulizer gas (N_2) pressure, 60 psi.

The MS was controlled by MS Workstation 6.6 software.

Sample preparation

GK Iringo, *GK Kormorán* and *GK Zalán* were chosen as a probe oat species. They were grown in an experimental field in Kiszombor and Újszeged (Csongrád County, Hungary). The *M. pruriens* seeds were grown in greenhouse. The seeds were finely ground with a laboratory grinder and 1 g of the powder was soaked in 6 ml of an aqueous solution of 0.1% (m/v) ascorbic acid and 1% (v/v) MeOH. The mixture was shaken vertically with a Stuart STR4 vertical shaker for 5 h, then centrifuged at 4500 rpm for 5 min. The supernatant was filtered through a GF/B glass microfiber filter. Twenty µl of 0.6 µg/ml internal standard α-methyldopa solution was added to 1 ml of the filtered extract.

Results and Discussion

The development of this method related not only to L-DOPA, but also to its biological precursor, L-tyrosine. α-Methyldopa was selected as internal standard and added to the samples immediately before the analysis in order to correct for the fluctuations in the MS performance.

Because of the H^+-accepting property of the amino group (El Aribi et al. 2004) positive ion mode was applied for the detection of the analytes. Under ESI conditions, L-DOPA (L-tyrosine and α-methyldopa too) can be effectively transformed into a protonated ion. The fragmentation of $[(M+H)]^+$ yields different fragment ions (Fig. 1), the most abundant in the case of L-DOPA being $[(M+H)\text{-}NH_3]^+$ at m/z 181 and $[(M+H)\text{-}H_2O\text{-}CO]^+$ at m/z 152. To obtain the highest $[(M+H)\text{-}NH_3]^+$ fragment peak intensity (m/z 181, 165 and 195 for L-DOPA, L-tyrosine and α-methyldopa, respectively), optimization of the ESI parameters was carried out.

The effects of the nebulizer gas pressure and temperature

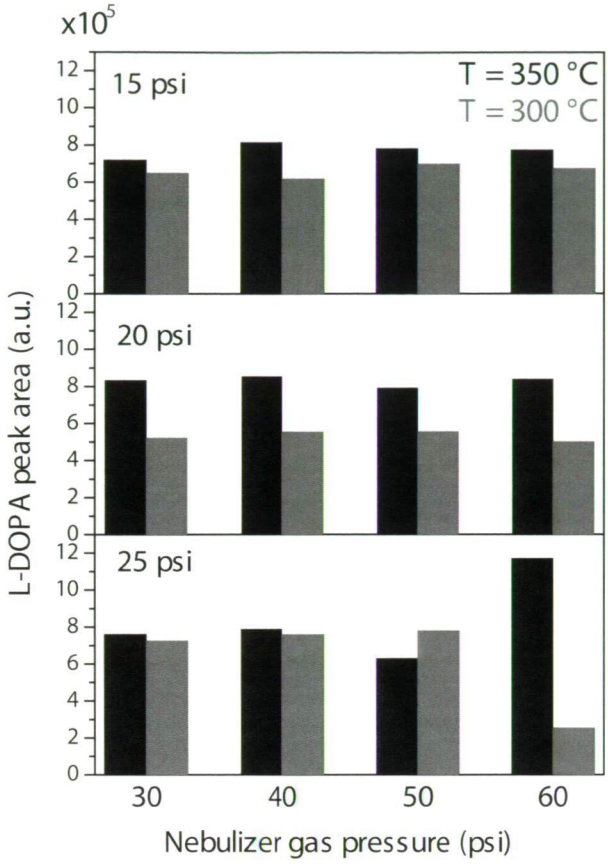

Figure 2. The effect of the nebulizer gas (x axis) and drying gas pressures (upper left hand corners) on the L-DOPA signal. The experiments were carried out at two different nebulizer gas temperatures (350 and 300 °C, black and grey bars).

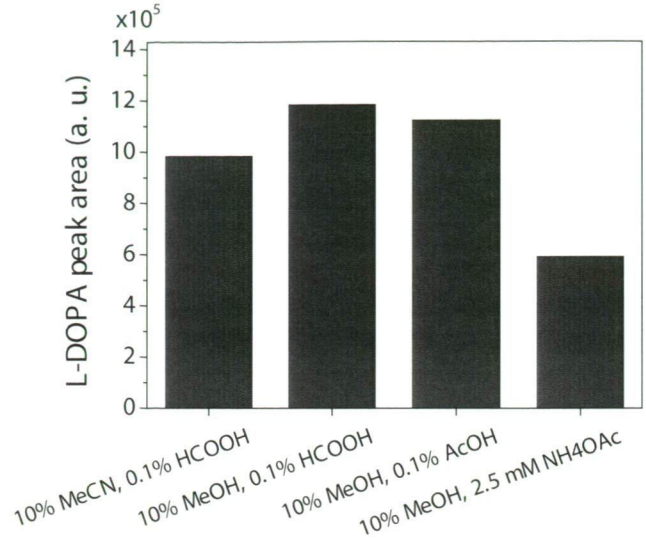

Figure 3. The effect of different mobile phase composition on the L-DOPA signal.

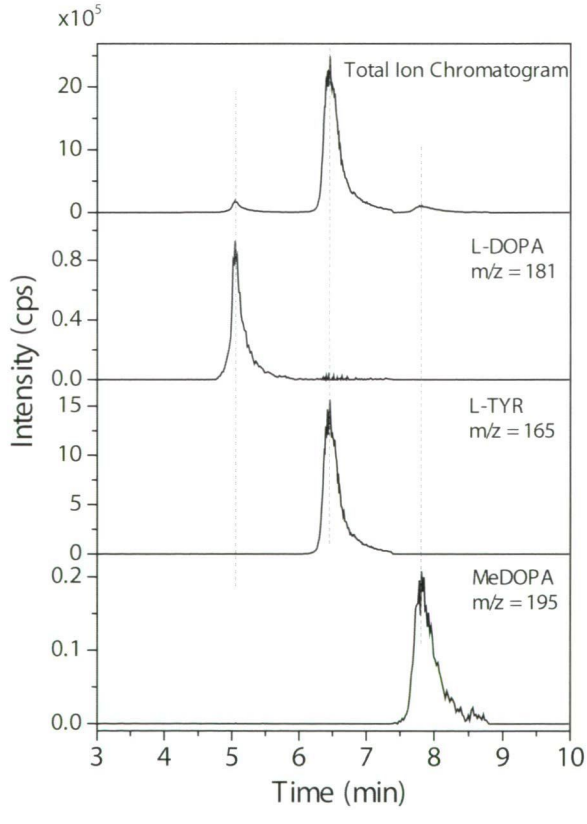

Figure 4. Total ion chromatogram and selected ion chromatograms for L-DOPA, L-tyrosine and α-methyldopa of the *GK Kormorán* variety.

and the drying gas pressure were studied. The results revealed that the investigated parameters did not have significant effects on the ionization efficiency of L-DOPA (Fig. 2). However, an outstanding intensity was observed at a nebulizer gas pressure of 60 psi and a drying gas pressure of 25 psi at a nebulizing gas temperature of 350 °C.

After the establishment of the MS parameters, the influence of the mobile phase composition on the efficiency of L-DOPA ionization was investigated via flow injection analysis by using acetonitrile, methanol, formic acid, acetic acid and ammonium acetate. It was found that formic acid and acetic acid were more suitable than ammonium acetate as mobile phase additives (Fig. 3). No matter which individual solvent was used, there was no marked effect on the signal intensity. On the other hand, in the course of the HPLC separation, methanol provides higher selectivity, while acetonitrile has lower viscosity. In order to take advantage of both of these beneficial features, ACN/MeOH mixture was chosen as eluent B at 75/25 (v/v), and eluent A also contained 3% (v/v) of eluent B. Gradient elution proved suitable for the total separation of the L-DOPA, L-tyrosine and α-methyldopa signals (Fig. 4).

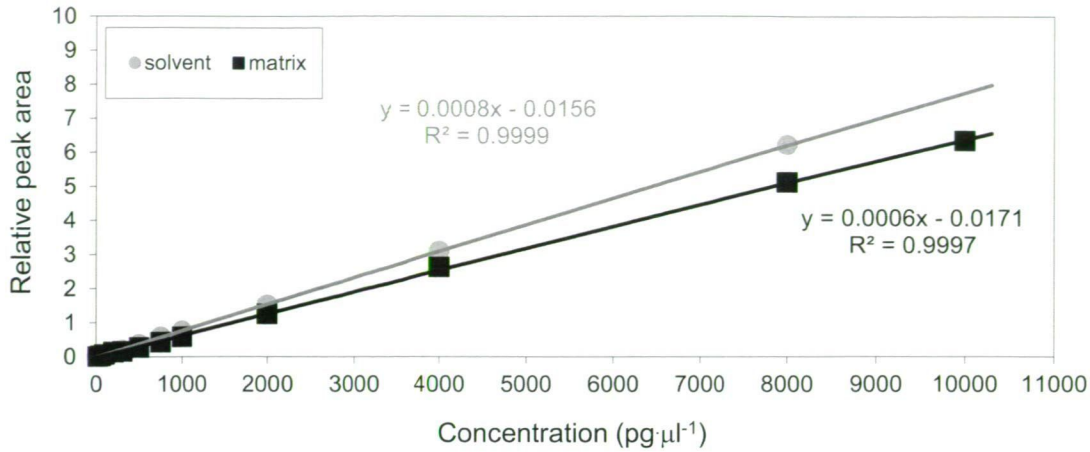

Figure 5. Calibration curves created by dilution with the extraction solvent (0.1% (m/v) ascorbic acid and 1% (v/v) MeOH) and corn extract (blank matrix).

In order to test the linearity of the response versus the amount of L-DOPA injected, various concentrations of standard solutions in the range from 10 to 10 000 pg/µl were analyzed. Figure 5 presents two calibration curves. The stock solution of the analyte was diluted with the extraction solvent, or with corn extract (blank matrix). Both plots exhibited good linearity throughout the whole concentration range. Observations in plant analytical chemistry (Dams et al. 2003; Lattanzio et al. 2007) indicate that the slopes of the calibration curves differed due to the matrix effect. The ionization of L-DOPA is suppressed by the matrix components: the response is 1.35 times higher in the absence of the matrix.

During validation of the method the mean recoveries of four replicates at three different spiking levels (0.6, 3 and 6 mg/kg) were 95.2%, 99.6% and 95.2%, respectively. The repeatability of the measurements was calculated by performing four injections of one of the spiked sample extracts. RSD % was found to be better than 4%, as were the intraday precision and accuracy. The limit of detection was 15 pg or 18 µg/kg (*S/N*=3).

The validated method was applied for the determination of the L-DOPA contents of different oat varieties. Some *M. pruriens* seeds were also analyzed, for comparison (Table 1.). It was concluded that the concentration of L-DOPA in oat varies within the interval 2-20 mg/kg, which is three orders of magnitude lower than that in *M. pruriens* samples. A further important observation was made that the L-DOPA content depends not only on the variety, but also on the time of harvesting and the production site.

Table 1. L-DOPA content of some selected oat species and *Mucuna pruriens* samples.

Sample	L-DOPA content (mg/kg)
GK Iringó	10.02
GK Zalán	2.17
GK Kormorán (Kiszombor, 2007.)	7.83
GK Kormorán (Kiszombor, 2008.)	2.27
GK Kormorán (Kiszombor, 2009.)	3.88
GK Kormorán (Újszeged, 2009.)	11.89
M. pruriens 1.	37423
M. pruriens 2.	64019

Acknowledgements

This research was supported by the European Union and the State of Hungary, co-financed by the European Social Fund in the framework of TÁMOP-4.2.4.A/ 2-11/1-2012-0001 'National Excellence Program'.

References

Bertoldi C, Leo M, Braca A, Ercoli L (2009) Bioassay-guided isolation of allelochemicals from *Avena sativa* L.: allelopathic potential of flavone C-glycosides. Chemoecology 19:169-176.

Bourcier S, Benoist JF, Clerc F, Rigal O, Taghi M, Hoppilliard Y (2006) Detection of 28 neurotransmitters and related compounds in biological fluids by liquid chromatography/tandem mass spectrometry. Rapid Commun Mass Spectrom 20:1405-1421.

Dams R, Huestis MA, Lambert WE, Murphy CM (2003) Matrix effect in bio-analysis of illicit drugs with LC-MS/MS: influence of ionization type, sample preparation, and biofluid. J Amer Soc Mass Spectrom 14:1290-1294.

Daxenbichler ME, VanEtten CH, Hallinan EA, Earle FR, Barclay AS (1971) Seeds as sources of L-DOPA. J Med Chem 14:463-465.

El Aribi H, Orlova G, Hopkinson AC, Siu KWM (2004) Gas-phase fragmentation reactions of protonated aromatic amino acids: concomitant and consecutive neutral eliminations and radical cation formations. J Phys Chem A 108:3844-3853.

Lattanzio VM, Solfrizzo M, Powers S, Visconti A (2007) Simultaneous determination of aflatoxins, ochratoxin A and *Fusarium* toxins in maize by liquid chromatography/tandem mass spectrometry after multitoxin immunoaffinity cleanup. Rapid Commun Mass Spectrom 21:3253-3261.

Manini P, Andreoli R, Cavazzini S, Bergamaschi E, Mutti A, Niessen WNA (2000) Liquid chromatography-electrospray tandem mass spectrometry

of acidic monoamine metabolites. J Chromatogr B 744:423-431.

Nagashayana N, Sankarankutty P, Nampoothiri MRV, Mohan PK, Mohanakumar KP (2000) Association of (L)-DOPA with recovery following Ayurveda medication in Parkinson's disease. J Neurol Sci 176:124-127.

Nishihara E, Parvez MM, Araya H, Fujii Y (2004) Germination growth response of different plant species to the allelochemical L-3,4-dihydroxyphenylalanine (L-DOPA). Plant Growth Reg 42:181-189.

Schumacher WJ, Thill DC, Gary LA (1983) Allelopathic potential of wild oat (*Avena fatua*) on spring wheat (*Triticum aestivum*) growth. J Chem Ecol 9:1235-1245.

Shalini S, Reddy RY (2011) Method development and validation of levodopa and carbidopa in a combined dosage form by RP-HPLC method. Int J Pharm Technol 3:2943-2960.

Tsunoda M (2006) Recent advances in methods for the analysis of catecholamines and their metabolites. Anal Bioanal Chem 386:506-514.

Volume 58(2):139-146, 2014
Acta Biologica Szegediensis
http://www2.sci.u-szeged.hu/ABS

ARTICLE

Expression of a bacterial β-carotene hydroxylase in canthaxanthin producing mutant *Mucor circinelloides* strains

Árpád Csernetics[1]*, Eszter Tóth[1], Anita Farkas[1], Gábor Nagy[1], Ottó Bencsik[1], Palanisamy Manikandan[2,3], Csaba Vágvölgyi[1] and Tamás Papp[1]

[1]Department of Microbiology, Faculty of Science and Informatics, University of Szeged, Szeged, Hungary, [2]Department of Laboratory Medical Sciences, College of Applied Medical Sciences, Majmaah University, Kingdom of Saudi Arabia, [3]Aravind Eye Hospital and Postgraduate Institute of Ophthalmology, Coimbatore, Tamil Nadu, India

ABSTRACT Xanthophylls, primarily hydroxyl- and keto-derivatives of β-carotene (such as zeaxanthin, β-cryptoxanthin, canthaxanthin, echinenone and astaxanthin) have powerful antioxidant activity. Due to several positive effects on human and animal health, industrial application of xanthophylls shows an increasing tendency. In our previous study, carotenoid biosynthesis of the β-carotene producing zygomycetes, *Mucor circinelloides* was modified by integrating the β-carotene ketolase encoding gene (*crtW*) of *Paracoccus* sp. N81106 into the genome. The isolated mutants accumulated mainly canthaxanthin and echinenone. Although, the fungus has β-carotene hydroxylase activity the astaxanthin production remained low even under different cultivation conditions, whereby canthaxanthin accumulation was further enhanced. In this study, the β-carotene hydroxylase encoding gene (*crtZ*) of the same bacterium was introduced into these canthaxanthin producing mutants of *M. circinelloides* either on autonomously replicating plasmids or by integrating it into the genome using the REMI method. Increased astaxanthin accumulation was observed in the transformants, which together with zeaxanthin and β-cryptoxanthin content could be further enhanced several fold by the modification of the cultivation conditions. An effective method for the extraction of carotenoids from *Mucor* mycelia grown in liquid culture was also developed. **Acta Biol Szeged 58(2):139-146 (2014)**

KEY WORDS

Paracoccus sp. N81106
β-carotene hydroxylase
heterologous expression
carotenoid extraction
astaxanthin

Mucor circinelloides (Mucoromycotina) is an intensively studied carotenoid producing zygomycetes; well-developed transformation systems are available for the fungus and most of the genes involved in the carotenoid biosynthesis have been isolated and characterized (Velayos et al. 2000a, 2000b, 2003, 2004; Papp et al. 2006, 2010; Csernetics et al. 2011). Carotenoids are tetraterpene molecules and synthesized via the mevalonate – isoprenoid pathway in fungi. Condensation of two molecules of geranylgeranyl pyrophosphate, several dehydrogenation and two cyclisation steps lead to the formation of β-carotene in *M. circinelloides* (Fig. 1.), which is the major carotenoid compound in the fungus, but intermediates (such as lycopene and γ-carotene) are also accumulated (Velayos et al. 2000a, 2000b; Csernetics et al. 2011; Papp et al. 2013). Furthermore, *M. circinelloides* shows a weak β-carotene hydroxylase activity, therefore it is able to synthesize zeaxanthin (3,3′-dihydroxy-β,β-carotene) and β-cryptoxanthin (3-hydroxy-β,β-carotene) (Papp et al. 2006, 2013; Csernetics et al. 2011). At the same time, several microorganisms, such as *Paracoccus* sp. N81106 able to accumulate canthaxanthin (β,β-carotene-4,4'-dione), echinenone (β,β-carotene-4-on) and astaxanthin (3,3′-dihydroxy-β,β-carotene-4,4′-dione) as well; formation of astaxanthin from β-carotene requires a β-carotene hydroxylase and a ketolase activity (Misawa et al. 1995). These xanthophylls have powerful antioxidant properties and their preventive action against different types of cancer, age-related macular degeneration, heart- or bone disease makes them dietary important (Chew et al. 1999; Nishino et al. 2002; Mares-Perlman et al. 2002; Guerin et al. 2003; Beatty et al. 2004; Yamaguchi 2004; Kumaresan et al. 2008). Besides, they are frequently used in pharmaceutical and cosmetic industry and also in feed additives (Bhosale and Bernstein 2005). Today, most of the commercially available xanthophylls are synthesized chemically. Biosynthesis of astaxanthin is limited to microorganisms and along with other carotenoids an increasing demand can be observed to replace chemical synthesis with natural sources (Bhosale and Bernstein 2005).

In our previous studies, *crtW* and *crtZ* genes of the *Paracoccus* sp. N81106, encoding β-carotene ketolase and hydroxylase, respectively, were expressed in *M. circinelloides*

Accepted Dec 11, 2014
*Corresponding author. E-mail: csernetics.arpad@gmail.com

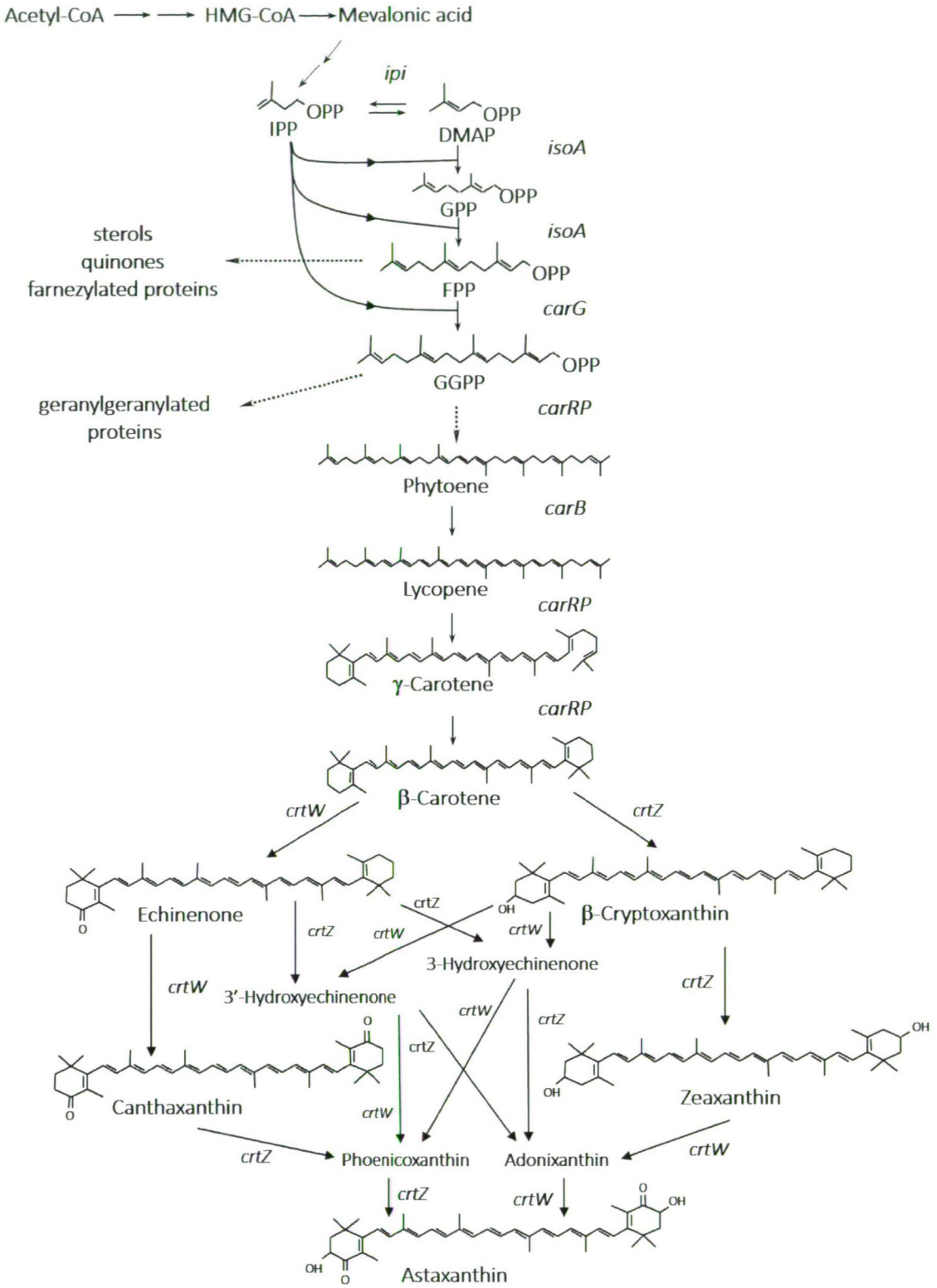

Figure 1. Carotenoid biosynthesis pathway in *M. circinelloides* and possible steps of the β-carotene – astaxanthin conversion in *M. circinelloides* transformants harbouring the *Paracoccus* sp. N81106 *crtW* and *crtZ* genes (based on Misawa et al. 1995). HMG-CoA – 3-hydroxy-3-methylglutaryl-CoA; IPP – isopentenyl pyrophosphate; DMAP – dimethylallyl pyrophosphate; GPP – geranyl pyrophosphate; FPP – farnesyl pyrophosphate; GGPP – geranylgeranyl pyrophosphate. *M. circinelloides* genes: *ipi* – IPP isomerase; *isoA* – FPP synthase; *carG* – GGPP synthase; *carRP* – phytoene synthase/lycopene cyclase; *carB* – phytoene desaturase. *Paracoccus* sp. N81106 genes: *crtZ* – β-carotene hydroxylase and *crtW* – β-carotene ketolase.

MS12 strain on autonomously replicating plasmids (Papp et al. 2006). Introduction of the *crtZ* enhanced the zeaxanthin and β-cryptoxanthin accumulation, while introduction of the *crtW* lead to the presence of canthaxanthin, echinenone and astaxanthin in low amount. Co-expression of the *crtZ* and *crtW* genes increased the canthaxanthin and β-cryptoxanthin production compared to the introduction of only the single *crtW* (Papp et al. 2006). Integration of the *Paracoccus crtW* gene into the *Mucor* genome by double homologous recombination and restriction enzyme-mediated integration (REMI) led to transformants accumulating 123-148 μg g^{-1} canthaxanthin and 117-135 μg g^{-1} echinenone [dry mass] (Papp et al. 2013). At the same time, production of astaxanthin remained low in these transformants. It is supposed that the endogenous β-carotene hydroxylase has poor activity and able to convert canthaxanthin to astaxanthin with low efficiency (Papp et al. 2013). Another explanation could be that *Mucor* β-carotene hydroxylase does not able to catalyse this conversion but the low amounts of zeaxanthin and β-cryptoxanthin accumulated by the fungus may serve as substrates to the *Paracoccus* β-carotene ketolase to form low amount of astaxanthin.

In this study, our aim was to express the *crtZ* gene of *Paracoccus* sp. N81106 in canthaxanthin producing mutants of *M. circinelloides* to enhance the astaxanthin accumulation. The *crtZ* was introduced on autonomously replicating plasmids and, in parallel, it was integrated into the *Mucor* genome using the REMI method. Carotenoid content of the resulting transformants and effect of different culturing conditions on their carotenoid composition were also investigated.

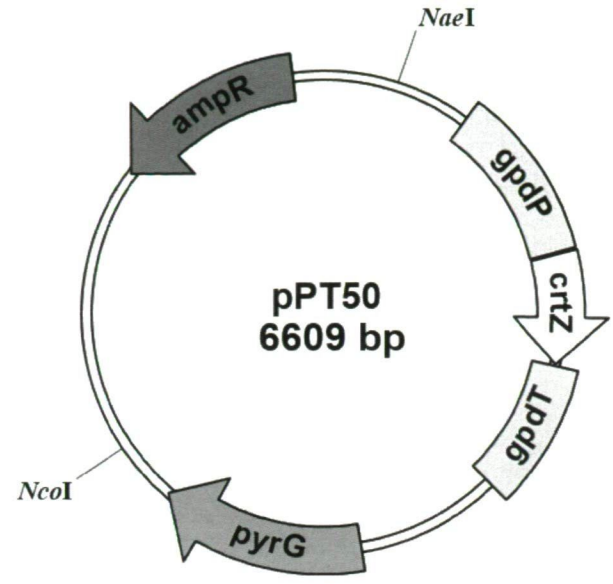

Figure 2. Plasmid construction used to transform the canthaxanthin producing mutants MS12+pCA8lf/1 and MS12+pPT51'R3/2. The plasmid harbours the *Paracoccus* sp. N81106 *crtZ* gene encoding a β-carotene hydroxylase between the *Mucor gpd1* promoter and terminator regions. The *Mucor pyrG* gene is responsible for the complementation of the uracil auxotrophy and *ampR* (gene for ampicillin resistance) for the bacterial selection. The fragment obtained by digesting with the restriction enzymes *Nae*I and *Nco*I corresponds to pPT50'R used for REMI transformation.

Materials and Methods

Strains, media and growth conditions

The *M. circinelloides* strains, MS12+pCA8lf/1 and MS12+pPT51'R3/2, which have *leuA*$^+$, *pyrG*$^-$, *crtW*$^+$ genotype (Papp et al. 2013) and are derived from the *leuA*$^-$, *pyrG*$^-$mutant MS12 (Benito et al. 1992), were used in the transformation experiments. These strains are auxotrophic for uracil and harbours the *crtW* gene encoding the β-carotene ketolase of *Paracoccus* sp. N81106 (formerly *Agrobacterium aurantiacum*) integrated into their genome by homologous double recombination (MS12+pCA8lf/1) or REMI (MS12+pPT51'R3/2) methods. Both strains accumulate mainly canthaxanthin and echinenone and small amount of astaxanthin (Papp et al. 2013).

Escherichia coli TOP10F$^-$ was used in plasmid amplifications. *E. coli* was cultivated on Luria-Bertani medium (LB, 10 g tryptone; 5 g yeast extract; 10 g NaCl and 20 g agar for solid medium per litre) containing 100 μg mL^{-1} ampicillin at 37 °C.

For growth tests, nucleic acid and carotenoid extraction, *M. circinelloides* strains were cultivated on solid minimal medium (YNB, 10 g glucose; 0.5 g yeast nitrogen base without amino acids; 1.5 g $(NH_4)_2SO_4$, 1.5 g sodium glutamate and 20 g agar per litre) supplemented with uracil and leucine (0.5 mg mL^{-1}) if required. Fungal cultures were grown for 4 days at 25 °C under continuous light. Effect of cultivation temperature on carotenoid accumulation of the fungal strains was tested on YNB plates at 20, 25, 30 and 37 °C. To examine the effect of carbon sources on carotenoid production, glucose was replaced with fructose, trehalose, mannose, galactose, glycerol-L-monoacetate, dihydroxyacetone and L-aspartic acid in a final concentration of 1% in YNB. Combinations of different carbon sources were also tested. The carotenoid content was also determined from liquid cultures when strains were grown in YNB medium without agar for 6 days on 25 °C under continuous light and shaking (110 rpm). Mycelia were separated from the media by filtration using 0.45 μm pore size filters (Millipore).

For growth test, 10^5 spores were inoculated onto the centre of YNB plates. To test the mitotic stability of the transformants solid malt extract medium (MEA, 10 g glucose; 10 g malt extract; 5 g yeast extract and 20 g agar per litre) was used as a complete medium.

Molecular techniques

Purification of plasmid DNA was performed with the Viogene Mini Plus and Midi Plus Plasmid DNA Extraction Systems (Viogene). DNA fragments were purified from agarose gel

Table 1. Different methods and solvents tested to improve the carotenoid extraction efficiency from liquid cultures.

Extraction method	Pre-treatment		Extraction solvent
Conventional [a]	-		Acetone Petroleum ether DMSO, partition in petroleum ether DMSO, partition in hexane
Reduction of the moisture content	Lyophilisation for 45 min. Drying at 40 °C overnight		Acetone and petroleum ether
	Desiccation with Na_2SO_4	10% 20% 50% 100%	
Pre-treatment with lactic acid	0.2 M 0.3 M 0.4 M 0.5 M 2 M 3 M 4 M 5 M	heating to 120 °C heating to 50 °C	Acetone

[a] The method, which was used for solid cultures and described in Materials and Methods, is regarded as the conventional method.

using the Silica Bead DNA Gel Extraction Kit (Thermo Scientific). General procedures for plasmid DNA manipulation, transformation of *E. coli* and Southern blotting were performed by following standard methods (Sambrook et al. 1989). For fungal DNA preparation, mycelium was disrupted with a pestle and mortar in liquid nitrogen and DNA was isolated according to Iturriaga et al. (1992). *CrtZ* gene probe for Southern hybridization was constructed by amplifying a DNA fragment from the plasmid pPT50 using the crtZ1 (5' ATG ACC AAT TTC CTG ATC 3') and crtZ2 (5' CGT GCG CTC CTG CGC CTC 3') primers and the digoxigenin-based PCR DIG Probe Synthesis Kit (Roche). The DIG Nucleic Acid Detection Kit (Roche) was used for immunological detection of the nucleic acid blots, following the instructions of the manufacturer.

Plasmid construction and transformation

The plasmid pPT50 harbouring the *crtZ* gene of *Paracoccus* sp. N8106 under the control of the promoter and terminator regions of the *Mucor* glyceraldehyde-3-phosphate dehydrogenase (*gpd1*) gene was used in all transformation experiments (Fig. 2) (Papp et al. 2006). As a selection marker, the plasmid holds the *Mucor pyrG* encoding the orotidine-5'-phosphate decarboxylase, which complements the uracil auxotrophy of *M. circinelloides* strains MS12+pCA8lf/1 and MS12+pPT51'R3/2.

For PEG/$CaCl_2$-mediated transformation, protoplasts of *M. circinelloides* were prepared following the next steps: spores of MS12+pCA8lf/1 and MS12+pPT51'R3/2 were harvested from four days old cultures and inoculated into small drops onto cellophane sheets placed on YNB media supplemented with uracil and grown at 25 °C for 16 h. Colonies were washed in protoplast-forming solution (10 mM sodium-phosphate buffer, pH 6.4; 0.8 M sorbitol; 1.5% home-made snail enzyme) and incubated at 25 °C for 3 h under continuous gentle shaking. Protoplasts were separated from the mycelia by filtration through 3 sheets of gauze. Protoplasts were collected by centrifugation (3200 rpm, 15 min, 4 °C), washed with SMC buffer (50 mM $CaCl_2$; 10 mM 3-(N-morpholino) propanesulfonic acid and 0.8 M sorbitol) and re-suspended in 0.25 ml SMC. Thereafter, the PEG/$CaCl_2$-mediated transformation of MS12+pCA8lf/1 and MS12+pPT51'R3/2 protoplasts with circular plasmid was performed according to van Heeswijck and Roncero (1984). For REMI, the pPT50 plasmid was digested with *Nae*I - *Nco*I enzymes (to avoid the re-circularization) and the resulting pPT50'R linear fragment, which harboured the *crtZ* gene fused with the *gpd1* promoter and terminator regions and the *pyrG* gene, was introduced into the recipient MS12+pCA8lf/1. The REMI transformation of protoplasts was performed according to the PEG/$CaCl_2$-mediated transformation method, except that 30-30 U restriction enzymes used for preparation of the linearized DNA were added to the protoplasts together with 5-10 µg linear fragment and the solution was incubated for 0.5 h on ice and 1.5 h at 33 °C. Transformants were selected on the basis of auxotrophy complementation on YNB solid medium. Introduction of the pPT50 plasmid into MS12+pCA8lf/1 and MS12+pPT51'R3/2 resulted the MS12+pCA8lf/1+pPT50 and MS12+pPT51'R3/2+pPT50, while introduction of the pPT50'R fragment into MS12+pCA8lf/1 resulted the MS12+pCA8lf/1+pPT50'R transformants.

Carotenoid extraction and analysis

Carotenoids were extracted from 500 mg mycelial powder

with 700 µl acetone and vortexing (Papp et al. 2006). This extraction step was repeated until the pellet was found to be devoid of pigments. Extracts were collected in 50 ml Falcon tube, combined and partitioned in an equal volume of 10% diethyl ether in petroleum ether. To facilitate the separation 2 ml distilled water was added and centrifuged (3200 rpm, 8 min, 4 °C). The petroleum ether fraction was dried under nitrogen. To determine the dry mass, 500 mg mycelial powder was dried at 70 °C overnight.

The carotenoid extraction was performed from liquid cultures, as well. Filtrated *Mucor* mycelia was disrupted with liquid nitrogen and was partitioned to test different extraction methods, such as lyophilisation, drying at 40 °C or desiccation with sodium-sulphate with different concentrations, solvents (such as acetone, petroleum ether and DMSO) and acid pre-treatment combined with heating (0.2-5 M lactic acid at 50-120 °C) (Table 1). Other steps of the extraction were performed as described above.

For high-performance liquid chromatography (HPLC), samples and standards were analysed by using a modular Shimadzu low-pressure gradient HPLC system. The dried samples were re-dissolved in 100 µl tetrahydrofuran supplemented with butylated hydroxytoluene (100 µg mL^{-1}) directly before the analysis and 2 µl was subjected to HPLC analysis on a Phenomenex Prodigy column (4.6 x 250, ODS 3 µm). The separation was performed with a gradient (where min/solvent A%/solvent B% was 0/99/1; 8/60/40; 13/46/54; 15/0/100; 18/0/100; 21/99/1; 25/99/1) using 4% water-96% methanol as solvent A and 100% methyl-terc-butyl ether as solvent B, at a flow rate of 1 mL min^{-1}. The detection wavelength was 450 nm and the column thermostat temperature was 35 °C. For identification of carotenoids the following standards were used: astaxanthin, lycopene, β-carotene (Sigma), β-cryptoxanthin, canthaxanthin, zeaxanthin (Carl Roth) and echinenone (DHI Water and Environment). For γ-carotene, standard was purified by HPLC from *Mucor azygosporus*.

Results and discussion

Introduction of the *crtZ* gene into MS12+pCA8lf/1 and MS12+pPT51'R3/2 strains

Introduction of the pPT50 circular plasmid into canthaxanthin and echinenone producing MS12+pCA8lf/1 and MS12+pPT51'R3/2 mutants resulted in 20-25 transformants/10^5 protoplasts. The transformation frequency was similar to those in our previous studies, in which autonomously replicating plasmids harbouring the bacterial *crtW* and *crtZ* genes were used to transform the MS12 strain (Papp et al. 2006; Csernetics et al. 2011). The REMI transformation method was applied successfully for zygomycetes firstly by our research group (Papp et al. 2013). Similarly to those experiments, two to three colonies could be isolated per transformation of 10^6 MS12+pCA8lf/1 protoplasts using the pPT50'R linear DNA. Southern hybridization analysis verified the presence of the exogenous DNA in the transformants (results not shown), which proved to be mitotically stable on selective (YNB) and non-selective (MEA) media after ten consecutive cultivation cycles and no differences in their growing ability was observed compared to the recipient or the wild-type strains. Five-five isolates per transformation experiments were selected for further analysis.

Carotenoid content of the transformants

Carotenoid content of five-five transformants was analysed at the 4th and 10th cultivation cycle after the transformation by HPLC. Strains MS12, MS12+pCA8lf/1 and MS12+pPT51'R3/2 were used as controls (Table 2). After the 4th cultivation cycle, low amount of astaxanthin and decreased canthaxanthin and echinenone content were observed in all transformants. After the 10th consecutive cultivation cycle on YNB, MS12+pCA8lf/1+pPT50/1-5 and MS12+pPT51'R3/2+pPT50/1-5 accumulated 737 and 611 µg g^{-1} [dry mass] total carotenoid and 6 and 14 µg g^{-1} [dry mass] astaxanthin, respectively. Astaxanthin content was around 1-2% of the total carotenoids in these transformants. Compared to the recipient strains, significantly increased echinenone, β-carotene and γ-carotene content and decreased canthaxanthin content were also observed, mainly in MS12+pPT51'R3/2+pPT50/1-5 (Table 2). Integration of the *crtZ* gene into the genome of MS12+pCA8lf/1 resulted in 741 µg g^{-1} [dry mass] average total carotenoid content and, similarly to the transformants harbouring the *crtZ* gene on autonomously replicating plasmids, canthaxanthin, echinenone and β-carotene remained the major carotenoid components. These integrative transformants accumulated significantly higher amounts of total carotenoids, as well as canthaxanthin, echinenone and zeaxanthin than those harbouring the *crtW* and *crtZ* genes on autonomously replicating plasmids (Papp et al. 2006). However, they produced similar amounts of astaxanthin. As higher level of astaxanthin accumulation was observed by introducing the *crtZ* gene on autonomously replicating plasmids than by integrating it into the genome (Table 2), MS12+pCA8lf/1+pPT50/1-3 and MS12+pPT51'R3/2+pPT50/1-3 transformant were selected for further investigations.

Effect of the cultivation conditions on the carotenoid accumulation

Carotenoid accumulation of MS12+pCA8lf/1+pPT50/1-3 and MS12+pPT51'R3/2+pPT50/1-3 was analysed at different cultivation temperatures and compositions of media (Table 3). Effect of carbon sources on the carotenoid production of MS12+pCA8lf/1 was analysed in our previous study and the tested carbon sources were selected based on these results (Papp et al. 2013). Cultivation on fructose, trehalose and mannose as sole carbon sources increased

Table 2. Total carotenoid content and composition of the transformants, MS12 and the recipient MS12+pCA8lf/1 and MS12+pPT51'R3/2 strains.

Strain	Total carotenoid	β-carotene	β-cryptoxanthin	Zeaxanthin	Echinenone	Canthaxanthin	Astaxanthin	Lycopene	γ-carotene
MS12	422±25	268±18	25±3	6±2	-	-	-	14±3	23±4
MS12+pPT51'R3/2	511±27	56±11	16±4	10±2	103±4	110±10	2±1	11±2	32±4
MS12+pPT51'R3/2+pPT50/1-5	611±55	201±23	11±1	12±2	137±15	36±11	14±2	19±6	65±10
MS12+pCA8lf/1	534±29	38±10	27±5	4±2	114±11	151±19	2±1	21±5	34±4
MS12+pCA8lf/1+pPT50/1-5	737±75	146±15	24±4	14±4	203±36	103±14	6±4	24±7	87±15
MS12+pCA8lf/1+pPT50'R/1-5	741±112	236±37	14±4	6±3	171±15	145±47	3±1	12±1	36±11

Average values (μg g^{-1} [dry mass]) were calculated from carotenoid content of five transformants in three independent carotenoid extractions and measurements.

the total carotenoid, zeaxanthin and echinenone content of MS12+pPT51'R3/2+pPT50/1-3 in comparison with cultivation on glucose. Astaxanthin accumulation significantly increased on fructose, L-aspartic acid and mannose; on the latter, 28 μg g^{-1} [dry mass] astaxanthin content was measured (Table 3). Glucose, mannose, trehalose and fructose had also positive effect on the carotenoid content of both MS12+pCA8lf/1 and MS12+pPT51'R3/2 (Papp et al. 2013).

Effects of combinations of carbon sources (such as dihydroxyacetone and L-aspartic acid combined with glucose, trehalose and mannose) on the carotenoid content of MS12+pPT51'R3/2+pPT50/1-3, MS12+pCA8lf/1+pPT50/1-3 and the recipient strains were also tested. Most combinations resulted in slight increase in the total carotenoid content. However, glucose combined with dihydroxyacetone led to the highest total carotenoid content in all strains (Table 3), approximately 2-3 times higher amounts were measured than on glucose or dihydroxyacetone, separately. Simultaneously, enhanced β-cryptoxanthin, canthaxanthin and echinenone production was detected in MS12+pCA8lf/1 and MS12+pPT51'R3/2 and increased astaxanthin, zeaxanthin, β-cryptoxanthin, canthaxanthin and echinenone accumulation was observed in MS12+pPT51'R3/2+pPT50/1-3 and MS12+pCA8lf/1+pPT50/1-3 (Table 3). Application of glucose and dihydroxyacetone supposedly resulted the induction and increased activity of the *gpd1* promoter, which enhanced the expression of the *crtW* and *crtZ* genes. Dihydroxyacetone as sole carbon source resulted decreased total carotenoid content, however, the proportion of xanthophylls within it increased in MS12+pPT51'R3/2+pPT50/1-3.

We also tested the effect of the cultivation temperature on the carotenoid content. Temperature is an important environmental factor affecting the biosynthesis of carotenoids (Bhosale 2004). Cultivation at 30 °C had a positive effect on the total carotenoid and astaxanthin content compared to cultivation at 25 °C in the case of MS12+pPT51'R3/2+pPT50/1-3. The transformants were able to survive at 37 °C as well, with lower production of carotenoids. Similarly, transformants harbouring the *Paracoccus crtW* gene integrated into the genome (MS12+pCA8lf/1 and MS12+pPT51'R3/2) were able to survive at 37 °C, in contrast with the wild-type MS12 (Papp et al. 2013). Xanthophylls, including astaxanthin has better antioxidant activity than β-carotene and may protect cells against increased levels of reactive oxygen species and may contribute in higher thermo tolerance through decreasing the fluidity and stabilizing the structure of the membranes (Palozza and Krinsky 1992; Tjahjono et al. 1994; Liang et al. 2009).

Development of carotenoid extraction method for liquid cultures

For fermentation developments, it would be advantageous if carotenoid and xanthophyll production in liquid culturing would be developed and optimized. Therefore, carotenoid production of our transformants was also tested in liquid cultures. It was observed that the extraction method used for mycelia harvested from solid media (Papp et al. 2006; Csernetics et al. 2011) is not effective for those from liquid media. Relatively high amounts of pigments remained after several extraction steps. It was presumed, that high moisture content of mycelia or formation of thicker cell wall in liquid media may cause the low efficiency of the carotenoid extraction. Thus, different methods were tested to improve the extraction efficiency. The conventional method was used as a control (Table 1).

To reduce the moisture content, lyophilization for 45 min. or overnight drying at 40 °C was applied together with acetone and petroleum ether extractions. Sodium-sulphate, which has desiccating effect, was also tested. It was applied in 10, 20, 50 and 100% (m/m) of mycelial mass combined with acetone extraction. Among the tested processes, lyophilisation combined with acetone extraction proved to be the most effective. In case of the astaxanthin producer *Phaffia rhodozyma*, which has thick cell wall, DMSO or acid pretreatment is used for cell lysis before carotenoid extraction (Sedmak et al. 1990; Xiao et al. 2009). Therefore, different acids were tested to enhance cell lysis and avoid degradation of astaxanthin and lactic acid was found to be the most appropriate for this purpose (Ni et al. 2008). Extraction with DMSO and partition of carotenoids in hexane instead of

Table 3. Carotenoid composition of transformants under different cultivation conditions.

Strain	Carbon source/ temperature	Total	β-carotene	β-crypto-xanthin	Zeaxan-thin	Echinenone	Canthax-anthin	Astaxan-thin	Lycopene	γ-carotene
MS12+pPT51'R3/2+pPT50	Glucose	611±55	201±23	11±1	12±2	137±15	36±11	14±2	19±6	65±10
MS12+pCA8lf/1+pPT50		737±75	146±15	24±4	14±4	203±36	103±14	6±4	24±7	87±15
MS12+pPT51'R3/2+pPT50	Fructose	694±72	233±21	10±2	16±2	165±22	23±4	17±4	16±5	68±25
MS12+pCA8lf/1+pPT50		705±81	134±19	19±3	11±1	195±31	97±11	6±1	22±7	81±31
MS12+pPT51'R3/2+pPT50	L-aspartic acid	400±49	72±9	7±1	13±3	101±14	19±2	17±3	10±2	44±12
MS12+pCA8lf/1+pPT50		259±25	32±7	9±2	6±2	64±12	47±13	5±2	6±1	26±15
MS12+pPT51'R3/2+pPT50	Trehalose	806±92	309±31	21±4	16±4	159±18	29±7	12±3	17±5	71±23
MS12+pCA8lf/1+pPT50		409±31	57±15	12±3	10±2	108±27	80±9	6±2	10±1	33±11
MS12+pPT51'R3/2+pPT50	Mannose	734±62	175±19	7±1	17±2	202±20	39±4	28±3	21±4	80±21
MS12+pCA8lf/1+pPT50		497±59	75±11	23±7	10±3	143±19	74±9	5±1	19±6	59±15
MS12+pPT51'R3/2+pPT50	Galactose	635±65	261±31	17±2	13±2	123±13	22±2	8±2	12±2	50±18
MS12+pCA8lf/1+pPT50		579±53	124±22	15±3	16±3	150±17	86±7	7±1	17±7	54±11
MS12+pPT51'R3/2+pPT50	Glycerol-L-mono-acetate	465±35	200±16	14±3	9±4	67±9	23±11	6±1	6±2	22±3
MS12+pCA8lf/1+pPT50		588±57	201±21	8±2	12±4	124±23	75±17	5±2	13±5	45±7
MS12+pPT51'R3/2+pPT50	Dihydroxyacetone	395±41	54±7	16±5	29±5	70±16	69±21	11±2	5±1	17±4
MS12+pCA8lf/1+pPT50		207±16	24±6	6±1	8±2	30±7	58±22	5±1	4±2	11±3
MS12+pPT51'R3/2+pPT50	Glucose, on 20 °C	614±44	262±31	20±7	10±2	90±17	20±2	6±1	20±7	51±11
MS12+pCA8lf/1+pPT50		653±71	168±19	13±5	13±4	171±19	68±11	3±1	19±5	71±9
MS12+pPT51'R3/2+pPT50	Glucose, on 30 °C	694±61	206±11	18±4	12±4	105±23	31±17	30±5	21±4	73±27
MS12+pCA8lf/1+pPT50		507±67	94±19	16±4	10±3	98±21	49±15	6±2	32±9	87±24
MS12+pPT51'R3/2+pPT50	Glucose, on 37 °C	447±36	199±14	10±2	4±1	26±6	3±1	4±1	16±6	55±31
MS12+pCA8lf/1+pPT50		500±81	182±19	9±1	3±1	73±11	16±7	1±0.5	23±12	73±37
MS12+pPT51'R3/2	Glucose + Dihydroxyacetone	959±189	36±15	123±25	10±2	161±24	300±55	2±1	133±34	128±29
MS12+pPT51'R3/2+pPT50		989±183	62±24	102±31	30±7	223±35	115±42	35±4	74±19	128±44
MS12+pCA8lf/1		1171±227	44±11	151±31	2±1	225±41	443±71	3±1	161±41	159±33
MS12+pCA8lf/1+pPT50		1032±205	50±23	113±27	27±8	211±45	299±34	29±3	125±21	137±54

Average carotenoid values (μg g^{-1} [dry mass]) were calculated from biological replicates in three independent carotenoid extractions and measurements.

petroleum ether significantly increased the carotenoid yield. In our tests, 0.2-0.5 and 2-5 M lactic acid was added to the mycelial powder and the resulting samples were heated to 120 °C and 50 °C, respectively. After a centrifugation step, the extraction was continued with the repeated addition of acetone and vortexing. In most of the tested cases, mycelia became completely colourless after 6-8 extraction steps. Finally, extraction with DMSO or 4 M lactic acid combined with heating to 50 °C were found to be the most effective for carotenoid extraction, which resulted 120-200% effectiveness in comparison with the conventional method. Additionally, HPLC analysis verified that these conditions did not resulted in significant degradation of pigments. Carotenoid composition of MS12+pPT51'R3/2+pPT50/1-3 was analysed from mycelia cultivated in liquid YNB medium (containing glucose as carbon source) using the above described method. Total carotenoid content was around 398 μg g^{-1} [dry mass] and 10-25% increase in the proportion of canthaxanthin, echinenone, β-cryptoxanthin, zeaxanthin and astaxanthin content was observed, however it was still below of the xanthophyll content of mycelia harvested from solid media.

Acknowledgement

The research of Árpád Csernetics and Csaba Vágvölgyi was supported by the European Union and the State of Hungary, co-financed by the European Social Fund in the framework of TÁMOP-4.2.4.A/2-11/1-2012-0001 'National Excellence Program'. The infrastructure and research equipment was supported by OTKA NN 106394.

References

Beatty S, Nolan J, Kavanagh H, O'Donovan O (2004) Macular pigment optical density and its relationship with serum and dietary levels of lutein and zeaxanthin. Arch Biochem Biophys 430(1):70-76.

Benito EP, Díaz-Mínguez JM, Iturriaga EA, Campuzano EA, Eslava AP (1992) Cloning and sequence analysis of the *Mucor circinelloides pyrG* gene encoding orotidine-5'-monophosphate decarboxylase: use of *pyrG* for homologous transformation. Gene 116(1):59-67.

Bhosale P (2004) Environmental and cultural stimulants in the production of carotenoids from microorganisms. Appl Microbiol Biotechnol 63:351-361.

Bhosale P, Bernstein PS (2005) Microbial xanthophylls. Appl Microbiol Biotechnol 68(4):445-455.

Chew BP, Park JS, Wong M, Wong TS (1999) A comparison of the anticancer activities of dietary beta-carotene, canthaxanthin and astaxanthin in mice in vivo. Anticancer Res 19 (3A):1849-1853.

Csernetics Á, Nagy G, Iturriaga EA, Szekeres A, Eslava AP, Vágvölgyi C, Papp T (2011) Expression of three isoprenoid biosynthesis genes and their effects on the carotenoid production of the zygomycete *Mucor circinelloides*. Fungal Genet Biol 48(7):696-703.

Guerin M, Huntley ME, Olaizola M (2003) *Haematococcus* astaxanthin: applications for human health and nutrition. Trends Biotechnol

21(5):210-216.

Iturriaga EA, Díaz-Mínguez JM, Benito EP, Álvarez MI, Eslava AP (1992) Heterologous transformation of *Mucor circinelloides* with the *Phycomyces blakesleeanus leu1* gene. Curr Genet 21:215-223.

Kumaresan N, Sanjay KR, Venkatesh KS, Kadeppagari R-K, Vijayalakshmi G, Umesh-Kumar S (2008) Partially saturated canthaxanthin purified from *Aspergillus carbonarius* induces apoptosis in prostate cancer cell line. Appl Microbiol Biotechnol 80(3):467-473.

Liang J, Tian Y, Yang F, Zhang J, Skibsted LH (2009) Antioxidant synergism between carotenoids in membranes. Astaxanthin as a radical transfer bridge. Food Chem 115(4):1437-1442.

Mares-Perlman JA, Millen AE, Ficek TL, Hankinson SE (2002) The body of evidence to support a protective role for lutein and zeaxanthin in delaying chronic disease. Overview. J Nutr 132(3):518S-524S.

Misawa N, Satomi Y, Kondo K, Yokoyama A, Kajiwara S, Saito T, Ohtani T, Miki W (1995) Structure and functional analysis of a marine bacterial carotenoid biosynthesis gene cluster and astaxanthin biosynthetic pathway proposed at the gene level. J Bacteriol 177:6575-6584.

Ni H, Chen Q-H, He G-Q, Wu G-B, Yang Y-F (2008) Optimization of acidic extraction of astaxanthin from *Phaffia rhodozyma*. J Zhejiang Univ Sci B 9(1):51-59.

Nishino H, Murakosh M, Ii T, Takemura M, Kuchide M, Kanazawa M, Mou XY, Wada S, Masuda M, Ohsaka Y, Yogosawa S, Satomi Y, Jinno K (2002) Carotenoids in cancer chemoprevention. Cancer Metastasis Rev 21(3-4):257-264.

Palozza P, Krinsky NI (1992) Astaxanthin and canthaxanthin are potent antioxidants in a membrane model. Arch Biochem Biophys 297:291-295.

Papp T, Csernetics Á, Nagy G, Bencsik O, Iturriaga EA, Eslava AP, Vágvölgyi C (2013) Canthaxanthin production with modified *Mucor circinelloides* strains. Appl Microbiol Biotechnol 97(11):4937-4950.

Papp T, Csernetics Á, Nyilasi I, Ábrók M, Vágvölgyi C (2010) Genetic transformation of zygomycetes fungi. In: Rai M, Kövics G (eds) Progress in mycology, Springer, Scientific Publishers, Jodhpur, pp. 75-94.

Papp T, Velayos A, Bartók T, Eslava AP, Vágvölgyi C, Iturriaga EA (2006) Heterologous expression of astaxanthin biosynthesis genes in *Mucor circinelloides*. Appl Microbiol Biotechnol 69(5):526-531.

Sambrook J, Fitsch EF, Maniatis T (1989) Molecular cloning: a laboratory manual. Cold Spring Harbor Press, Cold Spring Harbor.

Sedmak JJ, Weerasinghe DK, Jolly SO (1990) Extraction and quantitation of astaxanthin from *Phaffia rhodozyma*. Biotechnol Tech 4(2):107-112.

Tjahjono AE, Hayama Y, Kakizono T, Terada Y, Nishio N, Nagai S (1994) Hyper-accumulation of astaxanthin in a green alga *Haematococcus pluvialis* at elevated temperatures. Biotechnol Lett 16:133-138.

Xiao A, Ni H, Cai H, Li L, Su W, Yang Q (2009) An improved process for cell disruption and astaxanthin extraction from *Phaffia rhodozyma*. World J Microbiol Biotechnol 25:2029-2034.

Yamaguchi M (2004) Osteogenesis promoter containing β-cryptoxanthin as the active ingredient. Japanese patent CT Int Appl 42 pp. WO 2004037236.

van Heeswijck R, Roncero MIG (1984) High frequency transformation of *Mucor* with recombinant plasmid DNA. Carlsberg Res Commun 49:691-702.

Velayos A, Blasco JL, Alvarez MI, Iturriaga EA, Eslava AP (2000a) Blue-light regulation of the phytoene dehydrogenase (*carB*) gene expression in *Mucor circinelloides*. Planta 210(6):938-946.

Velayos A, Eslava AP, Iturriaga EA (2000b) A bifunctional enzyme with lycopene cyclase and phytoene synthase activities is encoded by the *carRP* gene of *Mucor circinelloides*. Eur J Biochem 267(17):1-12.

Velayos A, Fuentes-Vicente M, Aguilar-Elena R, Eslava AP, Iturriaga EA (2004) A novel fungal prenyl diphosphate synthase in the dimorphic zygomycete *Mucor circinelloides*. Curr Genet 45(6):371-377.

Velayos A, Papp T, Aguilar-Elena R, Fuentes-Vicente M, Eslava AP, Iturriga EA, Álvarez MI (2003) Expression of the *carG* gene, encoding geranylgeranyl pyrophosphate synthase, is up-regulated by blue light in *Mucor circinelloides*. Curr Genet 43(2):112-120.

Volume 58(2):147-156, 2014
Acta Biologica Szegediensis
http://www2.sci.u-szeged.hu/ABS

ARTICLE

Thermodynamic and kinetic characteristics of an α-amylase from *Bacillus licheniformis* SKB4

Saptadip Samanta[1], Arpan Das[3], Suman Kumar Halder[3], Arijit Jana[3], Sanjay Kar[2], Pradeep Kumar Das Mohapatra[3], Bikash Ranjan Pati[3], Keshab Chandra Mondal[3]*

[1]Department of Physiology, Midnapore College, Midnapore, Paschim Medinipur 721101, West Bengal, India, [2]Department of Botany, Midnapore College, Midnapore, Paschim Medinipur 721101, West Bengal, India, [3]Department of Microbiology, Vidyasagar University, Midnapore, 721102, West Bengal, India

ABSTRACT An amylolytic bacterial strain, *Bacillus licheniformis* SKB4 produced maximum amylase at pH 6.5 at 42 °C, and at late stationary phase (24 h) of growth. Starch and peptone were found the best supporting carbon and nitrogen source with C:N ratio of 1:2 for amylase production. The purified enzyme was non-responsive to most of the metal ions except K^+ and Mg^{++} (1.0 mM). The enzyme was stable and active at pH 6.5. The enzyme showed optimum temperature at 90 °C with 10 min of half life ($t_{½}$) at 100 °C. The Q_{10} of the enzyme was 1.0. The thermodynamic principles like activation energy, free energy for substrate binding and transition state of the enzyme were found 31.53, 5.53 and -17.4 KJ/Mol of starch, respectively. The kinetic constant like V_{max}, K_m, K_{cat} and catalytic efficiency (K_{cat}/K_m) for starch were found to be 1.04 μmol mg^{-1} min^{-1}, 6.2 mg ml^{-1}, 2 × 10^3 S^{-1} and 3.22 × 10^2 ml mg^{-1} S^{-1}, respectively. All these findings suggested that this amylase has unique characteristics for starch hydrolysis in respect to thermostability and kinetic properties. **Acta Biol Szeged 58(2):147-156 (2014)**

KEY WORDS

α-amylase
Bacillus licheniformis
thermodynamic characteristics
enzyme kinetics

Alpha-amylase (EC 3.2.1.1, 1,4-α-D-glucan glucano hydrolase, endoamylase) hydrolyzes starch, glycogen and related polysaccharides randomly by cleaving the internal α-1,4-glucosidic linkages and have great success by replacing the chemical hydrolysis of starch. α-Amylases account for ~30% of the enzyme market (Shivramakrishnan et al. 2006) and it is widely used in various industries like alcohol, brewing, sugar for liquefaction of starch; in textile industry for desizing of fabrics, etc (Gupta et al. 2003). The exploitation of amylase in world market is estimated to increase by 4% annually, significantly uses in detergents (37%), textiles (12%), starch (11%), baking (8%) and animal feed (6%) industries (Deb et al. 2013). Bacterial α-amylases, particularly from the *Bacillus* species are of special interest for their large-scale production under simple cultivation system and of remarkable thermostability (Prakash and Jaiswal 2010). Heat-resistant enzymes offer commercial opportunities because higher temperatures can overcome the viscosity problems of substrate (e.g. starch) and accelerated endothermic reactions (Kikani et al. 2012).

Microbial enzyme production is generally subjected to the influence of different parameters of culture condition; therefore it is necessary to standardize the cultural and nutritional conditions of the organism. In industry, submerged fermentation process is generally employed for the production of microbial enzymes due to the easy control of different physico-chemical parameters, less chance of contamination and enzyme remain in the culture fluid somehow as purified form (Coronado et al. 2000; Gangadharan et al. 2006).

In view of the versatile appliances of thermophilic α-amylase in different sectors, attempt has been made to optimize the submerged culture condition and characterize some relevant properties of the purified α-amylase from *Bacillus licheniformis* SKB4.

Materials and Methods

Microorganism

Bacillus licheniformis SKB4, a soil isolate (Samanta et al. 2009) was used for the present study.

Culture condition for amylase production

Enzyme production was carried out in 250-ml Erlenmeyer flask containing 50 ml basal medium (pH 6.5) containing (g l^{-1}): starch, 5; peptone, 10; beef extract, 5; KH_2PO_4, 3; $MgSO_4$ 0.5; $CaCl_2$; 0.02. It was inoculated with 1% (v/v) freshly prepared inoculum and incubated on a rotary shaker (120 rpm) at 42 °C for 28 h. The growth of the bacteria was measured at 620 nm. The pH of the culture medium was also measured in different time intervals. The culture supernatant obtained by centrifugation (5000 rpm for 10 min) was considered as crude source of enzyme and assayed for amylase activity.

Accepted Dec 8, 2014
*Corresponding author. E-mail: mondalkc@gmail.com

Optimization of culture conditions

To determine the optimal cultural condition for enzyme production, the most effective level of individual parameters, *viz.*, initial medium pH (3.0-10.0), growth temperature (30 °C - 50 °C), soluble sugars (glucose, mannose, galactose, fructose, inositol, arabinose, sucrose, lactose, maltose, rhamnose, xylose, ribose, raffinose, starch in 0.1-0.5 g % w/v concentrations) and nitrogen sources (peptone, beef extract, tryptone, urea, yeast extract, thiourea, NH_4NO_3, $(NH_4)_2HPO_4$, $(NH_4)H_2PO_4$, $NaNO_3$ in 0.1-0.5 g % w/v concentrations) were studied following one variable at a time (OVAT) optimization protocol.

Assay of α-amylase

Amylase activity was determined by studying its saccharolytic properties according to Bernfield (1955). Briefly, the reaction mixture consisted 0.5 ml of 1% (w/v) starch, 0.4 ml of phosphate buffer (10 mM, pH 6.5) and 0.1 ml of enzyme solution and incubated for 5 min at 90 °C. The reaction was stopped by addition of 1 ml of 3,5 dinitrosalicylate (DNS) reagent. The quantity of reducing sugar was measured colorimetrically at 530 nm using glucose as standard sugar. The unit of amylase was defined as the amount of enzyme which produced 1μmol of reducing sugar as glucose in 1 min under specified condition.

Purification of amylase

The concentrated culture broth was brought to 35% saturation with analytical grade $(NH_4)_2SO_4$ and kept overnight at 4 °C. The supernatant was separated by centrifugation (10 000 × g for 10 min) and the precipitate was discarded after examining its amylolytic activity. Then 80% saturation was brought by adding additional $(NH_4)_2SO_4$ and was allowed to stand overnight at 4 °C. The precipitate was collected by centrifugation (12 000 × g for 30 min at 4 °C) and dissolved in 10 mM phosphate buffer (pH 6.5). The precipitate was then dialyzed against the same buffer for 24 h with a periodical change of buffer solution. The dialyzed enzyme was then applied to a DEAE cellulose column (Merck, Mumbai, India) and the enzyme was eluted with a linear gradient of KCl (0.01-0.1M). The active fraction in the flow through were collected and concentrated in lyophilizer. At the next stage, the amylase solution put on a Sephadex G-100 column (1.5 x 92 cm) that pre-equilibrated with 10 mM phosphate buffer (pH 6.5) and then eluted with the same buffer. The active enzyme fraction were collected and concentrated and stored at 4 °C for further use.

Effect of metal ions on amylase activity

Different metal ions (at a concentration of 1-100 mM) in assay buffer (10 mM phosphate buffer pH 6.5) were incubated with the enzyme at 37 °C for 30 min. The residual activities were examined under standard assay conditions.

Influence of pH on amylase activity and stability

The optimum pH of enzyme activity was measured at different pH levels from 3.0-11.0 [10 mM citrate buffer (pH 3.0-5.8), 10 mM phosphate buffer (pH 6.0-8.0) and 10 mM bi-carbonate buffer (pH 9.0 to 11.0)]. To determine the pH stability, the enzyme solution was mixed with suitable buffer at different pH values (10 mM, pH 3.0-11.0) and incubated at 4 °C for 24 h and then residual activity was measured at optimum temperature.

Determination of optimum temperature and apparent half life ($t_{1/2}$) of amylase

The optimum temperature of enzyme activity was determined by incubating the reaction mixture separately at different tem-

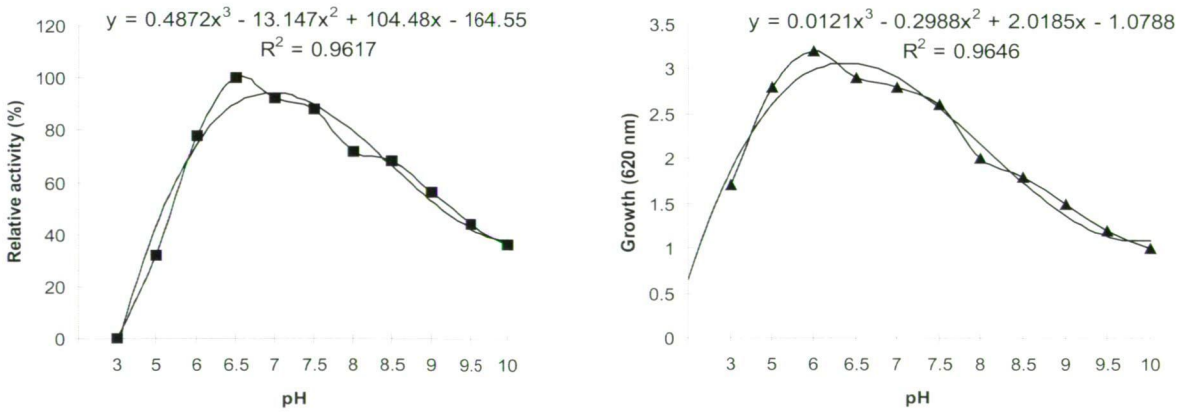

Figure 1. Effect of initial medium pH on amylase production (▪) and growth (▲) of *B. licheniformis* SKB4. The pH of medium adjusted after sterilization. Bacteria were grown on a rotary shaker (120 rpm) at 42 °C for 28 h.

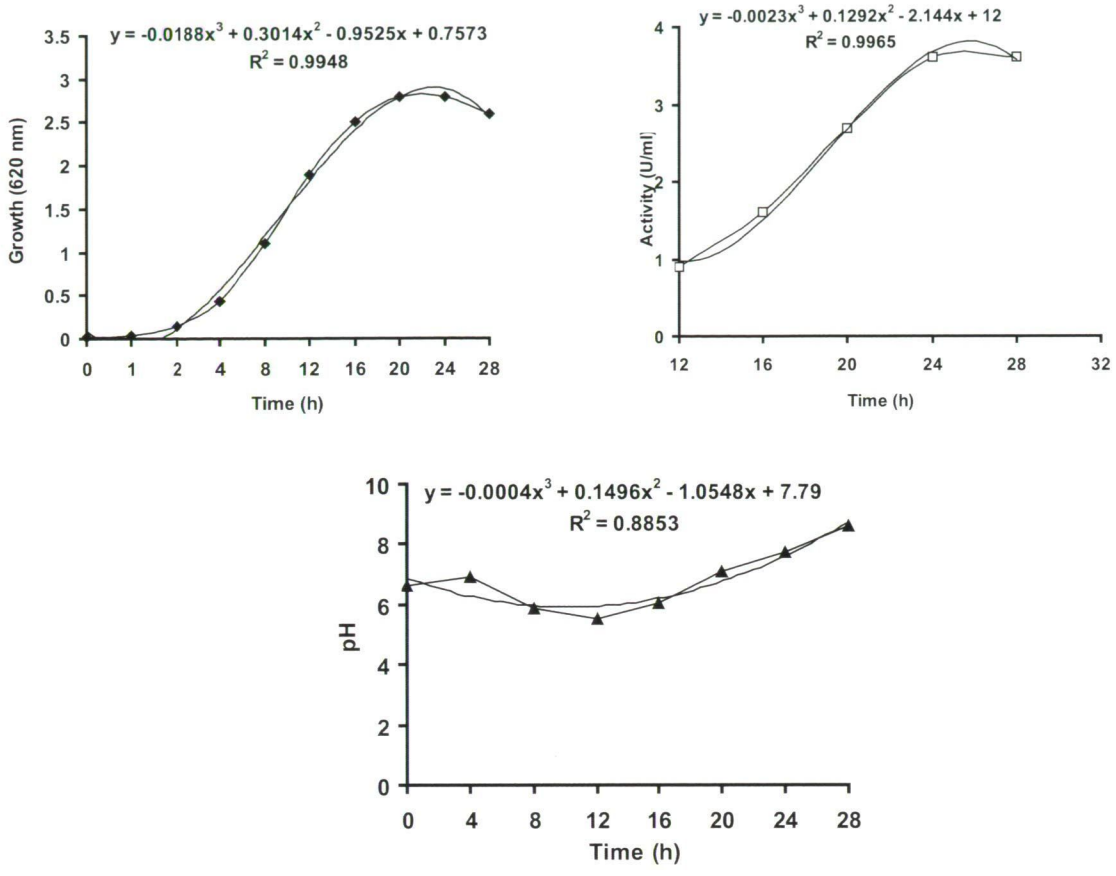

Figure 2. Cell growth (♦) and enzyme production (□) of *B. licheniformis* SKB4. Incubation period was 28 h at 42 °C on a rotary shaker (120 rpm). Initial medium pH adjusted at 6.5. The pH (▲) of the growing medium increased during growth of the bacteria.

perature from 30-100 °C. The apparent half life ($t_{1/2}$) of amylase at 100 °C was estimated on the basis of thermostability of enzyme in the absence of substrate. The enzyme solution was taken in a stoppered test tube and placed in a water bath at 100 °C. The enzyme solution was taken out after regular interval and assayed immediately after addition of substrate. $t_{1/2}$ was estimated at when 50% activity was restored.

Thermodynamic characteristics of amylase activity

The activation energy (Ea) for substrate hydrolysis under the given experimental conditions was determined by plotting the data in an Arrhenius plot (Das et al. 2012). The free energy for substrate binding and transition state formation was calculated using the following derivations (Saqib et al. 2010):

$\Delta G^*_{E\text{-}S}$ (free energy of substrate binding) = -RT *ln* Ka

Where, Ka = $1/K_m$, R is the universal gas constant (8.314 JK^{-1} mol^{-1}) and T is the absolute temperature (K).

$\Delta G^*_{E\text{-}T}$ (free energy of transition state formation) = -RT *ln* (K_{cat}/K_m)

The temperature coefficient (Q_{10}) is the rate of an enzymatic catalytic reaction changes for every 10 °C rise in temperature, was calculated by the Dixon and Webb equation (Dixon and Webb 1979).

$ln\ Q_{10} = E_a \times 10/RT^2$

Where, Ea is the activation energy of the enzyme (J mol^{-1}).

Determination of kinetic constants for substrate

The Michaelis constant (K_m), maximum reaction velocity (V_{max}), turn over number (K_{cat}) and catalytic efficiency (K_{cat}/K_m) of purified amylase for starch were determined by using Lineweaver and Burk plot (Lineweaver and Burk 1934).

Results and Discussion

Effect of initial medium pH and incubation time on amylase production

pH is one of the important determinant for growth and overall activities of microbes. The catalytic activity and three dimensional structure of enzyme are of particularly very sensitive to hydrogen ion concentration. The experimental organism, *B.*

Table 1. Effect of soluble sugar on growth and amylase formation of *B. licheniformis* SKB4. Fermentation condition: temperature 42 °C, initial medium pH 6.5, incubation time 28 h. Data represented as the average of three separate experiments.

Carbon source	Concentration (g% w/v)	Growth (620 nm)	Enzyme activity (U/ml)
Control (without C source)		1.10	0.10
Glucose	0.1	2.40	0.23
	0.3	2.40	0.15
	0.5	3.6	0.10
Mannose	0.1	2.25	0.03
	0.3	3.60	0.05
	0.5	3.20	0.26
Galactose	0.1	3.00	0.15
	0.3	3.15	0.20
	0.5	3.30	0.27
Fructose	0.1	2.85	0.12
	0.3	3.60	0.09
	0.5	3.60	0.07
Inositol	0.1	2.10	0.06
	0.3	3.30	0.10
	0.5	3.90	0.10
Arabinose	0.1	2.70	0.06
	0.3	2.40	0.09
	0.5	2.25	0.09
Sucrose	0.1	2.25	0.21
	0.3	2.55	0.17
	0.5	3.00	0.05
Lactose	0.1	2.40	0.11
	0.3	2.40	0.27
	0.5	1.80	0.50
Maltose	0.1	2.55	0.11
	0.3	2.85	0.21
	0.5	3.00	0.30
Rhamnose	0.1	1.86	0.02
	0.3	3.15	0.08
	0.5	3.45	0.05
Xylose	0.1	2.40	0.08
	0.3	3.30	0.08
	0.5	3.90	0.10
Ribose	0.1	2.40	0.18
	0.3	2.10	0.15
	0.5	3.30	0.04
Raffinose	0.1	2.40	0.06
	0.3	3.30	0.06
	0.5	3.60	0.03
Starch	0.1	2.6	0.45
	0.3	2.7	0.65
	0.5	3.0	0.90

Table 2. Effect of different nitrogen sources on growth and amylase production of *B. licheniformis* SKB4 (incubation time 28 h, initial medium pH 6.5, temperature 42 °C). Data represented as the average of three separate experiments.

Nitrogen source	Concentration (g% w/v)	Growth (620 nm)	Enzyme activity (U/ml)
Control		0.08	0.10
NH_4NO_3	0.1	0.10	0.08
	0.3	0.20	0.07
	0.5	0.32	0.02
$(NH_4)_2HPO_4$	0.1	0.45	0.10
	0.3	0.62	0.14
	0.5	0.80	0.08
$(NH_4)H_2PO_4$	0.1	0.30	0.07
	0.3	0.72	0.05
	0.5	0.65	0.03
$NaNO_3$	0.1	0.22	0.07
	0.3	0.46	0.04
	0.5	0.58	0.04
Urea	0.1	0.90	0.08
	0.3	0.85	0.05
	0.5	0.55	0.05
Beef extract	0.1	2.0	0.10
	0.3	3.0	0.16
	0.5	3.5	0.18
Peptone	0.1	2.2	0.17
	0.3	2.8	0.20
	0.5	3.2	0.32
Tryptone	0.1	0.95	0.10
	0.3	0.95	0.06
	0.5	1.30	0.07
Yeast extract	0.1	0.90	0.12
	0.3	2.6	0.12
	0.5	2.8	0.10
Thiourea	0.1	0.35	0.10
	0.3	0.10	0.03
	0.5	0.10	0.03

licheniformis SKB4 grew well over a wide range of pH, *i.e.*, 3.0 to 10.0, produced maximum amylase at pH 6.5 (Fig. 1), but it showed maximum growth at pH 6.0. Most of the starch degrading bacterial strains are reported to produce enzyme in a pH range between 6.0 and 7.0 (Haq et al. 2002; Gupta et al. 2003; Rasooli et al. 2008).

B. licheniformis SKB4 initiated to synthesize amylase from the 12th h of active log phase, and maximum amount was noted during its late stationary phase (24 h) (Fig. 2). Similar pattern of amylase synthesis was also observed by Boži et al. (2011) in *Bacillus subtilis* IP 5832. Wanderley et al. (2004) suggested that effective induction of amylase did not occur until the stationary phase of growth and it related to the depletion of readily available carbon source. Moreover, maximum α-amylase production by *B. licheniformis* Shahed-07 occurred when cell growth reached to the stationary phase (26 h), suggesting that enzyme secretion is not growth related rather it depends on the quantity of cell mass (Rasooli et al. 2008).

In relation to growth, pH of the media was tended to acidic up to 12 h of growth, but, thereafter changed towards alkalinity (Fig. 2). The initial decrease of pH is due to fast growth of the organisms which produced acids from carbohydrate fermentation, and the latter change of pH towards alkalinity may due to cell lysis (de Oliveira et al. 2010). Similar fashion of cell growth, enzyme production and changes in pH of the culture media were observed in case of *Bacillus* sp. IMD 434

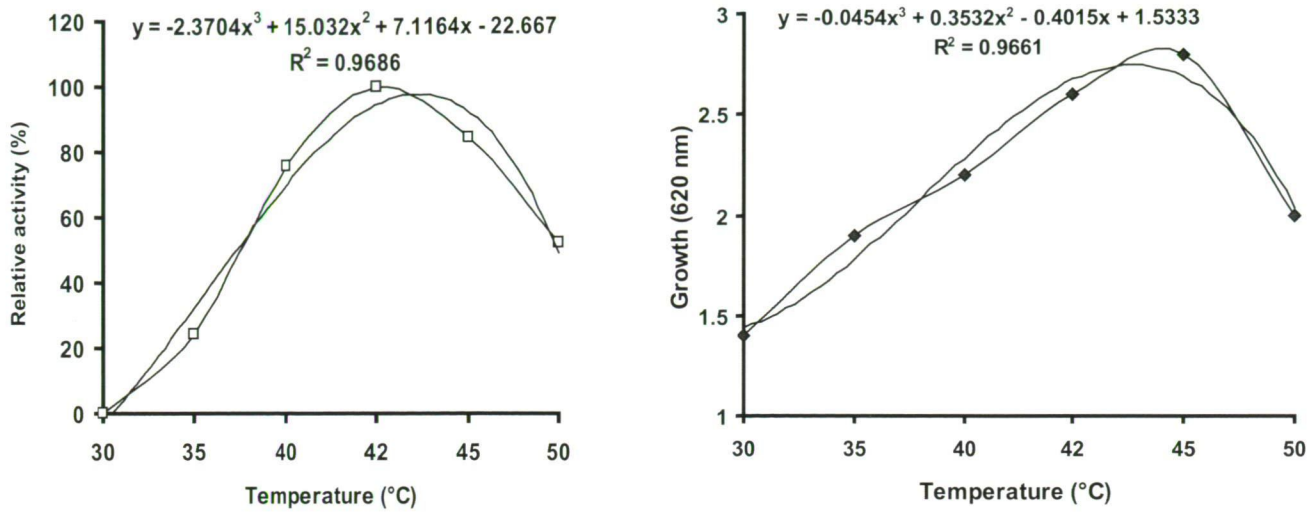

Figure 3. Effect of incubation temperature on amylase production (□) and growth (♦) of *B. licheniformis* SKB4. The pH of medium adjusted at 6.5. Bacteria were grown on a rotary shaker (120 rpm) for 28 h at different temperatures (30-50 °C).

(Hamilton et al. 1999) and *Bacillus* sp. IMD 370 (Mc Tigue et al. 1995).

Effect of temperature on amylase production

The studied bacterium, *B. licheniformis* SKB4 grown well at 30 °C, but it produced notable quantity of amylase at 35 °C. Maximum level of enzyme production was found at 42 °C, but highest growth was achieved at 45 °C (Fig. 3). Previously, it was reported that maximum level of α-amylase production by *B. subtilis* 147 (Avdiiuk and Varbanets 2008) and *Bacillus* sp. GHA1 (Ahmadi et al. 2010) occurred at 42 °C. Aiba et al. (1983) reported that the high temperature may inactivate the expression of genes responsible for the starch degrading enzymes.

Effect of carbon and nitrogen sources on amylase production

A range of soluble sugars at various concentrations (0.1-0.5%, w/v) were tested for growth and amylase production of *B. licheniformis* SKB4 and the results are summarized in Table 1. Among the carbon sources, starch was found to be best inducer for amylase synthesis followed by lactose > maltose > galactose > mannose. Whereas, other sugars like fructose, inositol, arabinose, rhamnose, xylose, and raffinose could be considered as poor producer of amylase. Similar type of results was also noted in *B. licheniformis* (Chandra et al. 1980, Rasooli et al. 2008). Aiyer (2004) and Rasooli et al. (2008) also suggested that starch is a good inducer for amylase synthesis in *B. licheniformis*. Glucose, sucrose and ribose in 0.1% (w/v) concentration act as moderate carbon source for amylase production (Table 1), but enzyme synthesis was inhibited at their higher concentrations (>0.1%, w/v). Similar type of findings was also noted in case of *Bacillus polymyxa* and *B. subtilis* (Nickless et al. 2001) and their amylase producing gene was turned off (catabolite repression) in presence of glucose or fructose. The bacterial cells growing on easily utilizable carbon sources such as glucose or sucrose did not need to waste valuable energy for the biosynthesis of amylase. Therefore, the gene for amylase is turned off (Nickless et al. 2001). Haseltine et al. (1996) argued that a sensory system facilitated the detection of exogenous starch which acted as mediator for induction of α-amylase synthesis. The present findings suggest that the *B. licheniformis* SKB4 α-amylase induction by starch and repression by glucose was subjected to multiple forms of regulations.

It was found that enzyme production increased along with starch concentration upto 0.5% (w/v) and above it decreased (Fig. 4). But growth of the bacteria reached highest level at 1% (w/v) starch concentration. Rukhaiyar and Srivastava (1995) explained that culture broth viscosity has increased at high concentration of starch which interfere the oxygen transfer leading to limitation of dissolved oxygen for the growth of bacteria as well as its enzyme synthesis.

The effect of nitrogen sources over the concentration range of 0.1 to 0.5% (w/v) on growth and amylase production of *B. licheniformis* SKB4 was tested and represented in Table 2. Among the various nitrogen sources, peptone (0.5%, w/v) favoured maximum amylase production. The increasing order of amylase production by the stimulatory nitrogen sources can be arranged as: peptone (0.5%, w/v) > beef extract (0.5%, w/v) > $(NH_4)_2HPO_4$ (0.3%, w/v) > yeast extract (0.1%, w/v). Low concentration of nitrogen is inadequate for the enzyme production and excess nitrogen is equally detrimental causing inhibition of microbial growth as well

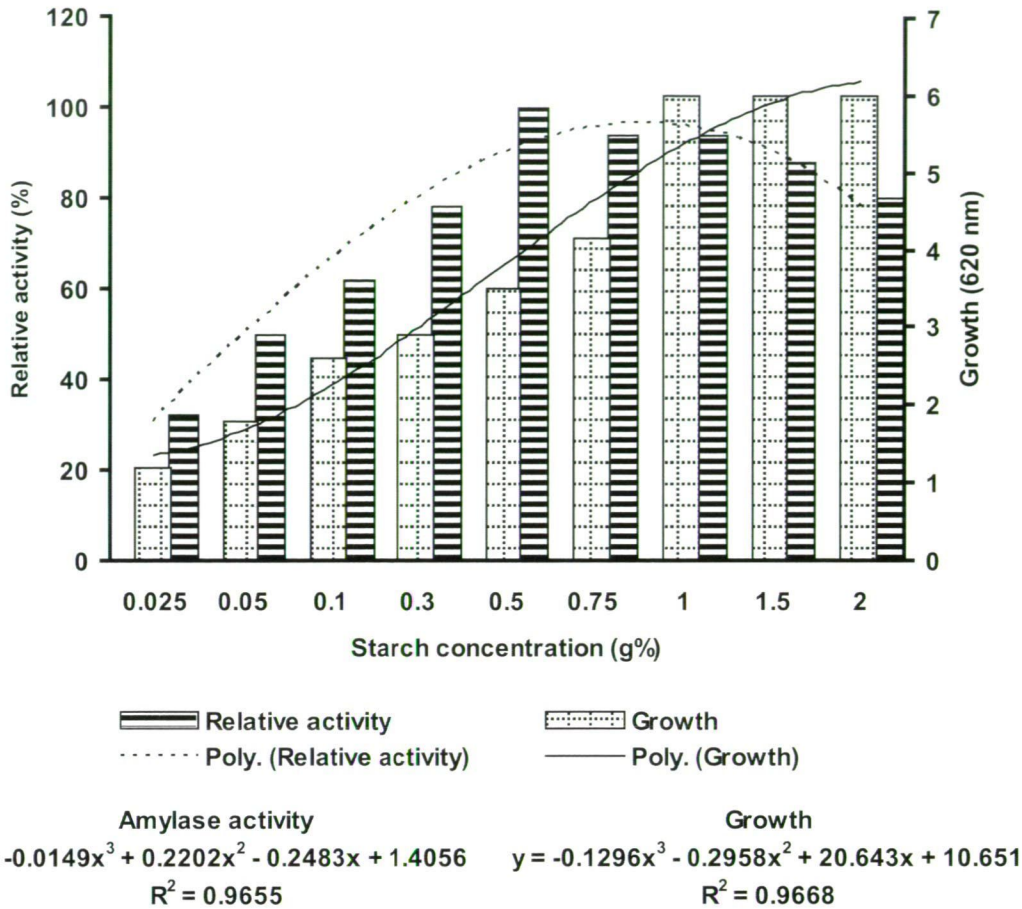

Figure 4. Effect of starch concentration on growth and amylase production of *B. licheniformis* SKB4. Basal medium contained starch at various concentration (0.025-2.0 % w/v), initial pH 6.5, temperature 42 °C, incubation time 28 h.

as enzyme synthesis (Aiyer 2004). Mc Tigue et al. (1995) also reported that peptone was a better nitrogen source for amylase production of .*B. licheniformis* SPT 278 than that of other organic and inorganic nitrogen sources. The maximum amylase yield was achieved when peptone concentration was at 1.0% with C/N ratio of reached 0.5 (Fig. 5, Table 3). This indicated that the nature and relative concentrations of carbon and nitrogen sources are important for amylase production from *B. licheniformis* SKB4. Earlier reports also revealed the C/N ratio of 1:1 to 1:2 was very effective for α-amylase production by different strains of *Bacillus* sp. (Aiyer 2004, Avdiiuk and Varbanets 2008).

Table 3. Effect of C/N ratio on amylase production.

C/N ratio	Activity of enzyme (%)
2.5	44
1.0	72
0.66	86
0.50	100
0.33	100

Effect of metal ions on enzyme activity

The effectiveness of a group of metal ions on the activity of purified amylase (M_w 60 kDa) was tested and represented in Table 4. Among them, Mg^{2+} and K^+ only increased the enzyme activity at very low concentration (1 mM). It was observed that Zn^{2+}, Fe^{2+}, Cu^{2+} inactivated the enzyme activity at higher concentration (0.1 M), whereas, Hg^{2+} inhibited at lower concentration. This observation indicated that the activity of amylase from *B. licheniformis* SKB4 may not metal dependent. The results were comparable with the findings of other studies (Shaw et al. 1995; Rao et al. 2002).

Effect of pH on stability and activity of amylase

The optimum pH of the amylase activity was found at 6.5 (Fig. 6). The enzyme was stable at this condition (Fig. 6). The enzyme retained considerable activity in the pH range of 6.0–9.0. It also retained about 58% and 18% of its original

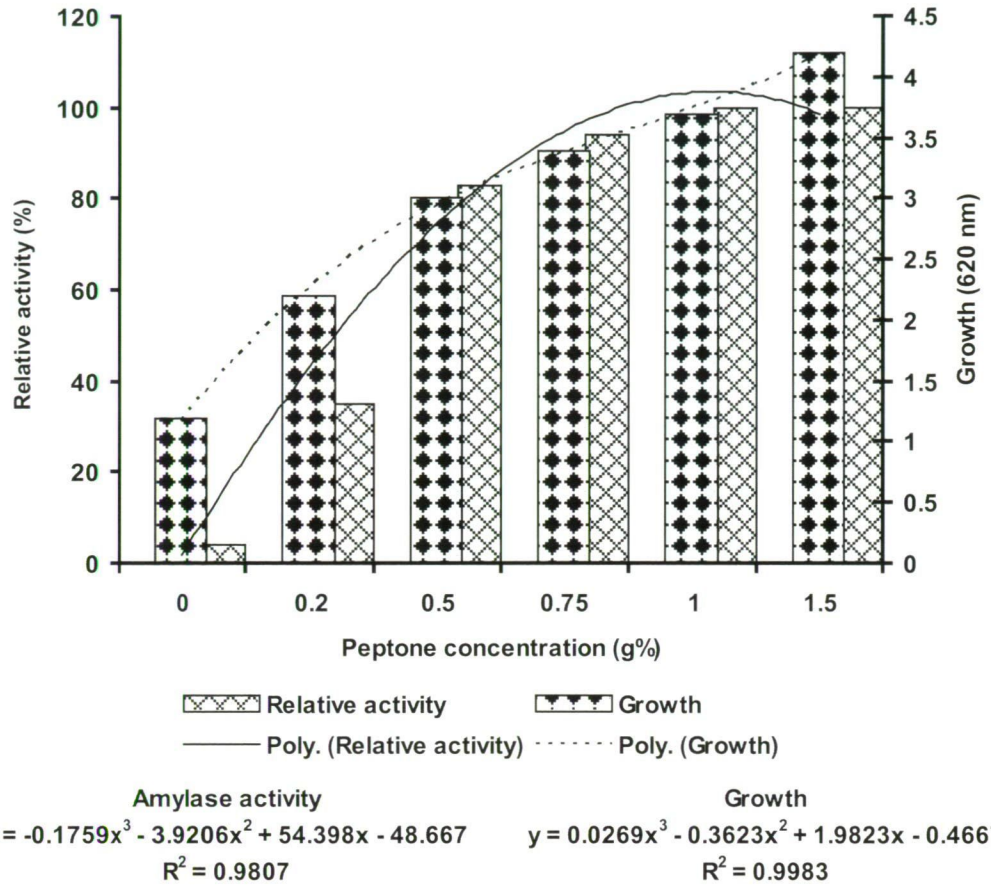

Figure 5. Effect of peptone concentration on growth and amylase production of *B. licheniformis* SKB4. Basal medium contained various concentration of peptone (0.2-1.5% w/v). Initial pH, temperature and incubation were 6.5, 42 °C and 28 h, respectively.

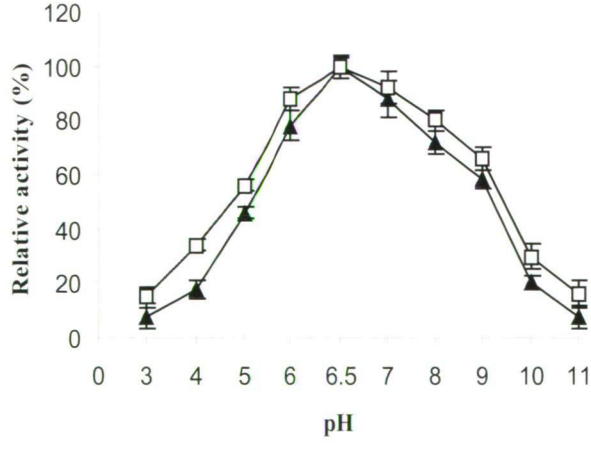

Figure 6. Effect of pH on enzyme activity (▲) and stability (□) of *B. licheniformis* SKB4 amylase. pH of the reaction buffer was varied (3-11). Amylase activity measured at 90 °C.

activity at pH 9.0 and 4.0, respectively. Our results are comparable with α-amylase from *B. subtilis* ITBCCB148 (Yandri et al. 2010) and *Bacillus cereus* GUF8 (Mahdavi et al. 2010).

Effect of temperature on amylase activity

Activity of α-amylase from *B. licheniformis* SKB4 was measured over a temperature range of 30 °C to 100 °C. The enzyme showed optimum activity at 90 °C (Fig. 7). It was also observed that 90% of its original activity was retained at 70 °C after 1 h incubation (Fig. 8). Other reports indicated that α-amylase from *B. licheniformis* (Adeyanju et al. 2007), *B. cereus* MK (Mrudula and Kokila 2010) were also active at 90 °C.

The half-life ($t_{1/2}$) of α-amylase of *B. licheniformis* SKB4 was 10 min at 100 °C and the temperature coefficient value (Q_{10}) was found to be 1.0 (Table 5). The Q_{10} for enzymes generally achieved between the range of 1 and 2 (Singh and Chhatpar 2011).

Determination of kinetic and thermodyanamic indices

The kinetic constants of the α-amylase like K_m (the Michaelis constant) and V_{max} (the maximum reaction rate) for starch

Table 4. Effect of metal ions on the activity of purified *B. licheniformis* SKB4 amylase. Enzyme activity was measured at pH 6.5 and 90 °C. Data represented as the average of three separate experiments.

Metal ions	Concentrations (M)	Relative activity (%)	% of change
Control		100	-
$MnCl_2$	0.1	20	80 (-)
	0.01	80	20 (-)
	0.001	86.6	13.4 (-)
$ZnCl_2$	0.1	0	100 (-)
	0.01	23	77 (-)
	0.001	76.6	23.4 (-)
$HgCl_2$	0.1	0	100 (-)
	0.01	8	92 (-)
	0.001	13	87 (-)
$CoCl_2$	0.1	20	80 (-)
	0.01	63	37 (-)
	0.001	76.6	23.4 (-)
$FeCl_3$	0.1	10	90 (-)
	0.01	86.6	13.4 (-)
	0.001	93	7 (-)
$CaCl_2$	0.1	24	76 (-)
	0.01	76	24 (-)
	0.001	93	7 (-)
KCl	0.1	86.6	13.4 (-)
	0.01	95	5 (-)
	0.001	103	3 (+)
$MgCl_2$	0.1	80	20 (-)
	0.01	86.6	13.4 (-)
	0.001	110	10 (+)
$CuCl_2$	0.1	0	100 (-)
	0.01	46.6	53.4 (-)
	0.001	60	40 (-)

(+) indicates stimulatory effect, (-) indicates inhibitory effect.

were found to be 6.2 mg ml^{-1} and 1.04 µmol mg^{-1} min^{-1} (Table 5), respectively, at 90 °C and pH 6.5. The K_m and V_{max} of α-amylase from *Bacillus stearothermophilus* GRE1 were also found to be 4.78 mg ml^{-1} and 6.67 mg ml^{-1} min^{-1}, respectively (Hossain et al. 2006). The turn over number (K_{cat}), which is the second-order rate constant for the conversion of the enzyme-substrate complex to the product, was calculated as 2×10^3 S^{-1} (Table 5). The apparent second-order rate constant, also called catalytic efficiency (K_{cat}/K_m), was 3.22×10^2 ml mg^{-1} S^{-1} (Table 5). All these characteristics are unique in the studied amylase, indicating its higher catalytic efficiency against starch like homopolysaccharides. α-Amylase from a mutant strain of *B. licheniformis* EMS-6 also showed similar K_{cat} and K_{cat}/K_m values (Haq et al. 2010).

Thermodynamic parameters provide a detailed portrait of inside of many chemical and biological reactions (Tanaka and Hoshino 2003). The activation energy (E_a) of the amylase of *B. licheniformis* SKB4 for starch hydrolysis was found to be 31.53, KJ/mol at 90 °C (Table 5). Previously it was reported that α-amylase from *B. licheniformis* EMS-6 was 25.14 KJ/mol (Haq et al. 2010). The free energy for substrate binding

Table 5. Summary of different kinetics and thermodynamic properties of purified *B. licheniformis* SKB4 amylase. Thermodynamic parameters were calculated at 90 °C.

Parameters	Purified amylase
K_m (mg/ml)	6.2
V_{max} (µmol/mg/min)	1.04
K_{cat} (S^{-1})	2×10^3
K_{cat} / K_m (ml mg^{-1} S^{-1})	3.22×10^2
E_a (KJ mol^{-1})	31.53
Q_{10}	1.0
$\Delta G_{E\text{-}S}$ (KJ mol^{-1})	5.53
$\Delta G_{E\text{-}T}$ (KJ mol^{-1})	-17.4
$T_{1/2}$ (min) (100 °C)	10

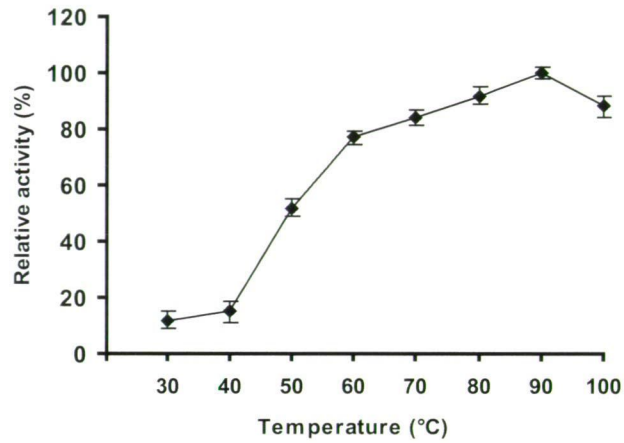

Figure 7. Effect of temperature on the activity of *B. licheniformis* SKB4 amylase. Temperature range of the reaction was 30-100 °C and amylase activity measured at pH 6.5.

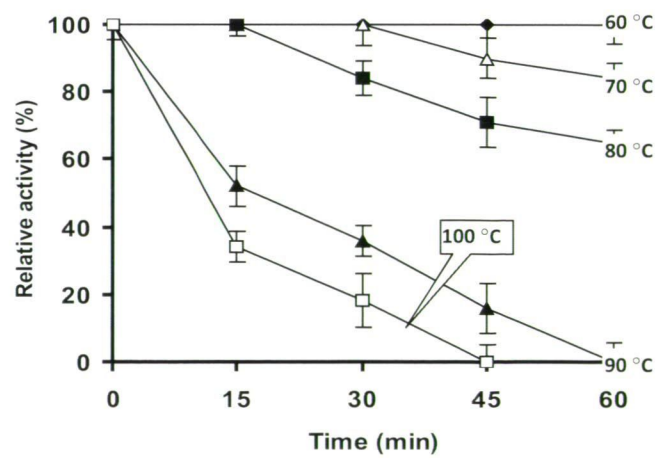

Figure 8. Study of thermostability of amylase from *B. licheniformis* SKB4 in absence of substrate after 1 h incubation. Amylase activity measured at pH 6.5 and 90 °C.

($\Delta G^*_{E\text{-}S}$) and transition state for formation of an activated enzyme substrate complex ($\Delta G^*_{E\text{-}T}$) of the enzyme at 90 °C were found to be 5.53 and –17.4 KJ/mol, respectively (Table 5). The free energy is required for the formation of activation complex and catalytic activity. The values of $\Delta G^*_{E\text{-}S}$ and $\Delta G^*_{E\text{-}T}$ indicated higher affinity of enzyme towards soluble starch for hydrolysis. The values of $\Delta G^*_{E\text{-}S}$ $\Delta G^*_{E\text{-}T}$ for glucoamylase from *Arachniotus citrinus* were found to be –2.95 and –17.7 kJ mol^{-1}, respectively (Perveen et al. 2006).

The present study revealed that *B. licheniformis* SKB4 is a potential strain for alpha amylase production in presence of soluble starch as substrate and complex nitrogen sources such as peptone. The high thermostability and metal independence of this amylase will be very effective for soluble starch hydrolysis. Various kinetic and thermodynamic parameters of the enzyme suggested that it has great affinity to catalyze soluble starch and suitable for many commercial applications, such as pharmaceutical, detergent and food industries.

Acknowledgements

The authors are very grateful to Vidyasagar University, Midnapore, West Bengal for the infrastructural and financial support.

References

Adeyanju MM, Agboola FK, Omafuvbe BO, Oyefuga OH, Adebawo OO (2007) A thermostable extracellular α-amylase from *Bacillus licheniformis* isolated from cassava steep water. Biotechnology 6(4):473-480.

Ahmadi A, Ghobadi S, Khajeh K, Nomanpour B, Dalfard AB (2010) Purification of -amylase from *Bacillus* sp. GHA1 and its partial characterization. J Iran Chem Soc 7:432-440.

Aiba S, Kitai K, Imanaka T (1983) Cloning and expression of thermostable α-amylase gene from *Bacillus stearothermophilus* in *Bacillus stearothermophilus* and *Bacillus subtilis*. Appl Environ Microbiol 46(5):1059-1065.

Aiyer PVD (2004) Effect of C:N ratio on alpha amylase production by *Bacillus licheniformis* SPT 278. Afr J Biotechnol 3(10):519-522.

Avdiiuk KV, Varbanets LD (2008) Optimization of cultivation conditions of the α-amylase producer *Bacillus subtilis* 147. Mikrobiol Z 70:10-16.

Bernfeld P (1955) Amylases alpha/beta. Methods Enzymol 1:149-158.

Boži N, Ruiz J, Santin JL, Vuj i Z (2011) Optimization of the growth and α-amylase production of *Bacillus subtilis* IP 5832 in shake flask and laboratory fermenter batch cultures. J Serb Chem Soc 76(7):965-972.

Chandra AK, Medda S, Bhadra AK (1980) Production of extracellular thermostable α-amylase by *Bacillus licheniformis*. J Ferment Technol 58:1-10.

Coronado MJ, Vargas C, Hofemeister J, Ventosa A, Nieto JJ (2000) Production and biochemical characterization of an α-amylase from the moderate halophile *Halomonas meridian*. FEMS Microbiol Lett 183:67-71.

Das A, Ghosh U, Mahapatra PK, Pati BR, Mondal KC (2012) Study on thermodynamics and adsorption kinetics of purified endoglucanase (CMCase) from *Penicillium notatum* NCIM NO-923 produced under mixed solid-state fermentation of waste cabbage and bagasse. Braz J Microbiol 43:1103-1111.

de Oliveira AN, de Oliveira LA, Andrade JS (2010) Partial characterization of amylases of two indigenous Central Amazonian rhizobia strains. Braz Arch Biol Technol 53(1):35-45.

Deb P, Talukdar SA, Mohsina K, Sarker PK, Sayem SMA (2013) Production and partial characterization of extracellular amylase enzyme from *Bacillus amyloliquefaciens* P-001. Springerplus 2:154.

Dixon M, Webb EC (1979) Enzyme Kinetics. In Dixon M, Webb EC, eds., Enzymes, 3rd edition. Academic Press, New York. 47-206.

Eisenthal R, Danson MJ, Hough DW (2007) Catalytic efficiency and k_{cat}/K_M: a useful comparator? Trends Biotechnol 25(6):247-249.

Gangadharan D, Sivaramakrishnan S, Nampoothiri KM, Pandey A (2006) Solid culturing of *Bacillus amyloliquefaciens* for α-amylase production. Food Technol Biotechnol 44:269-274.

Goyal N, Sidhu GS, Chakrabarti ST, Gupta JK (1995) Thermostability of alpha amylase produced by *Bacillus sp.* E2 - a thermophilic mutant. World J Microbiol Biotechnol 11:593-594.

Gupta R, Gigras P, Mohapatra H, Goswami VK, Chauhan B (2003) Microbial α-amylases: a biotechnological perspective. Proc Biochem 38:1599-1616.

Hamilton LM, Kelly CT, Fogarty WM (1999) Purification and properties of the raw starch-degrading α-amylase of *Bacillus* sp. IMD 434. Biotechnol Lett 21:111-115.

Haq I, Javed MM, Hameed U, Adnan F (2010) Kinetics and thermodynamic studies of alpha amylase from *Bacillus licheniformis* mutant. Pak J Bot 42(5):3507-3516.

Haq I, Rani VS, Ashraf H, Qadeer MA (2002) Biosynthesis of α-amylases by chemically treated mutant of *Bacillus subtilis*. J Biol Sci 2:73-75.

Haseltine C, Rolfsmeier M, Blum P (1996) The glucose effect and regulation of α-amylase synthesis in the hyperthermophilic archaeon *Sulfolobus solfataricus*. J Bacteriol 178:945-950.

Hossain SMZ, Haki GD, Rakshit SK (2006) Optimum production and characterization of thermostable amylolytic enzymes from *B. stearothermophilus* GRE1. Can J Chem Eng 84:368-374.

Kikani BA, Singh SP (2012) The stability and thermodynamic parameters of a very thermostable and calcium independent α-amylase from a newly isolated bacterium, *Anoxybacillus beppuensis* TSSC-1. Process Biochem 47:1791-1798.

Kole MM, Gerson DF (1989) Ammonium controlled fed-batch fermentation for amylase production. J Ferment Bioeng 68:423-427.

Laderman KA, Davis BR, Krutzsch HC, Lewis MS, Grico YV, Privalov BR, Anfinsen CB (1993) The purification and characterization of an extremely thermostable α-amylase from the hyperthermophilic archaebacterium *Pyrococcus furiosus*. J Biol Chem 268:24394-24401.

Lineweaver H, Burk O (1934) The determination of enzyme dissociation constants. J Am Chem Soc 56:658-666.

Mahdavi A, Sajedi RH, Rassa M, Jafarian V (2010) Characterization of an α-amylase with broad temperature activity from an acid-neutralizing *Bacillus cereus* strain. Iran J Biotechnol 8:103-111.

Malhotra R, Noorvez SM, Satyanarayana T (2000) Production and partial characterization of thermostable and calcium-independent alpha-amylase of an extreme thermophile *Bacillus thermooleovorans* NP54. Lett Appl Microbiol 31:378-384.

Mc Tigue MA, Kelly CT, Doyle EM, Fogarty WM (1995) The alkaline amylase of the alkalophilic *Bacillus* sp. IMD 370. Enzyme Microb Technol 17:570-573.

Mrudula S, Kokila R (2009) Production of thermostable α-amylase by *Bacillus cereus* MK in solid state fermentation: partial purification and characterization of the enzyme. Internet J Microbiol 8(1)

Nickless DM, Sobieski RJ, Crupper SS (2001) Genetic regulation of amylase expression in *Bacillus*. Bioscene 27:27-29.

Perveen R, Rashid MH, Saleem M, Khalid AM, Rajoka MI (2006) Kinetic and thermodynamic properties of an immobilized glucoamylase from a mesophilic fungus, *Arachniotus citrinus*. Protein Pept Lett 13:665-671.

Prakash O, Jaiswal N (2010) α-Amylase: an ideal representative of thermostable enzymes. Appl Biochem Biotechnol 160:2401-2414.

Rao DM, Purnima A, Ramesh, DV, Ayyanna C (2002) Purification of α-amylase from *Bacillus licheniformis* by chromatofocusing and gel filtration chromatography. World J Microbiol Biotechnol 18:547-550.

Rasooli I, Astaneh SDA, Borna H, Barchini KA (2008) A thermostable α-amylase producing natural variant of *Bacillus* sp. isolated from soil in Iran. Am J Agric Biol Sci 3:591-596.

Rukhaiyar R, Srivastava SK (1995) Effect of various carbon substrate on α-amylase production from *Bacillus* species. J Microbial Biotechnol 10(2):76-82.

Samanta S, Jana M, Maity C, Kar S, Mohapatra PKD, Pati BR, Mondal KC (2009) The potential of immobilized bacterial α-amylase on coconut coir, a smart carrier for biocatalysts. Biocatal Biotransformation 27(2):131-135.

Saqib AAN, Hassan M, Khan NF, Baig S (2010) Thermostability of crude endoglucanase from *Aspergillus fumigatus* gown under solid-state fermentation (SSF) and submerged fermentation (SmF). Proc Biochem 45:641-646.

Shaw JF, Lin FP, Chen SC, Chen HC (1995) Purification and properties of an extracellular α-amylase from *Thermus* sp. Bot Bull Acad Sin 36:195-200.

Sivaramakrishnan S, Gangadharan D, Nampoothiri KM, Soccol CR, Pandey A (2006) α- Amylases from microbial sources - an overview on recent developments. Food Technol Biotechnol 44(2):173-184.

Singh AK, Chhatpar HS (2011) Purification and characterization of chitinase from *Paenibacillus* sp. D1. Appl Biochem Biotechnol 164:77-88.

Suman S, Ramesh K (2010) Production of a thermostable extracellular amylase from thermophilic *Bacillus* species. J Pharm Sci Res 2:149-154.

Tanaka A, Hoshino E (2003) Secondary calcium binding parameter of *Bacillus amyloliquefaciens* α-amylase obtained from inhibition kinetics. J Biosci Bioeng 96(3):262-267.

Wanderley KJ, Torres FAG, Moraes LMP, Ulhoa CJ (2004) Biochemical characterization of α-amylase from the yeast *Cryptococcus flavus*. FEMS Microbiol Lett 231:165-169.

Yandri, Suhartati T, Hadi S (2010) Purification and characterization of extracellular α-amylase enzyme from locale bacteria isolate *Bacillus subtilis* ITBCCB148. Eur J Sci Res 39(1):64-74.

Volume 58(2):157-162, 2014
Acta Biologica Szegediensis
http://www2.sci.u-szeged.hu/ABS

ARTICLE

Antidermatophytic effect of *Bacillus mojavensis* SZMC 22228 and its secreted chymotrypsin-like protease

László Galgóczy[1]*, Melinda Guba[1], Enikő Sajben[1], Mónika Vörös[1], Miklós Takó[1], Rentsenkhand Tserennadmid[2], Csaba Vágvölgyi[1]

[1]Department of Microbiology, University of Szeged, Szeged, Hungary, [2]Institute of Biology, Mongolian Academy of Sciences, Ulaanbaatar, Mongolia

ABSTRACT The aim of the present study was to investigate the antifungal effect of *Bacillus mojavensis* SZMC 22228 against different dermatophytes and to isolate the antidermatophytic compound from the bacterial ferment broth. *B. mojavensis* SZMC 22228 and its cell-free ferment broth effectively inhibited the growth of clinical reference strain of *Microsporum canis*, *Microsporum gypseum*, *Trichophyton mentagrophytes*, *Trichophyton rubrum* and *Trichophyton tonsurans* in agar diffusion test *in vitro*. An antidermatophytic, ~25 kDa protein (*B. mojavensis* SZMC 22228 antidermatophyitc protein, BMAP) was purified from the antifungally active, cell-free ferment broth using size exclusion and ion-exchange chromatography. BMAP showed antifungal effect against all of the investigated dermatophytes both in agar diffusion and broth microdilution susceptibility tests. *M. gypseum* proved to be the most susceptible dermatophyte to BMAP (MIC=40 µg/ml), all the other investigated fungi were less susceptible (MIC=80 µg/ml). The enzymatic activity of this protein was investigated in microtiter plate assay using hydrolase specific chromogenic substrates. BMAP showed high proteolytic activity towards N-Succ-Ala-Ala-Pro-Phe-*p*NA, and proved to be a chymotrypsin-like protease. These results suggest that the antidermatohytic activity of *B. mojavensis* SZMC 22228 correlates with its chymotrypsin-like protease production. After further investigations, the purified BMAP could be a promising base of a novel antidermatophytic strategy. **Acta Biol Szeged 58(2):157-162 (2014)**

KEY WORDS

Bacillus mojavensis
dermatophytes
antifungal effect
protein isolation
extracellular chymotrypsin-like protease

The worldwide distributed dermatophytes are a group of keratinophilic fungi. They are highly adapted to digest keratinous debris thus these fungi are capable of invading the superficial layer of the skin, hair, and nails of humans and other vertebrates (Bond 2010; Leite Jr et al. 2014). Approximately 40% of the human population is affected in worldwide (Leite Jr et al. 2014), but the spectrum of isolated dermatophytes is diverse in time and geography (Havlickova et al. 2008; Seebacher et al. 2008). They rarely cause life-threatening infection in healthy individuals, but they may have a debilitating effect on the patients and affect their quality of life (Rotta et al. 2012). However, it is a well-known fact that the incidence of superficial and fatal systemic dermatophyte infections has been increasing continuously during recent years as a consequence of the rise in the number of immunocompromised patients (Rotta et al. 2012). The choice of the appropriate therapy in the cases of these patients is not simple because of the possible drug interactions and severe side effects (Dias et al. 2103). The more frequent occurrence of antimycotic resistant dermatophyte strains further sharpens this problem (Jones 1990; Mukherjee et al. 2003; Martinez-Rossi et al. 2008). Therefore, there is a substantial demand for new safely applicable antidermatophytic compounds without side effects.

Biologically active substances secreted by the members of *Bacillus* genus are promising compounds of drug industry for development of novel antifungal agents (Tserkovniak et al. 2009). The plant endophyte *Bacillus mojavensis* is a relatively new member of the *Bacillus* genus (Nair et al. 2002; Bacon and Hinton 2011). This species is closely related to *Bacillus subtilis* complex, but it can be distinguishable based on the fatty acid composition, DNA sequence, and the resistance to genetic transformation (Bacon and Hinton 2011). Several studies reported that *B. mojavensis* actively secretes different compounds with remarkable or potential antifungal activity, *e.g.* lipopeptides such as surfactin, iturin, fengycin; proteases, cellulases (Youcef-Ali et al. 2014). Due to this feature *B. mojavensis* is also known as an effective biocontrol agent against plant and post-harvest pathogenic filamentous fungi (Bacon and Hinton 2011).

This paper describes the antidermatophytic activity of a *B. mojavensis* strain isolated from mumijo, a traditional Mongolian medicine (Galgóczy et al. 2011); furthermore, the

Accepted Sept 30, 2014
*Corresponding author. E-mail: galgoczi@gmail.com

isolation and identification of an extracellular chymotrypsin-like protease (*B. mojavensis* SZMC 22228 antidermatophyitc protein, BMAP) which plays a role in it.

Materials and Methods

Strains and media

The following clinical reference dermatophyte strains were used in the present study: *Microsporum canis* (American Type Culture Collection, USA; ATCC 36299), *Microsporum gypseum* (ATCC 24102), *Trichophyton mentagrophytes* (ATCC 9533), *Trichophyton rubrum* (ATCC 28188) and *Trichophyton tonsurans* (ATCC 28942). All these isolates were maintained on potato dextrose agar (PDA, Sigma-Aldrich, St Louis, MO, USA) slants at 4 °C. For inoculum preparation they were subcultured onto oatmeal agar (10 g/l oatmeal, 1.5 g/l KH_2PO_4, 1 g/l $NaNO_3$, 1 g/l $MgSO_4$, 20 g/l agar) to induce conidium production (Jessup et al. 2000; Ghannoum et al. 2006). Antifungal activity tests were performed in PDA plates. *B. mojavensis* SZMC 22228 was maintained on LB (10 g/l tryptone, 2 g/l yeast extract, 10 g/l NaCl, 20 g/l agar, pH 7.0) slant and was grown in low salt LB broth (LSLB: 10 g/l tryptone, 5 g/l yeast extract, 5 g/l NaCl, pH 7.0) for investigation of antifungal activity of the cell-free ferment broth and for purification of the BMAP.

Isolation and molecular identification of *B. mojavensis* SZMC 22228

B. mojavensis was isolated from a Mongolian mumijo preparation (Galgóczy et al. 2011) and indentified for partial sequencing of the *gyrA* gene according to Reva et al. (2004). After sequencing (performed at LGC Genomics GmbH, Berlin, Germany) of the amplified partial *gyrA* gene, the result was compared with similar sequences available in the National Center for Biotechnology Information (NCBI) database using Basic Local Alignment Search Tool (BLAST) (Altschul et al. 1990).

Purification of *B. mojavensis* SZMC 22228 antidermatophytic protein (BMAP)

BMAP was isolated from the ferment broth of *B. mojavensis* SZMC 22228, which was cultivated in 250-ml Erlenmeyer flask containing 100 ml LSLB inoculated with 10^5 bacteria, and incubated at 30 °C for 48 h under continuous shaking (160 rpm). After bacterial cell harvest (30 min, 10.000×*g*, 4 °C), the supernatant was filtered (MILLEX-HP, pore size: 0.45 µm, Millipore, Billerica, MA, USA) then the extracellular protein fraction was precipitated with 80% of ammonium sulfate at 4 °C for 24 h. Precipitated proteins were collected by centrifugation (30 min, 10.000×*g*, 4 °C) and resuspended in 10 ml of 20 mM Tris buffer (pH 7.2). This protein solution was dialyzed (Snake Skin dialysis tubing, 3.5K MWCO, Thermo Scientific, Logan, UT, USA) against 20 mM Tris buffer (pH 7.2) in 1:100 volume ratio based on the instruction of manufacturer at 4 °C for 48 h with buffer changing after 24 h.

The different molecular weight protein fractions of the ten-fold concentrated sample were separated with size exclusion chromatography. The column (20×250 mm, Sephadex G-50, GE Healthcare, Uppsala, Sweden) was equilibrated with 20 mM Tris buffer (pH 7.2). Protein fractions were eluted (flow rate: 2 ml/min) with the above mentioned buffer. Protein fractions which showed high antidermatophytic activity in agar diffusion test (data not shown) were pooled, concentrated to six-fold, and then this solution was separated with centrifugal ultrafiltration (Corning® Spin-X® UF 20 ml Centrifugal Concentrator, 30,000 MWCO Membrane, Corning, Tewksbury, MA, USA). The <30 kDa fraction (showed antidermatophytic effect in agar diffusion test, data not shown) was dialyzed against 20 mM Tris buffer (pH 7.2), then purified with ion-exchange chromatography on a CM Sepharose Fast Flow (Sigma-Aldrich, St Louis, MO, USA) column (13×60 mm, equilibrated with 20 mM Tris buffer (pH 7.2) at a flow rate of 1 ml/min. The proteins were eluted with a NaCl gradient (0.1-1.0 M) prepared in the equilibrating buffer. The protein fractions were dialyzed against 20 mM Tris buffer (pH 7.2); finally, they were sterilized by filtration (MILLEX-HP, pore size: 0.45 µm, Millipore, Billerica, MA, USA) and their antidermatophytic activity was investigated in agar diffusion test. Protein content of the different fractions was checked in SDS-PAGE (NuPAGE Novex 4-12% Bis-Tris Gel, 1.0 mm, 10 well, Invitrogen-Life Technologies, Eugene, OR, USA) visualized with Coomassie Brilliant Blue R-250 and silver staining. Purification experiments were repeated three times.

Antidermatophytic activity assays

Fungal inocula were prepared as described previously (Galgóczy et al. 2008). An agar diffusion technique was used to estimate the antagonism ability of *B. mojavensis* SZMC 22228 and the size of growth inhibition caused by the cell-free bacterial ferment broth (filtered through MILLEX-HP, pore size: 0.45 µm) and the purified BMAP. Solid culture medium (PDA) was overlaid with 1 ml of potato dextrose broth (PDB, Sigma-Aldrich, St Louis, MO, USA; pH 7.0) that were inoculated with 10^6 microconidia/ml and was dried. For the investigation of antagonism ability, 10 µl 10^4 bacteria/ml suspended in LB was dropped on the surface of this plate and was dried. For investigation of the antifungal activity of *B. mojavensis* SZMC 22228 cell-free ferment broth and purified BMAP, an agar diffusion technique was used: 100 µl of sterile bacterial ferment broth or BMAP (160 µg/ml) diluted in 20 mM Tris buffer (pH 7.2) were filled into the wells of inoculated PDA plates. Sterile LSLB or Tris buffer (pH 7.2) was used as negative control. Diameters of the inhibition zones were measured after incubation at 30 °C for 72 h.

Table 1. Antidermatophytic activity of the *Bacillus mojavensis* SZMC 22228, its cell-free ferment broth and the 160 µg/ml purified ~25 kDa antidermatophytic protein (BMAP) in agar diffusion test on PDA after incubation at 30 °C for 72 h.

Species	Diameter of inhibition zone (mm)		
	B. mojavensis SZMC 22228	Cell-free ferment broth	160 µg/ml BMAP
Microsporum canis ATCC 36299	58.0±10.5	14.3±2.1	15.3±2.9
Microsporum gypseum ATCC 24102	48.0±2.9	18.3±2.1	23.7±3.1
Trichophyton mentagrophytes ATCC 9533	53.3±14.5	12.0±3.0	14.7±1.5
Trichophyton rubrum ATCC 28188	32.7±11.6	15.0±2.6	17.30±0.6
Trichophyton tonsurans ATCC 28942	56.7±12.6	16.3±2.1	18.3±2.3

Standard deviations (±SD) derived from three replicates (N=3).

Minimal inhibitory concentrations (MIC) of BMAP against the investigated dermatophytes were determined in broth microdilution susceptibility test using flat-bottom 96-well microtiter plate. One hundred microliter of BMAP diluted in PDB was mixed with 100 µl of microconidial suspension (10^5 microconidia/ml) prepared also in PDB. The final concentrations of BMAP were 160, 80, 40, 20, 10, 5, 2.5 and 1.25 µg/ml. The plates were incubated at 30 °C for 72 h, and the optical densities were then measured at 620 nm with microtiter plate reader (ASYS Jupiter HD-ASYS Hitech, Salzburg, Austria). Two hundred microliter fresh PDB was used as background for the spectrophotometric calibration. To determine MICs, optical densities of the untreated control cultures (100 µl of microconidial suspension mixed with 100 µl PDB) were referred to 100% of growth, in each case. MIC was defined as the lowest BMAP concentration at which growth was not detected on the basis of the OD_{620} values as compared with the untreated control. Antifungal activity experiments were repeated three times.

Enzymatic activity assays

The enzymatic activity of BMAP was determined in 96-well microtiter plate by the use of N-bz-Phe-Val-Arg-*p*NA, N-α-bz-L-Arg-*p*NA, N-acetyl-L-Leu-*p*NA, N-Succ-Ala-Ala-Pro-Phe-*p*NA, *p*-nitrophenyl-N-acetyl-β-D-glucosaminide, *p*-nitrophenyl-N,N'-diacetyl-β-D-chitobioside, *p*-nitrophenyl-β-D-N,N',N''-triacetylchitotriose, *p*-nitrophenyl-β-D-cellobioside, and *p*-nitrophenyl-β-glucopyranoside. All substrates were purchased from Sigma-Aldrich (St Louis, MO, USA). Twenty microliter of 1 mg/ml substrate was given to 80 µl of 40 µg/ml BMAP (diluted in 20 mM Tris buffer; pH 7.2) and incubated for 3 h at 30 °C. The reaction was stopped by addition of 25 µl 10% (w/v) sodium carbonate and the *p*-nitrophenol or *p*-nitroaniline release was measured at 405 nm using an ASYS Jupiter HD microplate reader. Twenty microliter of 1 mg/ml substrate mixed with 20 mM Tris buffer (pH 7.2) was used as background for the spectrophotometric calibration. Enzymatic activity assays were repeated three times.

Results

Isolation and identification of *B. mojavensis* SZMC 22228

The BLAST analysis of the amplified partial *gyrA* sequence revealed 99% similarity to the partial *gyrA* sequence of *B. mojavensis* NRRL BD-600 strain (accession number: EU138644). Based on this result, the *Bacillus* strain isolated from Mongolian mumijo preparation was identified as *B. mojavensis*. This *B. mojavensis* strain was deposited in the Szeged Microbiological Collection (SZMC, http://www2.sci.u-szeged.hu/microbiology/collection.htm) under the SZMC 22228 number, and the partial *gyrA* gene sequence in the European Nucleotide Archive under the HG964636 identifier.

Antifungal activity of *B. mojavensis* SZMC 22228 and its ferment broth

The isolated *B. mojavensis* SZMC 22228 effectively inhibited the growth of *M. canis*, *M. gypseum*, *T. mentagrophytes*, *T. rubrum* and *T. tonsurans* in different rates (Table 1). The cell-free ferment broth of *B. mojavensis* SZMC 22228 also showed antidermatophytic activity on these isolates in the applied agar diffusion test (Table 1). In these tests *M. canis* (58.0±10.5 mm inhibition zone caused by *B. mojavensis* SZMC 22228) and *M. gypseum* (18.3±2.1 mm inhibition zone caused by the cell-free ferment broth of *B. mojavensis* SZMC 22228) were the most susceptible dermatophytes (Table 1).

Purification of *B. mojavensis* SZMC 22228 antidermatophytic protein (BMAP) and its antifungal activity

Gel electrophoresis revealed the presence of a protein with a molecular mass of approx. 25 kDa in the purified fraction of the ferment broth which had antidermatophytic activity (BMAP, Figure 1). After purification the final yield of BMAP from three independent productions was 3.64±0.53 mg. One hundred sixty microgram per milliliter BMAP was able to inhibit the growth of *M. canis*, *M. gypseum*, *T. mentagrophytes*, *T. rubrum* and *T. tonsurans* causing inhibition halos with different diameters in agar diffusion tests (Table 1). *M. gypseum* (inhibition zone: 23.7±3.1 mm) was the most susceptible isolate (Table 1). Based on these results we suppose that the isolated ~25 kDa molecular weight BMAP plays a role in the antidermatophytic effect. The purified BMAP maintained

its antifungal activity against all investigated dermatophytes in broth microdilution susceptibility test, and also the *M. gypseum* proved to be the most susceptible fungus (MIC = 40 µg/ml). All the other dermatophytes were less susceptible (MIC = 80 µg/ml).

Enzymatic activity assays

BMAP did not show enzymatic activity towards N-acetyl-L-Leu-*p*NA, *p*-nitrophenyl-N-acetyl-β-D-glucosaminide, *p*-nitrophenyl-N,N'-diacetyl-β-D-chitobioside, *p*-nitrophenyl β-D-N,N',N''-triacetylchitotriose, *p*-nitrophenyl-β-D-cellobioside, *p*-nitrophenyl-β-glucopyranoside, *p*-nitrophenyl-N-acetyl-β-D-glucosaminide; but hydrolysed the N-α-bz-L-Arg-*p*NA, N-bz-Phe-Val-Arg-*p*NA, N-Succ-Ala-Ala-Pro-Phe-*p*NA proteolytic substrates. The most effective proteolytic activity was exerted on N-Succ-Ala-Ala-Pro-Phe-*p*NA (Figure 2). Based on these results and the amount of the released *p*-nitroaniline from digested proteolytic substrates (Figure 2), BMAP is considered as a chymotrypsin-like protease.

Discussion

Several *B. mojavensis* strains are considered as biocontrol agents because they can enhance plant growth and protect the plant against its fungal pathogens due to the produced surfactin, iturin, fengycin and various enzymes. Although, the factors which are responsible for growth enhancement are unknown but the antifungal mechanism of the biocontrol strains is well-characterized especially on *Fusarium verticillioides* (Bacon and Hinton 2011). Growth inhibition ability of *B. mojavensis* on other plant pathogenic (*e.g. Ambrosiella macrospora*, *Botrytis cinerea*, *Fusarium oxysporum*, *Fusarium moniliforme*, *Macrophomina phaseolina*, *Mucor rammanianus*, *Alternaria solani*, *Phytophthora meadii*, *Pythium aphanidermatum* and *Rhizoctonia solani*), and (opportunistic) human pathogenic (such as *Aspergillus flavus*, *Aspergillus niger*, *Candida utilis*, *Candida albicans* and *Rhizopus* spp.) fungi was demonstrated by previous studies (Nair et al. 2002; Maachiaet al. 2011; Youcef-Ali et al. 2014). In our work we observed that *B. mojavenis* SZMC 22228 can inhibit effectively the growth of different dermatophytes. Such kind antifungal activity of *B. mojavenis* has not been reported in the literature yet; however, data are available about the antidermatophytic effect of other *Bacillus* species. Previously, it was proven that *Bacillus amyloliquefaciens* HNA3 exerts growth inhibition effect on *T. mentagrophytes* (Nastro et al. 2011) and different *B. subtilis* isolates on *Trichophyton* and *Microsporum* spp. (Kumar et al. 2005, 2009; Lukmanova et al. 2008). Kumar et al. (2009) observed that a peptide belonging to the group of antifungal antibiotic peptides is responsible for this effect. Compared to this finding, a ~25 kDa extracellular chymotrypsin-like protease (BMAP) plays

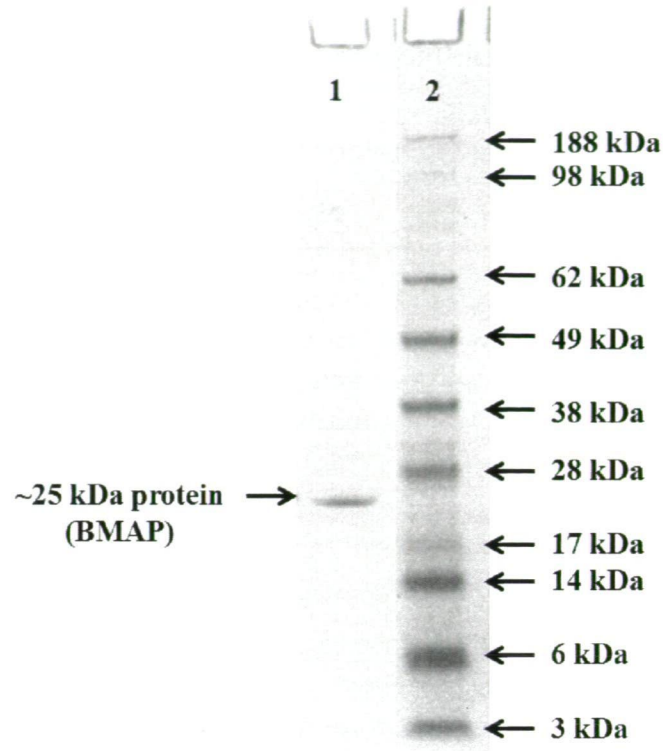

Figure 1. Bis-Tris SDS PAGE (4-12%) of the antidermatophytically active purified ~25 kDa protein (BMAP) from the ferment broth of *Bacillus mojavensis* SZMC 22228. Lane 1, purified ~25 kDa BMAP; lane 2, molecular weight marker (SeeBlue Plus2 Pre-Stained Standard, Invitrogen-Life Technologies, Eugene, OR, USA).

a role in the antidermatophyotic activity of *B. mojavensis* SZMC 22228.

Numerous species of *Bacillus* have been involved in industrial protease production and *B. mojavensis* is also considered as a great source of different (alkaline) proteases (Schallmey et al. 2004). Three different alkaline proteases from *B. mojavensis* A21 strain have been isolated, which show differences in their molecular weight (15-29 kDa) and enzymatic features, such as specific activity, pH and thermal optimum/stability, and calcium-dependence (Haddar et al. 2009a, 2009b). Proteases showing same substrate specificity as BMAP were isolated from the ferment broth of *B. mojavensis*-related *B. subtilis* strains. A 30 and 43-46 kDa molecular weight fibrinolytic enzymes with high activity to N-Succ-Ala-Ala-Pro-Phe-*p*NA chromogenic substrate were purified from the ferment broth of *B. subtilis* DC33 and *Bacillus* sp. nov. SK006 (Wang et al. 2006; Hua et al. 2008). The antifungal activity of these proteases has not been investigated yet, but few reports demonstrated a correlation between the biocontrol function of *Bacillus* strains and their extracellular protease production (Luo et al. 2013). Information about the

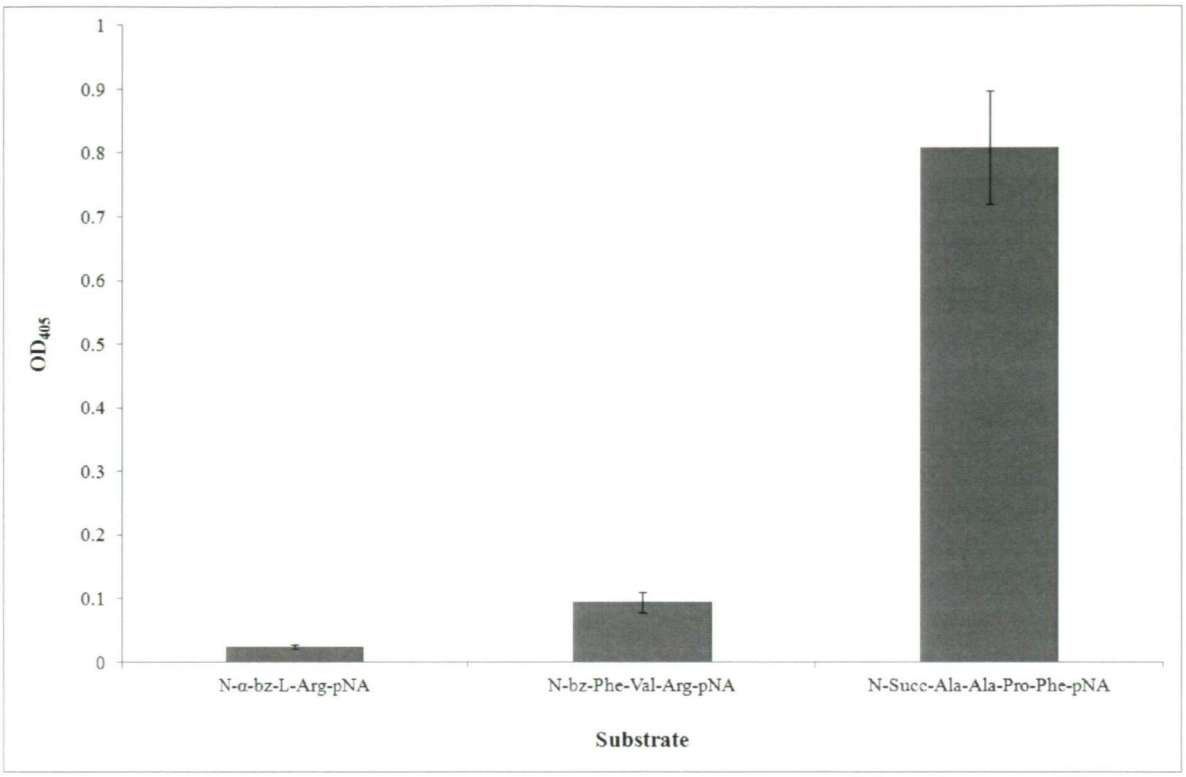

Figure 2. Substrate activity of the of the purified ~25 kDa antidermatophytic protein (BMAP) at 30 °C after 3 h. Standard deviations (±SD) derived from three replicates (N=3).

antifungal activity of extracellular proteases is available in the case of *B. mojavensis*-related *B. subtilis*. Its culture filtrate which had protease activity inhibited the growth of aflatoxigenic Aspergilli (Thakaew and Niamsup 2013). Basurto-Cadena et al. (2012) found connection between the presence of proteases and antagonistic activity of *B. subtilis* against plant pathogenic fungi such as *F. verticillioides* and *R. solani*. In a more detailed study, it was observed that the 41.38 kDa alkaline protease P6 from *B. subtilis* N7 effectively inhibits the spore germination and mycelial growth of *F. oxysporum* f.sp. *cucumerium* (Luo et al. 2013). Until the present study, antidermatophytic effect of bacterial proteases has not been described in the literature.

Our results indicate that the isolated ~25 kDa BMAP could be a promising agent in the treatment of dermatophytosis, however, further *in vitro* and *in vivo* investigations and characterization experiments (such as MALDI-TOF analysis, N-terminal sequencing, enzyme kinetics, pH and thermal optimum/stability, ion-dependence, hematolytic and toxic effect, etc.) are needed.

Acknowledgments

The research of L.G., M.G., M.T. and Cs.V. was supported by the European Union and the State of Hungary, co-financed by the European Social Fund in the framework of TÁMOP 4.2.4.A/2-11-1-2012-0001 'National Excellence Program'.

References

Altschul SF, Gish W, Miller W, Myers EW, Lipman DJ (1990) Basic local alignment search tool. J Mol Biol 215:403-410.

Bacon CW, Hinton DM (2011) *Bacillus mojavensis*: Its endophytic nature, the surfactins, and their role in the plant response to infection by *Fusarium verticillioides*. In Maheshwari DK, ed., Bacteria in Agrobiology: Plant Growth Responses. Springer-Verlag Berlin, Heidelberg, pp. 21-39.

Basurto-Cadena MG, Vázquez-Arista M, García-Jiménez J, Salcedo-Hernández R, Bideshi DK, Barboza-Corona JE (2012) Isolation of a new Mexican strain of *Bacillus subtilis* with antifungal and antibacterial activities. SciW J 2012:384978.

Bond R (2010) Superficial veterinary mycoses. Clin Dermatol 28:226-236.

Dias MF, Bernardes-Filho F, Quaresma-Santos MV, Amorim AG, Schechtman RC, Azulay DR (2013) Treatment of superficial mycoses: review - part II. An Bras Dermatol 88:937-944.

Galgóczy L, Papp T, Pócsi I, Hegedus N, Vágvölgyi C (2008) In vitro activity of *Penicillium chrysogenum* antifungal protein (PAF) and its combination with fluconazole against different dermatophytes. A Van Leeuw J Microb 94:463-470.

Galgóczy L, Guba M, Papp T, Krisch J, Vágvölgyi Cs, Tserennadmid, R (2011) In vitro antibacterial effect of a mumijo preparation from Mongolia. Afr J Microbiol Res 5:3832-3835.

Ghannoum MA, Chaturvedi V, Espinel-Ingroff A, Pfaller MA, Rinaldi MG, Lee-Yang W, Warnock DW (2004) Intra- and interlaboratory study of a method for testing the antifungal susceptibilities of dermatophytes. J Clin Microbiol 42:2977-2979.

Haddar A, Bougatef A, Agrebi R, Sellami-Kamoun A, Nasri M (2009a) A novel surfactant-stable alkaline serine-protease from a newly isolated *Bacillus mojavensis* A21. Purification and characterization. Process Biochem 44:29-35.

Haddar A, Agrebi R, Bougatef A, Hmidet N, Sellami-Kamoun A, Nasri M. (2009b) Two detergent stable alkaline serine-proteases from *Bacillus mojavensis* A21: purification, characterization and potential application as a laundry detergent additive. Bioresour Technol 100:3366-3373.

Havlickova B, Czaika VA, Friedrich M (2008) Epidemiological trends in skin mycoses worldwide. Mycoses 51 Suppl 4:2-15.

Hua Y, Jiang B, Mine Y, Mu W (2008) Purification and characterization of a novel fibrinolytic enzyme from *Bacillus* sp. nov. SK006 isolated from an Asian traditional fermented shrimp paste. J Agric Food Chem 56:1451-1457.

Jessup CJ, Warner J, Isham N, Hasan I, Ghannoum MA (2000) Antifungal susceptibility testing of dermatophytes: establishing a medium for inducing conidial growth and evaluation of susceptibility of clinical isolates. J Clin Microbiol 38:341-344.

Jones HE (1990) Problems of resistant dermatophytes. J Am Acad Dermatol 23:779-781.

Kumar A, Saini P, Shrivastava JN (2005) Biological control of dermatophytic fungus *Trichophyton* species by *Bacillus subtilis*. Hindustan Antibiot Bull 47-48:36-40.

Kumar A, Saini P, Shrivastava JN (2009) Production of peptide antifungal antibiotic and biocontrol activity of *Bacillus subtilis*. Indian J Exp Biol 47:57-62.

Leite DP Jr, de Souza Amadio JV, de Almeida Alves Simões S, Martins de Araújo S, Rodrigues da Silva NM, Anzai MC, Hahn RC (2014) Dermatophytosis in military in the central-west region of Brazil: literature review. Mycopathologia 177:65-74.

Lukmanova KA, Gizatullina SV, Magazov RSh, Melent'ev AI, Galimzianova NF, Aktuganov GE (2008) Antagonistic activity of bacteria from *Bacillus genus* against dermatophyte fungi. Zh Mikrobiol Epidemiol Immunobiol 4:21-33.

Luo Y, Sun L, Zhu Z, Ran W, Shen Q (2013) Identification and characterization of an anti-fungi *Fusarium oxysporum* f. sp. *cucumerium* protease from the *Bacillus subtilis* strain N7. J Microbiol 51:359-366.

Maachia SB, Errakhi R, Mathieu F, Chérif M, Lebrihi A (2011) Identification and partial characterization of antifungal and antibacterial activities of two *Bacillus* sp. strains isolated from salt soil in Tunisia. Afr J Microbial Res 5:4956-4966.

Martinez-Rossi NM, Peres NT, Rossi A (2008) Antifungal resistance mechanisms in dermatophytes. Mycopathologia 166:369-383.

Mukherjee PK, Leidich SD, Isham N, Leitner I, Ryder NS, Ghannoum MA (2003) Clinical *Trichophyton rubrum* strain exhibiting primary resistance to terbinafine. Antimicrob Agents Chemother 47:82-86.

Nair JR, Singh G, Sekar V (2002) Isolation and characterization of a novel *Bacillus* strain from coffee phyllosphere showing antifungal activity. J Appl Microbiol 93:772-780.

Nastro RA, Di Costanzo A, Gesuele R, Trifuoggi M, Inglese M, Guida M (2011) Influence of temperature on the production of antibiotic molecules in *Bacillus amyloliquefaciens* strain HNA3. In Méndez-Vilas A, ed., Science against microbial pathogens: communicating current research and technological advances. Formatex, Badajoz, pp. 1307-1310.

Reva ON, Dixelius C, Meijer J, Priest FG (2004) Taxonomic characterization and plant colonizing abilities of some bacteria related to *Bacillus amyloliquefaciens* and *Bacillus subtilis*. FEMS Microbiol Ecol 48:249-259.

Rotta I, Otuki MF, Sanches AC, Correr CJ (2012) Efficacy of topical antifungal drugs in different dermatomycoses: a systematic review with meta-analysis. Rev Assoc Med Bras 58:308-318.

Schallmey M, Singh A, Ward OP (2004) Developments in the use of *Bacillus* species for industrial production. Can J Microbiol 50:1-17.

Seebacher C, Bouchara JP, Mignon B (2008) Updates on the epidemiology of dermatophyte infections. Mycopathologia 166:335-352.

Thakaew R, Niamsup H (2013) Inhibitory activity of *Bacillus subtilis* BCC 6327 metabolites against growth of aflatoxigenic fungi isolated from bird chili powder. Int J Biosc Biochem Bioinfo 3:27-32.

Tserkovniak LS, Roi AO, Kurdysh IK (2009) Synthesis of amino acids of *Bacillus subtilis* IMV V-7023 in the medium with glycerophosphates. Mikrobiol Z 71:18-23.

Wang CT, Ji BP, Li B, Nout R, Li PL, Ji H, Chen LF (2006) Purification and characterization of a fibrinolytic enzyme of *Bacillus subtilis* DC33, isolated from Chinese traditional Douchi. J Ind Microbiol Biotechnol 33:750-758.

Youcef-Ali M, Kacem Chaouche N, Dehimat L, Bataiche I, Kara Ali M, Cawoy H, Thonart P (2014) Antifungal activity and bioactive compounds produced by *Bacillus mojavensis* and *Bacillus subtilis*. Afr J Microbial Res 8:476-484.

Volume 58(2):163-166, 2014
Acta Biologica Szegediensis
http://www2.sci.u-szeged.hu/ABS

ARTICLE

Deletion series in the P1 protein of the *Sweet potato mild mottle virus* identifies the shortest fully functional RNA silencing suppressor domain

Edit Zsuzsanna Szabó[1], Lajos Kemény[1,2], Lóránt Lakatos[1,2]*

[1]Department of Dermatology and Allergology, Faculty of Medicine, University of Szeged, Szeged, Hungary, [2]MTA-SZTE Dermatological Research Group, Szeged, Hungary

ABSTRACT RNA silencing is a part of the plant innate immune system that could effectively cope with intruders, like viruses. However, viruses evolved proteins that can suppress RNA silencing thus supporting virus spreading in the host. To counteract RNA silencing, suppressor proteins attack different players of RNA silencing pathway. The P1 protein of the *Sweet potato mild mottle* virus binds and inactivates small RNA loaded RISC complexes. Using a deletion series in the P1 protein we aimed to identify the possible smallest working version of P1. Our results revealed that the minimal RNA silencing suppressor domain of P1 is as small as 210 amino acids in size.

Acta Biol Szeged 58(2):163-166 (2014)

KEY WORDS

RNA silencing
plant
Sweet potato mild mottle virus
RNA silencing suppressor

RNA silencing is a post-transcriptional gene regulation mechanism conserved in almost all eukaryotes and involved in many essential biological processes, from development, physiological activity to the regulation of abiotic and biotic stress responses by micro RNAs (miRNA), genome defense by 24 nucleotide (nt) long small interfering RNAs (siRNAs) and in particular antiviral defense by 21 nt siRNAs. RNA silencing negatively regulates genes expression (Herr and Baulcombe 2004).

The trigger of RNA silencing can be pri-miRNAs for miRNAs or double stranded (ds) RNAs as replicative forms of plant viruses. Trigger RNAs are processed into si- and miRNAs by the RNAse III type enzymes Dicers, then small RNAs are loaded into the Argonaute (AGO) protein containing protein complexes called RNA induced silencing complex (RISC). This process is referred to as RISC assembly. In RISC, one strand of the small RNA is eliminated resulting in the single stranded (ss) small RNA containing RISC complex (active RISC). Active RISC complexes are able to hamper gene expression either by cleaving the target RNA or by inhibiting the translation of the target RNA (Hutvagner and Simard 2008). Thus, Argonaute (AGO) proteins play a key role in RNA silencing.

In the last few years, several AGO binding proteins were identified. Most of them contain GW/WG (Gly-Trp/Trp-Gly) domains, which mediate the interaction with AGO. This group of proteins was named GW/WG proteins after the founding member GW182 protein of human. GW182 in animals binds AGO and mediates the interaction with the polyA binding proteins to repress the translation of the target RNA (Pfaff et al. 2013). In *Schizosaccharomyces pombe*, transcriptional silencing involves AGO and TAS3 that shows high similarity to animal GW182 proteins (Pfaff et al. 2013). In plants, heterochromatin silencing exploits a couple of GW/WG proteins, such as the second largest subunit of the RNA polymerase V complex and SPT5 protein (Bies-Etheve et al. 2009; Herr et al. 2005). Moreover, the GW/WG protein SUO was identified in Arabidopsis thaliana to be involved in miRNA driven RNA silencing (Yang et al. 2012). Thus, these GW/WG proteins have a positive effect on RNA silencing and are absolutely required for the efficient carrying RNA silencing into execution.

Two viral proteins bearing WG/GW domains were found to have a negative effect on RNA silencing. The p38 protein of the *Turnip crinkle virus* (TCV) sequesters small RNA unloaded AGO1 (Azevedo et al. 2010). However, the P1 RNA silencing suppressor protein of the *Sweet potato mild mottle virus* (SPMMV) is markedly different from that of p38. SPMMV P1 binds AGO1 loaded with si- or miRNAs, thus inhibiting target cleavage of active RISC complexes. Mutational analysis revealed three WG/GW motifs, resembling the AGO binding platform conserved in plants and metazoans, at the N-terminal part of P1, which are required for AGO binding and silencing suppressor activity (Giner et al. 2010).

Recently, we found that the first 383 amino acid (aa) region of the SPMMV P1 renders RNA silencing suppressor activity (Giner et al. 2010). Thus, our aim was to find the smallest region of the P1 protein bearing fully functional suppressor activity. Our results based on a series of truncation of

Accepted Dec 18, 2014
*Corresponding author. E-mail: lakatos.lorant@med.u-szeged.hu

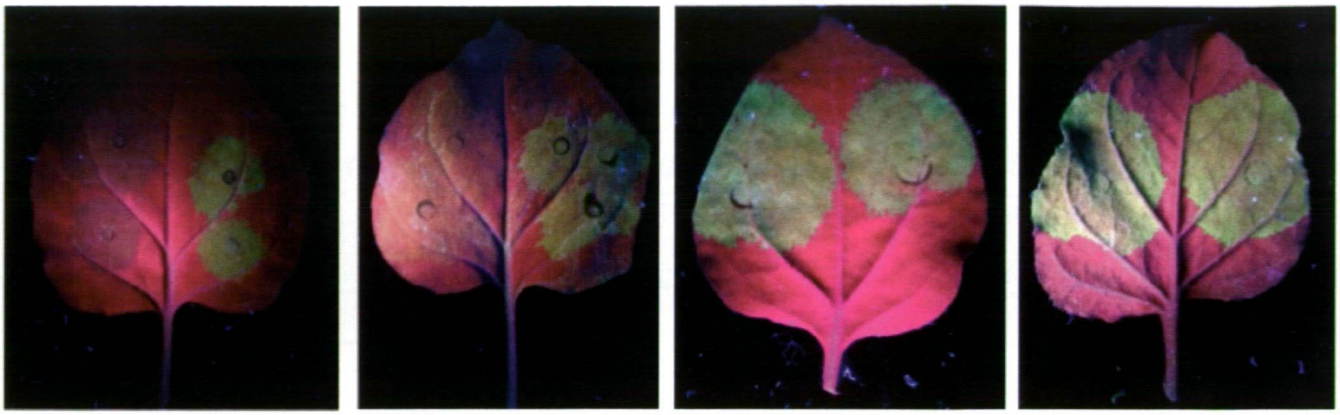

Figure 1. RNA silencing suppressor activity of the truncated mutants. The first panel shows empty vector infiltrated sample, used as negative control. The mutant of interest was infiltrated as shown in the second, third and fourth panel. On the right side of each panel $P1_{1-383}$ was infiltrated, as positive control.

the P1 protein from the C-terminal end showed that the 1-210, but not 1-120, amino acids region is fully functional.

Materials and Methods

Plant materials

Wild-type *Nicotiana benthamiana* plants grown in soil under normal growth conditions were used for, virus infection and agroinfiltration. Plants were grown in Phytotron (Versatile Environmental Test Chambers; Sanyo, Tokyo, Japan) under a 14-h light (50 mE m±2s±1) and 10-h dark regime at 23 °C.

Agroinfiltration

Agroinfiltration was essentially carried out as described earlier (Silhavy et al. 2002). Plasmid DNA was introduced into the *Agrobacterium tumefaciens* C58C1 strain by triparental mating (Wise et al. 2006). *Agrobacterium* strains harboring the expression plasmids were cultured at 28 °C in LB medium in the presence of 5 μg/ml tetracycline and 100 μg/ml kanamycin. Cultures were centrifuged at room temperature with 1000 g to pellet the bacteria, then resuspended in the induction solution containing 10 mM MES (pH 5.6), 10 mM $MgCl_2$ and 150 μM acetosyringone. Optical density of the cultures were determined and diluted to an OD_{600} of 0.3 for suppressor and 0.1 for reporter genes. Diluted and mixed *Agrobacterium* strains were incubated in the induction solution for 1-3 hours at room temperature before infiltration.

Primers used in this study

P1-5'-end: 5'GGGGATTCCCTAGAATGGGGAAATCCAAACTC 3'
$P1_{1-360}$-3'-end: 5' TGAATTCTCATGCCACCGTGATGGGACACACCATAGC 3'
$P1_{1-305}$-3'-end: 5' TGAATTCTCATGTCTTTGTAACCCACATAACTGC 3'
$P1_{1-210}$-3'-end: 5' TGAATTCTCAAATTGAGAAAACAGTTTCCTCAAAAACC 3'
$P1_{1-120}$-3'-end: 5' TGAATTCTCAGTTATCAAGTACATTGTCGTCGCGCTTGTT 3'

Western blot analysis

To the blot analysis, samples were collected in 2 cm diameter. The samples were extracted in 2x sodium dodecyl sulfate (SDS) loading puffer and boiled for 5 minutes, after sample preparation 10% sodium dodecyl sulfate polyacrylamide gel electrophoresis (SDS-PAGE) was run. Blocking was carried out in 5% dry milk in phosphate buffered saline (PBS) at every turn. Anti-HA (anti-influenza hemagglutinin, 1:3000 in 5% dry milk) and anti-GFP (anti-green fluorescent protein, 1:5000) was used for HA and GFP tagged samples, respectively. Anti rabbit HRP (anti-rabbit IgG conjugated to horseradish peroxidase, 1:5000) was used as secondary antibody. At the co-immunoprecipitation anti-Ha and anti-myc antibody was used (1:5000 in 2% dry milk; secondary antibody was anti-rabbit HRP, 1:5000).

Results and Discussion

It was previously demonstrated that the N-terminal 383 amino acid region of SPMMV P1 possessed the silencing suppressor domain (Giner et al. 2010). If the N-terminally HA-tagged full length SPMMV P1 was infiltrated into *N. benthamiana* plants and immunoprecipitated, the minority of the HA-tagged protein was proven full length (Lakatos, unpublished). This result might not be surprising, since it is already known that

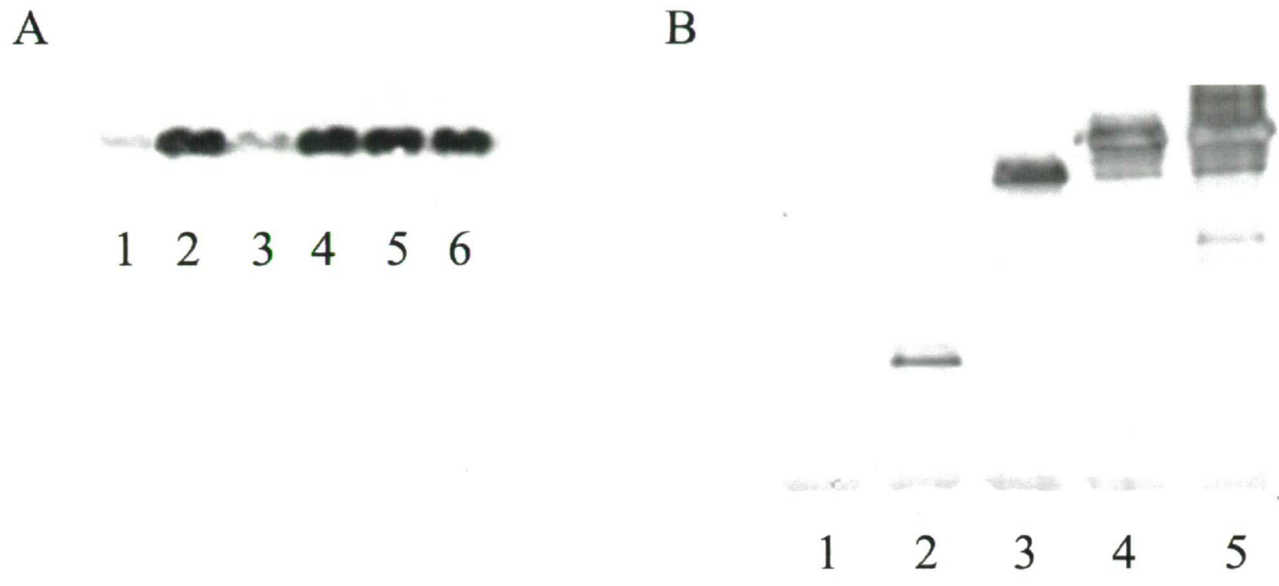

Figure 2. Expression analysis of GFP and the truncated suppressor mutants. Panel A, GFP detected by anti-GFP polyclonal antibody; lanes: 1, empty vector+GFP171; 2, GFP-171+ $P1_{1-383}$; 3, GFP-171+ $P1_{1-120}$; 4, GFP-171+ $P1_{1-210}$, 4 GFP-171+ $P1_{1-305}$, 5, GFP-171+ $P1_{1-360}$; GFP-171+ $P1_{1-383}$. Panel B, suppressor mutants detected by anti-HA antibody; lanes: 1, GFP-171+ $P1_{1-120}$; 2 GFP-171+ $P1_{1-210}$; 3 GFP-171+ $P1_{1-305}$; 4 GFP-171+ $P1_{1-360}$; GFP-171+ $P1_{1-383}$; lower panel represents the loading control.

maturation of the huge potyviral polypeptide translated occurs via the intrinsic protease activities of the polypeptide. Even P1 has a protease domain in its C-terminal, which is required for liberation of P1 from the primary translation product (Valli et al. 2007). Thus, the C-terminal truncation of P1 can be a consequence of its own protease activity, but the action of the plant proteases could not be excluded.

Our aim was to find out, whether these shorter versions of P1 still have RNA silencing suppressor activity. To answer this question, we systematically performed C-terminal truncations on the SPMMV P1 protein. To this end, we amplified the P1 coding region with P1-5'-end primer (annealing to the translational start codon) and $P1_{1-360}$-, $P1_{1-305}$-, $P1_{1-210}$- and $P1_{1-120}$-3'-end primers resulting in 360-, 305-, 210- and 120-aa versions of P1. PCR products were cloned into the TOPO II vector (Invitrogen) and sequenced from both sides. These inserts were cloned into pSanyi plant expression vector (Kertesz et al. 2006) to express them as fusion protein with a HA-tag at their N-terminal end. *Agrobacterium* strains harboring these constructs were coinfiltrated with reporter construct GFP-171.1 (Parizotto et al. 2004) to check for silencing suppressor activity in *N. benthamiana* (Giner et al. 2010). SPMMV $P1_{1-383}$ was used as a control, because this truncated version was known to have silencing suppressor activity. Forty eight hours post-infiltration, visual inspection of the infiltrated leaves was carried out under UV light. We found that the SPMMV $P1_{1-383,}$ $P1_{1-360}$, $P1_{1-305}$, and $P1_{1-210}$ infiltrated leaves showed bright green fluorescence under UV light, indicating RNA silencing suppressor activity. However, the $P1_{1-120}$ infiltrated leaves were rather red, which demonstrated lack of silencing suppressor activity (Fig. 1). Then, Western blotting was carried out to detect GFP protein in the infiltrated leaves. Consistently with our visual inspection, strong GFP expression was found in the protein extracts of $P1_{1-383,}$ $P1_{1-360}$, $P1_{1-305}$, and $P1_{1-210}$ infiltrated leaves, while significantly less GFP was detected, when GFP-171 or GFP-171 and $P1_{1-120}$ were infiltrated (Fig. 2A). These experiments clearly revealed that silencing suppressor function was lost in the case of the $P1_{1-120}$ mutant. We showed earlier that SPMMV P1 contains three WG/GW motifs at positions 15, 101 and 131 (Giner et al. 2010). Although, we found that changing W131 to A (alanine) did not significantly affect the silencing suppressor function, but in the case of the $P1_{1-120}$ mutant, excluding W131 and ten more amino acids might be detrimental for silencing suppressor activity (Giner et al. 2010). Finally, the expression of the N-terminally HA-tagged truncated silencing suppressor proteins were examined by western blotting. Our results showed that extracts of leaves infiltrated with $P1_{1-210,}$ $P1_{1-305}$, $P1_{1-360}$, and $P1_{1-383}$ showed high suppressor expression in increasing protein size (Fig 2B). On the other hand, leaves infiltrated with $P1_{1-120}$ did not express the corresponding protein. Of note, that extracts used in this experiment contained nearly the same amount of protein, as shown in the protein loading panel (Figure 2B). However, the SPMMV $P1_{1-120}$ protein, which did not show suppressor activity, could be detected only when they coinfiltrated in plants with *Tobacco etch virus* HC-Pro (data not shown) (Azevedo et al. 2010; Szabo et al. 2012).

The prototype RNA silencing suppressor inhibiting preassembled RISC is the SPMMV P1 protein, which consists of 759 amino acids. As it was shown before, this large protein in size contains the RNA silencing suppressor domain at the N-terminal part (Giner et al. 2010) and a protease domain conserved in the *Potivirideae* family (Valli et al. 2007). Shorter versions of P1 were found in unrelated experiments implicated the functionality of these proteins. Thus, we narrowed the silencing suppressor domain to the N-terminal 210 amino acids of SPMMV P1. This truncated protein has full silencing suppressor activity, compared to longer versions.

Acknowledgments

This study was supported by the Hungarian Research Fund (OTKA) grants (NN107787 and NN11024) to LL. LK was funded by the European Union and co-financed by the European Social Fund (TÁMOP-4.2.2.A-11/1/KONV-2012-0035 and TÁMOP 4.2.4.A-2013/2-A2-SZJÖ-TOK-13.

References

Azevedo J, Garcia D, Pontier D, Ohnesorge S, Yu A, Garcia S, Braun L, Bergdoll M, Hakimi MA, Lagrange T, Voinnet O (2010) Argonaute quenching and global changes in Dicer homeostasis caused by a pathogen-encoded GW repeat protein. Genes Dev 24:904-915.

Bies-Etheve N, Pontier D, Lahmy S, Picart C, Vega D, Cooke R, and Lagrange T (2009) RNA-directed DNA methylation requires an AGO4-interacting member of the SPT5 elongation factor family. EMBO Rep 10:649-654.

Giner A, Lakatos L, Garcia-Chapa M, Lopez-Moya JJ, Burgyan J (2010) Viral protein inhibits RISC activity by argonaute binding through conserved WG/GW motifs. PLoS Pat 6:e1000996.

Herr AJ, Baulcombe DC (2004) RNA silencing pathways in plants. Cold Spring Harbor Symposia on Quantitative Biology 69:363-370.

Herr AJ, Jensen MB, Dalmay T, Baulcombe DC (2005) RNA polymerase IV directs silencing of endogenous DNA. Science 308:118-120.

Hutvagner G, Simard MJ (2008) Argonaute proteins: key players in RNA silencing. Nat Rev Mol Cell Biol 9:22-32.

Kertesz S, Kerenyi Z, Merai Z, Bartos I, Palfy T, Barta E, Silhavy D (2006) Both introns and long 3'-UTRs operate as cis-acting elements to trigger nonsense-mediated decay in plants. Nucleic Acids Res 34:6147-6157.

Parizotto EA, Dunoyer P, Rahm N, Himber C, Voinnet O (2004) In vivo investigation of the transcription, processing, endonucleolytic activity, and functional relevance of the spatial distribution of a plant miRNA. Genes Dev 18:2237-2242.

Pfaff J, Hennig J, Herzog F, Aebersold R, Sattler M, Niessing D, Meister G (2013) Structural features of Argonaute-GW182 protein interactions. Proc Nat Acad Sci U S A 110:E3770-3779.

Silhavy D, Molnar A, Lucioli A, Szittya G, Hornyik C, Tavazza M, Burgyan J (2002) A viral protein suppresses RNA silencing and binds silencing-generated, 21- to 25-nucleotide double-stranded RNAs. EMBO J 21:3070-3080.

Szabo EZ, Manczinger M, Goblos A, Kemeny L, Lakatos L (2012) Switching on RNA silencing suppressor activity by restoring argonaute binding to a viral protein. J Virol 86:8324-8327.

Valli A, Lopez-Moya JJ, Garcia JA (2007). Recombination and gene duplication in the evolutionary diversification of P1 proteins in the family Potyviridae. J Gen Virol 88:1016-1028.

Wise AA, Liu Z, Binns AN (2006) Three methods for the introduction of foreign DNA into *Agrobacterium*. Methods Mol Biol 343:43-53.

Yang L, Wu G, Poethig RS (2012) Mutations in the GW-repeat protein SUO reveal a developmental function for microRNA-mediated translational repression in *Arabidopsis*. Proc Nat Acad Sci U S A 109:315-320.

Volume 58(2):167-170, 2014
Acta Biologica Szegediensis
http://www2.sci.u-szeged.hu/ABS

ARTICLE

Identification of potential mycotoxin producing fungi on agricultural products in Hungary and Serbia

Nikolett Baranyi[1], Sándor Kocsubé[1], Noémi Kiss[1], Andrea Palágyi[1], Mónika Varga[2], Beáta Tóth[2], János Varga*[1]

[1]Department of Microbiology, Faculty of Science and Informatics, University of Szeged, Szeged, Hungary, [2]Cereal Research Nonprofit Ltd., Szeged, Hungary

ABSTRACT One of the most important effects of climate change is the occurrence of thermotolerant mycotoxin producing fungi in countries with temperate climate, causing mycotoxin contamination of agricultural products. Indeed, a shift has recently been observed in the occurrence of aflatoxin producing fungi in Europe, with consequent aflatoxin contamination in agricultural commodities including maize and milk in several European countries including Serbia, Croatia, Slovenia, Romania and Ukraine. These observations led us to examine the occurrence of mycotoxin producing Aspergilli in agricultural products in Hungary and Serbia. The samples were collected from cereal fields in Hungary and North-Serbia (Vojvodina) after harvest in 2012. Surface-sterilized cereal seeds were placed on selective media and the isolated fungal strains were identified using morphological methods. The species identification of selected isolates was carried out using sequence-based methods. Several potentially aflatoxigenic *A. flavus* isolates were identified on maize. Further examinations of mycotoxin producing abilities of the isolates, and their occurrence in milk and milk-derived products are in progress.

Acta Biol Szeged 58(2):167-170 (2014)

KEY WORDS

climate change
fungi
Aspergillus
aflatoxins
mycotoxins

Mycotoxins are secondary metabolites of filamentous fungi, which are harmful to animals and humans, and are able to provoke various disease symptoms (Varga et al. 2009). Aflatoxins are the most thoroughly studied mycotoxins, which are produced by species assigned to the *Aspergillus* genus. They were discovered when the toxicity of animal feeds containing contaminated peanut meal led to the death of more than 100,000 turkeys from acute liver necrosis in the early sixties (Turkey-X disease; Blout 1961, Sargeant et al. 1961, van der Zijden et al. 1962). *Aspergillus flavus* was identified as the producing fungus, and aflatoxins were named after the toxic agent. Aflatoxins have both toxic and carcinogenic properties, posing serious threats to both animal and human health (Bennett and Klich 2003). Aflatoxin B_1 is the most toxic aflatoxin, being a potent genotoxic carcinogen in laboratory animals and there is a strong evidence for its liver carcinogenity in humans (Wild and Turner 2002). Comprehensive studies have shown that aflatoxin is a risk factor for human hepatocellular carcinoma, especially in Asia and sub-Saharan Africa (Groopman et al. 2005). Although lethality is an uncommon outcome of aflatoxicosis in humans, several deaths were attributed to that (Nyikal et al. 2004). Because of its toxicity, over 100 countries restrict the content of aflatoxins in the food and feed supplies (van Egmond et al. 2007).

Accepted Nov 28, 2014
*Corresponding author. E-mail: jvarga@bio.u-szeged.huu

Aflatoxins are a group of structurally related difuranocoumarins that were named as aflatoxin B_1, B_2, G_1, and G_2 based on their fluorescence under UV light (blue or green) and their relative chromatographic mobilities during thin-layer chromatography. Aflatoxin B_1 is the most potent natural carcinogen known (Squire 1981, IARC 2012), and is usually the major aflatoxin produced by toxigenic strains. Aflatoxin M_1, a hydroxylated metabolite is found primarily in animal tissues and fluids (milk and urine) as a metabolic product of aflatoxin B_1 (Varga et al. 2009).

The most important producer, *A. flavus* is also an important pathogen of various cultivated plants including maize, cotton and peanut, and causes serious yield losses throughout the world. Since aflatoxin production is favoured by moisture and high temperature, *A. flavus* is able to produce aflatoxins in warmer, tropical and subtropical climates (Varga et al. 2009). Consequently, aflatoxin contamination of agricultural products in countries with temperate climate, including Central European countries was not treated as a serious health hazard. However, climate change associated with global warming seems to change the scenario. Recently, several papers have dealt with the effects of climate change on the appearance of aflatoxin producing fungi and aflatoxins in foods (Paterson and Lima 2010, Tirado et al. 2010). Based on these studies, aflatoxin producing fungi and consequently aflatoxins are expected to become more prevalent with climate change

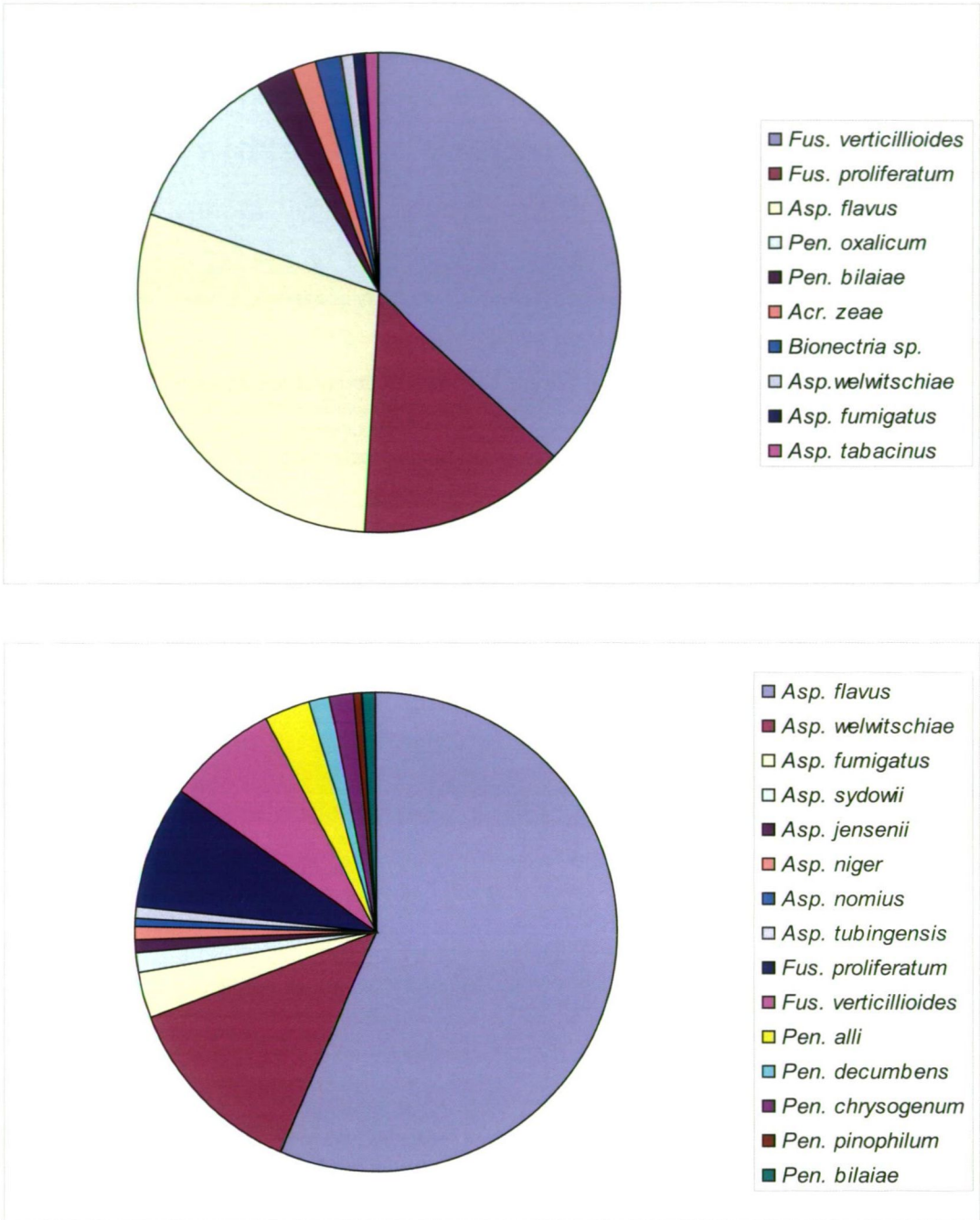

Figure 1. Distribution of potentially mycotoxin producing fungi in maize samples collected after harvest (top), and in samples stored in warehouses (bottom).

in countries with temperate climate. Indeed, several recent reports have indicated the occurrence of aflatoxin producing fungi and consequently aflatoxin contamination in agricultural commodities in several European countries that did not face with this problem before.

Regarding Hungary, Richard et al. (1992) examined the mycotoxin producing abilities of 22 isolates collected from various sources in Hungary, and none of the isolates were found to produce aflatoxins. Besides, Borbély et al. (2010) have examined mycotoxin levels in cereal samples and mixed feed samples collected in eastern Hungary, and detected aflatoxin B_1 levels above the EU limit in 4.8% of the samples. Additionally, more recently, Dobolyi et al. (2013) identified aflatoxin producing *A. flavus* from maize kernel collected in

various parts of Hungary. Furthermore, Tóth et al. (2013) have examined the occurrence of potential mycotoxigenic fungi on Hungarian maize kernels between 2010 and 2012. Several potentially mycotoxigenic *Aspergillus* isolates were identified on maize. In 2010 the weather was very rainy, while in 2011 and 2012 the weather conditions were more hot and dry. In 2010, a large number of *Penicillium* species occurred in the samples, possibly due to the colder weather conditions. In 2011 and 2012, Aspergilli were observed in larger quantities than previously, possibly due to the dry and hot weather conditions. These observations led us to examine the occurrence of potential aflatoxigenic species in maize kernels collected in Hungary and Serbia (Vojvodina).

Materials and Methods

Sample collection

The samples were collected from various maize growing regions of Hungary and Serbia in 2012. The samples were surface sterilized, and plated onto dichloran rose bengal (DRBC) media (King et al. 1979). Plates were incubated at 25 °C in darkness and monitored periodically for characteristic mycelium growing from the kernels. Outgrowing mycelia were purified and transferred to malt extract agar (MEA). Isolates were subcultured as single conidia on MEA, PDA (potato dextrose agar) and CYA (Czapek yeast agar) plates (Samson et al. 2004).

Genotypic studies

The cultures used for the molecular studies were grown on YPD (1% yeast extract, 1% peptone, 1% D-glucose) broth for 5 days, on 25 °C. DNA was extracted from the mycelia using the Masterpure™ yeast DNA purification kit (Epicentre) according to the instructions of the manufacturer. Part of the calmodulin gene was amplified and sequenced as described previously (Pildain et al. 2008). The primers used were: cmd5 (5 -CCGAGTACAAGGAGGCCTTC-3) and cmd6 (5 -CCGATAGAGGTCATAACGTGG-3) (Hong et al. 2005). Calmodulin sequences were compared using nucleotide-nucleotide BLAST (blastn) with default settings (http://blast.ncbi.nlm.nih.gov, Altschul et al. 1990) to the GenBank database, and to our own sequence database. Species identification was determined from the lowest expected value of the BLAST output.

Examination of aflatoxin producing abilities

The *Aspergillus flavus* isolates were grown on 2 ml YES (2% yeast, 20% sucrose) solution. The isolates were incubated for 7 days at 25 °C and at 30 °C in darkness. The aflatoxin extraction were carried out in 2 ml dichloromethane. For the examination of the aflatoxin producing abilities of the isolates thin layer chromatography (TLC) and enzyme-linked immunosorbent assay (ELISA) methods were used.

The used aflatoxin standard included aflatoxin B_1, B_2, G_1 and G_2. Camag Linomat 5 syringe system, Merck Millipore TLC Silica gel 60, and toluene:ethyl-acetate:formic acid 6:3:1 mixture were used for TLC analysis. To quantify the aflatoxin levels, ELISA analysis (AgraQuant® Total Aflatoxin Assay 1/20) was performed according to the instructions of the manufacturer (Romer Labs).

Results and Discussion

Several *Aspergillus* species have been identified recently, which are able to produce aflatoxins (Varga et al. 2009). These species can readily be distinguished using sequence analysis of part of their β-tubulin or calmodulin genes (Varga et al. 2011). In this study, we examined the occurrence of potential aflatoxigenic fungi on maize in several parts of Hungary and Serbia in 2012. *Fusarium* species (mainly *F. proliferatum* and *F. verticillioides*) and *A. flavus* were mostly present in samples collected during harvest in 2012 (Fig. 1). Other *Aspergillus* and *Penicillium* species were also detected. Besides these potentially mycotoxigenic species, *Acremonium zeae*, a potential biocontrol organism against maize pathogens (Wicklow et al. 2005), *Penicillium bilaiae*, which is used as a phosphate-solubizing organism (Leggett et al. 2007), and a *Bionectria* species which was found to be able to degrade zearalenone (Takahashi-Ando et al. 2002) were also identified.

Fusarium species dominated in samples collected after harvest, while *Aspergillus* species were predominant in stored samples. Occurrence of *A. flavus* was 76% in stored samples, and 33% in samples collected after harvest (Fig. 1). Regarding the samples collected during harvest in 2012, some samples were contaminated by aflatoxins. These highly carcinogenic mycotoxins were detected in 2 field samples came from Serbia (3.16 and 0.82 μg/kg). However, these values are below the EU limit (10 μg/kg; http://eur-lex.europa.eu/legal-content/EN/TXT/PDF/?uri=CELEX:32010R0165&from=EN). Fumonisins were detected in most of the samples. In two maize samples (from Curug and Pancevo), the amount was above the EU limit (data not shown).

We have also chosen 10-10 *A. flavus* isolates and tested their aflatoxin producing abilities at 25 °C and 30 °C. We have observed some differences in the aflatoxin production at different temperatures (data not shown). We are planning to examine the aflatoxin M_1 content and the aflatoxin producing abilities of *Aspergillus* strains from Hungarian cheese samples too using HPLC and ELISA methods.

Acknowledgements

The research of N.B., and S.K. was supported by the European Union and the State of Hungary, co-financed by the European Social Fund in the framework of TÁMOP 4.2.4.A/2-11-1-2012-0001 "National Excellence Program – Elaborating and operating an inland student and researcher personal support system convergence program". This work

was also supported by OTKA grants K84122 and K84077, and by the European Union through the Hungary-Serbia IPA Cross-border Cooperation Programme (ToxFreeFeed, HU-SRB/1002/122/062).

References

Altschul SF, Gish W, Miller W, Myers EW, Lipman DJ (1990) Basic local alignment search tool. J Mol Biol 215:403-410.

Bennett JW, Klich M (2003) Mycotoxins. Clin Microbiol Rev 16:497–516.

Blout WP (1961) Turkey "X" disease. Turkeys 9:52-77.

Borbély M, Sipos P, Pelles F, Győri Z (2010) Mycotoxin contamination in cereals. J Agroalim Proc Techn 16:96-98.

Dobolyi C, Sebők F, Varga J, Kocsubé S, Szigeti G, Baranyi N, Szécsi Á, Tóth B, Varga M, Kriszt B, Szoboszlay S, Krifaton C, Kukolya J (2013) Occurrence of aflatoxin producing *Aspergillus flavus* isolates in maize kernel in Hungary. Acta Aliment 42:451-459.

Groopman JD, Johnson D, Kensler TW (2005) Aflatoxin and hepatitis B virus biomarkers: a paradigm for complex environmental exposures and cancer risk. Cancer Biomark 1:5–14.

Hong SB, Go SJ, Shin HD, Frisvad JC, Samson RA (2005). Polyphasic taxonomy of *Aspergillus fumigatus* and related species. Mycologia 97:1316-1329.

IARC (International Agency for Research on Cancer) (2012) A review of human carcinogens. Vol. 100F: Chemical agents and related occupations. IARC Working Group on the Evaluation of Carcinogenic Risks to Humans, Lyon, France.

King AD Jr, Hocking AD, Pitt JI (1979) Dichloran-rose bengal medium for enumeration and isolation of molds from foods. Appl Environ Microbiol 37:959–964.

Leggett M, Cross J, Hnatowitch G, Holloway G (2007) Challenges in commercializing a phosphate-solubilizing microorganism: *Penicillium bilaiae*, a case history. First International Meeting on Microbial Phosphate Solubilization. Dev Plant Soil Sci 102:215-222.

Nyikal J, Misore A, Nzioka C, Njuguna C, Muchiri E, Njau J, Maingi S, Njoroge J, Mutiso J, Onteri J, Langat A, Kilei IK, Nyamongo J, Ogana G, Muture B, Tukei P, Onyango C, Ochieng W, Tetteh C, Likimani S (2004) Outbreak of aflatoxin poisoning - Eastern and Central Provinces, Kenya, January–July 2004. Morbid Mortal Week Rep 53:790-793.

Paterson RRM, Lima N (2010) How will climate change affect mycotoxins in food? Food Res Int 43:1902-1914.

Pildain MB, Frisvad JC, Vaamonde G, Cabral D, Varga J, Samson RA (2008) Two novel aflatoxin-producing *Aspergillus* species from Argentinean peanuts. Int J Syst Evol Microbiol 58:725-735.

Richard JL, Bhatnagar D, Peterson S, Sandor G (1992) Assessment of aflatoxin and cyclopiazonic acid production by *Aspergillus flavus* isolates from Hungary. Mycopathologia 120:183-188.

Samson RA, Hoekstra ES, Lund F, Filtenborg O, Frisvad JC (2004) Methods for the detection, isolation and characterisation of food-borne fungi. Introduction to food- and airborne fungi 2004, pp. 283-297.

Sargeant K, Sheridan A, O Kelley J, Carnaghan RBA (1961) Toxicity associated with certain samples of groundnut. Nature 192:1096-1097.

Squire RA (1981) Ranking animal carcinogens: a proposed regulatory approach. Science 214:877-880.

Tirado MC, Clarke R, Jaykus LA, McQuatters-Gollop A, Frank JM (2010) Climate change and food safety: A review. Food Res Int 43:1745-1765.

Takahashi-Ando N, Kimura M, Kakeya H, Osada H, Yamaguchi I (2002) A novel lactonohydrolase responsible for the detoxification of zearalenone: enzyme purification and gene cloning. Biochem J 365:1-6.

Tóth B, Kótai É, Varga M, Pálfi X, Baranyi N, Szigeti G, Kocsubé S, Varga J (2013) Climate change and mycotoxin contamination in Central Europe: an overview of recent findings. Rev Agricult Rural Devel 2:461-466.

van der Zijden ASM, Blanche Koelensmid WAA, Boldingh J, Barrett CB, Ord WO, Philip J (1962) *Aspergillus flavus* and Turkey X disease: isolation in crystalline form of a toxin responsible for Turkey X disease. Nature 195:1060-1062.

van Egmond HP, Schothorst RC, Jonker MA (2007) Regulations relating to mycotoxins in food: perspectives in a global and European context. Anal Bioanal Chem 389:147-157.

Varga J, Frisvad JC, Samson RA (2009) A reappraisal of fungi producing aflatoxins. World Mycotoxin J 2:263-277.

Varga J, Frisvad JC, Pildain MB, Vaamonde G, Cabral D, Samson RA (2011) Two new aflatoxin producing species, and an overview of *Aspergillus* section *Flavi*. Stud Mycol 69:57-80.

Wicklow DT, Roth S, Deyrup ST, Gloer JB (2005) A protective endophyte of maize: *Acremonium zeae* antibiotics inhibitory to *Aspergillus flavus* and *Fusarium verticillioides*. Mycol Res 109:610-618.

Wild CP, Turner PC (2002) The toxicology of aflatoxins as a basis for public health decisions. Mutagenesis 17:471-481.

Volume 58(2):171-177, 2014
Acta Biologica Szegediensis
http://www2.sci.u-szeged.hu/ABS

ARTICLE

Typing of methicillin resistant and sensitive *Staphylococcus aureus* isolated from Tamilnadu, India using DNA fingerprints by pulsed-field gel electrophoresis

Kathirvel Rajaduraipandi[1], Donald Morrison[2], Mariappa Mani[3], Guruvu Nambirajan[4], Kanesan Panneerselvam[4], Coimbatore Subramanian Shobana[5], Venkatapthy Narendran[6], Palanisamy Manikandan*[6,7]

[1]The Erode Diagnostic Laboratory, Erode - 638009, Tamilnadu, India, [2]Scottish MRSA Reference Laboratory, Microbiology Department, Stobhill Hospital, Glasgow, UK, [3]Microbiological Laboratory, Coimbatore - 641002, Tamilnadu, India, [4]Department of Microbiology, M.R. Government Arts College, Mannargudi, India - 614001, [5]Department of Microbiology, PSG College of Arts and Science, Avinashi road, Coimbatore - 641 014, Tamilnadu, India, [6]Aravind Eye Hospital and Postgraduate Institute of Ophthalmology, Coimbatore - 641014, Tamilnadu, India, [7]Department of Medical Laboratory Sciences, College of Applied Medical Sciences, Majmaah University, Kingdom of Saudi Arabia

ABSTRACT MRSA infection is alarming particularly in hospital set ups/community. We typed 43 isolates of *Staphylococcus aureus* (MRSA and MSSA) based on genomic DNA restriction fragment length polymorphisms (RFLPs). The genomic DNA of the test isolates was digested with *Sma*I enzyme, fractionated by PFGE and the patterns were assessed by dendrogram for percentage similarity. The *Sma*I restricted genomic DNA of 19 MRSA and 24 MSSA identified 27 different PFGE patterns, in which 11 and 16 were from MRSA and MSSA, respectively. Prevalence predominance was observed in few types/subtypes of MSSA (type B and subtype I-1) and MRSA (sub type A-2) and high percentage of similarity was noticed among the subtypes of PFGE types such as P and I of MSSA. During the epidemiological studies, to understand the dissemination of endemic/epidemic MRSA and MSSA, PFGE-based typing of pathogens may be used as a reliable and effective typing method.
Acta Biol Szeged 58(2):171-177 (2014)

KEY WORDS

Staphylococcus aureus
methicillin-resistant
MRSA
MSSA
PFGE
molecular epidemiology

Methicillin-resistant *Staphylococcus aureus* (MRSA) has emerged as a global health concern and poses a continuous threat to medical care since the first strain was isolated in the United Kingdom in 1961 (Chambers 2001; Yamamoto et al. 2012; Nelson and Gallagher 2012; Uhlemann et al. 2013; Udo et al. 2014). MRSA is becoming majorly responsible for a wide spectrum of nosocomial and community associated infections worldwide (Mehndiratta and Bhalla 2012; Stryjewski and Corey 2014) and cause endemic and epidemic infections in many parts of the world including India (Pulimood et al. 1996; Stryjewski and Corey 2014).

The treatment and eradication of MRSA is becoming difficult and they may further increase the number of infections, the costs and the length of hospital stays (Vidhani et al. 2001; Patel 2007; Elixhauser and Steiner 2007). Also, MRSA strains are commonly resistant to multiple antimicrobials, in particular to all beta-lactams (except for the newer anti-MRSA compounds), which narrows the treatment possibilities and changes the spectrum of antibiotics used for therapy (Qureshi et al. 2004; Rajaduraipandi et al. 2006; Bartoloni et al. 2014; Ben Nejma et al. 2014). Now, health care facilities of all types experience such MRSA with significant and consistent increase in prevalence and with very obvious clinical impact. This increased prevalence of MRSA could be due to increased transmission of various strains among people or emergence of new strains (Uemura et al. 2004). Therefore, the knowledge of endemic MRSA strains in each place will be valuable in the surveillance and epidemiological investigation of MRSA clones/outbreaks for which epidemiological typing would be indispensable (Fujino et al. 2004; Bartoloni et al. 2014).

Based on PFGE typing, which is one of the most widely used molecular approaches of epidemiological analyses, the clonal nature of MRSA can be identified in order to understand the sources and routes of MRSA transmission (Hosoda et al. 2002; Goering et al. 2008). This will help the implementation of appropriate infection control measures and the effective empiric treatment protocols during the clinical management of MRSA infections, besides assisting our understanding of the diverse evolutionary trajectories of MRSA lineages globally (Bartoloni et al. 2014). As epidemiologically related isolates share the same genetic features, DNA-based typing techniques can be applied for an accurate epidemiological evaluation of MRSA. In this study we describe the application of DNA fingerprints generated by PFGE

Accepted Dec 21, 2014
*Corresponding author. E-mail: manikandanpalanisamy@gmail.com

Table. Test MRSA and MSSA isolates subjected to PFGE.

S. No.	Collection centers	Type of clinical specimen	Total No. of MRSA (*n*=19)	Isolate number for PFGE	MRSA PFGE pattern	Type of clinical specimen	Total No. of MSSA (*n*=24)	Isolate number for PFGE	MSSA PFGE pattern
1	Coimbatore	Blood	1	13	F2	Pus	4	23,26,33,35	B
		Pus	1	15	S	Pus	4	1,31,41,42	I-1
		Pus	1	16	T	Pus	1	8	Q
2	Palayam	Pus	1	20	U	Throat	2	24,30	C
						Pus	1	4	P-1
						Pus	1	5	P-2
3	Salem	Pus	5	9,11,19,21,32	A-2	Urine	1	25	D
						Syn. fluid	1	28	G
4	Trichy	Urine	2	7,22	A-1	Pus	1	3	I-2
							1	6	I-3
							1	18	I-4
							1	14	I-5
5	Coonoor	Syn. fluid	2	10,29	H	Pus	1	12	R
6	Erode	Sputum	2	17,43	O	Sputum	2	37	M-1
		Blood	2	2,27	F-1	Pus	1	40	N
7	Karur	Pus	1	34	K	Sputum	1	38,39	M-2
		Pus	1	36	L				

Syn. fluid = Synovial fluid

to determine and compare the PFGE patterns of endemic MRSA and MSSA strains isolated from different centers of Tamilnadu, India.

Materials and Methods

Identification of *S. aureus*

The clinical samples collected from Microbiological Laboratory at Coimbatore, and from six of its sub-centers in Tamilnadu for a period of 24 months were aseptically handled and processed (Table 1). The morphotypes (cellular types) were done for all the samples based on the Gram staining method. The samples were also inoculated into respective preliminary screening media according to the standard laboratory procedures (Bannerman 1999) and incubated at 37 °C for 24 h. The microscopically identified isolates were further confirmed based on biochemical test results. All isolates of *S. aureus* were tested for the production of free coagulase enzyme using tube coagulase test. The results were confirmed using the standard coagulase-producing *S. aureus* strain ATCC-25923.

Screening for MRSA

All the confirmed *S. aureus* isolates were tested for methicillin resistance using 1µg oxacillin disc on Mueller Hinton agar incubated at 35 °C and their methicillin resistance/sensitivity was documented. Furthermore, the antibiotic susceptibility pattern was studied by disc diffusion test following the guidelines of the Clinical and Laboratory Standards Institute (CLSI 2010). The antibiotics used were Penicillin-G (10 unit); Ampicillin (10 µg); Cephalexin (30 µg); Cephotaxime (30 µg); Erythromycin (15 µg); Gentamycin (10 µg); Amikacin (30 µg); Netillin (30 µg); Ciprofloxacin (5 µg); Ofloxacin (5 µg); Norfloxacin (10 µg); Co-trimoxazole (25 µg); Vancomycin (30 µg) and Linezolid (30 µg).

Pulsed-Field Gel Electrophoresis (PFGE)

A total of forty-three isolates of *S. aureus* (19 MRSA and 24 MSSA) were selected based on antimicrobial susceptibility patterns and subjected to PFGE. Three well characterized MRSA clones, EMRSA-15 (Clonal Complex [CC22]), EMRSA-16 [CC30] and SMRSA-105 [CC5]) were also included in the study for comparative evaluation. NCTC 8325 was used as a gel reference standard. PFGE typing of *Sma*I (Gibco, BRL, UK) digested DNA was performed by a modification of a previously described method (Bannerman et al. 1995). A colony was inoculated into brain heart infusion broth and incubated overnight at 37 °C without agitation. The pellet from 0.4 ml of this culture was washed in 0.8 ml NET buffer (10 mM Tris, 1 mM EDTA, 10 mM NaCl), resuspended in 0.25 ml NET buffer and mixed with 200 units of achromopeptidase (Sigma) (Leonard et al. 1995) and an equal volume of 2% SeaPlague agarose (Flowgen) at 50 °C. The cell/agarose suspension was loaded into block molds (BioRad) and allowed to solidify at 4 °C. Cells were lysed by incubation at 50 °C for 60 min in lysis buffer (6 mM Trizma base, 100 mM EDTA, 1 M NaCl, 0.5% Brij 58, 0.2% sodium deoxycholate, 0.5% lauroyl sarcosine). The blocks were washed three times for 10 min each at room temperature in TE buffer (10 mM Trizma base, 1 mM EDTA). One quarter of each agarose block was digested with 30 units of *Sma*I for 3 h according to the manufacturer's instructions and loaded into the wells of a 1% PFGE certified agarose gel

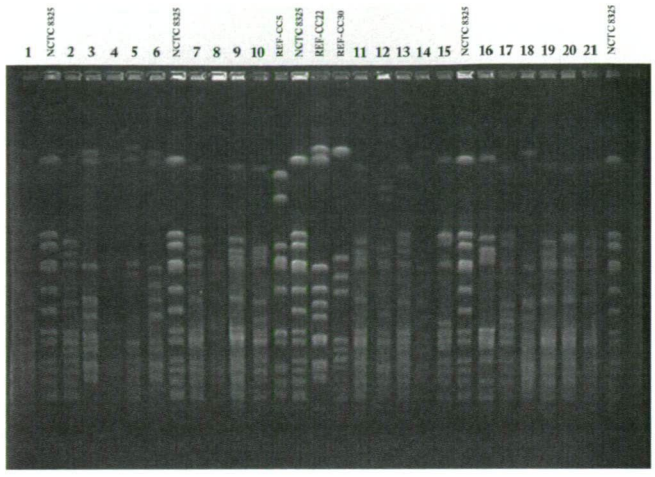

Figure 1. *SmaI* digested genomic DNA fingerprints of MRSA and MSSA isolates by pulsed field gel electrophoresis (PFGE).

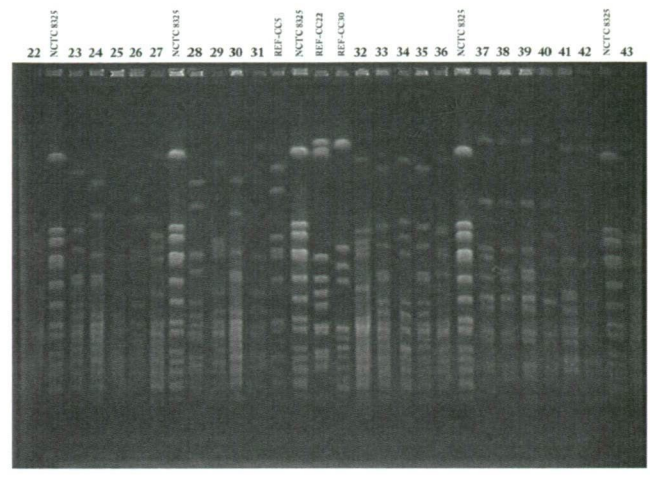

Figure 2. *SmaI* digested genomic DNA fingerprints of MRSA and MSSA isolates by pulsed field gel electrophoresis (PFGE).

(BioRad). Electrophoresis was performed in 0.5×TBE buffer (44.5 mM Trizma base, 44.5 mM boric acid, 1 mM EDTA) (Biowhittaker) by the contour-clamped homogenous electric field method with a CHEF Mapper system (BioRad). The fragments were separated with a linear ramped pulse time of 6.8 to 63.8 seconds over a period of 23 h at 14 °C and the gels were stained with 1 μg/mL ethidium bromide (Sigma) solution for 30 min, visualized under UV and photographed. Differences between isolates were recorded by visual comparison of DNA fingerprints and their PFGE patterns were determined. First, the patterns were examined to identify the common pattern (usually recognized as type A). Subsequently, the size and number of the fragments in the common pattern were compared with the fragments that made up the patterns of the other isolates. On the basis of fragment-for-fragment comparisons, each isolate's pattern was then classified. Patterns that were different from common patterns by six or more band differences were considered unrelated types (as type B, type C etc.). Patterns that differ from the common pattern (i.e type A) by two or three fragment differences were considered to be subtypes (such as A1, A2 etc.) of the common pattern (Tenover et al. 1995).

Statistical Analysis

Data are represented in figures, descriptive as mean ± SD, 95% Confidence Interval with normal approximation has been calculated around estimates of prevalence. Chi Square test in case of proportions and Student's *t*-test in case of means were used for analyses.

Results

The PFGE restriction patterns of the 43 isolates as well as known reference and control strains were visually examined. Presence of 12-15 well resolved bands of approx. 670 to <80 kb were confirmed. The reproducibility of banding patterns was confirmed using reference strains and control strains on different gels. Upon PFGE typing of 19 MRSA (47.5% of 250), a total of 11 different PFGE patterns were identified and were further grouped under 9 types (Table 1).

Upon PFGE typing among 19 of 250 MRSA, a total number of 11 different PFGE patterns were identified in which 9 types were confirmed (Table 1). It was found that each type was differing from others by 6 to 7 bands. For example, PFGE types O and H; A and F differed from each other by 6 bands with a similarity between 90% and 95%. Types such as T and O, K and L were found to be 95% related. Further, these MRSA strains were observed to represent different geographical areas of this region. PFGE type O was isolated in sputum specimen from Erode (western part of Tamil Nadu state) and type H in synovial fluid collected from a hilly area called Coonoor (a town in the Nilgiris district, Tamil Nadu state, located at an altitude of 1,850 m above sea level). The two PFGE types A and F carried sub-types/variants such as A1, A2 and F1, F2 respectively and among subtypes A and F only one band difference was noticed. The most frequent pattern A2 represented 26% of the 19 MRSA isolates and all of these were isolated from a single (Salem; a western district of Tamil Nadu state) center. Other subtypes were found to represent varying geographical areas. Subtypes A1, F1 and F2 were isolated from Trichy (central part of Tamilnadu state), Erode and Coimbatore (western part of Tamilnadu state) and the dendrogram-based analysis estimated 95% similarity among the subtypes of each type (Fig. 3).

Similarly, of 24 MSSA, 16 PFGE patterns were identified and further categorized in to 10 PFGE types (Table 1). Types D and Q, C and B were observed to be 95% related and all were geographically found to be from different places

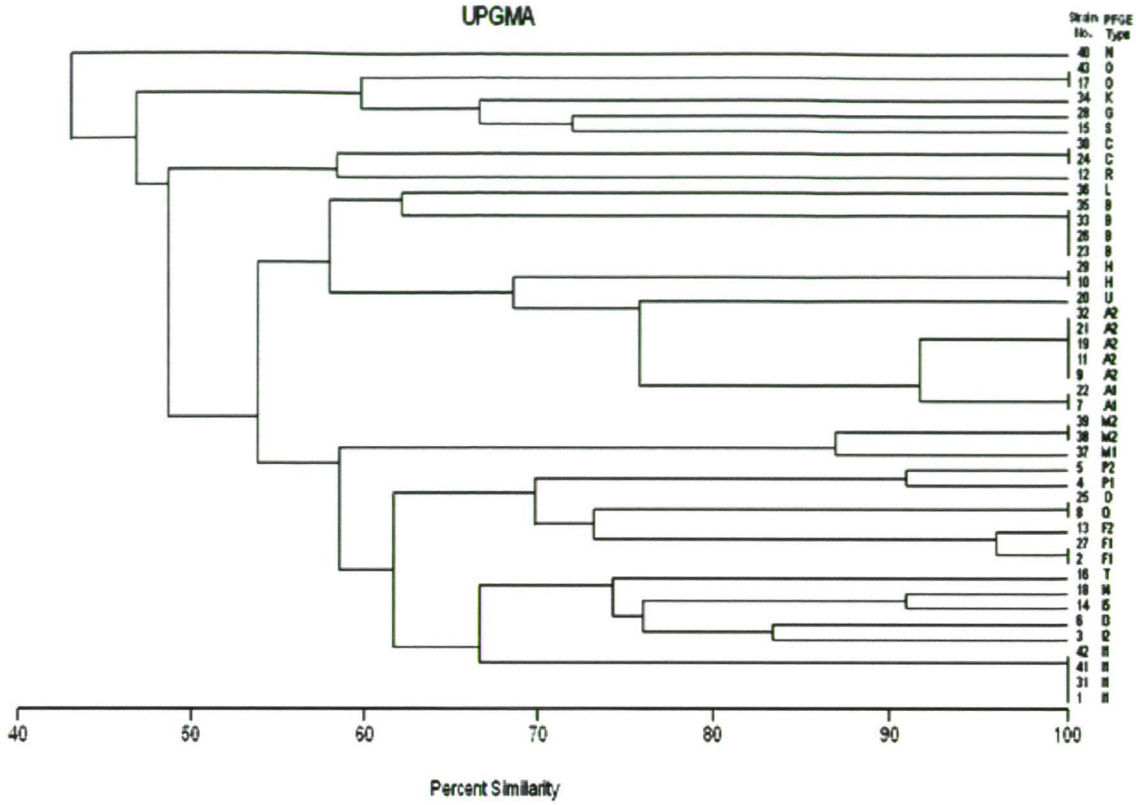

Figure 3. Dendrogram showing the percentage similarity among PFGE patterns (*SmaI*) of MRSA and MSSA genomic DNA.

(type Q and B from Coimbatore; type C from Palayam, type D from Salem). Furthermore, types I, M and P in MSSA carried varying number of sub types and the most frequent PFGE subtype I-1 made up 16% of the 24 MSSA isolates. All the strains of I-1 subtypes were isolated from pus specimens of a single hospital in Coimbatore. However, subtypes I-2 through I-5 were from another geographical area (Trichy). Subtypes I-2 and I-3, and sub types I-4 and I-5 were 95% related, whereas, subtype I-1 was only 90% related to other types. Similarly, subtypes P-1and P-2, and M1 and M2 shared 95% similarity.

The PFGE types of all the *S. aureus* strains tested were compared with three recognized major international types/ clones. Three of the major international clonal complexes of *S. aureus* were found among 24 MSSA isolates analyzed using PFGE. PFGE type I is a variant of EMRSA – 15, which belongs to the MLST clonal complex - 22. PFGE type P is a MSSA variant of EMRSA-16, which belongs to the MSST clonal complex - 30 and, PFGE type R belongs to the MLST clonal complex 5.

Discussion

Bacterial pathogens with antimicrobial resistance are more difficult and expensive to treat as they may increase other complications and could lengthen hospital stay (Elixhauser and Steiner 2007). In this respect, emergence of hospital and community associated MRSA is causing worldwide concern (Mehta et al. 1998; Maree et al. 2007; Ray et al. 2011; Sujatha, 2014). Many tertiary care hospitals refer MRSA as an important nosocomial pathogen (Anupurba et al. 2003; Thati et al. 2011; Ahmed et al. 2012; Mir and Srikanth 2013; Kali et al. 2013) and therefore frequent surveillance and accurate epidemiological typing is indispensable to understand and identify the sources and routes of transmission so as to control its further spread (Fujino et al. 2004; Adesida et al. 2007).

Epidemiological studies involve different typing methods to explore the epidemiology of MRSA and pulsed field gel electrophoresis (PFGE) has been recommended as a 'gold standard' (Mehndiratta and Balla 2012) for typing MRSA isolates because it can distinguish among several concurrent epidemic strains. As a result of the rich diversity of the chromosomal digestion profiles and clarity, this typing method has been used in several epidemiological studies of MRSA infections (Erdenizmenli et al. 2004; Wolter el al. 2008; Tenover and Goering, 2009; Shabir et al. 2010; Pereira et al. 2014).

In this study, PFGE played a vital role in typing the MRSA and MSSA isolates obtained from various parts of Tamilnadu and also in understanding the most predominant

and potential strains of this region. This was a multicenter study, in which PFGE patterns of the test strains (both MRSA and MSSA) collected from different districts of Tamilnadu state were studied and their patterns were compared among themselves as well as with the PFGE patterns of major international reference clones. A total of 9 and 10 PFGE types were identified from 19 MRSA and 24 MSSA isolates, respectively. Ichiyama et al. (1991) had proposed PFGE as a useful method for investigating the source, transmission and spread of nosocomial MRSA infections and reported 31 distinctive fragment patterns among 111 infecting and colonizing MRSA isolates from inpatients of six different hospitals under Nagoya University in Japan. Based on the PFGE restriction patterns, their study confirmed the involvement of 4 types of test strains causing epidemic infections among patients. In a similar type of study, Wei and Grubb (1992) classified 26 clinical isolates of MRSA collected from six Australian hospitals into 17 groups based on RFLPs of chromosomal DNA using PFGE and also highlighted the sensitivity of PFGE in typing MRSA both within and between hospitals.

A multicenter study assessed the optimal resolution and interlaboratory reproducibility of results from genotyping *S. aureus* by PFGE (van Belkum et al. 1997) and it was observed that several isolates did not give a 100% match at different centers, indicating that the standardization of PFGE depends on controlling a variety of experimental factors. However, in comparison with conventional typing methods such as phage typing and antibiotyping, PFGE's potential in discriminating MRSA during epidemiological studies is still significant (Loureiro et al. 2000). This has also been acknowledged by several workers (Shopsin and Kreiswirth 2001; Sasaki et al. 2002; Fujino et al. 2004). Struelens et al. (1992) also demonstrated the discriminatory ability of PFGE with typing ability index of 0.982 when compared to the indices of 0.959 and 0.947 for antibiotyping and phage typing, respectively. The first report on EMRSA - 15 variant from the United States employed PFGE as the only epidemiological tool (Wolter et al. 2008) and identified the pathogen. In this study, neither MRSA nor MSSA isolates can be more heterogeneous, because the difference in diversity among MRSA and MSSA isolates may not be significant and statistically valid, especially when we look at types rather than patterns, as 9 PFGE types were determined among MRSA and only 10 PFGE types in MSSA. However, Carles-Nurit et al. (1992) found that the *Sma*I restriction pattern in each of 20 MSSA strains collected from a single hospital over a period of 4 months was unique, whereas only seven RFLP patterns were seen among 27 test MRSA strains. The authors also confirmed these findings through nearly similar *Apa*I restriction patterns supporting low diversity among the MRSA isolates tested. This proved that MSSA strains were more diverse than MRSA.

Although MRSA PFGE subtype A2 was found to be the commonest pattern, it may not be widespread geographically as all these isolates were obtained from a single center. Other MRSA subtypes were also confined to a particular center, and no isolates of a single subtype were found in varying centers of this region. The MRSA isolates of subtype A2 were isolated at different time intervals from the same center during the study, suggesting the continued presence of these strains in that area.

All the MSSA PFGE subtype I-1 strains were isolated from patients' pus specimens of a single orthopedic hospital in Coimbatore. Large interval was noticed between the isolation time of each of these isolates and the patients were found to form pus only after their admission, showing the dissemination of this strain locally. The identification of subtypes is becoming possible, as there are alterations in *Sma*I macrorestriction digestion patterns resulting from gain or loss of restriction sites due to point mutation, insertions or deletions. Generally, a number of subtypes are generated from a well-studied MRSA clone and the DNA profiles of the test strains generated by PFGE techniques appear stable and reproducible even after several times of subculturing. Among the sub-types of major MSSA clones such as P and M and MRSA PFGE subtypes of clones A and F of this study, more than 95% similarity was calculated and it was found that the strains were genetically related and had evolved and disseminated within this area. However, one of the MSSA subtypes I-1 of clone I shared only 90% similarity with the rest of the subtypes (I-2 through I-5) and this should be a distantly related strain of this group. Stewart et al. (1993) estimated the genetic distances between MRSA with unusual methicillin resistance by analyzing DNA polymorphisms. The authors observed that the majority of the isolates were belonging to one group with only minor genetic differences between the isolates that showed varying resistance to methicillin, and suggested that this was the evidence of the development of resistant variants from a particular clonal type during outbreaks.

More interestingly, in this study we compared the PFGE types of MRSA and MSSA with representatives of three major international clonal complexes of *S. aureus* and identified the presence of all three of them in South India.

No data were available about international travel or contact in the case of the patients involved. This fact suggests that these three clones may also be important causes of *S. aureus* infections in India. EMRSA-15 is the dominant MRSA in the UK, followed by EMRSA-16 (Ellington et al. 2010). In Scotland, EMRSA-16 and EMRSA-15, represented 80.0% and 15.4% of all MRSA, respectively (Monnet et al. 2004; Goering et al. 2008). EMRSA-16 and other clones within Clonal Complex 30 are found worldwide (Chen et al. 2013). EMRSA-16 is the second most common MRSA in the USA and is a common cause of community acquired MRSA in both the USA and Australia. USA100, also known as the New York/Tokyo clone was the most common pulse-field type (PFT) in the USA (44%) and Japan and is found in many

other countries worldwide. However, a first report appeared in the literature about the incidence of an EMRSA-15 variant in the United States in 2008 (McDougal et al. 2003; Wolter et al. 2008). MSSA variants of these three MRSA clones have been widely reported. Although none of the MRSA clones found in this study belonged to these three clones, it is clear that the mobile genetic element known as staphylococcal cassette chromosome mec (SCCmec) which confers methicillin resistance is able to transfer into these clones and given the right selective pressure it is possible that this may happen in this region.

As MRSA infection is alarming particularly in hospital set ups/community and in unique cases such as diabetic and immunocompromised patients, quick, efficient and reliable characterization of strains and identification of clonal spread within a region need to be done. The PFGE-based DNA fingerprinting is a useful method for investigating the transmission patterns of nosocomial MRSA infections. The understanding of MRSA epidemiology in the respective regions and identification of the DNA restriction patterns of the most infecting/prevalent strain(s) by PFGE could assist the monitoring of the spread of these strains. Also, infected patients can be isolated and provided with better treatment so as to bring out effective control and prevention strategies. We undertook this study to determine the type or clonality of MRSA and MSSA in a specific region and also to identify the level of diversity among the tested isolates.

MRSA subtype A2 alone represented 26% of the 19 MRSA, while MSSA type I represented 33% of the 24 MSSA examined. The predominance of certain types/subtypes in the studied area could be due to the effective spread of particular strains. Although the probable reason for the speedy transmission is ambiguous, it may be related with the virulence factors of the particular strain. A clear clinical understanding of predominant and widespread endemic MRSA/MSSA could be derived by analysing their virulence factors as well as by typing isolates representing other regions of state Tamilnadu. When epidemiological surveys of this kind are carried out continuously, effective control measures can be implemented by identifying specific MRSA clones that are responsible for frequent infections.

Acknowledgement

We would like to thank the Scottish MRSA reference Laboratory, Microbiology Department, Stobhill Hospital, Glasgow, UK G21 3UW for the part of PFGE.

References

Ahmed MO, Elramalli AK, Amri SG, Abuzweda AR, Abouzeed YM (2012) Isolation and screening of methicillin-resistant *Staphylococcus aureus* from health care workers in Libyan hospitals. East Mediterr Health J 18:37-42.

Adesida SA, Abioye OA, Bamiro BS, Brai BI, Smith SI, Amisu KO, Ehichioya DU, Ogunsola FT, Coker AO (2007) Associated risk factors and pulsed field gel electrophoresis of nasal isolates of *Staphylococcus aureus* from medical students in a tertiary hospital in Lagos, Nigeria. Braz J Infect Dis 11:63-69.

Anupurba S, Sen MR, Nath G, Sharma BM, Gulati AK, Mohapatra TM (2003) Prevalence of methicillin resistant *Staphylococcus aureus* in a tertiary referral hospital in Eastern Uttar Pradesh. Indian J Med Microbiol 21:49-51.

Bannerman TL (1999) *Staphylococcus*, *Micrococcus*, and other catalase positive cocci that grow aerobically. In Murray PR, Baron EJ, Tenover FC, Yolten RH, ed., Manual of Clinical Microbiology. American Society of Microbiology, Washington DC, pp. 384-404.

Bannerman TL, Hancock GA, Tenover FC, Miller JM (1995) Pulsed-field gel electrophoresis as a replacement for bacteriophage typing of *Staphylococcus aureus*. J Clin Microbiol 33:551-555.

Ben Nejma M, Merghni A, Mastouri M (2014) Genotyping of methicillin resistant *Staphylococcus aureus* strains isolated from hospitalized children. Int J Pediatr.2014; Article ID 314316 doi: 10.1155/2014/314316.

Bartoloni A, Riccobono E, Magnelli D, Villagran AL, Di Maggio T, Mantella A, Sennati S, Revollo C, Strohmeyer M, Giani T, Pallecchi L, Rossolini GM (2014) Methicillin-resistant *Staphylococcus aureus* (MRSA) in hospitalized patients from the Bolivian Chaco. Int J Infect Dis in press, doi: 10.1016/j.ijid.2014.12.006

Chen L, Chavda KD, Solanki M, Mediavilla JR, Mathema B, Schlievert PM, Kreiswirth BN (2013) Genetic variation among Panton-Valentine leukocidin-encoding bacteriophages in *Staphylococcus aureus* clonal complex 30 strains. J Clin Microbiol 51:914-919.

Clinical and Laboratory Standards Institute (2010). Performance Standards for Antimicrobial Susceptibility Testing; Twenty-First Informational Supplement. CLSI document M100-S20 Wayne PA: Clinical and Laboratory Standards Institute.

Chambers HF (2001) The changing epidemiology of *Staphylococcus aureus*? Emerg Infect Dis 7:178-182.

Carles-Nurit MJ, Christophle B, Broche S, Gouby A, Bouziges N, Ramuz M (1992) DNA polymorphisms in methicillin-susceptible and methicillin-resistant strains of *Staphylococcus aureus*. J Clin Microbiol 30:2092-2096.

Elixhauser A and Steiner C (2007) Infections with methicillin resistant *Staphylococcus aureus* (MRSA) in U.S. hospitals, 1993-2005. HCUP Statistical Brief #35. Agency for Healthcare Research and Quality, Rockville, MD. http://www.hcup-us.ahrq.gov/reports/statbriefs/sb35.pdf

Ellington MJ, Hope R, Livermore DM, Kearns AM, Henderson K, Cookson BD, Pearson A, Johnson AP (2010) Decline of EMRSA-16 amongst methicillin-resistant *Staphylococcus aureus* causing bacteraemias in the UK between 2001 and 2007. J Antimicrob Chemother 65:446-448.

Erdenizmenli M, Yapar N, Senger SS, Ozdemir S, Yuce A (2004) Investigation of colonization with methicillin-resistant and methicillin-susceptible *Staphylococcus aureus* in an outpatient population in Turkey. Jpn J Infect Dis 57:172-175.

Fujino T, Sekiguchi J, Kawana A, Konosaki H, Nishimura H, Saruta K, Kudo K, Kondo T, Yazaki Y, Kuratsuji T, Kirikae T (2004) Molecular epidemiology of methicillin-resistant *Staphylococcus aureus* in a Tokyo hospital in 2003. Jpn J Infect Dis 57:83-85.

Goering RV, Morrison D, Al-Doori Z, Edwards GF, Gemmell CG (2008) Usefulness of mec-associated direct repeat unit (dru) typing in the epidemiological analysis of highly clonal methicillin-resistant *Staphylococcus aureus* in Scotland. Clin Microbiol Infect 14:964-969.

Hosoda M, Toyama J, Hasada K, Fujino T, Ohtsuki R, Kirikae T (2002) A clonal expansion of methicillin-resistant *Staphylococcus aureus* (MRSA) in a tuberculosis ward. Jpn J Infect Dis 55:219-221.

Ichiyama S, Ohta M, Shimokata K, Kato N, Takeuchi J (1991) Genomic DNA fingerprinting by pulsed-field gel electrophoresis as an epidemiological marker for study of nosocomial infections caused by methicillin-resistant *Staphylococcus aureus*. J Clin Microbiol 29:2690-2695.

Kali A, Stephen S, Sivaraman U, Kumar S, Joseph NM, Srirangaraj S, Easow JM (2013) Bacteriophage types of methicillin-resistant *Staphylococcus aureus* in a tertiary care hospital. Australas Med J. 6:496-503.

Leonard RB, Mayer J, Sasser M, Woods ML, Mooney BR, Brinton BG,

Newcomb-Gayman PL, Carroll KC (1995) Comparison of MIDI Sherlock system and pulsed-field gel electrophoresis in characterizing strains of methicillin-resistant *Staphylococcus aureus* from a recent hospital outbreak. J Clin Microbiol 33:2723-2727.

Loureiro MM, de Moraes BA, Quadra MR, Pinheiro GS, Suffys PN, Asensi MD (2000) Molecular epidemiology of methicillin resistant *Staphylococcus aureus* isolated from newborns in a hospital in Rio de Janeiro, Brazil. Mem Inst Oswaldo Cruz 95:777-782.

Maree CL, Daum RS, Boyle-Vavra S, Matayoshi K, Miller LG (2007) Community-associated methicillin-resistant *Staphylococcus aureus* isolates causing healthcare-associated infections. Emerg Infect Dis 13:236-242.

McDougal LK, Steward CD, Killgore GE, Chaitram JM, McAllister SK, Tenover FC (2003). Pulsed-field gel electrophoresis typing of oxacillin-resistant *Staphylococcus aureus* isolates from the United States: establishing a national database. J Clin Microbiol 41:5113-5120.

Mehndiratta PL, Bhalla P (2012) Typing of Methicillin resistant *Staphylococcus aureus*: a technical review. Indian J Med Microbiol 30:16-23.

Mehta AP, Rodrigues C, Sheth K, Jani S, Hakimiyan A, Fazalbhoy N (1998) Control of methicillin resistant *Staphylococcus aureus* in a tertiary care center. A five year study. J Med Microbiol 16:31-34.

Mir AB and Srikanth (2013) Prevalence and antimicrobial susceptibility of methicillin resistant *Staphylococcus aureus* and coagulase-negative Staphylococci in a tertiary care hospital. Asian J Pharm Clin Res 6:231-234.

Monnet DL, MacKenzie FM, López-Lozano JM, Beyaert A, Camacho M, Wilson R, Stuart D, Gould IM (2004) Antimicrobial drug use and methicillin-resistant *Staphylococcus aureus*, Aberdeen, 1996-2000. Emerg Infect Dis 10:1432-1441.

Nelson MU, Gallagher PG (2012) Methicillin-resistant Staphylococcus aureus in the neonatal intensive care unit. Semin Perinatol 36:424-430.

Patel S (2007) The impact of MRSA on wound healing. Wound Essent 2:144-148.

Pereira V, Riboli D, da Cunha M (2014) Characterization of the clonal profile of MRSA isolated in neonatal and pediatric intensive care units of a University Hospital. Ann Clin Microbiol Antimicrob 13:50.

Pulimood TB, Lalitha MK, Jesudson MV, Pandian R, Selwyn JJ. (1996) The spectrum of antimicrobial resistance among methicillin resistant *Staphylococcus aureus* (MRSA) in a tertiary care centre in India. Indian J Med Res 103:212-215.

Qureshi AH, Rafi S, Qureshi SM, Ali AM (2004) The current susceptibility patterns of methicillin resistant *Staphylococcus aureus* to conventional anti Staphylococcus antimicrobials at Rawalpindi. Pak J Med Sci 20:361-364.

Rajaduraipandi K, Mani KR, Panneerselvam K, Mani M, Bhaskar M, Manikandan P (2006) Prevalence and antimicrobial susceptibility pattern of methicillin resistant *Staphylococcus aureus*: a multicentre study. Indian J Med Microbiol 24:34-38.

Ray P, Gautam V, Singh R (2011) Methicillin-resistant *Staphylococcus aureus* (MRSA) in developing and developed countries: implications and solutions. Reg Health Forum 15:74-82.

Sasaki R, Fujino T, Saruta K, Kawasaki J, Shigeto N, Kirikae T (2002) Molecular epidemiological surveillance of methicillin-resistant *Staphylococcus aureus* in a Hiroshima community hospital in 2002. Jpn J Infect Dis 55:93-95.

Shabir S, Hardy KJ, Abbasi WS, McMurray CL, Malik SA, Wattal C, Hawkey PM (2010) Epidemiological typing of meticillin-resistant *Staphylococcus aureus* isolates from Pakistan and India. J Med Microbiol 59:330-337.

Shopsin B, Kreiswirth BN (2001) Molecular epidemiology of methicillin-resistant *Staphylococcus aureus*. Emerg Infect Dis 7:323-326.

Stewart PR, el-Adhami W, Inglis B, Franklin JC (1993) Analysis of an outbreak of variably methicillin-resistant *Staphylococcus aureus* with chromosomal RFLPs and mec region probes. J Med Microbiol 38:270-277.

Struelens MJ, Deplano A, Godard C, Maes N, Serruys E (1992) Epidemiologic typing and delineation of genetic relatedness of methicillin-resistant *Staphylococcus aureus* by macrorestriction analysis of genomic DNA by using pulsed-field gel electrophoresis. J Clin Microbiol 30:2599-2605.

Stryjewski ME, Corey GR (2014) Methicillin-resistant *Staphylococcus aureus*: an evolving pathogen. Clin Infect Dis 58:S10-S19.

Sujatha MB (2014) Drug treatment of MRSA infections. Kerala J Orthop 27:81-85.

Tenover FC, Arbeit RD, Goering RV, Mickelsen PA, Murray BE, Persing DH, Swaminathan B (1995) Interpreting chromosomal DNA restriction patterns produced by pulsed-field gel electrophoresis: criteria for bacterial strain typing. J Clin Microbiol 33:2233-2239.

Tenover FC, Goering RV (2009) Methicillin-resistant *Staphylococcus aureus* strain USA300: origin and epidemiology. J Antimicrob Chemother 64:441-446.

Thati V, Shivannavar CT, Gaddad SM (2011) Vancomycin resistance among methicillin resistant *Staphylococcus aureus* isolates from intensive care units of tertiary care hospitals in Hyderabad. Indian J Med Res 134:704-708.

Udo EE, Al-Lawati BA, Al-Muharmi Z, Thukral SS (2014) Genotyping of methicillin-resistant *Staphylococcus aureus* in the Sultan Qaboos University Hospital, Oman reveals the dominance of Panton-Valentine leucocidin-negative ST6-IV/t304 clone. New Microbes New Infect 2:100-105.

Uemura E, Kakinohana S, Higa N, Toma C, Nakasone N (2004) Comparative chracterization of *Staphylococcus aureus* isolates from throats and noses of healthy volunteers. Jpn J Infect Dis 57:21-24.

Uhlemann AC, Hafer C, Miko BA, Sowash MG, Sullivan SB, Shu Q, Lowy FD (2013) Emergence of sequence type 398 as a community- and healthcare-associated methicillin-susceptible *Staphylococcus aureus* in Northern Manhattan. Clin Infect Dis 57:700-703.

van Belkum A, van Leeuwen W, Verkooyen R, Saçilik SC, Cokmus C, Verbrugh H (1997) Dissemination of a single clone of methicillin-resistant *Staphylococcus aureus* among Turkish hospitals. J Clin Microbiol 35:978-981.

Vidhani S, Mehndiratta PL, Mathur MD (2001) Study of methicillin resistant *S. aureus* (MRSA) isolates from high-risk patients. Ind J Med Microbiol 19:13-16.

Wei MQ, Grubb WB (1992) Typing of Australian methicillin-resistant *Staphylococcus aureus* strains by pulsed field gel electrophoresis. J Med Microbiol 37:187-191.

Wolter DJ, Chatterjee A, Varman M, Goering RV (2008) Isolation and characterization of an epidemic methicillin-resistant *Staphylococcus aureus* 15 variant in the central United States. J Clin Microbiol 46:3548-3549.

Yamamoto T, Hung WC, Takano T, Nishiyama A (2012) Genetic nature and virulence of community-associated methicillin-resistant *Staphylococcus aureus*. Biomedicine 3:2-18.

Volume 58(2) 2014
Acta Biologica Szegediensis
http://www2.sci.u-szeged.hu/ABS

DISSERTATION SUMMARIES

Investigation of the relationship of hydrogenase enzymes and photosynthesis in *Thiocapsa roseopersicina*

Ildikó K. Nagy

Department of Biotechnology, University of Szeged, Szeged, Hungary

The photosynthetic purple sulphur bacterium, *Thiocapsa roseopersicina* harbours four functional [NiFe] hydrogenases. Two of them are attached to the periplasmic membrane (Hyn, Hup) and the other two are apparently localized in the cytoplasm (Hox1, Hox2). It prefers to utilize reduced sulphur compounds for anaerobic photochemolithotrophic growth, but simple organic substrates such as glucose and acetate can also be used as carbon, energy and electron sources.

There is a facultative lithoautrophic proteobacterium, *Ralstonia eutropha* which has a soluble hydrogenase gene, *hoxI*. In *R. eutropha* the HoxI protein has an established role in the *in vivo* photosynthetic electron transport similar to that of the Hox1E in *T. roseopersicina*. The in frame deletion of *hox1E* gene causes complete loss of *in vivo* hydrogenase activity in *T. roseopersicina* and in addition, this loss-of-function mutation was not complemented by *hoxI* gene.

Various constructs harbouring the *hoxI* gene were transferred into different *T. roseoperscina* hydrogenase mutant strains.

Functional studies aimed the investigation of the role of *hoxI* in the modulation of Hox1 enzyme. Therefore, experiments were carried out under conditions when only Hox1 hydrogenase was functional (elevated sodium-thiosulphate concentration in the medium). The strain expressing the *hoxI* gene was shown to evolve significantly higher amount of hydrogen *in vivo* compared to the control (empty plasmid in the same strain).

The global gene expression changes were studied in three different strains by sequencing-based Whole Transcriptome Analysis (WTA): the strain which contains the complete Hox1 hydrogenase, the *hox1E* mutant strain and the *hox1E* mutant strain harbouring the heterologous *hoxI* gene.

The WTA results were divided into two groups. The first group deals with the genes, which showed decreased expression in response to *hox1E* deletion (two genes organized into one operon and coding for the NADH dehydrogenase subunit 5 protein and a hypothetical transmembrane protein coupled to NADH-ubiquinone oxidoreductase chain 5 homolog). The low expression levels of these genes were not complemented by the *hoxI* gene. The second group represents genes, which products are involved in the organization of the photosynthetic reaction center and the light harvesting complex. These genes also showed reduced expression in the *hox1E* mutant strain, however the addition of the *hoxI* gene restored their expression levels.

Currently we are investigating the metabolic background of the gene expression changes by deploying different molecular and functional experiments as well as mutant analysis studies. Light dependence of the Hox1 hydrogenase is under investigation, this might shed light on the interaction of Hox1 hydrogenase and photosynthesis.

This research was supported by the European Union and the State of Hungary, co-financed by the European Social Fund in the framework of TÁMOP 4.2.4.A A2-ACSJD-13-0524 'National Excellence Program.

Supervisor: Gábor Rákhely and Gergely Maróti
E-mail: rakhelyg@brc.hu and marotig@brc.hu

Instructions to Authors

Submission of manuscripts

Submission of a manuscript to *Acta Biologica Szegediensis* automatically involves the assurance that it has not been published and will not be published elsewhere in the same form. Manuscripts should be written in English (consistent with either UK or US spelling). Since poorly-written material will not be considered for publication, authors are encouraged to have their manuscripts corrected for language and usage by a trusted expert. There are no explicit length limitations. However, a normal research article will occupy 4-8 printed pages; reviews might be considerably longer.

Manuscripts should be submitted to the Editor-in-Chief as an electronic attachment to **csaba@bio.u-szeged.hu**. All submitted manuscripts should be complete in themselves and firmly supported by properly detailed experimental data. *Instructions to Authors* is published in each issue and also available at **http://www2.sci.u-szeged.hu/ABS**. Correspondence relating to the status of the manuscripts, proofs, publication, reprints and advertising should be sent also to **abs@bio.u-szeged.hu**.

Manuscript format

The following file formats are acceptable for the main manuscript document: Microsoft word (doc, docx) and Rich text format (rtf). All pages should be printed with full double spacing, 2.5 cm margins, and a nonjustified right margin. A standard 12 point typeface (e.g. Times New Roman, Helvetica or Courier) should be used throughout the manuscript, with symbol font for Greek letters. Footnotes are not permitted. Each page should be numbered at the bottom as follows:

Page 1. Title page: Complete title, first name, middle initial, last name of each author; affiliations of the authors; mailing and e-mail addresses and phone and fax numbers of the corresponding author and a running title of no more than 48 characters.

Page 2. Abstract: no more than 200 words, followed by 4-6 key words. The abstract should not contain any undefined abbreviations and references.

Beginning on page 3: Introduction, Materials and Methods, Results, Discussion, Acknowledgments, References, Tables, Figures. Each section should be begun on a new page.

For reagents and instruments, the manufacturer's name should be given in parentheses. If microorganisms are used in the study, the collection or the strain number should be given; new isolates must be deposited in a publicly available culture collection. New nucleotide and amino acid sequences must be submitted in freely available databases (i.e. EMBL/GenBank) and the accession number should be provided. GenBank/EMBL accession number of the used amino acid or nucleic acid sequences also should be presented. Sources for all antibodies should be indicated. Customary abbreviations in common use need not be defined in the text (e.g. DNA, ATP or PCR). Other abbreviations should be defined at first mention and used consistently thereafter. Authors are required to use approved gene symbols and names; protein names should be in plain type. Quantitative results must be presented as graphs or tables and supported by appropriate experimental design and statistical tests. Only SI units may be used. For studies that involve animals or human subjects, the institutional, national or international guidelines that were followed should be indicated.

Acknowledgments

This section can include sources of the financial support received for the work and recognition for colleagues who assisted in the study or the manuscript preparation or provided unpublished data.

References

Only work that has been published or is in the press may be referred to. Personal communications should be acknowledged in the text and accompanied by written permission. In the text, references should be cited by name and year, e.g. Bloom (1983) or (Schwarz-Sommer et al. 1990) or (Maxam and Gilbert 1977) or (Schwarz-Sommer et al. 1990, Maxam and Gilbert 1977). In the References, references should be listed alphabetically by first authors (including all coauthors) and chronologically for a given author (beginning with the most recent date of publication). Where the same author has more than one publication in a year, lower case letters should be used (e.g. 1999a, 1999b, etc.). Periods should not be used after authors' initials or abbreviated journal titles (e.g. *Acta Biologica Szegediensis* should be cited as Acta Biol Szeged). Inclusive page numbers should be used. Examples:

Bloom FE (1983) The endorphins: a growing family of pharmacologically pertinent peptides. Annu Rev Pharmacol Toxicol 23:151-170.

Coons AH (1978) Fluorescent antibody methods. In Danielli JF, ed., General Cytochemical Methods. Academic Press, New York, 399-422.

Maxam AM, Gilbert WA (1977) A new method for sequencing DNA. Proc Natl Acad Sci USA 74:560-564.

Monod J, Changeux J-P, Jacob F (1963) Allosteric proteins and cellular control systems. J Mol Biol 6:306-329.

Schwarz-Sommer Z, Huijser P, Nacken W, Saedler H, Sommer H (1990) Genetic control of flower development by homeotic genes in *Antirrhinum majus*. Science 250:931-936.

Tables

Tables should be numbered consecutively with Arabic numerals. The first table in the text should be referred to as Table 1, and so on. A brief title should be included above the table. Each table should be double spaced, without vertical or horizontal lines, and on a separate sheet. Material in text should not be duplicated and methods should not be described.

Figure legends

Figures should be numbered consecutively with Arabic numerals. The first figure in the text should be referred to as Fig. 1, and so on. The following information should be provided in the figure legend: Figure number (using as Figure 1), short title of figure and the detailed legend. Material in the legend should not be duplicated and methods should not be described. The size of scale bars should be indicated when appropriate.

Figures

All figures should be submitted in separate files. Preferred file formats are TIFF or EPS. In some cases, MSOffice files are also acceptable. Adequate resolution (at least 300 dpi, preferably 600 dpi) should be used in making the original image. If figures are submitted with the main text, each of them should be presented in a separate page after the tables.